Radiolabelling of Aryl Boronic Esters with ^{18}F and ^{123}I: Method Development and Application

Greg J. McSweeney

A thesis submitted to the board of the faculty of Physical Sciences in partial fulfilment of the requirements for the degree of Doctor of Philosophy at the University of Oxford



Merton College

Trinity Term 2017

Author's Declaration

The work presented in this thesis was conducted at the Chemistry Research Laboratory at the University of Oxford under the supervision of Prof. Véronique Gouverneur. All the work is my own, except where otherwise stated, and has not been submitted for any other degree at this or any other university.

Greg McSweeney

October 2017

Radiolabelling of Aryl Boronic Esters with ^{18}F and ^{123}I: Method Development and Application

Abstract

Greg J. McSweeney, University of Oxford, a thesis submitted for the degree of Doctor of Philosophy, Trinity 2017

The overarching theme of this thesis is the application of aryl boronic esters to the fields of PET and SPECT radiochemistry.

Chapter 1 provides an introduction to positron emission tomography (PET) and single photon emission computed tomography (SPECT), in conjunction with an introduction to the utility of arylboranes as precursors for radioisotope incorporation.

In **chapter 2**, a general method for the copper-mediated nucleophilic ^{123}I-iodination of (hetero)aryl boronic pinacol esters and acids is disclosed. This methodology was applied toward the successful radiosynthesis of four commonly used SPECT radiotracers, [^{123}I]DPA- 713, [^{123}I]IMPY, [^{123}I]MIBG and [^{123}I]IPEB.

In **chapter 3**, the copper-mediated nucleophilic ^{18}F-fluorination of aryl boronic pinacol esters, developed in the Gouverneur group, has been applied to the field of prosthetic group ^{18}F-radiochemistry. This protocol was utilised to synthesise four popular prosthetic groups in a single radiosynthetic step.

Chapter 4 describes the radiosynthesis and biological evaluation of [^{18}F]DPA-713 and [^{18}F]CF_3DPA-713, two novel analogues of the Translocator Protein (TSPO) ligand *N,N*-diethyl-2-(4-methoxyphenyl)-5,7-dimethylpyrazolo[1,5-a]pyrimidine-3-acetamide-713 (DPA-713).

Finally, **chapter 5** details experimental procedures and characterisation for all compounds.

Acknowledgements

I would like to express my gratitude to Prof. Véronique Gouverneur for giving me the opportunity to do my D.Phil studies in her research group.

The funding for this project was provided by the EPSRC to which I am extremely thankful.

During the course of this thesis I was fortunate to work with some amazing collaborators in Prof. Daniel Anthony and Dr. Alex Dickens.

I would like to extend a word of thanks to Thomas C. Wilson for all the work and commitment he put into the iodine-123 project. Although it was extremely difficult at times we got there in the end.

To Dr. Sean Preshlock, you are a legend!. Thank you for all of your help and support throughout my time in Oxford.

The VG group has been such an amazing place to work over the last few years. Thanks to all members past and present for the constant support and entertainment during long days in the lab, for the KFC trips, the tea breaks and for the Friday football.

Many people are required to keep the CRL running and I would like to say a huge word of thanks to the analytical staff as well as the rest of the CRL support staff.

Thank you to Dr. Keary M. Engle, Dr. Samuel Calderwood and Dr. Robert Leśniak for proofing this thesis.

I would like to thank all of the people that I have met throughout my time in Oxford and my friends back home in Ireland. Particular thanks should go to Robert Leśniak, Cleo Petherick, Stephen Fielden, Samuel Calderwood, Sangseraima Ujeed Robert Carlsson, Matthew Collins, Stephen Hyde, Mark Ryan and Paul Ward.

I would like to thank my parents Ken and Ann for their unwavering support and guidance, words cannot describe just how much you mean to me. You stood with me everyday of this difficult journey and will forever inspire me with your courage, compassion and strength. I love you both.

To my sister Julie-Ann, I don't think you could ever know just how much of an inspiration you are to me.

Finally, to my sister Kate and my Grandad Daniel thank you for always watching over me.

Table of Contents

Front Matter

Author's Declaration i

Abstract iii

Acknowledgements v

Table of Contents ix

Abbreviations and Acronyms xiii

Chapter 1: Arylboranes as versatile precursors for PET & SPECT radiochemistry 1

1.1 Molecular Imaging 1

1.2 Positron Emission Tomography 1

1.2.1 Production of carbon-11 5

1.2.2 Production of fluorine-18 5

1.3 Single Photon Emission Computed Tomography 7

1.3.1 Production of iodine-123 9

1.4 Arylboranes as versatile precursors for PET and SPECT 9

1.4.1 Synthesis of arylboranes 10

1.4.1.1 Electrophilic trapping of organometallic intermediates 10

1.4.1.2 Transition metal coupling 11

1.4.1.3 C-H activation 13

1.4.1.4 Metal free borylation 15

1.4.2 Application of aryl boranes as precursors for radiosynthesis 16

1.4.2.1 Carbon-11 incorporation from aryl boranes 17

1.4.2.2 Fluorine-18 incorporation from arylboranes 21

1.4.2.3 Iodine-123 incorporation from aryl boranes 26

1.5 Thesis outline 27

1.6 References 28

Chapter 2: Radiosynthesis of SPECT tracers *via* copper-mediated ^{123}I-iodination of (hetero)aryl boron reagents **33**

2.1 Introduction 35

2.2 Aim of study 37

2.3 Preliminary Investigations 38

2.3.1 Proposed mechanism 42

2.3.2 Iodine-123 optimisation 44

2.4 Substrate Scope investigation 47

2.4.1 Calculation of radiochemical conversion 48

2.5 Radiolabelling of clinically relevant SPECT radiotracers 50

2.5.1 Synthesis of [^{123}I]IMPY 50

2.5.2 Synthesis of [^{123}I]DPA-713 53

2.5.3 Divergent Radiohalogenation 55

2.6 Conclusions 60

2.7 References 61

Chapter 3: Access to ^{18}F-aryl prosthetic groups *via* copper-mediated nucleophilic ^{18}F-fluorination 63

3.1 Introduction 65

3.2 Preliminary investigations 69

3.2.1 Synthesis of boronate precursors and ^{19}F prosthetic group analogues 70

3.3 ^{18}F-labelling of aryl prosthetic groups 72

3.4 Post labelling conjugation 73

3.4.1 Copper-catalysed alkyne azide cycloaddition 73

3.4.2 Thiol-alkylation with **[^{18}F]3.15** 75

3.4.3 Acylation with [^{18}F]3.1 77

3.5 ^{18}F-Labelling of aryl isocyanide 81

3.5.1 Preliminary investigations 82

3.5.1.1 Synthetic efforts toward **3.30** 83

3.5.1.2 Synthesis of **3.32** a reference for ^{18}F incorporation 84

3.5.1.3 Optimisation of dehydration parameters for isocyanide formation 84

3.5.2 Use of **3.32** for proposed post-labelling conjugation 86

3.5.3 Attempted radiosynthesis of ^{18}F-aryl isocyanide 88

3.6 Conclusion and future work 91

3.7 References 92

Chapter 4: [^{18}F]DPA 713 a novel second generation radioligand for PET imaging of neuroinflammation 95

4.1 Introduction 97

4.2 TSPO Specific Radioligands 98

4.3 Aim of study 101

4.4 Synthetic strategy 103

4.4.1 Strategy for synthesis of 3-iodo-DPA-713 104

4.5 Synthetic efforts toward 3-iodo-DPA-713 104

4.5.1 Synthesis of [^{19}F]CF_3DPA-713 reference for fluorine-18 incorporation 107

4.6 Synthesis of aryl boronate precursor for ^{18}F-fluorination 108

4.7 Radiochemistry 111

4.7.1 ^{18}F-Trifluoromethylation 111

4.7.2 ^{18}F-Fluorination 113

4.8 Biological Studies 115

4.8.1 Statistical Analysis 115

4.8.2 Imaging of LPS induced neuroinflammation using [^{18}F]4-9 116

4.8.3 Imaging of LPS-induced neuroinflammation using [^{18}F]4-10 117

4.8.4 [^{18}F]4-10 binds to the TSPO expression surrounding a focal MS-like lesion in mice 118

4.8.5 [^{18}F]4-10 has a greater binding affinity for TSPO in mice 120

4.9 Conclusions and future work 122

4.10 References 123

Chapter 5: Experimental Data **127**

5.1 General Experimental 129

5.2 Chapter 2: Radiosynthesis of SPECT tracers via copper mediated ^{123}I-iodination of (hetero)aryl boron reagents 131

5.2.1 General Procedures 131

5.2.2 Substrate Synthesis 134

5.2.3 Radiochemistry 146

5.3 Chapter 3: Access to ^{18}F aryl prosthetic groups *via* copper-mediated nucleophilic ^{18}F-fluorination 163

5.3.1 Substrate Synthesis 163

5.3.2 Radiochemistry 175

5.4 Chapter 4: ^{18}F-DPA 713 a novel second generation radioligand for PET imaging of neuroinflammation 188

5.4.1 General Procedures 188

5.4.2 Substrate Synthesis 190

5.4.3 Attempted Iodination of DPA-713 204

5.4.4 Radiochemistry 209

5.4.5 Biological Methods 219

5.5 References 222

Abbreviations and Acronyms

α	Alpha, alpha particle
β+	Positron
γ	Gamma
δ	Chemical shift (ppm)
d	Deuterium
n	Neutron
p	Proton
λ	Wavelength
μ	Micro
μL	Microlitre
μm^2	Square Micrometre
ν	Neutrino
ν	Wavenumbers (cm^{-1})
°C	Celsius
aq.	Aqueous
β-[123I]CIT	2-Beta-carboxymethoxy-3-beta-[4-iodophenyl] tropane
$(C_2H_5O)_2P(O)H$	Diethylphosphite
$[^{123}I]NaI$	Sodium [123I]Iodide
$[^{125}I]NaI$	Sodium [125I]Iodide
$[^{18}F]KF$	Potassium [18F]Fluoride
$[^{18}F]$5FB	2,3,5,6-Tetrafluorophenyl- [18F]pentafluorobenzoate
$[^{18}F]$FBA	4-[18F]Fluorobenzaldehyde
$[^{18}F]$FBAM	*N*-[6-(4-[18]FFluorobenzylidene)aminooxyhexyl]maleimide
$[^{18}F]$FBBr	1-([18F]Fluoro)-4-bromobenzene
$[^{18}F]$FBeAcMeCC	Prop-2-yn-1-yl 4-([18F]fluoro)benzoate
$[^{18}F]$FBeAmMeCC	4-([18F]Fluoro)-*N*-(prop-2-yn-1-yl)benzamide
$[^{18}F]$FBEM	*N*-[2-(4-[18F]Fluorobenzamido)ethyl]maleimide
$[^{18}F]$FBeMeN3	1-(Azidomethyl)-4-([18F]fluoro)benzene
$[^{18}F]$FBenzA	(4-([18F]Fluoro)phenyl)methanamine
$[^{18}F]$FBenzAc	4-[18F]Fluorobenzoic Acid
$[^{18}F]$FBI	1-([18F]Fluoro)-4-iodobenzene
$[^{18}F]$FBnBrA	2-Bromo-*N*-(4-[18F]fluorobenzyl)acetamide
$[^{18}F]$FPM	1-(4-[18F]Fluorophenyl)-1H-pyrrole-2,5-dione
$[^{18}F]$FSB	*N*-Succinimidyl 4-[18F]fluorobenzoate
[d.c.]	Decay Corrected
[n.d.c.]	Non-decay Corrected
$^{11}CH_3I$	^{11}C-Methyl iodide
18-crown-6	1,4,7,10,13,16-Hexaoxacyclo-octadecane
Å	Angstrom
Ac_2O	Acetic Anhydride
ACBD3	Acyl-Coenzyme A Binding Domain Containing 3

AcOH	Acetic Acid
AgOTf	Silver Triflate
Ala	L-Alanine
Ar-Bpin	Aromatic Boronic Ester
ATAD3A	ATPase Family, AAA Domain Containing 3A
$B(iOPr)_3$	Triisopropyl Borate
$B(OMe)_3$	Trimethyl Borate
$B_2(OH)_2$	Tetrahydroxydiboron
B_2Pin_2	Bis(pinacolato)diboron
BathoPhen	4,7-Diphenyl-1,10-phenanthroline
BBB	Blood-brain Barrier
BBN	Bombesin
BCG	Bacillus Calmette–Guérin
$BnNH_2$	Benzylamine
Boc_2O	Di-tert-butyl Dicarbonate
Bpin	Pinacol Boronate Ester
Bpnd	Binding Potential
br. s	Broad Singlet
$BrCOCH_2Br$	2-Bromoacetyl Bromide
$Bu_4N[^{18}F]F$	Tetra-*n*-butylammonium [18F]Fluoride
CCl_4	Carbon Tetrachloride
CI	Chemical Ionisation
Cl-T	Chloramine-T
$ClCF_2CO_2Me$	Methyl Chlorodifluoroacetate
cm^2	Square Centimetre
CNS	Central Nervous System
$Co(OAc)_2$	Cobalt(II) Acetate
COD	Cyclooctadiene
COE	Cyclooctene
CsF	Caesium Fluoride
CT	Computed Tomography
$Cu(OAc)_2$	Copper(II) Acetate
$Cu(OCOCF_3)_2$	Copper(II) Trifluoroacetate
Cu(OTf)2	Copper(II) Triflate
$Cu(OTf)_2(py)_4$	Tetrakis(pyridine)copper(II) Triflate
Cu_2O	Copper(I) Oxide
CuAAC	Copper-catalysed Alkyne Azide Cycloaddition
CuBr	Copper(I) Bromide
CuI	Copper(I) Iodide
CuOTf(benz)	Copper(I) Trifluoromethanesulfonate Benzene Complex
CuOTf(MeCN)4	Tetrakis(acetonitrile)copper(I)triflate
CuSO4	Copper(II) Sulfate
CuTC	Copper(I) Thiophene-2-carboxylate

CYP-450	Cytochrome P450
CYP11A1	Cytochrome P450 Family 11 Subfamily A Member 1
d	Doublet
DA	Dopaminergic
DAA1106	*N*-(2-Phenoxy-5-fluorophenyl)-*N*-(2,5-dimethoxybenzyl)acetamide
dba	Dibenzylideneacetone
DCE	1,2-Dichloroethane
DCM	Dichloromethane
Dehyd	Dehydrating
DIC	*N,N'*-Diisopropylcarbodimide
DIPEA	*N,N'*-Diisopropylethylamine
DMA	Dimethylacetamide
DMAP	4-Dimethylaminopyridine
DMEDA	1,2-Dimethylethylenediamine
DMF	Dimethylformamide
DMSO	Dimethyl Sulfoxide
DOPA	Dihydroxyphenylalanine
DPA-713	*N,N*-Diethyl-2-(4-methoxyphenyl)-5,7-dimethylpyrazolo[1,5-a]pyrimidine-3-acetamide-713
DPA-714	*N,N*-Diethyl-2-[4-(2-fluoroethoxy)phenyl]-5,7-dimethylpyrazolo[1,5-a]pyrimidine-3-acetamide
dppe	1,2-Bis(diphenylphosphino)ethane
dppf	Diphenylphosphinoferrocene
DSC	*N,N'*-Disuccinimidyl Carbonate
dtbpy	4-4'-Di-tert-butyl-2-2'-dipyridyl
EAE	Experimental Allergic Encephalomyelitis
EDG	Electron Donating Group
EoB	End-of-bombardment
equiv	Equivalent
ESI	Electrospray Ionisation
Et_2O	Diethylether
EtOAc	Ethyl Acetate
EtOH	Ethanol
FDA	6-Fluorodopamine
FI	Field Ionisation
FMIBG	1-[(3-Fluorophenyl)methyl]guanidine
FMT	6-Fluoro-meta-tyrosine
FMTEB	3-Fluoro-5-((2-methylthiazol-4-yl)ethynyl)benzonitrile
FPEB	3-Fluoro-5-(pyridin-2-ylethynyl)benzonitrile
GBq	gigaBecquerel
GE-180	Flutriciclamide
GRPR	Gastrin-releasing Receptor
GSH	Glutathione
h	Hour

H_2O_2	Hydrogen Peroxide
H_2SO_4	Sulfuric Acid
H_3PO_2	Hypophosphorous Acid
HABs	High-affinity Binders
HBPin	Pinacolborane
HBr	Hydrogen Bromide
HCl	Hydrogen Chloride
HI	Hydrogen Iodide
HPLC	High-performance Liquid Chromatography
HRMS	High Resolution Mass Spectra
hv	Light Energy
Hz	Hertz
IMCR	Isocyanide Multi-component Reactions
IMM	Inner Mitochondrial Membrane
IMPY	Imidazolepyrazole
IPEB	3-Iodo-5-(pyridin-2-ylethynyl)benzonitrile
IR	Infrared
Kryptofix	Kryptofix 2.2.2, 4,7,13,16,21,24-hexaoxa-1,10-diaza-bicyclo[8.8.8]-hexacosane
$K_2C_2O_4$	Potassium Oxalate
K_2CO_3	Potassium Carbonate
K_3PO_4	Tripotassium Phosphate
kDa	kiloDalton
KF	Potassium Fluoride
KHF_2	Potassium Hydrogen Difluoride
KI	Potassium Iodide
K_i	Inhibitory Constant
$KMnO_4$	Potassium Permanganate
KOAc	Potassium Acetate
LABs	Low-affinity Binders
LAM	Low Atomic Mass
$LiAH_4$	Lithium Aluminium Hydride
LiBr	Lithium Bromide
LiHMDS	Lithium Bis(trimethylsilyl)amide
LiOTf	Lithium Triflate
LRMS	Low Resolution Mass Spectra
LPS	Lipopolysaccharide
m	Multiplet
MABs	Mixed-affinity Binders
MBP	Myelin Basic Protein
MBq	megaBecquerel
MeCN	Acetonitrile
MeI	Methyl Iodide
MeOH	Methanol

min	Minute
mL	Millilitre
mm^2	Square Millimetre
MOG	Myelin Oligodendrocyte Glycoprotein
Mol	Molecular/mole
MP	Melting Point
MPL	Myelin Proteolipid Protein
MRI	Magnetic Resonance Imaging
MS	Multiple Sclerosis
n-BuLi	*n*-Butyllithium
$NaBH_4$	Sodium Borohydride
nAChR	Nicotinic Acetylcholine Receptor
NaH	Sodium Hydride
$NaHCO_3$	Sodium Bicarbonate
NaI	Sodium Iodide
NaN_3	Sodium Azide
NaOAc	Sodium Acetate
NaOH	Sodium Hydroxide
NaOMe	Sodium Methoxide
Nep	Neopentyl Glycol
NET	Norepinephrine Transporter Protein
NEt_3	Triethylamine
$NH_2NH_2.H_2O$	Hydrazine Hydrate
NH_4HCOO	Ammonium Formate
NHS	*N*-Hydroxysuccinimide
$Ni(cod)_2$	Nickel Dicyclooctadiene
nm	Nanometre
nM	Nano-Molar
NMP	*N*-Methyl-2-pyrrolidone
OMM	Outer Mitochondrial Membrane
p-TSCl	4-Toluenesulfonyl Chloride
$P(Cy)_3$	Tricyclohexylphosphine
$P(o\text{-tolyl})_3$	Tri-*o*-tolylphosphine
PBR28	*N*-Acetyl-*N*-(2-methoxybenzyl)-2-phenoxy-5-pyridinamine
PBS	Phosphate Buffered Saline
$Pd(dppf)Cl_2.DCM$	1,1′-Bis(diphenylphosphino)ferrocene]dichloropalladium(II), Complex with Dichloromethane
$Pd(PPh_3)_4$	Tetrakis(triphenylphosphine)palladium
Pd/C	Palladium on Carbon
$PdCl_2(PPh_3)_2$	Bis(triphenylphosphine)palladium(II) dichloride
PEG	Poly(ethylene glycol)
PET	Positron Emission Tomography
pH	Potential of Hydrogen

PhCHO	Benzaldehyde
PhCOOH	Benzoic acid
Phen	1,10-Phenanthroline
Pin	Pinacol
PK11195	*N*-Butan-2-yl-1-(2-chlorophenyl)-*N*-methylisoquinoline-3-carboxamide
pKa	Acid Dissociation Constant
PKA	Protein Kinase A
$POCl_3$	Phosphoryl Chloride
PPh_3	Triphenylphospine
PSL	Photostimulated Luminescence
q	Quartet
RCC	Radiochemical Conversion
RCP	Radiochemical Purity
RCY	Radiochemical Yield
R_f	Retention Factor
RGD	Arginylglycylaspartic acid
ROI	Region of Interest
rt	Room Temperature
s	Singlet
SA	Specific Radioactivity
SCH	Spinal Cord Homogenate
SET	Single Electron Transfer
$SOCl_2$	Thionyl Chloride
SPECT	Single Photon Emission Computed Tomography
StAR	Steroidogenic Acute Regulatory Protein
t	triplet
t-BuONO	*tert*-Butylnitrite
T.M	Transition Metal
$t_{1/2}$	Half-life
TBAT	Tetrabutylammoniumdifluorotriphenylsilicate
TCT	2,4,6-Trichloro-1,3,5-triazine
Temp	Temperature
TEMPO	(2,2,6,6-Tetramethylpiperidin-1-yl)oxyl
TFA	Trifluoroacetic Acid
THF	Tetrahydrofuran
TLC	Thin Layer Chromatography
Thr	L-Threonine
TMEDA	Tetramethylethylenediamine
TSPO	Translocator Protein
US	Ultrasound
UV	Ultraviolet
VDAC-1	Voltage-dependent Anion-selective Channel 1
WAX	Weak Anion Exchange

Author Contributions

All experiments described within this thesis are my own, except where otherwise stated. A list of all work carried out with/by others is given here:

For safety purposes when conducting experiments with ionising radiation no less than two people were present during radiosynthesis for **Chapters 2-4**.

Chapter 2

Compounds **2.21**, **2.22**, **2.25-2.27** were synthesised by Thomas C. Wilson. Radiosynthesis of compounds **[^{18}F]2.25** and **[^{18}F]2.21** was completed by Dr. Sean Preshlock, Dr. Stefan Verhoog and Dr. Samuel Calderwood. Experiments employing iodine-123 were carried out in collaboration with Dr. Sean Preshlock, Dr. Stefan Verhoog and Thomas C. Wilson.

Chapter 3

Experiments employing fluorine-18 were conducted in collaboration with Dr. Stefan Verhoog and Dr. Sean Preshlock.

Chapter 4

Experiments employing fluorine-18 were performed in collaboration with Dr. Sean Preshlock. Induction of Focal EAE, intrastriatal injection of LPS, histology and *in vitro/ex vivo* autoradiography experiments were carried out by Prof. Daniel Anthony and Dr. Alex Dickens.

Introduction

Chapter 1 : Arylboranes as versatile precursors for PET & SPECT radiochemistry

1.1 Molecular Imaging

Molecular imaging enables the real-time, non-invasive visualisation of biochemical events at the cellular and molecular level of intact living organisms.[1] Imaging techniques such as, Magnetic Resonance Imaging (MRI), Computed Tomography (CT) and Ultrasound (US) enable morphological/anatomical visualisation, but provide limited information on metabolic or molecular processes. In contrast, Positron Emission Tomography (PET) and Single Photon Emission Computed Tomography (SPECT) provide quantitative information at the molecular level, facilitating early detection of disease states and understanding of integrative biological events.[2,3]

Importantly, employing PET or SPECT imaging in concurrence with structural imaging techniques such as, CT and MRI can provide both physiological and anatomical information, which may not be determined by using either method independently.[4,5]

1.2 Positron Emission Tomography

PET is a powerful non-invasive functional imaging technique that employs positron-emitting radioactive tracers. The application of PET may: enable a greater understanding of biological pathways, provide important information on the *in vivo* pharmacokinetic and pharmacodynamic properties of compounds during drug discovery, and facilitate the diagnosis and treatment analysis of a wide variety of disease states.[6-8]

Radioisotopes frequently employed for PET are short-lived and decay primarily *via* positron emission (β^+). Radioisotope production is achieved *via* bombardment of a specific target material in a cyclotron*.[9] Carbon-11, nitrogen-13, oxygen-15 and fluorine-18 are archetypal low atomic mass (LAM) radionuclides utilised for PET. These LAM radionuclides can be directly substituted for their stable equivalent, (carbon-12, nitrogen-14, oxygen-16, fluorine-19) without perturbing the biological activity of the chemical probe under investigation. Table 1.2.1 details the production and decay processes of these LAM radionuclides.

Table 1.2.1: Production and decay of LAM PET radionuclides

Radionuclide	Production	Half-life ($t_{½}$ min)	Decay Process	Decay Product	Maximum β^+ energy (keV)	Range in H_2O (mm)
Carbon-11	$^{14}N(p,a)^{11}C$	20.4	99.8% β^+	^{11}B	960	4.1
Nitrogen-13	$^{16}O(p,a)^{13}N$	9.97	100% β^+	^{13}C	1190	5.4
Oxygen-15	$^{14}N(d,n)^{15}O$	2.04	99.9% β^+	^{15}N	1720	8.2
Fluorine-18	$^{18}O(p,n)^{18}F$	109.8	97% β^+	^{18}O	635	2.4

The half-life ($t_{½}$) of the radionuclide tethered to a chemical probe should be in proportion to the time-scale of the biological process under investigation; oxygen-15 ($t_{½}$ = 2.04 min. (Table 1.2.1)) is commonly utilised to examine cerebral blood-flow, a biological process with a short biological half-life.[10]

Synthetic procedures toward positron emitting chemical probes are designed to minimise decay of the β^+ emitter. Therefore, radioisotope installation is performed at a late stage of the synthesis. A timeframe of three isotope half-lives ($t_{½}$) from end-of-bombardment (EoB) to injection is commonly used as a guideline, therefore standard synthetic routes may need to be amended, increasing the complexity of radiotracer

*A compact particle accelerator capable of producing proton or deuteron beams.[9]

(exogenous radioactive probe) synthesis in comparison to their non-radioactive counterparts.[7]

Following the intravenous injection of the radioactive tracer, a set time period is allowed to pass prior to the PET scan to facilitate tracer accumulation in the tissues of interest. At the onset of radioactive decay *via* β^+ emission, an annihilation event ensues when the emitted positron meets an electron. This produces two coincident gamma (γ) rays (emitted γ-quanta pair). A scintillator surrounding the imaging target detects the emitted photons, converting them to electrical impulses *via* photomultiplier tube. Succeeding millions of these annihilation events, a spatial representation of the radiotracers *in vivo* activity is computed and rendered in the form of a 2 or 3 dimensional image (Figure 1.2.1).[11]

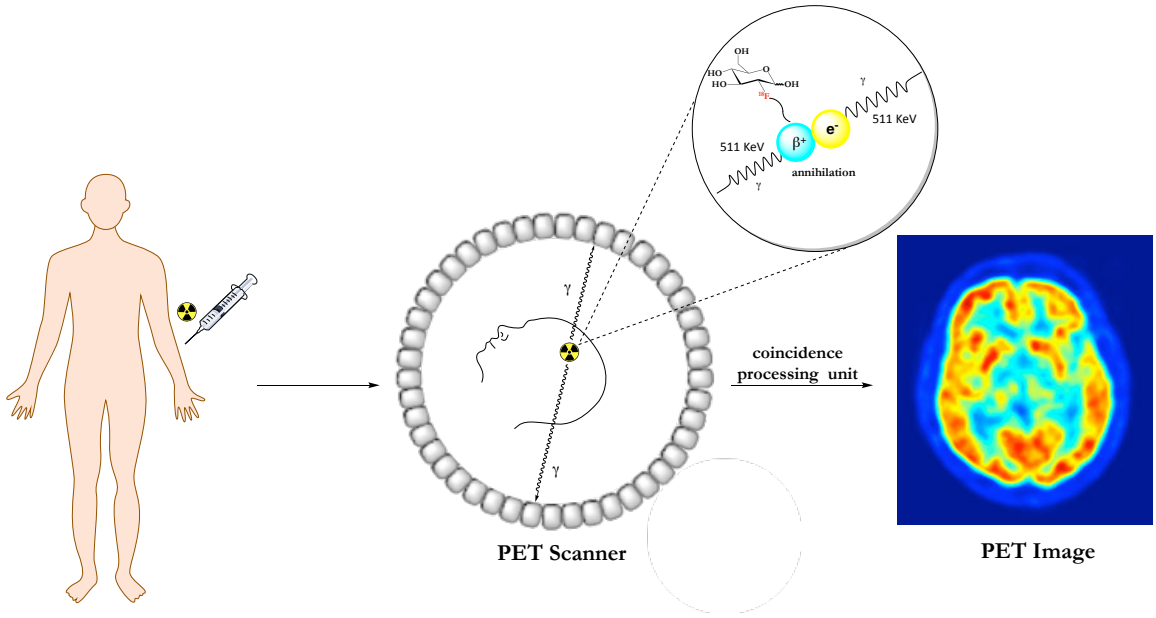


Figure 1.2.1: Molecular imaging *via* PET.

The energy of emission dictates the distance travelled by the positron prior to annihilation, which in turn, determines the resolution of the rendered image. A shorter linear emission range enables the site of annihilation to be determined more precisely, enhancing image resolution. Fluorine-18 has the shortest linear emission range (2.4 mm in H_2O) of all available radionuclides utilised for PET, resulting in the highest

image resolution.[7] Figure 1.2.2 details the decay process of fluorine-18 and the resulting annihilation event upon positron emission.

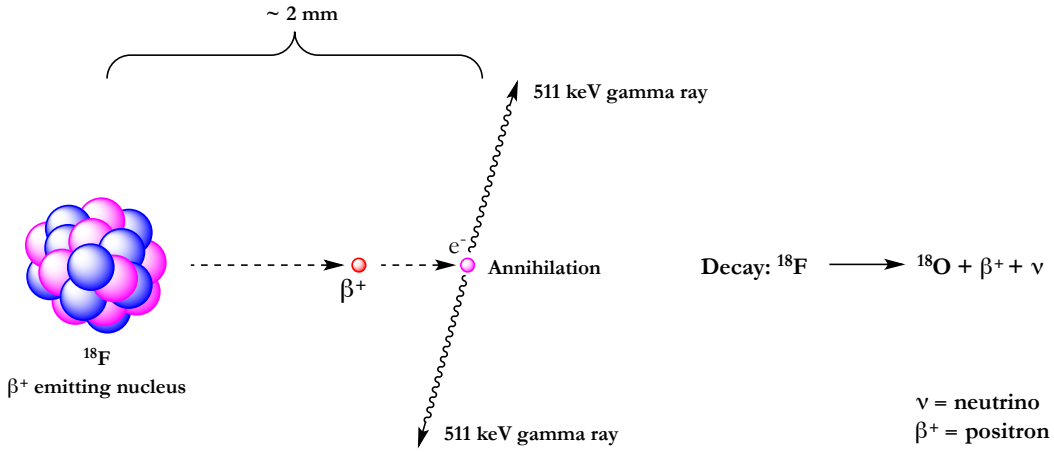


Figure 1.2.2: Mode of decay of ^{18}F & resulting annihilation event upon positron emission

Owing to their intrinsic properties, carbon-11 and fluorine-18 are the most utilised PET radionuclides.[8,12] The omnipresence of carbon-12 in chemical probes and natural products renders carbon-11 an important PET radioisotope. Its half-life of 20.4 minutes enables repeated studies in the same patient within short time intermissions. However, production and use of carbon-11 labelled radiotracers is limited to facilities with direct access to a cyclotron. Fluorine-18 has found widespread utility in PET due to its relatively long half-life (109.8 minutes), short linear emission range (2.4 mm in H_2O), low positron energy and high positron abundance during decay (β^+ emission of 97%). These properties enable high-resolution images to be obtained and permit the construction of complex chemical probes that require a number of synthetic steps succeeding radioisotope incorporation. Furthermore the transport of a pre-prepared fluorine-18 radiotracer to a hospital or academic institute that does not have direct access to a cyclotron is possible.[7,11]

1.2.1 Production of carbon-11

Carbon-11 is typically produced *via* proton bombardment of a nitrogen-14 target, by the $^{14}N(p,\alpha)^{11}C$ nuclear reaction.[13] The construction of carbon-11 containing chemical probes is usually facilitated from $^{11}CO_2$ or $^{11}CH_4$. Both of these primary synthons are constructed by doping the nitrogen-14 target with either oxygen-16 (20-20,000 ppm) or hydrogen-1 (5-10 %) respectively.[12] Figure 1.2.3 details an array of important carbon-11 precursors accessed from $^{11}CO_2$ and $^{11}CH_4$.[14]

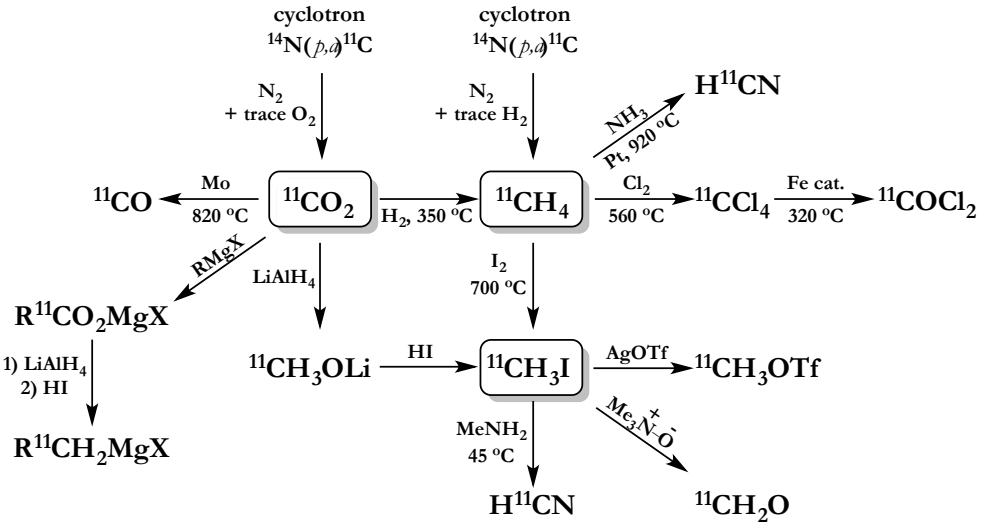


Figure 1.2.3: Pathways to important carbon-11 reagents from $^{11}CO_2$ and $^{11}CH_4$

^{11}C-Methyl iodide ($^{11}CH_3I$) is the most frequently utilised carbon-11 reagent accessed from $^{11}CO_2$ or $^{11}CH_4$. Radiosynthetic incorporation employing $^{11}CH_3I$ can be achieved by C-, N-, O- or S-methylation or *via* ^{11}C-C cross-coupling transformations.[7,14]

1.2.2 Production of fluorine-18

Fluorine-18 is produced as an aqueous solution of [^{18}F]fluoride or as gaseous [^{18}F]F_2. Deuterium irradiation of ^{20}Ne (200 μmol of F_2) and proton irradiation of $^{18}O_2$ (50 μmol of F_2) targets, yield carrier-added gaseous [^{18}F]F_2 in low specific radioactivity (SA) (Table 1.2.2). Specific radioactivity (SA) is defined as the quantity of radioactivity per unit mass of a radiolabeled compound, commonly quoted as gigaBecquerel per micromole (GBq/ μmol).[12]

Table 1.2.2: Methodologies for the production of ^{18}F sources

^{18}F source	Nuclear Reaction	Target	SA(GBq/μmol)
$[^{18}F]F_2$	$^{20}Ne(d,a)^{18}F$	$Ne + F_2$	0.37-0.74
$[^{18}F]F_2$	$^{18}O(p,n)^{18}F$	$^{18}O_2 + F_2$	1
$[^{18}F]F_2$	$^{18}O(p,n)^{18}F$	$H_2{}^{18}O$	55
$[^{18}F]F^-$	$^{18}O(p,n)^{18}F$	$H_2{}^{18}O$	5000

Routine $[^{18}F]F_2$ production is typically achieved *via* the $^{18}O(p,n)^{18}F$ nuclear reaction (Table 1.2.2). Initial proton bombardment of the $^{18}O_2$ target produces excited fluorine-18 atoms ($^{18}F^*$). These excited atoms ($^{18}F^*$) adhere to the nickel walls of the $^{18}O_2$ target. Introduction of carrier $^{19}F_2$ (~0.1% in Ne or Kr) and subsequent target irradiation elicits an isotopic exchange to form $[^{18}F]F_2$, in limited SA (~1 GBq/μmol).[15]

A "post-target" $[^{18}F]F_2$ radiosynthesis has been described by Bergman and Solin yielding $[^{18}F]F_2$ in higher SA (~55 GBq/μmol) (Table 1.2.2).[16] [^{18}F]Fluoride produced *via* the $^{18}O(p,n)^{18}F$ nuclear reaction is dried azeotropically and reacted with methyl iodide to form [^{18}F]fluoromethane ($[^{18}F]CH_3F$). Purification by gas chromatography and transfer with carrier $^{19}F_2$ to an electrical discharge chamber enables atomisation and $^{18}F/^{19}F$ isotopic exchange, yielding $[^{18}F]F_2$.

[^{18}F]Fluoride is predominantly utilised for fluorine-18 radiosynthetic incorporation due to the increased ease of operation and high SA compared to $[^{18}F]F_2$. Proton irradiation of ^{18}O-enriched water ($H_2{}^{18}O$) yields [^{18}F]fluoride with a SA of ~5000 GBq/μmol (Table 1.2.2). The [^{18}F]fluoride ions are collected from the cyclotron as a solution in $H_2{}^{18}O$.[17] Therefore, the fluorine-18 species in solution is weakly nucleophilic and highly solvated. Thus activation of the nucleophile is a necessity to increase its reactivity. This is accomplished *via* multi-step protocol (Figure 1.2.4). [^{18}F]Fluoride is trapped on an anion-exchange cartridge and subsequently eluted with an MeCN : H_2O solution containing a suitable cation.[18] Commonly utilised fluoride cations are potassium ions complexed with the polyether cryptand, Kryptofix 2.2.2 (K_{222})[19] or

tetraalkylammonium ions. Subsequent azeotropic distillation with MeCN curtails the quantity of water present and produces an [^{18}F]fluoride ion with increased reactivity. Dissolution of the azeotropic residue in polar aprotic solvent is typically conducted prior to fluorine-18 radiosynthetic manipulation.

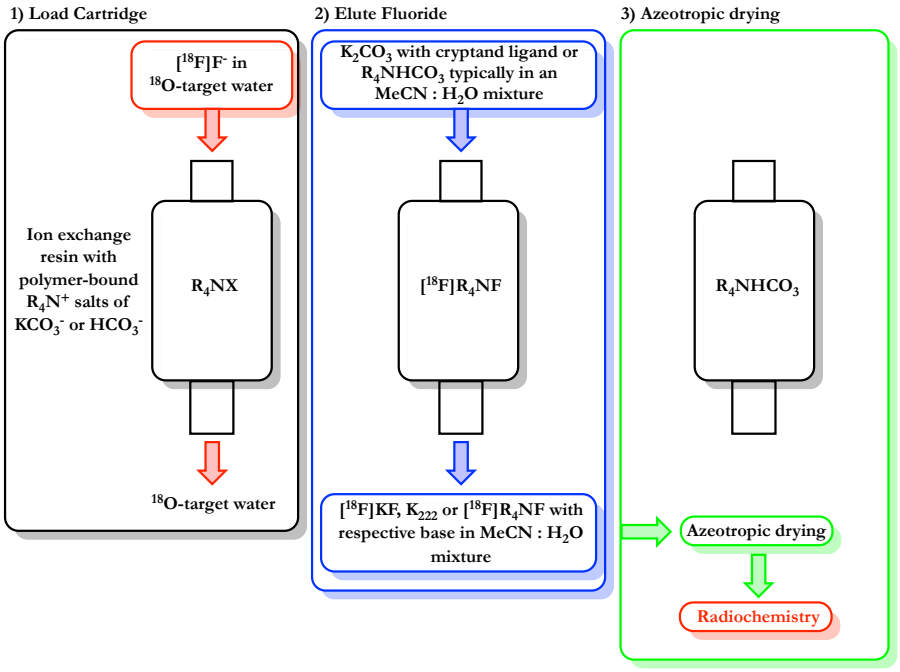


Figure 1.2.4: Typical protocol for the activation of aqueous [^{18}F]fluoride *via* ion-exchange resin

1.3 Single Photon Emission Computed Tomography

Single Photon Emission Computed Tomography (SPECT) imaging employs radionuclides that emit γ-rays directly. These emitted γ-rays are detected by a gamma-camera. Within the gamma camera a collimator facilitates localisation of parallel γ-rays allowing directional information to be obtained. Succeeding scintillation and signal amplification *via* photomultiplier tube, a tomographic reconstruction algorithm is applied to render a two or three-dimensional image. Figure 1.3.1 details the process used to obtain a SPECT image using iodine-123 (photon emission energy of 159keV).

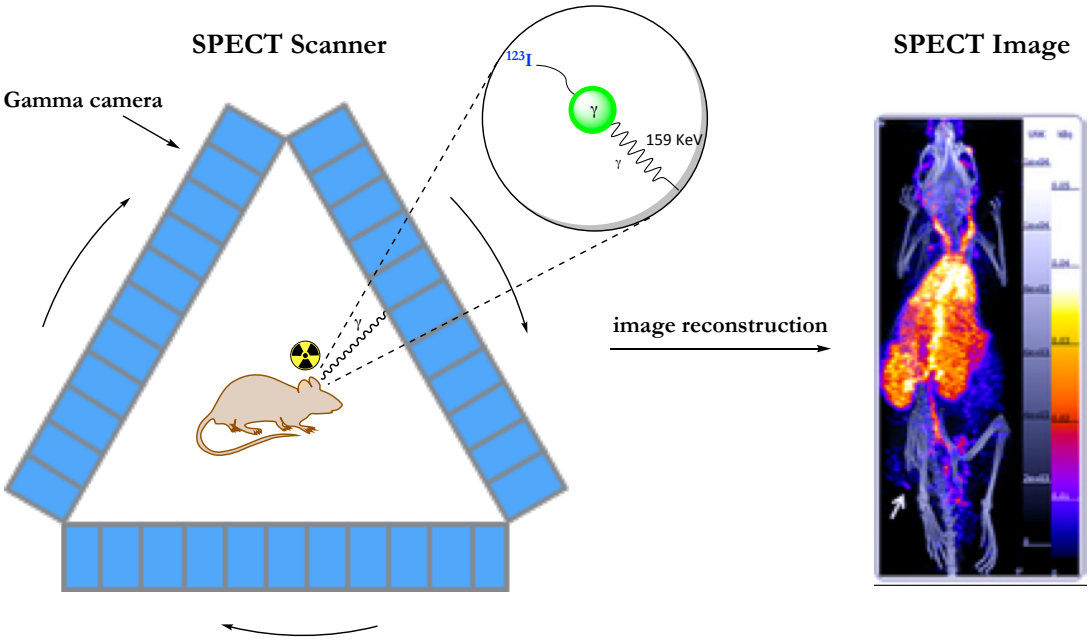


Figure 1.3.1: Schematic of Single Photon Emission Computed Tomography

In comparison to PET, the overall photon emission energies (MeV) are much lower for SPECT radionuclides. Furthermore, the need for physical collimators for image reconstruction i.e. the absence of electronic coincidence detection, results in decreased detection efficiency for SPECT. As a consequence, image resolution and sensitivity is typically superior for PET.† However, the employment of radionuclides with longer half-lives ($t_{1/2}$) and the lower expense of γ-cameras render SPECT more widespread in clinical environments. Table 1.3.1 describes the physical properties of the most commonly utilised SPECT radioisotopes.[8]

Table 1.3.1: Physical Properties of important SPECT Radioisotopes

Radionuclide	Half-life ($t_{1/2}$ hr)	Type of Emission	Principal Photon Emission Energy (MeV)
^{123}I	13.2	Electron Capture	0.16
^{99m}Tc	6	Isomeric Transition	0.14
^{111}In	67.9	Electron Capture	0.17/0.25
^{67}Ga	78.3	Electron Capture	0.09/0.19/0.30
^{201}Tl	73.1	Electron Capture	0.17

† PET sensitivity = 10^{-11}-10^{-12} mole/L. SPECT sensitivity = 10^{-10}-10^{-11} mole/L.[8]

The longer half-life of SPECT radionuclides allows increased time for radiosynthesis (improving operational ease), enables extended imaging time and facilitates biological wash-out of non-specific signal. Excluding iodine-123, the SPECT radionuclides mentioned in Table 1.3.1 typically require a chelating agent for radioisotope incorporation. However, iodine-123 is a unique SPECT radionuclide as radioisotope installation is frequently achieved *via* covalent iodine-carbon bond formation. This enables facile radiolabelling of small chemical probes, with limited structural perturbation in comparison to radionuclide chelation.

1.3.1 Production of iodine-123

Production of iodine-123 is typically realised *via* proton bombardment of a xenon-124 gaseous target (enriched to 99.8%).[20]

$$^{124}\mathbf{Xe\ (p,\ 2n)}^{123}\mathbf{Cs} \rightarrow \beta^{+} + {}^{123}\mathbf{Xe} \rightarrow \beta^{+} + {}^{123}\mathbf{I} \qquad \mathbf{(1)}$$

Upon proton irradiation, xenon-124 expels two neutrons forming caesium-123 (β^+ emitter with $t_{1/2}$ = 5.87 minutes). β^+ decay of caesium-123 induces formation of xenon-123. Gaseous xenon-123 is then separated from the original target material and allowed to decay in isolation, yielding pure iodine-123 *via* β^+ emission. Elution with dilute sodium hydroxide produces [^{123}I]NaI *via* halogen disproportionation reaction. Therefore, [^{123}I]NaI is typically made available as an aqueous solution of the iodide and hypoiodite in dilute sodium hydroxide.[21]

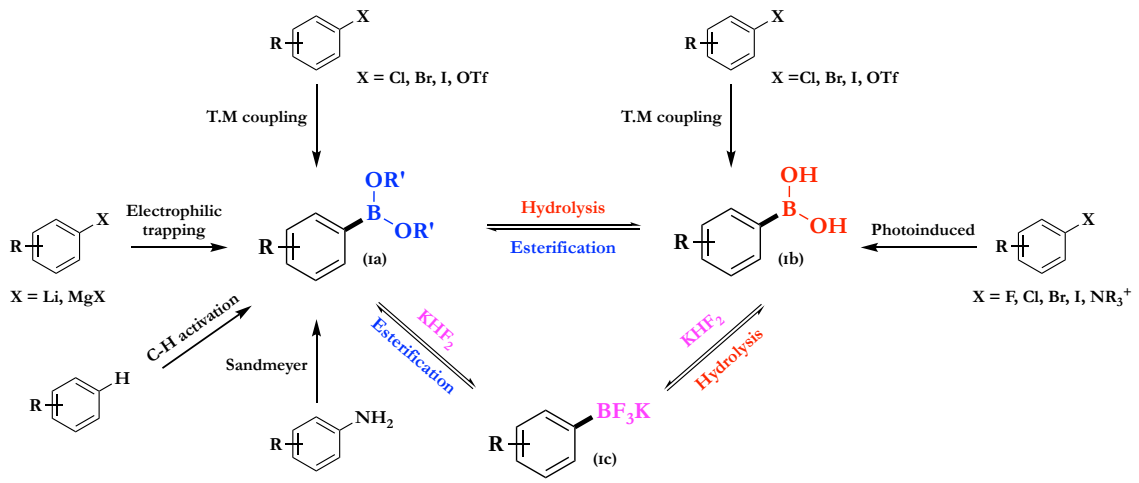
1.4 Arylboranes as versatile precursors for PET and SPECT

Amongst the abundance of precursors that can be employed for PET/SPECT imaging, arylboranes are of particular interest owing to their ease of synthesis and shelf-stable nature. Furthermore, with the advent of cross-coupling reactions, including the powerful Suzuki-Miyaura reaction, many arylborane reagents are available from commercial vendors.[22,23]

In this chapter we will discuss the synthesis of arylboranes in the form of boronic esters, acids and potassium trifluoroborate salts and how their application has facilitated access to a plethora of radioligands for PET and SPECT imaging.

1.4.1 Synthesis of arylboranes

Owing to the importance of arylboranes as synthetic intermediates in organic synthesis, a profusion of methods are available for their construction. Scheme 1.4.1 details a generic summary of the most prominent transformations employed to access these important motifs. Conveniently aromatic boranes in the form of boronic esters **(1a)**, acids **(1b)** and potassium trifluoroborate salts **(1c)** are easily interconverted *via* esterification, hydrolysis and fluorination (Scheme 1.4.1). Thus preparation of one motif (**1a, 1b** or **1c**), theoretically facilitates access to all three functional groups. The following sections of this thesis will disclose an overview of the most important preparative procedures utilised for the construction of arylboranes, with selected examples being discussed.

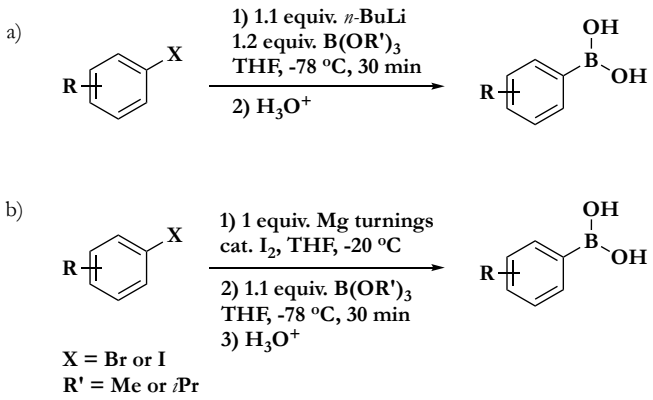


Scheme 1.4.1: Summary of prominent methods toward the construction of arylboranes

1.4.1.1 Electrophilic trapping of organometallic intermediates

One of the first methods discovered to prepare arylboranes is the reaction of a hard organometallic intermediate (lithium or magnesium) with a borate ester. This transformation first described by Khotinsky[24] in 1909 (magnesium) and Letsinger[25] in

1953 (lithium), enables the synthesis of aromatic boronic esters and acids from the corresponding aryl halide. Typically the organometallic species is generated *in situ* from a haloarene under cryogenic conditions. This is succeeded by transmetalation with a boric ester (e.g. trimethyl borate ($B(OMe)_3$) or triisopropyl borate ($B(iOPr)_3$)) to form an arylboronate. Subsequent hydrolysis facilitates formation of the arylboronic acid (Scheme 1.4.2). One disadvantage of this methodology is the low functional group tolerance exhibited during preparation of the organometallic reagent.

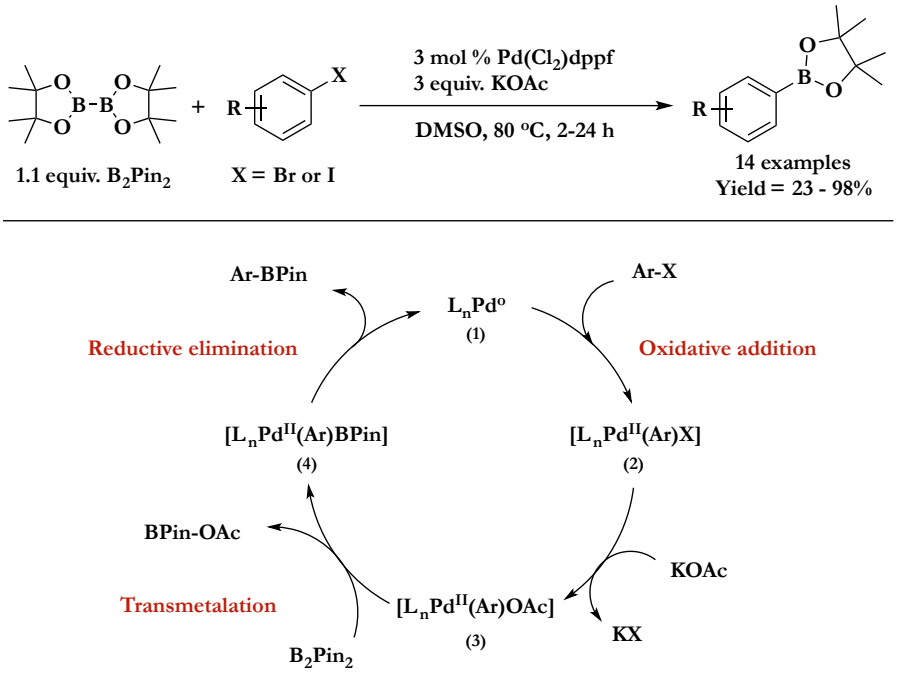


Scheme 1.4.2: Typical reaction conditions toward arylboronic acids *via* electrophilic trapping

1.4.1.2 Transition metal coupling

The direct aromatic borylation of aryl halides and triflates *via* transition metal catalysis, has emerged as a mild and efficient alternative to traditional organometallic mediated electrophilic borylation.[26,27] The most prominent transition metal catalysed transformation toward arylboranes, is the palladium catalysed cross-coupling reaction of haloarenes with bis(pinacolato)diboron (B_2Pin_2). Facile construction of arylboronic esters can be realised under mild reaction conditions using this methodology. This transformation was originally reported in 1995 by Miyaura[28] (Scheme 1.4.3). The reaction has a high functional group tolerance and is generally high yielding even under low catalyst loading. Mechanistically it is believed to proceed *via* a Pd^0/Pd^{II} redox couple. Oxidative addition of the organohalide to the Pd^0 catalyst **(1)** precedes

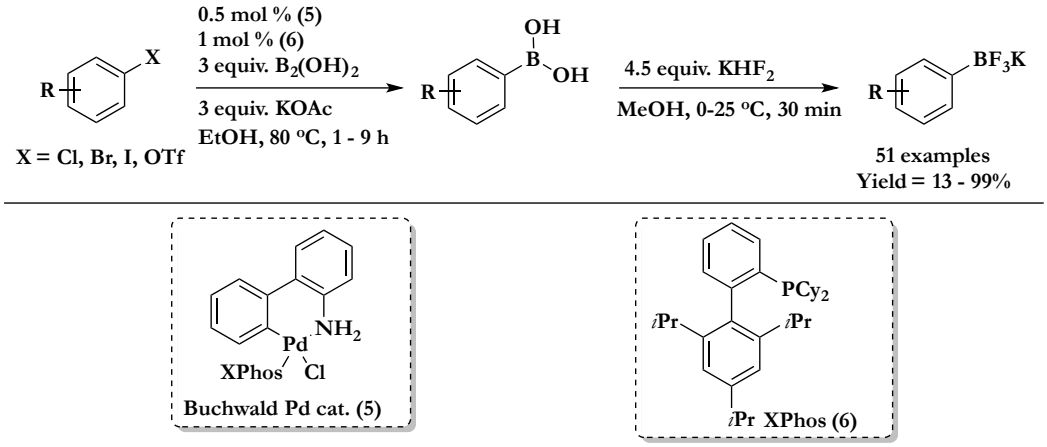
halide exchange with potassium acetate (KOAc)‡. The resulting (acetato)palladium(II) species **(3)** formed *in situ* facilitates transmetalation with B_2Pin_2[30] and subsequent reductive elimination yields the desired aromatic boronic ester (Ar-BPin) (Scheme 1.4.3).



Scheme 1.4.3: Original conditions of Miyaura borylation

Analogous to the Miyaura borylation for direct synthesis of arylboronates (Scheme 1.4.3), Molander[31,32] developed a simple and efficient palladium catalysed direct synthesis of aromatic boronic acids from halides and pseudohalides (Scheme 1.4.4). This important transformation utilises the second generation Buchwald XPhos§ preformed palladium catalyst **(5)**[33] and tetrahydroxydiboron ($B_2(OH)_2$) as boron nucleophile. The authors were able to demonstrate the wide applicability of this procedure on over 50 small molecule substrates containing a variety of electron rich and deficient functional groups.

‡ Use of potassium phenoxide as Lewis base has also been reported.[29]
§ XPhos = 2-Dicyclohexylphosphino-2′,4′,6′-triisopropylbiphenyl



Scheme 1.4.4: Direct formation of aryl boronic acids *via* palladium catalysis

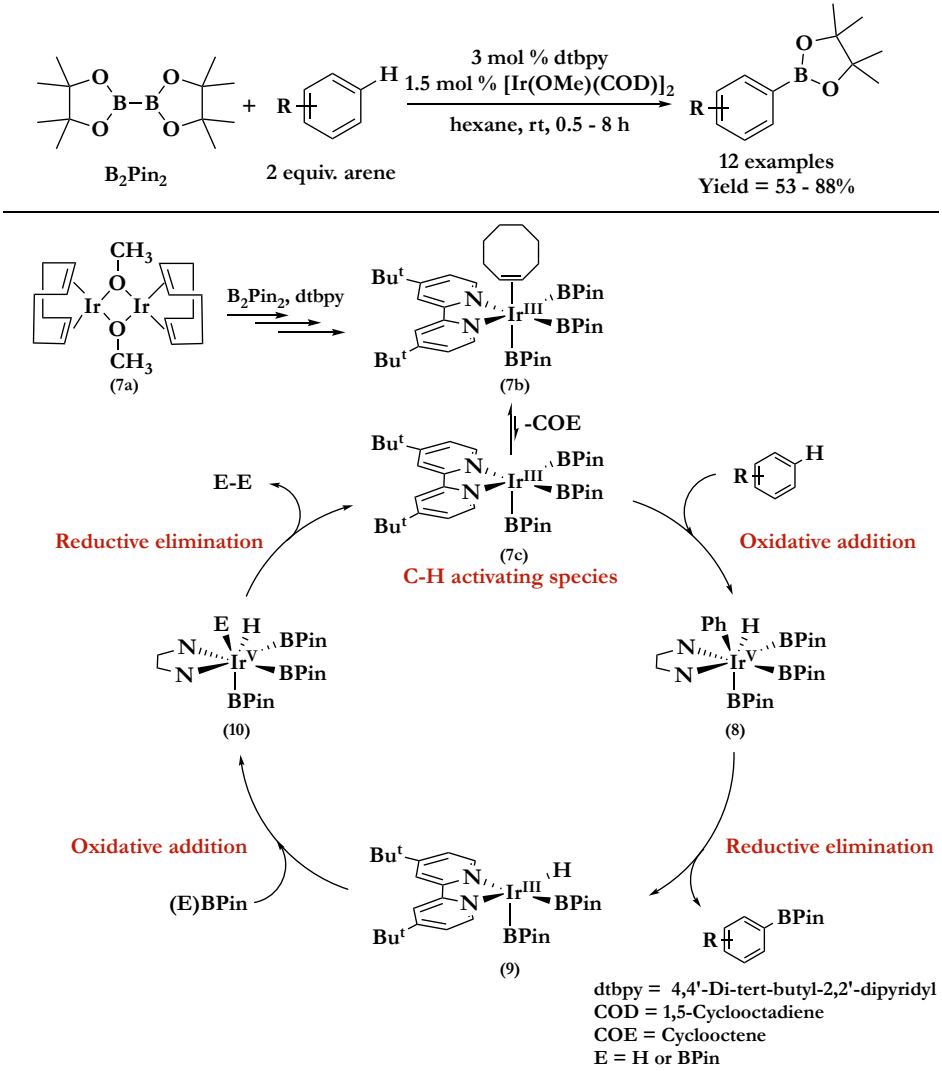
1.4.1.3 C-H activation

The development of transition metal catalysed C-H borylation has enabled the direct preparation of arylboranes from the corresponding aromatic hydrocarbons.[34,35] The most efficient preparation of arylboranes by C-H functionalisation, is the synthesis of aromatic boronic esters *via* iridium catalysis, co-discovered by Smith[36] and Ishiyama, Miyaura and Hartwig[37,38] in 2002. Scheme 1.4.5 details the conditions employed by Ishiyama, Miyaura and Hartwig.[38] This transformation has become the protocol of choice for direct C-H borylation owing to its mild reaction conditions and use of an air-stable boron reagent (B_2Pin_2) and precatalyst $[Ir(OMe)(cod)]_2$. The reaction proceeds at room temperature and is suitable for the direct C-H borylation of disubstituted and benzo-fused arenes.

Regiospecific borylation is observed for disubstituted arenes, with borylation occurring at C-H bonds *meta* or *para* to a substituent and functionalisation is not permitted at the *ortho* position. Additionally, 1,2-, 1,4- and 1,3-substituted arenes yield a single product[**] and potentially reactive functionalities on the aromatic ring are tolerated e.g. discriminate carbon-hydrogen selectivity over carbon-halogen.

[**] Reaction at the *ortho* carbon atom of the 1,4 isomer was retarded by steric congestion and borylation of 1,3 isomer proceeded selectively at the common *meta* carbon.[37,38]

A potential mechanism involving an Ir^{III}/Ir^{V} redox couple is shown in Scheme 1.4.5.[39] Following an induction period with **7a,** B_2Pin_2 and dtbpy, pre-catalyst **7b** is formed. Reversible dissociation of cyclooctene (COE) from **7b**, results in formation of the co-ordinatively unsaturated 16 electron active catalyst **7c**. Oxidative addition of arene to **7c**, yields **8** and subsequent reductive elimination of Ar-BPin results in formation of an iridium(III) hydride complex **(9)**. Further oxidative addition of either B_2Pin_2 or HBPin (formed *in situ*) to **10** and an ensuing reductive elimination producing HBPin or H_2, facilitates regeneration of the active catalyst **(7)**.

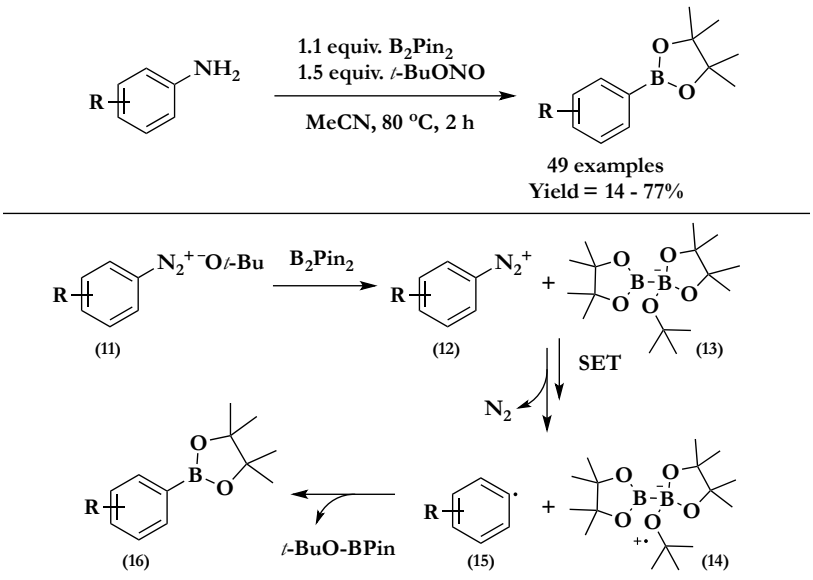


Scheme 1.4.5: Iridium catalysed C-H borylation of arenes

1.4.1.4 Metal free borylation

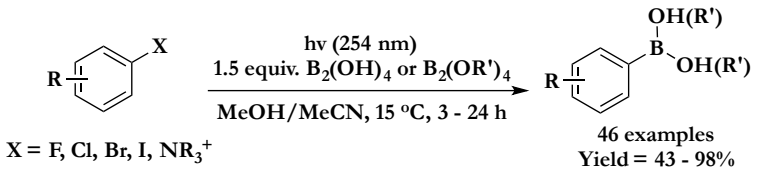
The exploration of metal-free reactions toward the construction of aryl boranes is an emerging branch of organic synthesis, where the use of heavy metals, expensive air sensitive catalysts and ligands can potentially be avoided.[40-45]

Wang[46,47] presented an elegant metal-free borylation of aromatic amines for construction of arylboronic esters (Scheme 1.4.6). The reaction is based on a Sandmeyer-type transformation where diazotisation of the arylamine starting material facilitates aromatic borylation from B_2Pin_2. The broad applicability and utility of this reaction was demonstrated on forty-nine representative examples. In addition, this transformation facilitates sequential borylation and Suzuki cross-coupling with iodobenzene. The sequential one-pot coupling was successfully performed on seventeen substrates in moderate to high yields (20-71%). Mechanistically the authors propose a single electron transfer (SET) radical recombination pathway (Scheme 1.4.6). Initially a *tert*-butoxide anion reacts with B_2Pin_2 forming a tetra-coordinated boron complex (**13**). SET between **12** and **13** results in the formation of an aryl radical **(15)** *via* nitrogen extrusion. The aromatic boronic ester **(16)** is then formed by reaction of **14** with **15**.



Scheme 1.4.6: Synthesis of pinacol arylboronates from aromatic amines

Mfuh[48] recently reported a metal- and additive-free, photoinduced borylation of haloarenes and quaternary ammonium salts (Scheme 1.4.7). Facile production of aryl boronic esters and acids under mild reaction conditions was achieved. The utility of this important transformation was exemplified by a practical gram-scale synthesis of representative aromatic boronic acids (three examples 1.1 – 1.8 g, 68 – 86% yield).



Scheme 1.4.7: Metal- and additive-free, photoinduced borylation of haloarenes and quaternary ammonium salts

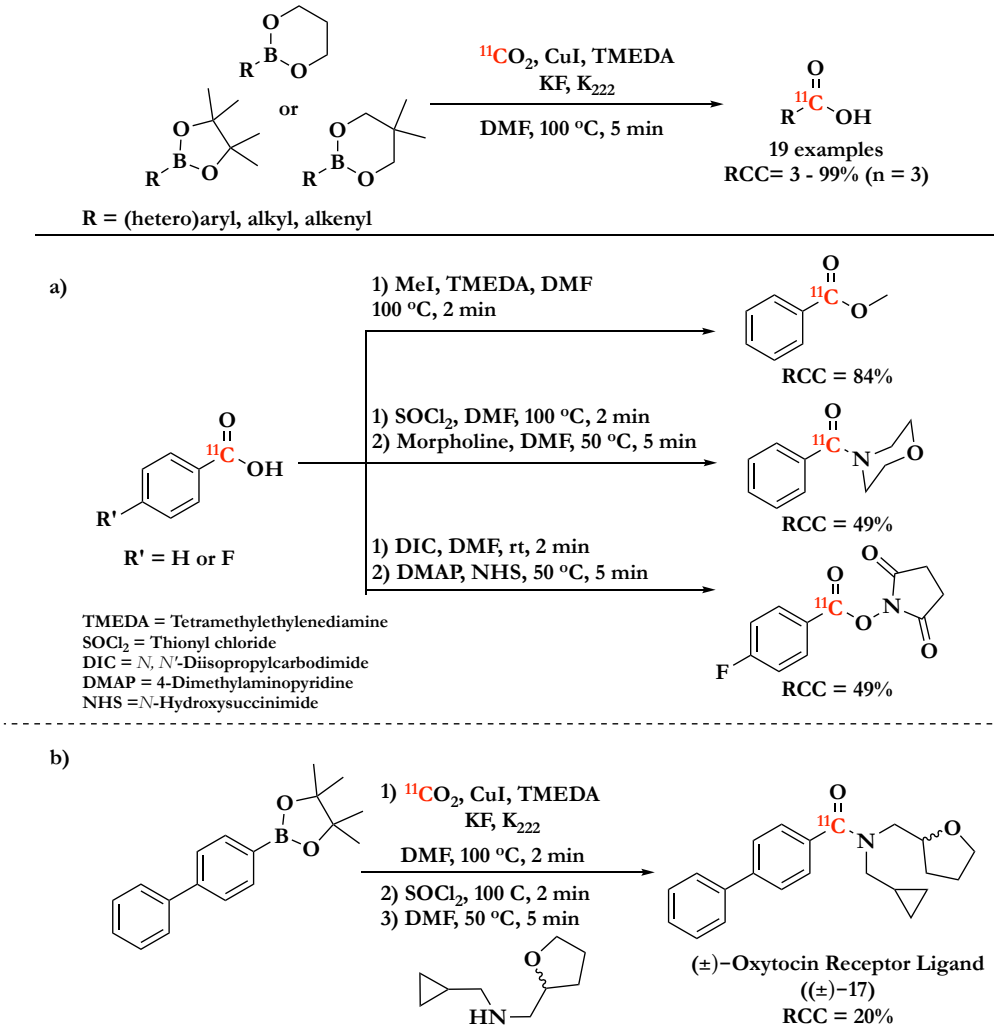
1.4.2 Application of aryl boranes as precursors for radiosynthetic incorporation

Arylboranes have found widespread application as synthetic precursors for a plethora of radiosynthetic transformations in the fields of PET and SPECT imaging. The following sections of this thesis will discuss the radiosynthesis of carbon-11, fluorine-18 and iodine-123 containing radioligands facilitated by arylborane chemistry.

An important note on radiosynthetic terminology is required before the proceeding sections. When discussing radiosynthesis, radiochemical reaction efficiency can be quantified by either radiochemical yield (RCY) or radiochemical conversion (RCC). In this thesis the term RCY will be used to refer to the total activity of isolated radiolabelled product, as a percentage of the starting activity of radioactive reagent. RCY may be decay corrected [d.c.] to time at start of synthesis, which negates total synthesis time, or may be non-decay corrected [n.d.c.]. The term RCC will be used to refer to the activity of a radiolabelled product as a percentage of the total activity at the end of the reaction and is by definition decay corrected. This is commonly quantified by radio-TLC and radio-HPLC.

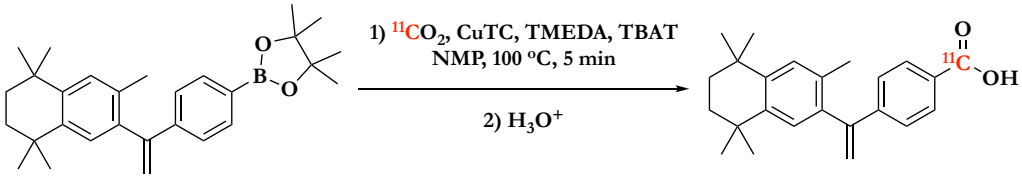
1.4.2.1 Carbon-11 incorporation from aryl boranes

In 2012 Pike[49] reported the direct carboxylation of various boronic esters under subatmospheric partial pressures of $^{11}CO_2$ (Scheme 1.4.8). Various (hetero)aryl, alkyl and alkenyl moieties were labelled, demonstrating the versatility of the reaction. However, observed RCCs tended to be lower with electron-poor substrates. Further derivatisation of the aryl carboxylation products to aromatic esters and amides, was achieved in moderate to high RCCs (Scheme 1.4.8 a)). The utility of this transformation was exemplified *via* one-pot synthesis of an oxytocin receptor ligand ((±)-17) in 20% RCC in a total synthesis time of 43 minutes from radionuclide production. (Scheme 1.4.8 b)).



Scheme 1.4.8: Cu-mediated carboxylation of boronic esters with [^{11}C]CO_2. a) Conversion of carboxylic acids to esters and amides. b) Radiosynthesis of oxytocin receptor ligand ((±)-17)

Vasdev[50] applied the copper-mediated carboxylation to the synthesis of [^{11}C]bexarotene (**18**), a retinoid X receptor agonist, applicable toward the treatment of T cell lymphoma.[51] **18** was synthesised in 15 ± 2% (n = 3) RCY [n.d.c] based on $^{11}CO_2$. Preliminary PET imaging studies with **18** in a non-human primate resulted in modest brain uptake (standardised uptake value = 0.8)[††] in regions with retinoid X receptor expression.

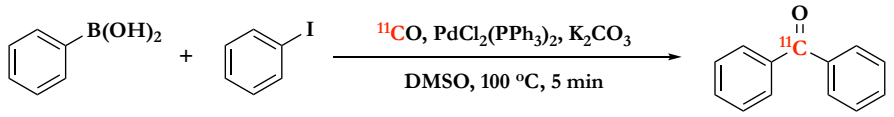


(18)
RCY = 15 ± 2 % (n = 3) [n.d.c]

CuTC = Copper thiophene-2-carboxylate
TBAT = Tetrabutylammoniumdifluorotriphenylsilicate
NMP = *N*-Metyhl-2-pyrrolidone

Scheme 1.4.9: Radiosynthesis of 18 *via* copper-mediated carboxylation

In 1997 Zeisler[52] presented the synthesis of carbon-11 labeled benzophenone (**19**) *via* carbonylative Suzuki cross-coupling reaction. **19** was synthesised in 69% RCY and >99% radiochemical purity (RCP) (Scheme 1.4.10).



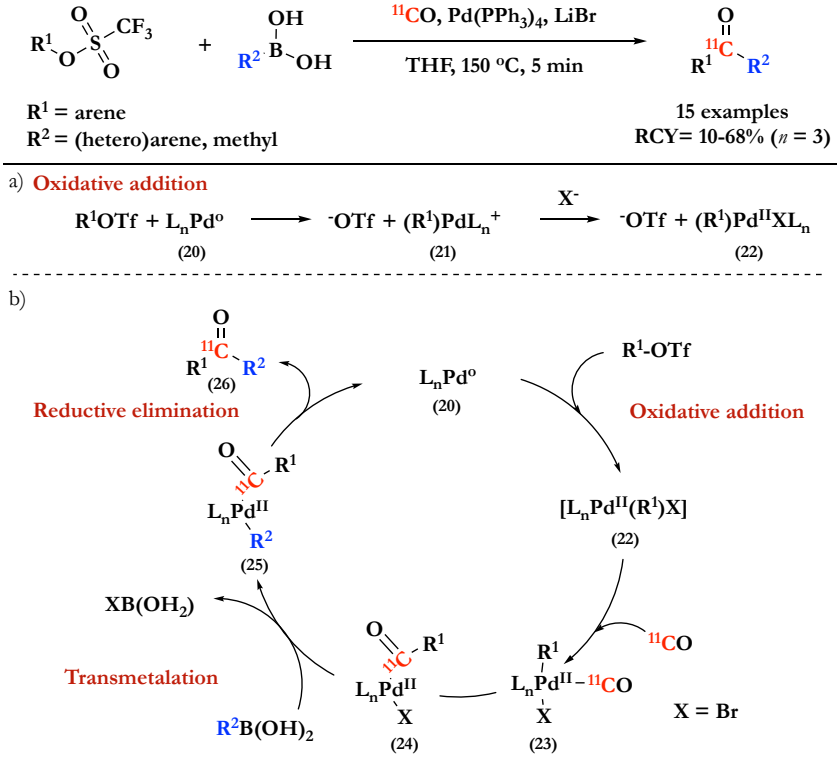
(19)
SA = 33.3 GBq/μmol
RCY = 69% [d.c] (n = 3)

Scheme 1.4.10: ^{11}C carbonylative Suzuki cross-coupling reaction

In an extension of this methodology, Raman and co-workers[53] coupled aryl triflates, with aryl and methylboronic acids, under low [^{11}C]CO concentration (10^{-5}M), to access 15 different radiolabelled ketones (Scheme 1.4.11). The reaction was heated to 150 °C for five minutes *via* micro-autoclave (200 μl). Products were obtained in 10–68% RCY [d.c] in high SA (150–640 GBq/μmol) and RCP (>98%).

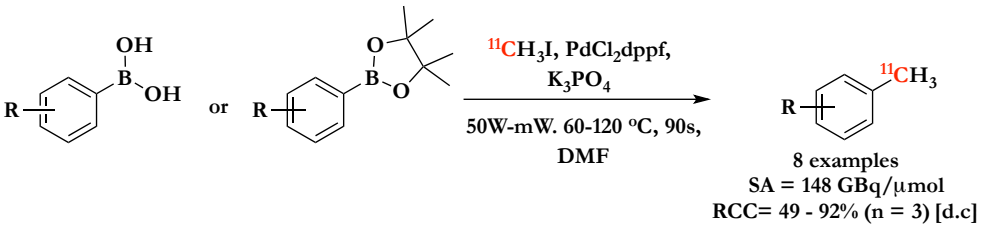
†† Standardised uptake value is the ratio of tissue radioactivity at a point in time C(T) over the injected dose of radioactivity per kilogram of body weight i.e. C(T)/[injection dose (MBq)/subject weight (kg)]

A potential catalytic cycle for this transformation is shown in Scheme 1.4.11. Initially, the oxidative addition of an aryl triflate (R^1-OTf) to **20** produces a cationic (aryl)palladium complex **(21)** (Scheme 1.4.11 a)).[54] **21** then reacts with excess halide (from lithium bromide) to form a neutral palladium species **(22)** *in situ*. Subsequent ^{11}CO coordination and 1,1 insertion to form **24**, is followed by transmetalation and reductive elimination to yield the desired ketone **(26)** (Scheme 1.4.11 b)).



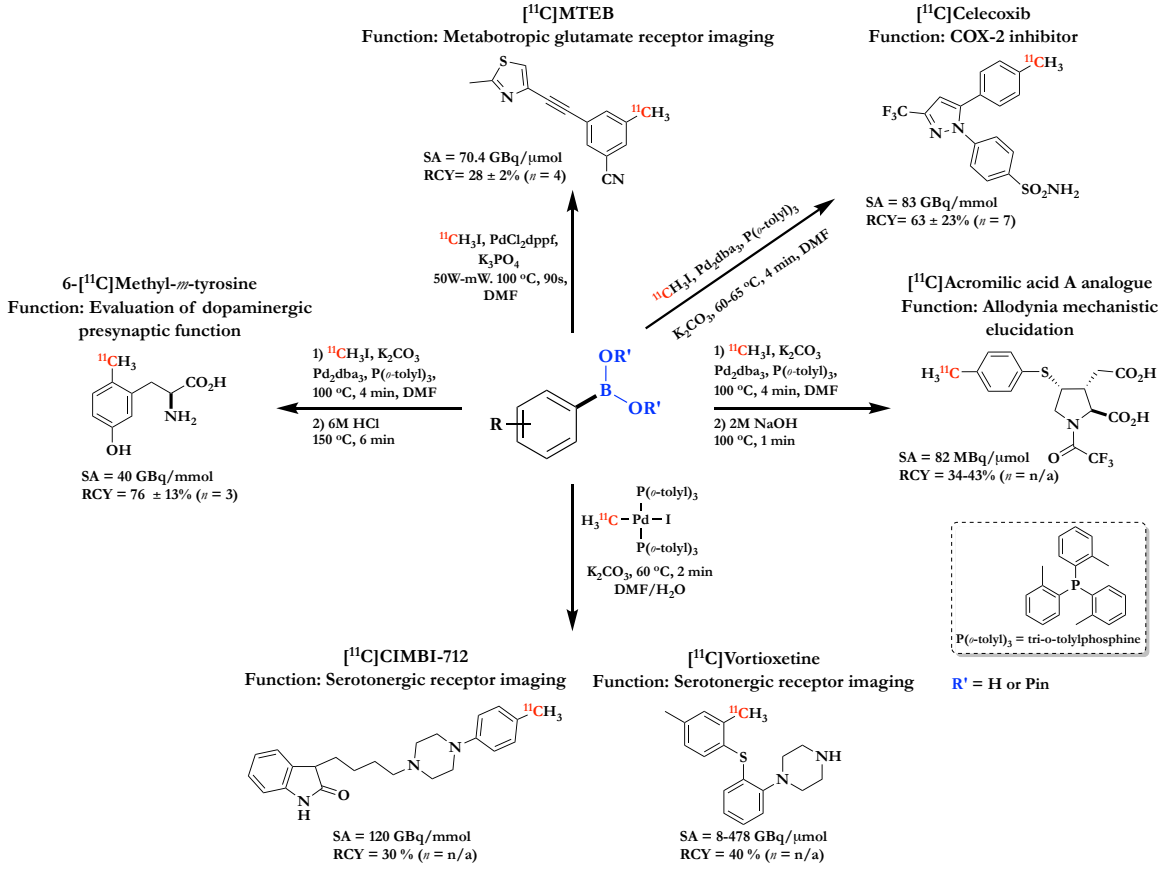
Scheme 1.4.11: ^{11}C carbonylative Suzuki cross-coupling reaction *via* aryl triflates

Although ^{11}C-methyl iodide ($^{11}CH_3I$) is the most frequently utilised synthon in modern carbon-11 radiosynthesis,[14] reported transformations between $^{11}CH_3I$ and arylboranes have been limited to the palladium-catalysed Suzuki reaction. An initial report by Hostetler[55] in 2005, disclosed the synthesis of ^{11}C-labelled functionalised toluene derivatives from the corresponding aryl boronic acids and esters (Scheme 1.4.12). Products were isolated in modest to high RCYs (56–92%), with high SA (148 GBq/μmol) and RCP (>95%), in less than 20 minutes succeeding production of $^{11}CH_3I$.



Scheme 1.4.12: Synthesis of ^{11}C-labelled functionalised toluene derivatives

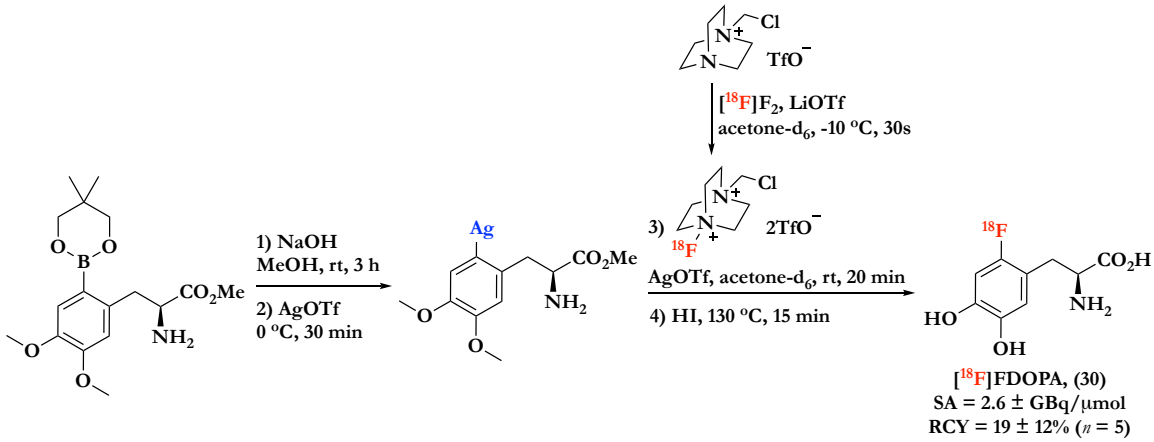
Since its inception by Hostetler,[55] the palladium-mediated Suzuki ^{11}C-methylation has found widespread utility toward the construction of a plethora of biologically important radioligands. Scheme 1.4.13 details a synthetic summary of selected radiotracers accessed *via* this methodology.[56-61]



Scheme 1.4.13: Synthesis and structures of selected radiotracers accessed *via* Suzuki ^{11}C-methylation

1.4.2.2 Fluorine-18 incorporation from arylboranes

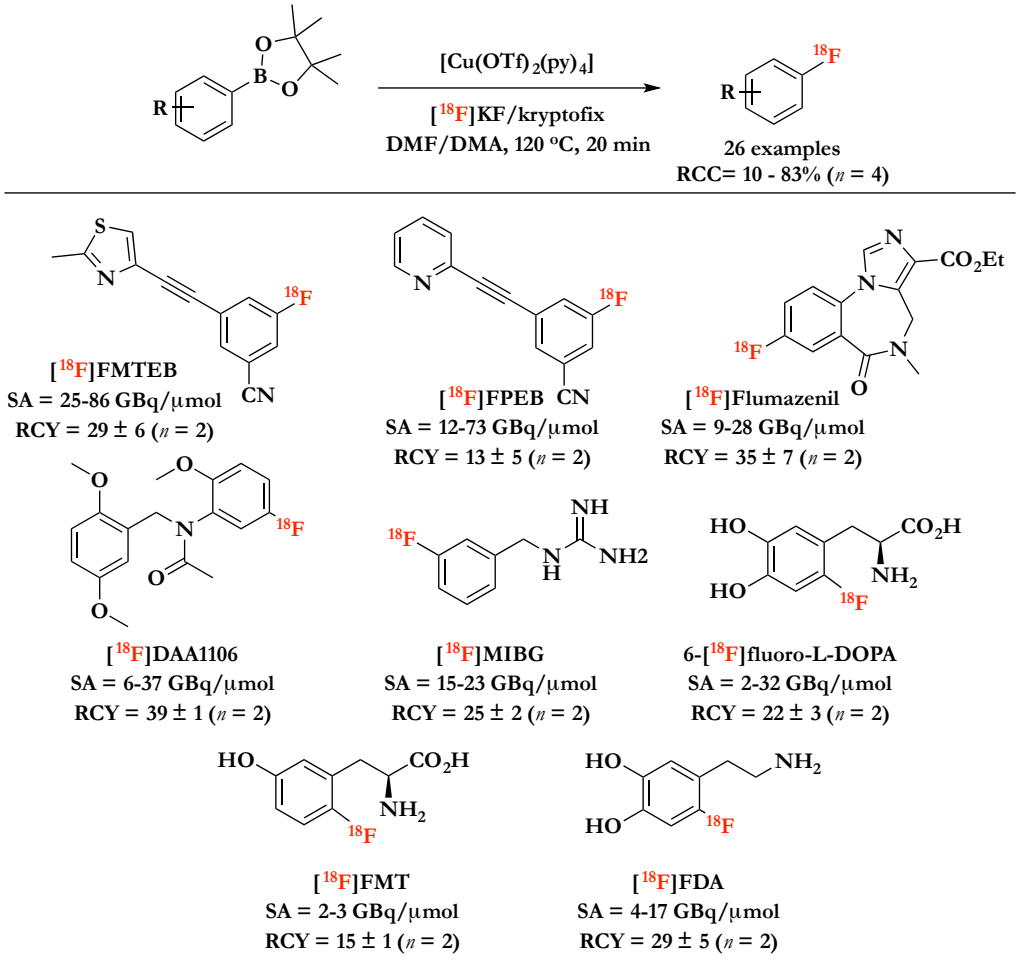
In 2013, Solin and Gouverneur[62] reported the silver-mediated electrophilic radiofluorination of an aryl boronic ester using [^{18}F]selectfluor® bis(triflate).



Scheme 1.4.14: Electrophilic radiofluorination toward 6-[^{18}F]fluoro-L-DOPA

6-[^{18}F]fluoro-L-DOPA, a radioligand typically utilised to study the dopaminergic system,[63] was synthesised in 19 ± 12% RCY with a specific activity of 2.6 GBq/μmol (Scheme 1.4.14). In 2014, Gouverneur[64] developed the first copper-mediated nucleophilic radiofluorination of (hetero)aryl boronic esters. This methodology facilitated access to a host of electron-rich (hetero)arenes from shelf-stable non-toxic precursors in modest to high RCCs. The reaction's utility was exemplified in a later publication,[65] with the production and isolation of eight clinically important radioligands (Scheme 1.4.15). This protocol was validated on two additional synthetic platforms, indicating its potential for broad application in PET.‡‡ Further utilisation of this methodology will be detailed in the proceeding chapters of this thesis.

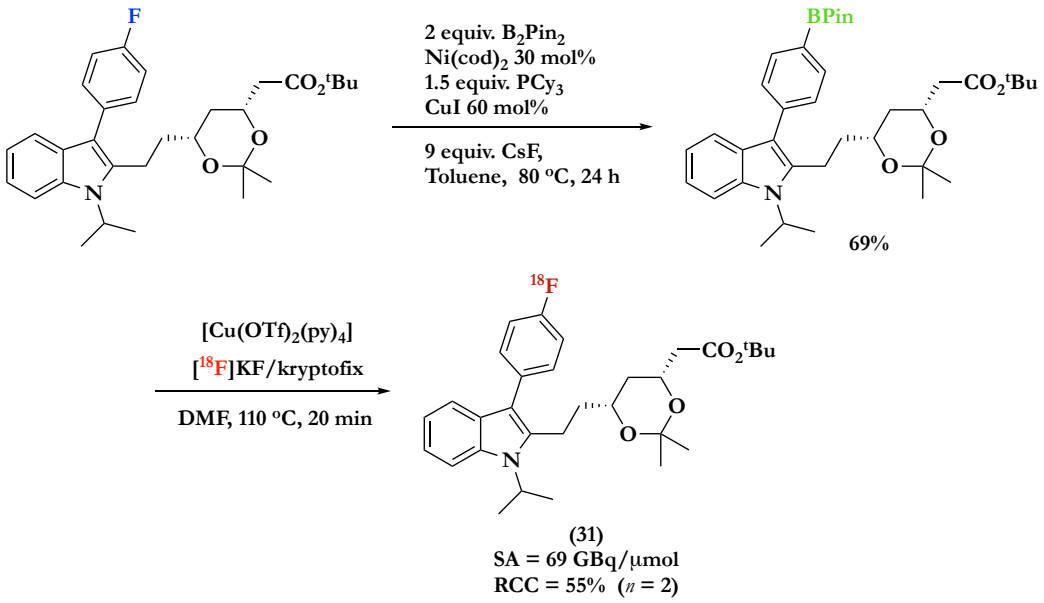
‡‡ During the course of writing this thesis further work on the radiofluorination of (hetero)aryl boronic esters was published.[66]



Scheme 1.4.15: Copper-mediated nucleophilic radiofluorination of (hetero)aryl boronic esters

Sanford and Scott[67] have recently disclosed an analogous procedure for the ^{18}F-fluorination of aryl boronic acids. The substrate scope and functional group tolerance of this transformation are similar to those observed by Gouverneur.[64,65]

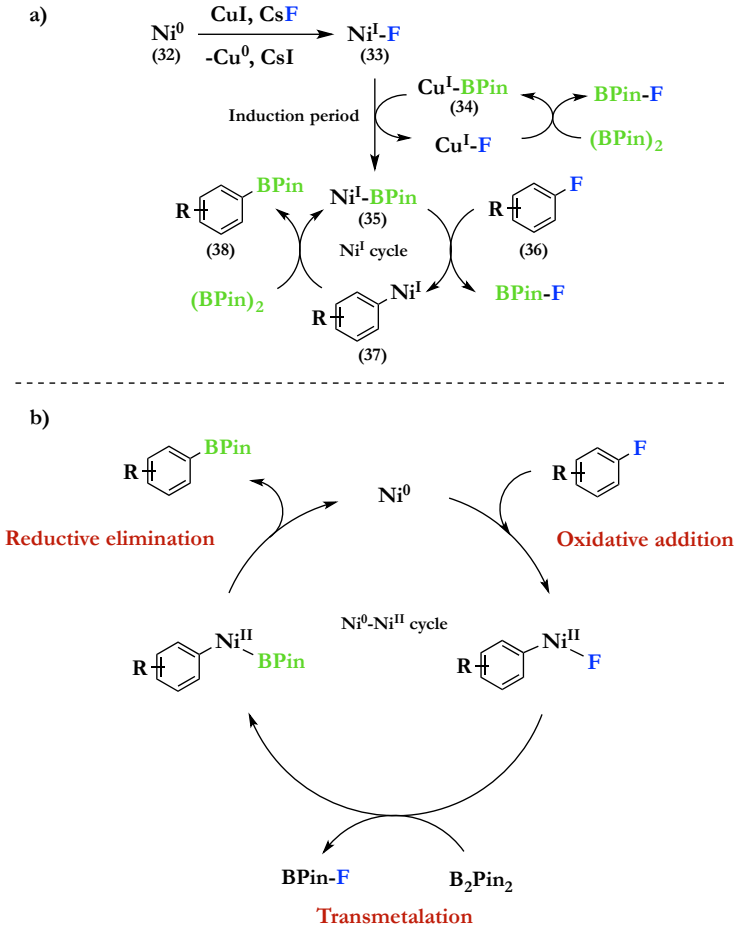
In 2015 Hosoya[68] developed a nickel-catalyzed defluoroborylation of fluoroarenes. This methodology facilitated a net two-step isotope exchange *via* an arylboronate, toward the synthesis of [^{18}F]dihydrofluvastin **(31)** (Scheme 1.4.16).



Scheme 1.4.16: Nickel-Catalyzed Defluoroborylation of Fluoroarenes

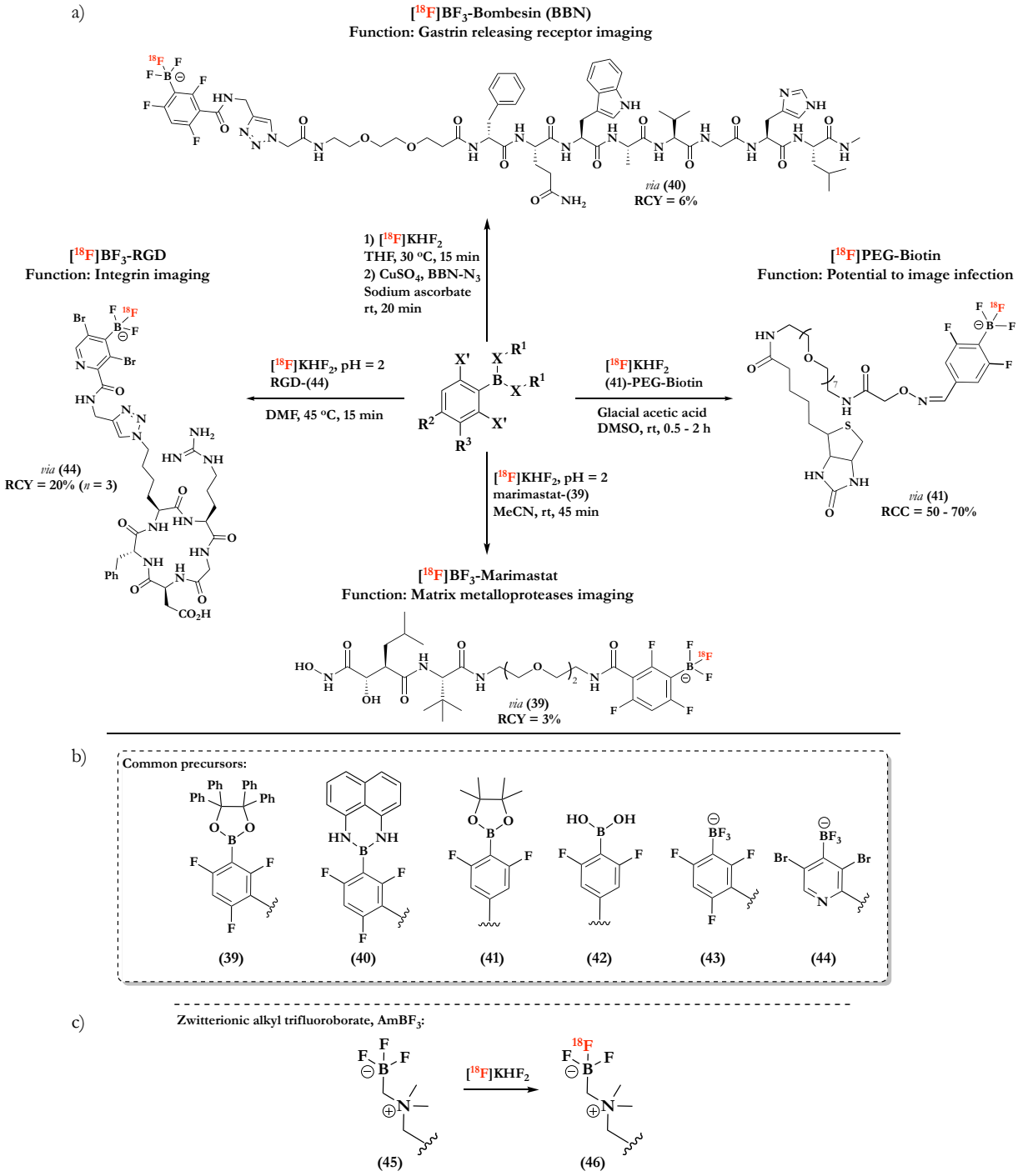
Details of two potential reaction mechanisms for the defluoroborylation of aryl fluorides are outlined in Scheme 1.4.17. The first mechanistic pathway proposed (Scheme 1.4.17 a)), proceeds *via* Ni(I) active catalyst **(35)**. Initially, Ni(I) fluoride **(33)** is formed *via* one-electron oxidation of a Ni(0) complex **(32)** with CuI.[69] Transmetalation of **33** with a borylcopper species **(34)** (formed *in-situ*), yields borylnickel(I) complex **35.** The ensuing C-F bond cleavage of fluoroarene **(36)** *via* **35,** is succeeded by borylation of Ni(I) complex **37** with B_2Pin_2. This ultimately affords the desired product **(38)**. Scheme 1.4.17 b) details a conventional cross-coupling mechanistic pathway, where C-F bond cleavage is facilitated by oxidative addition. Although the exact role of the copper iodide in this mechanism needs to be elucidated, experimental evidence disclosed by Hosoya[68] revealed that defluoroborylation does not proceed with electron-deficient arenes.[§§] Therefore this conventional cross-coupling mechanism seems less plausible.

[§§] Electron-deficient arenes are the preferred substrates for oxidative addition of C-X bonds.[70]



Scheme 1.4.17 Two potential mechanisms for nickel-mediated defluoroborylation

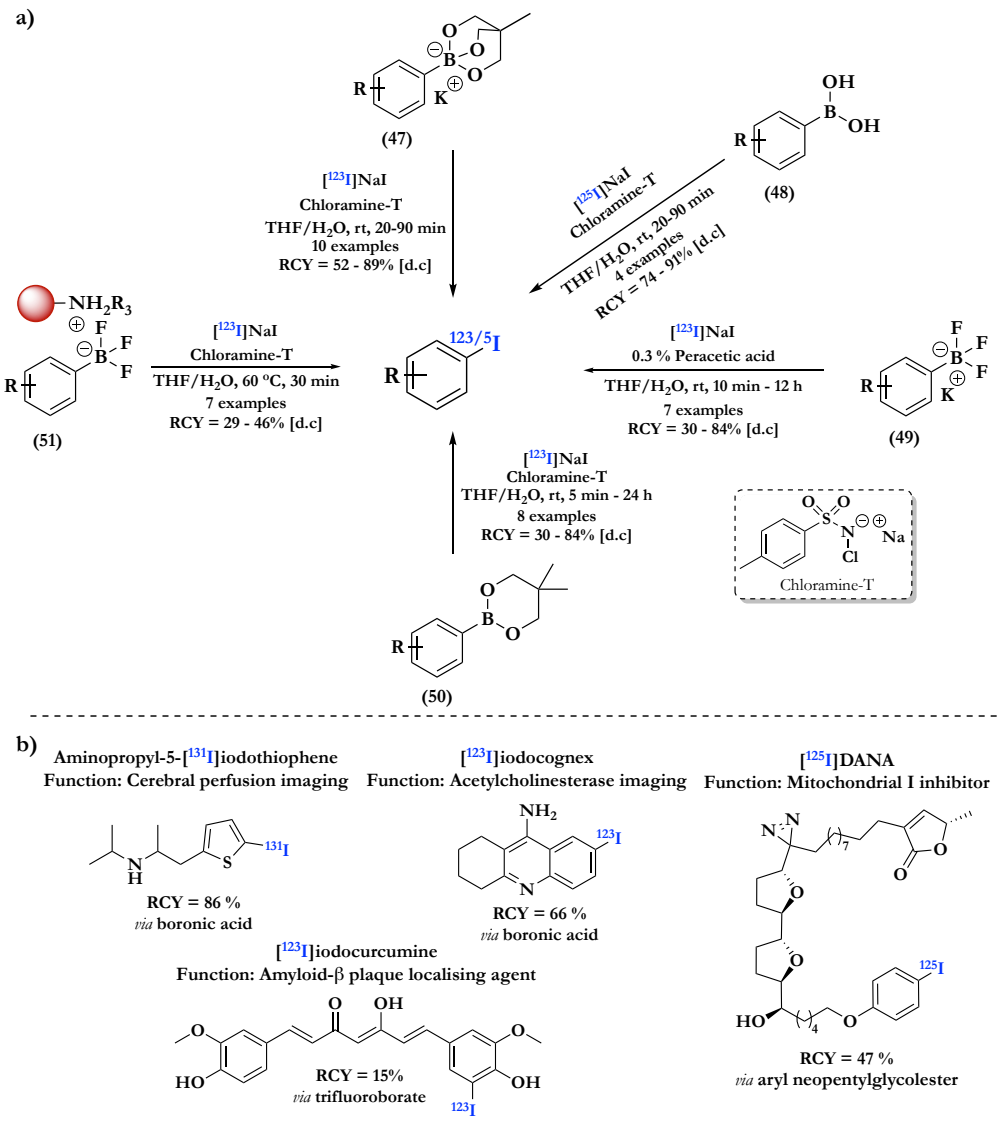
The direct labeling of arylboranes with nucleophilic [^{18}F]fluoride to yield [^{18}F]aryltrifluoroborates was developed in 2005 by Perrin.[71] Since its inception, this methodology has found widespread utility toward the radiosynthesis of a plethora of biomolecules (Scheme 1.4.18).[72-76] However, limitations associated with their solvolytic stability and the advent of a more stable zwitterionic alkyl [^{18}F]trifluoroborate **(46)**,[77,78] has precluded the need for labelled aromatic [^{18}F]trifluoroborates. As a consequence, current preclinical work predominantly involves the use of **46**.[76,79,80]



Scheme 1.4.18: a) Radiosynthesis of [^{18}F]aryltrifluoroborate containing biomolecules. b) Common aryl precursors employed for direct ^{18}F-aryltrifluoroborylation. c) Synthesis of increasingly stable zwitterionic alkyl [^{18}F]trifluoroborate (46).

1.4.2.3 Iodine-123 incorporation from aryl boranes

Kabalka and co-workers have disclosed the *ipso* electrophilic radioiodination of aryl potassium (hetero)aryltriolborates **(47)**,[81] boronic acids **(48)**,[82] trifluoroborate salts **(49)**,[83] neopentyl glycol boronate esters **(50)**[84] and polymer-supported organotrifluoroborates **(51)**[83] in the presence of chloramine-T (Scheme 1.4.19 a)).[***]



Scheme 1.4.19: Kabalka electrophilic radioiodination

[***] Radioiodination from aryl boranes has been successfully realised for iodine-123, 125 and 131. Each isotope is made available as an aqueous solution of the iodide and hypoiodite in dilute sodium hydroxide (**section 1.3.1**).[21] Therefore, radioincorporation with one of the aforementioned isotopes theoretically facilitates the installation of all three isotopes.

This methodology has been successfully utilised to access radioligands containing complex molecular scaffolds (Scheme 1.4.19 b)).[85-88] However, this radiochemistry has not been broadly implemented, potentially owing to limitations associated with the labeling of electron deficient precursors.

1.5 Thesis outline

This thesis is concerned with the application of aryl boronic esters to the fields of PET and SPECT synthetic radiochemistry.

In **chapter 2**, a general method for the copper mediated nucleophilic ^{123}I-iodination of (hetero)aryl boronic pinacol esters and acids is disclosed. This methodology was applied to the radiosynthesis of four commonly used SPECT radiotracers, [^{123}I]DPA-713, [^{123}I]IMPY, [^{123}I]MIBG and [^{123}I]IPEB.

In **chapter 3**, the copper-mediated nucleophilic ^{18}F-fluorination of aryl boronic pinacol esters,[64] developed in the Gouverneur group, has been applied to the field of prosthetic group ^{18}F-radiochemistry.

Chapter 4 describes the radiosynthesis and biological evaluation of [^{18}F]DPA-713 and [^{18}F]CF_3DPA-713, two novel analogues of the Translocator Protein (TSPO) ligand N,N-diethyl-2-(4-methoxyphenyl)-5,7-dimethylpyrazolo[1,5-a]pyrimidine-3-acetamide-713 (DPA-713).

Finally, **chapter 5** details experimental procedures and characterisation for all compounds.

1.6 References

(1) James, M. L.; Gambhir, S. S. *Physiol. Rev.* **2012**, *92* (2), 897–965.
(2) Willmann, J. K.; van Bruggen, N.; Dinkelborg, L. M.; Gambhir, S. S. *Nat. Rev. Drug Discovery* **2008**, *7* (7), 591–607.
(3) Massoud, T. F.; Gambhir, S. S. *Genes. Dev* **2003**, 545–580.
(4) Cherry, S. R. *Semin. Nucl. Med.* **2009**, *39* (5), 348–353.
(5) Riola-Parada, C.; García-Cañamaque, L.; Pérez-Dueñas, V.; Garcerant-Tafur, M.; Carreras-Delgado, J. L. *Revista Española de Medicina Nuclear e Imagen Molecular (English Edition)* **2016**, *35* (5), 306–312.
(6) Matthews, P. M.; Rabiner, E. A.; Passchier, J.; Gunn, R. N. *Br. J. Clin. Pharma.* **2012**, *73* (2), 175–186.
(7) Miller, P. W.; Long, N. J.; Vilar, R.; Gee, A. D. *Angew. Chem. Int. Ed.* **2008**, *47* (47), 8998–9033.
(8) Pimlott, S. L.; Sutherland, A. *Chem. Soc. Rev.* **2011**, *40* (1), 149–162.
(9) McQuade, P.; Rowland, D. J.; Lewis, J. S.; Welch, M. J. *Curr. Med. Chem.* **2005**, *12* (7), 807–818.
(10) Ter-Pogossian, M. M.; Herscovitch, P. *Semin. Nucl. Med.* **1985**, *15* (4), 377–394.
(11) *Positron Emission Tomography*; Bailey, D. L., Townsend, D. W., Valk, P. E., Maisey, M. N., Eds.; Springer-Verlag: London, 2005.
(12) Ametamey, S. M.; Honer, M.; Schubiger, P. A. *Chem. Rev.* **2008**, *108* (5), 1501–1516.
(13) Ferrieri, R. A.; Wolf, A. P. *Radiochemica Acta* **1983**, *34* (1-2), 69.
(14) Scott, P. J. H. *Angew. Chem. Int. Ed.* **2009**, *48* (33), 6001–6004.
(15) Nickles, R. J.; Hichwa, R. D.; Daube, M. E.; Hutchins, G. D.; Congdon, D. D. *Int. J. App. Rad. Iso.* **1983**, *34* (3), 625–629.
(16) Bergman, J.; Solin, O. *Nucl. Med. Biol.* **1997**, 677–683.
(17) *Handbook of Radiopharmaceuticals*; Welch, M. J., Redvanly, C. S., Eds.; John Wiley & Sons, Ltd: Chichester, UK, 2005.
(18) Coenen, H. H. In *Synthesis and applications of isotopically labelled compounds 1988*; 1989.
(19) Coenen, H. H.; Schüller, M.; Stöcklin, G.; Klatte, B.; Knöchel, A. *J. Labelled Compd. Radiopharm.* **1986**, *23* (5), 455–466.
(20) Bourguignon, M. H.; Pauwels, E. K.; Loc'h, C.; Mazière, B. *Eur. J. Nucl. Med.* **1997**, *24* (3), 331–344.
(21) Adam, M. J.; Wilbur, D. S. *Chem. Soc. Rev.* **2005**, *34* (2), 153–11.
(22) Miyaura, N.; Suzuki, A. *Chem. Rev.* **1995**, *95*, 2457–2483.
(23) Lennox, A. J. J.; Lloyd-Jones, G. C. *Chem. Soc. Rev.* **2014**, *43* (1), 412–443.
(24) Khotinsky, E.; Melamed, M. *Eur. J. Inorg. Chem.* **1909**, *42* (3), 3090–3096.
(25) Letsinger, R. L.; Skoog, I. H. *J. Org. Chem.* **1953**, *18* (7), 895-897.
(26) Chow, W. K.; Yuen, O. Y.; Choy, P. Y.; So, C. M.; Lau, C. P.; Wong, W. T.; Kwong, F. Y. *RSC Adv.* **2013**, *3* (31), 12518–12539.
(27) Nagashima, Y.; Takita, R.; Yoshida, K.; Hirano, K.; Uchiyama, M. *J. Am. Chem. Soc.* **2013**, *135* (50), 18730–18733.
(28) Ishiyama, T.; Murata, M.; Miyaura, N. *J. Org. Chem.* **1995**, 7508–7510.
(29) Takagi, J.; Takahashi, K.; Ishiyama, T.; Miyaura, N. *J. Am. Chem. Soc.* **2002**, *124* (27), 8001–8006.
(30) Miyaura, N.; Ishiyama, T.; Sasaki, H.; Ishikawa, M.; Sato, M, Suzuki, Akira. *J. Am. Chem. Soc.* **1989**, *111* (1). 314-321.
(31) Molander, G. A.; Trice, S. L. J.; Dreher, S. D. *J. Am. Chem. Soc.* **2010**, *132* (50), 17701–17703.

(32) Molander, G. A.; Trice, S. L. J.; Kennedy, S. M.; Dreher, S. D.; Tudge, M. T. *J. Am. Chem. Soc.* **2012**, *134* (28), 11667–11673.
(33) Kinzel, T.; Zhang, Y.; Buchwald, S. L. *J. Am. Chem. Soc.* **2010**, *132* (40), 14073–14075.
(34) Mkhalid, I. A. I.; Barnard, J. H.; Marder, T. B.; Murphy, J. M.; Hartwig, J. F. *Chem. Rev.* **2010**, *110* (2), 890–931.
(35) Hartwig, J. F. *Acc. Chem. Res.* **2012**, *45* (6), 864–873.
(36) Cho, J.-Y.; Tse, M. K.; Holmes, D.; Maleczka, R. E.; Smith, M. R. *Science* **2002**, *295* (5553), 305–308.
(37) Ishiyama, T.; Takagi, J.; Ishida, K.; Miyaura, N.; Anastasi, N. R.; Hartwig, J. F. *J. Am. Chem. Soc.* **2002**, *124* (3), 390–391.
(38) Ishiyama, T.; Takagi, J.; Hartwig, J. F.; Miyaura, N. *Angew. Chem.* **2002**, *114* (16), 3182–3184.
(39) Boller, T. M.; Murphy, J. M.; Hapke, M.; Ishiyama, T.; Miyaura, N.; Hartwig, J. F. *J. Am. Chem. Soc.* **2005**, *127* (41), 14263–14278.
(40) Yamamoto, E.; Izumi, K.; Horita, Y.; Ito, H. *J. Am. Chem. Soc.* **2012**, *134* (49), 19997–20000.
(41) Zhang, J.; Wu, H. H.; Zhang, J.; Zhang, J. *Eur. J. Org. Chem.* **2013**, *2013* (28), 6263–6266.
(42) Yamamoto, E.; Izumi, K.; Horita, Y.; Ukigai, S.; Ito, H. *Top. Catal.* **2014**, *57* (10-13), 940–945.
(43) Légaré, M.-A.; Courtemanche, M.-A.; Rochette, É.; Fontaine, F.-G. *Science* **2015**, *349* (6247), 513–516.
(44) Chen, K.; Cheung, M. S.; Lin, Z.; Li, P. *Org. Chem. Front.* **2016**, *3* (7), 875–879.
(45) Chernichenko, K.; Lindqvist, M.; Kótai, B.; Nieger, M.; Sorochkina, K.; Pápai, I.; Repo, T. *J. Am. Chem. Soc.* **2016**, *138* (14), 4860–4868.
(46) Mo, F.; Jiang, Y.; Qiu, D.; Zhang, Y.; Wang, J. *Angew. Chem. Int. Ed.* **2010**, *49* (10), 1846–1849.
(47) Qiu, D.; Jin, L.; Zheng, Z.; Meng, H.; Mo, F.; Wang, X.; Zhang, Y.; Wang, J. *J. Org. Chem.* **2013**, *78* (5), 1923–1933.
(48) Mfuh, A. M.; Doyle, J. D.; Chhetri, B.; Arman, H. D.; Larionov, O. V. *J. Am. Chem. Soc.* **2016**, *138*, 2985–2988.
(49) Riss, P. J.; Lu, S.; Telu, S.; Aigbirhio, F. I.; Pike, V. W. *Angew. Chem. Int. Ed.* **2012**, *51* (11), 2698–2702.
(50) Rotstein, B. H.; Hooker, J. M.; Woo, J.; Collier, T. L.; Brady, T. J.; Liang, S. H.; Vasdev, N. *ACS Med. Chem. Lett.* **2014**, *5* (6), 668–672.
(51) Rotstein, B. H.; Placzek, M. S.; Krishnan, H. S.; Pekošak, A.; Collier, T. L.; Wang, C.; Liang, S. H.; Burstein, E. S.; Hooker, J. M.; Vasdev, N. *Mol. Imaging* **2016**, *15* (0), 1–5.
(52) Zeisler, S. K.; Nader, M.; Theobald, A.; Oberdorfer, F. *Appl. Radiat. Isot.* **1997**, *48* (8) 1091–1095.
(53) Rahman, O.; Kihlberg, T.; Långström, B. *Eur. J. Org. Chem.* **2004**, *2004* (3), 474–478.
(54) Jutand, A.; Mosleh, A. *Organometallics* **1995**, *14* (4), 1810–1817.
(55) Hostetler, E. D.; Terry, G. E.; Donald Burns, H. *J. Labelled Compd. Radiopharm.* **2005**, *48* (9), 629–634.
(56) Hamill, T. G.; Krause, S.; Ryan, C.; Bonnefous, C.; Govek, S.; Seiders, T. J.; Cosford, N. D. P.; Roppe, J.; Kamenecka, T.; Patel, S.; Gibson, R. E.; Sanabria, S.; Riffel, K.; Eng, W.; King, C.; Yang, X.; Green, M. D.; O'malley, S. S.; Hargreaves, R.; Burns, H. D. *Synapse* **2005**, *56* (4), 205–216.

(57) Doi, H.; Ban, I.; Nonoyama, A.; Sumi, K.; Kuang, C.; Hosoya, T.; Tsukada, H.; Suzuki, M. *Chem.- Eur. J.* **2009**, *15* (16), 4165–4171.
(58) Kanazawa, M.; Furuta, K.; Doi, H.; Mori, T.; Minami, T.; Ito, S.; Suzuki, M. *Bioorg. Med. Chem. Lett.* **2011**, *21* (7), 2017–2020.
(59) Kanazawa, M.; Ohba, H.; Iwazaki, A.; Kakiuchi, T.; Tsukada, H. *Bioorg. Med. Chem. Lett.* **2015**, *23* (4), 729–734.
(60) Andersen, V. L.; Herth, M. M.; Lehel, S.; Knudsen, G. M.; Kristensen, J. L. *Tetrahedron Lett.* **2013**, *54* (3), 213–216.
(61) Andersen, V. L.; Hansen, H. D.; Herth, M. M.; Knudsen, G. M.; Kristensen, J. L. *Bioorg. Med. Chem. Lett.* **2014**, *24* (11), 2408–2411.
(62) Stenhagen, I. S. R.; Kirjavainen, A. K.; Forsback, S. J.; Jørgensen, C. G.; Robins, E. G.; Luthra, S. K.; Solin, O.; Gouverneur, V. *Chem. Commun.* **2013**, *49* (14), 1386–1388.
(63) Rakshi, J. S.; Uema, T.; Ito, K.; Bailey, D. L.; Morrish, P. K.; Ashburner, J.; Dagher, A.; Jenkins, I. H.; Friston, K. J.; Brooks, D. J. *Brain* **1999**, *122* (9), 1637–1650.
(64) Tredwell, M.; Preshlock, S. M.; Taylor, N. J.; Gruber, S.; Huiban, M.; Passchier, J.; Mercier, J.; Génicot, C.; Gouverneur, V. *Angew. Chem. Int. Ed.* **2014**, *53* (30), 7751–7755.
(65) Preshlock, S.; Calderwood, S.; Verhoog, S.; Tredwell, M.; Huiban, M.; Hienzsch, A.; Gruber, S.; Wilson, T. C.; Taylor, N. J.; Cailly, T.; Schedler, M.; Collier, T. L.; Passchier, J.; Smits, R. X.; Mollitor, J.; Hoepping, A.; Mueller, M.; Génicot, C.; Mercier, J. X. L.; Gouverneur, V. X. R. *Chem. Commun.* **2016**, *52*, 8361–8364.
(66) Taylor, N.; Emer, E.; Preshlock, S.; Schedler, M.; Tredwell, M.; Verhoog, S.; Mercier, J.; Génicot, C.; Gouverneur, V. E. *J. Am. Chem. Soc.* **2017**, jacs.7b03131–jacs.7b03131.
(67) Mossine, A. V.; Brooks, A. F.; Makaravage, K. J.; Miller, J. M.; Ichiishi, N.; Sanford, M. S.; Scott, P. J. H. *Org. Lett.* **2015**, *17* (23), 5780–5783.
(68) Niwa, T.; Ochiai, H.; Watanabe, Y.; Hosoya, T. *J. Am. Chem. Soc.* **2015**, 14313–14318.
(69) Schwab, M. M.; Himmel, D.; Kacprzak, S.; Kratzert, D.; Radtke, V.; Weis, P.; Ray, K.; Scheidt, E.-W.; Scherer, W.; de Bruin, B.; Weber, S.; Krossing, I. *Angew. Chem. Int. Ed.* **2015**, *54* (49), 14706–14709.
(70) Tsou, T. T.; Kochi, J. K. *J. Am. Chem. Soc.* **1979**, 6319–6332.
(71) Ting, R.; Adam, M. J.; Ruth, T. J.; Perrin, D. M. *J. Am. Chem. Soc.* **2005**, *127* (38), 13094–13095.
(72) Smith, T. A. D.; Simpson, M.; Cheyne, R.; Trembleau, L. *Appl. Radiat. Isot.* **2011**, *69* (10), 1395–1400.
(73) Li, Y.; Ting, R.; Harwig, C. W.; auf dem Keller, U.; Bellac, C. L.; Lange, P. F.; Inkster, J. A. H.; Schaffer, P.; Adam, M. J.; Ruth, T. J.; Overall, C. M.; Perrin, D. M. *MedChemComm* **2011**, *2* (10), 942–949.
(74) Li, Y.; Liu, Z.; Harwig, C. W.; Pourghiasian, M.; Lau, J.; Lin, K.-S.; Schaffer, P.; Benard, F.; Perrin, D. M. *Am. J. Nucl. Med. Mol. Imaging* **2013**, *3* (1), 57–70.
(75) Liu, Z.; Hundal-Jabal, N.; Wong, M.; Yapp, D.; Lin, K. S.; Bénard, F.; Perrin, D. M. *MedChemComm* **2014**, *5* (2), 171–179.
(76) Bernard-Gauthier, V.; Bailey, J. J.; Liu, Z.; Wängler, B.; Wängler, C.; Jurkschat, K.; Perrin, D. M.; Schirrmacher, R. *Bioconjugate Chem.* **2016**, *27* (2), 267–279.
(77) Liu, Z.; Chao, D.; Li, Y.; Ting, R.; Oh, J.; Perrin, D. M. *Chem. - Eur. J.* **2015**, *21* (10), 3924–3928.

(78) Liu, Z.; Pourghiasian, M.; Radtke, M. A.; Lau, J.; Pan, J.; Dias, G. M.; Yapp, D.; Lin, K.-S.; Benard, F.; Perrin, D. M. *Angew. Chem. Int. Ed.* **2014**, *53* (44), 11876–11880.
(79) Lin, K.-S.; nard, F. C. O. B. E.; Pourghiasian, M.; Kiesewetter, D. O.; Liu, Z.; Perrin, D. M.; Chen, X. *Nat. Protoc.* **2015**, *10* (9), 1423–1432.
(80) Perrin, D. M. *Acc. Chem. Res.* **2016**, *49* (7), 1333–1343.
(81) Akula, M. R.; Yao, M.-L.; Kabalka, G. W. *J. Labelled Compd. Radiopharm.* **2010**, *54* (3), 132–134.
(82) Kabalka, G. W.; Sastry, K. A. R.; Muralidhar, K. *J. Labelled Compd. Radiopharm.* **1982**, *19* (6), 795–799.
(83) Kabalka, G. W.; Mereddy, A. R. *Nucl. Med. Biol.* **2004**, *31* (7), 935–938.
(84) Kabalka, G. W.; Akula, M. R.; Zhang, J. *Nucl. Med. and Biol.* **2002**, *29*, 841–843.
(85) Goodman, M.; Kabalka, G.; Marks, R.; Knapp, F. J.; Lee, J.; Liang, Y. *J. Med. Chem.* **1992**, *35*, 280–285.
(86) Akula, M. R.; Zhang, J. H.; Kabalka, G. W. *J. Labelled Comp. Radiopharm.* **2001**, *44*, 260–261.
(87) Yamamoto, S.; Abe, M.; Nakanishi, S.; Murai, M.; Miyoshi, H. *Tetrahedron Lett.* **2011**, *52* (24), 3090–3093.
(88) Kabalka, G. W.; Yao, M.-L. *J. Organomet. Chem.* **2009**, *694* (11), 1638–1641.

Chapter 2

Radiosynthesis of SPECT tracers *via* copper-mediated ^{123}I-iodination of (hetero)aryl boron reagents

2.1 Introduction

Iodine-123 is an isotope of iodine commonly incorporated into bio-active molecules for SPECT-CT imaging.[1,2] **Figure 2.1.1** shows some clinically relevant radiotracers containing an iodine-123 radioisotope.[3-7]

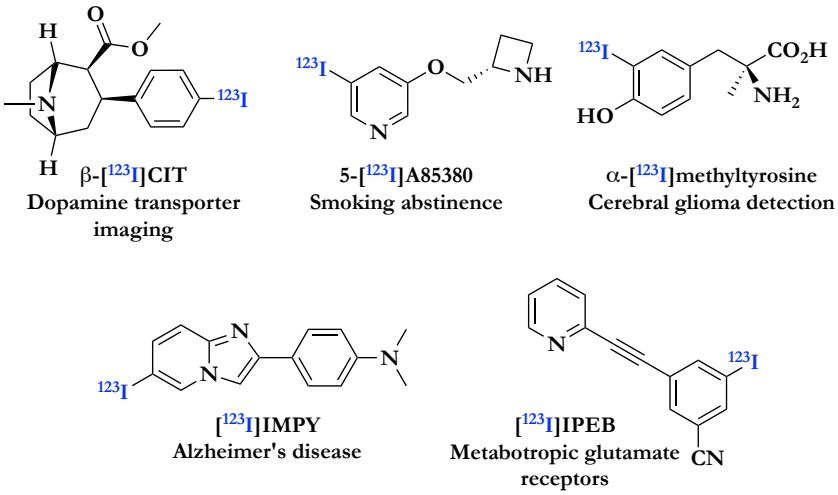
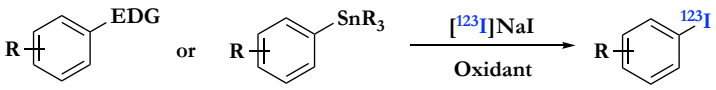


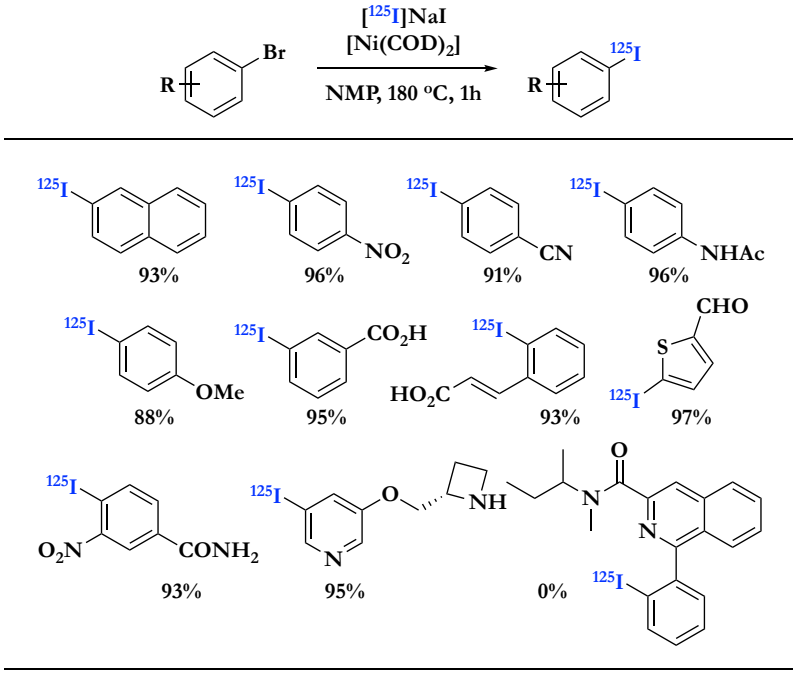
Figure 2.1.1: Commonly employed ^{123}I SPECT tracers

The two most conventional methods to synthesise SPECT tracers containing an iodoarene moiety are electrophilic aromatic substitution for electron rich arenes, or iododestannylation using [^{123}I]iodide and an external oxidant to form an "^{123}I^{+}" species *in situ*[1] (**Scheme 2.1.1**). Whilst oxidative iododestannylation of arylstannanes has facilitated direct radioiodination with high specific activity (SA) and radiochemical purity (RCP), organotin compounds are inherently toxic[8] and their use raises potential concerns relating to the presence of organotin residues in clinical preparations of radioiodinated imaging agents.



Scheme 2.1.1: Conventional methods toward aryl ^{123}I-iodination

To address this, alternative radiosynthetic methods have been developed.[9,10] For instance, in 2013 Sutherland[10] disclosed a nickel-mediated radioiodination of (hetero)aryl bromides using sodium [^{125}I]iodide ([^{125}I]NaI) (**Scheme 2.1.2**).

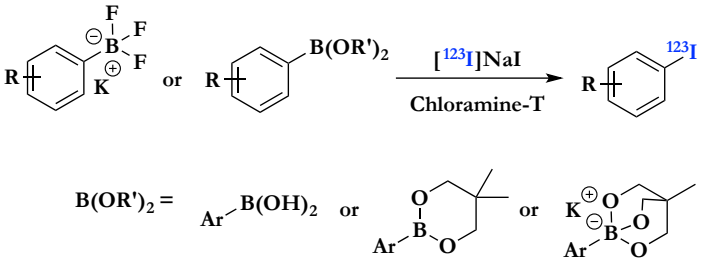


Scheme 2.1.2: Nickel-mediated radioiodination of (hetero)aryl bromides

This reaction employs $Ni(COD)_2$ an air-sensitive metal that requires an inert atmosphere and storage at 0 °C. The method has a large substrate scope and was successfully applied to the radiosynthesis of **5-[^{123}I]A85380**, a tracer used to image the α4β2 nicotinic acetylcholine receptor (nAChRs).[4] Starting with 74 MBq of activity, **5-[^{125}I]A85380** was isolated with a radiochemical yield (RCY) of 46 ± 8% (n = 3) and SA of 37 GBq/μmol. One limitation of this transformation is the labelling of sterically congested targets. Attempted radioiodination of **Br-PK11195** to yield **[^{125}I]PK11195** (a translocator protein ligand) was ineffective (**Scheme 2.1.2**). The authors suggest that the halogen exchange reaction with $Ni(COD)_2$ is potentially restricted by the steric environment associated with the *ortho* substituted bromo benzene of **Br-PK11195**.[10]

As discussed in **section 1.4.2.3**, Kabalka and co-workers have reported the electrophilic radioiodination of aryl boronic acids,[11] trifluoroborate salts,[12] potassium

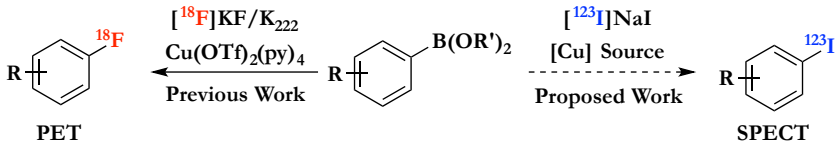
(hetero)aryltriolborates[13] and neopentyl glycol boronate esters[14] in the presence of [^{123}I]NaI and chloramine-T (**Scheme 2.1.3**). However, this radiochemistry has not been widely implemented, potentially owing to limitations associated with the labeling of electron deficient systems.



Scheme 2.1.3: Kabalka electrophilic aryl radioiodination

2.2 Aim of study

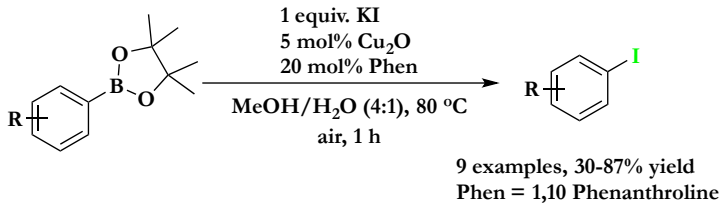
As mentioned previously (**section 1.4.2.2**), our group has disclosed the copper-mediated ^{18}F-fluorination of aryl boronic esters.[15,16] Here we saw an opportunity for expansion, firstly it was our aim to develop a novel radiosynthetic transformation that would enable the facile incorporation of both fluorine-18 and iodine-123 from a common aryl boronate precursor (**Scheme 2.2.1**).



Scheme 2.2.1: Proposed divergent radiosynthesis

This concept of divergent radiohalogenation could potentially advance the field of synthetic radiochemistry, facilitating the synthesis of either a PET or SPECT tracer from an identical starting material (**Scheme 2.2.1**). Secondly, we aimed to improve upon the conditions developed by Kabalka[17] (**Scheme 2.1.3**) by enabling the *ipso* radioiodination of electron-deficient arenes. In this context, a paper reported in 2013 by Hartwig,[18] a copper-mediated ^{127}I-iodination of aryl boronic esters (**Scheme 2.2.2**), served

as inspiration for our synthetic efforts toward the copper-mediated radioiodination of hetero(aryl) boranes using [^{123}I]NaI.



Scheme 2.2.2: Hartwig copper(I) oxide (Cu_2O) ^{127}I-iodination of aryl-Bpin

2.3 Preliminary Investigations

As a preliminary experiment, both Hartwig and Kabalka's protocols were repeated using [^{127}I]NaI with an array of electron rich and poor aryl-Bpin reaction partners **(Table 2.3.1).**

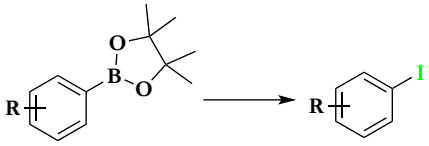
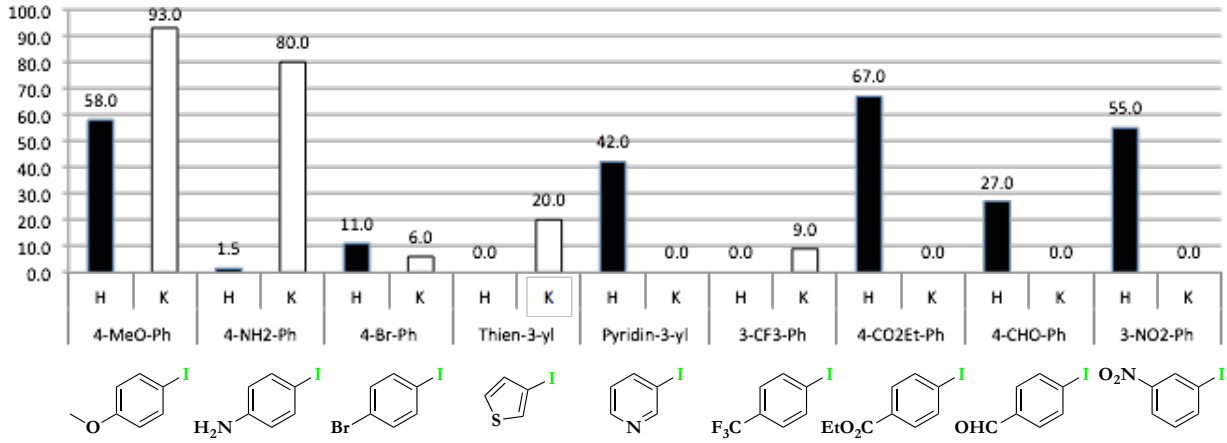


Table 2.3.1: Hartwig and Kabalka Iodination using [^{127}I]NaI

Hartwig (H): NaI 2eq, Cu_2O 5mol%, Phen 20mol%, MeOH/H_2O (4/1), 80°C, 30 min
Kabalka (K): NaI 1eq, Chloroamine-T 1.8eq, THF/1M NaOH (1/1), 80°C, 30 min*
*All ^{1}H NMR yields measured using ***tert*-butyl methyl ether** as internal standard



* Kabalka conditions trialed for 4-MeO-Ph at room temperature gave 71% yield.

Yields were obtained *via* ^{1}H NMR analysis using *tert*-butyl methyl ether as an internal standard. In accordance with the literature, Kabalka's conditions were more successful for electron rich substrates,[17] whilst iodination occurred on both electron rich and poor substrates using Hartwig's methodology (**Table 2.3.1**).

Therefore, Hartwig's iodination protocol was elected as a starting point for reaction optimisation studies owing to the general success observed for both electron rich and poor substrates. We began by screening a range of copper-chelating nitrogen containing ligands (**Table 2.3.2**, entries 1-6). As seen from **Table 2.3.2** entry 1, 1,10-phenanthroline was determined to be the ligand of choice for copper-mediated iodination. Entries 7-13 disclose our efforts at modifying both the solvent and temperature of the reaction using 1,10-phenanthroline. Unfortunately altering the ligand, solvent and temperature proved futile in improving upon the literature conditions.[18]

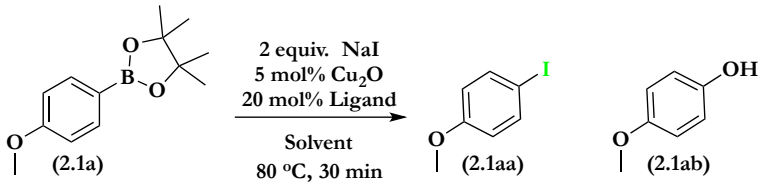


Table 2.3.2: Initial screening of Hartwig conditions

Entry	Ligand	Solvent	Temp[°C]	2.1a[%][a]	2.1aa[%][a]	2.1ab[%][a]
1	**1,10-Phen**	**MeOH/H_2O (4/1)**	**80**	**-**	**58**	**-**
2	1,2-dppe	MeOH/H_2O (4/1)	80	88	<5	-
3	2,2'-bipyridine	MeOH/H_2O (4/1)	80	-	<5	-
4	BathoPhen	MeOH/H_2O (4/1)	80	71	-	-
5	TMEDA	MeOH/H_2O (4/1)	80	-	<5	-
6	Pyridine	MeOH/H_2O (4/1)	80	11	<5	-
7	1,10-Phen	MeOH/NaOH 1% (4/1)	80	-	<5	-

8	1,10-Phen	*i*PrOH/H_2O (4/1)	80	14	8	24
9	1,10-Phen	THF/H_2O (4/1)	80	15	14	28
10	1,10-Phen	THF	80	85	<5	-
11	1,10-Phen	MeOH/H_2O (4/1)	120	-	<5	-
12	1,10-Phen	MeOH/H_2O (4/1)	50	33	16	10
13	1,10-Phen	MeOH/H_2O (1/1)	80	50	23	21

[a] Yields were obtained *via* ^{1}H NMR analysis using *tert*-butyl methyl ether as an internal standard

The direct hydroxylation of boronic acids and esters using Cu_2O and 1,10-phenanthroline in H_2O has previously been reported in 2010 by Xu.[19] Thus formation of oxidation byproduct **2.1ab** was unsurprising in the presence of copper, H_2O and O_2 (**Table 2.3.2** entries 8,9,12,13). In the same publication, Xu reported that the use of MeOH negated formation of **2.1ab**. This observation by Xu corroborates with the improved yield obtained for **2.1aa** when using MeOH/H_2O (4/1) (entry 1). Furthermore, increasing concentrations of H_2O, (MeOH/H_2O (1/1)), resulted in greater formation of **2.1ab** (entry 13).[†]

Next, a range of Cu(I) and Cu(II) catalysts were examined maintaining 1,10-phenanthroline as the ligand of choice (**Table 2.3.3**). Unfortunately, all yields and conversions for entries 2-8 were lower than the original conditions published by Hartwig using Cu_2O (**Table 2.3.3**, entry 1).[18] Importantly we found that, employing bench-stable copper (II) trifluoroacetate ($Cu(OCOCF_3)_2$) proved optimal, resulting in 65% yield (**Table 2.3.3**, entry 9).

[†]Lam has demonstrated *via* ^{18}O experimentation that oxidation byproducts can arise from H_2O in the presence of copper.[20,21]

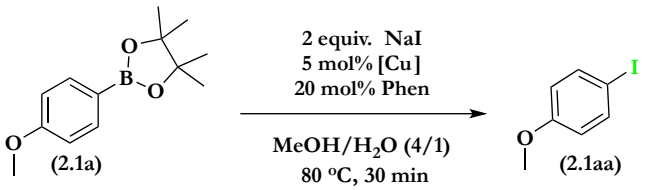


Table 2.3.3: Screening of Copper sources

Entry	Copper Source	2.1a[conversion%][a]	2.1aa[%][a]
1	Cu_2O	100	58
2	CuOTf(benz)	10	<5
3	CuBr	100	52
4	$CuOTf(MeCN)_4$	60	24
5	CuTC	54	25
6	$Cu(OAc)_2$	100	48
7	$Cu(OTf)_2pyr_4$	30	<5
8	$Cu(OTf)_2$	35	5
9	$Cu(OCOCF_3)_2$	100	65
10	Cu_2O	100	54[b]
11	**$Cu(OCOCF_3)_2$**	**100**	**74[b]**

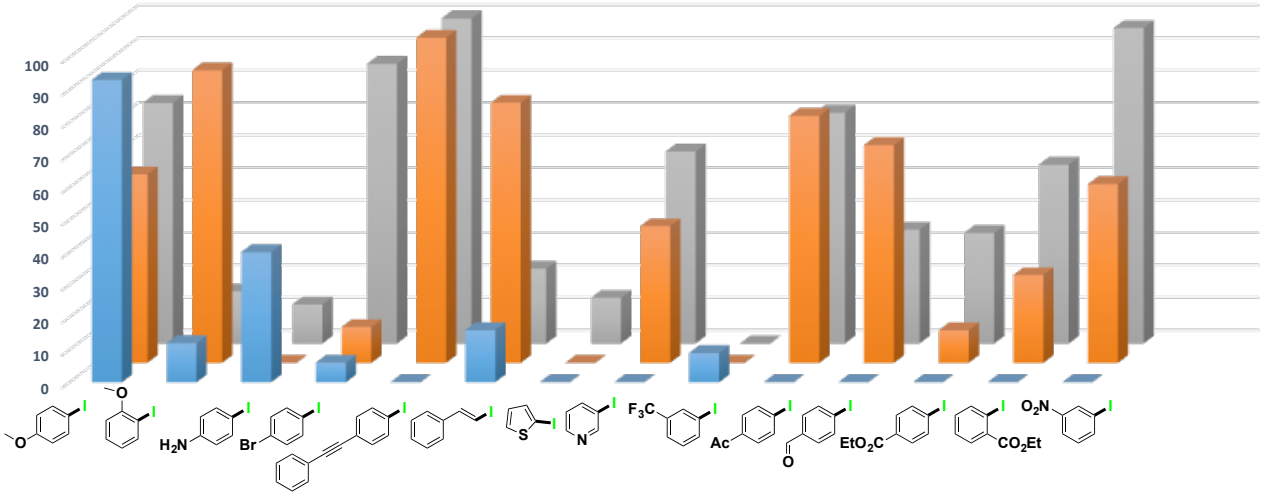
[a] Yields were obtained *via* ^{1}H NMR analysis using *tert*-butyl methyl ether as an internal standard.
[b] 1 equivalent of Sodium Iodide.

With [^{127}I]NaI as the limiting reagent, product formation increased to 74% yield with $Cu(OCOCF_3)_2$ (**Table 2.3.3**, entry 11). This is a significant result and boded well for later radiosynthetic experimentation.

As a consequence, a comparative substrate scope evaluation was undertaken. A selection of (hetero)aryl pinacol derivatives were subjected to the newly optimised $Cu(OCOCF_3)_2$ conditions in coincidence with those reported by Kabalka and Hartwig (**Table 2.3.4**). Pleasingly, the reaction employing $Cu(OCOCF_3)_2$ was found to tolerate a range of electron rich and poor functional groups, including amines, esters, thiophenes and aldehydes, in modest to high yields (**Table 2.3.4**, Novel Cu(II) conditions).

Table 2.3.4: Comparative substrate scope: Kabalka vs. Hartwig vs. Novel Cu(II) conditions

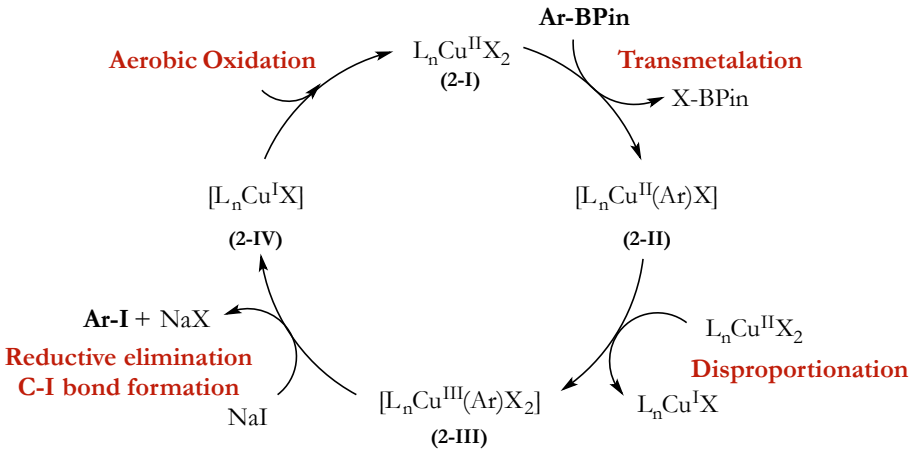
Series	Reaction Conditions
Kabalka	NaI 1eq, Cl-T 1.8eq, THF/1M NaOH (1/1), 80°C, 30 min
Hartwig	NaI 2eq, Cu_2O 5 mol%, Phen 20mol%, MeOH/H_2O (4/1), 80°C, 30 min
Novel Cu(II) cond.	NaI 1 eq, $Cu(OCOCF_3)_2$ 5 mol%, Phen 20mol%, MeOH/H_2O (4/1), 80°C, 30 min



2.3.1 Proposed mechanism

Seminal studies by Stahl[22] and Watson[23] on the copper-mediated aerobic oxidative coupling of aryl boronic esters, have provided key insights into the mechanism of the etherification and amination processes respectively. Both transformations have been proposed to commence *via* transmetalation of an aryl boronate ester with a copper(II) species, followed by formation of a copper(III) complex *via* disproportionation, subsequent reductive elimination and finally aerobic oxidation to complete the cycle.[22,24]

With this in mind, a mechanistic proposal for the copper-mediated iodination of aryl boronic esters is depicted in **Scheme 2.3.1.** Initially, a Cu(II) species **(2-I)** undergoes transmetalation with an aryl boronic ester **(Ar-BPin)** delivering aryl Cu(II) species **2-II.** Oxidation of **2-II** *via* disproportionation is believed to yield Cu(III) complex **2-III.** Rapid reductive elimination of **2-III** liberates the desired aryl iodide product **(Ar-I)** and complex **2-IV.** Reoxidation of **2-IV** with O_2 completes the catalytic cycle yielding Cu(II) species **2-I.**



Scheme 2.3.1: Proposed mechanism for copper-mediated iodination of aryl boronic esters

Analogous to the findings of Stahl and Watson and in support of the putative mechanism detailed in **Scheme 2.3.1**, experimental investigations under anaerobic conditions resulted in significant depletion of reaction yield (Table 2.3.5 entries 1-4). This dependence on O_2 for reaction efficiency alludes to aerobic oxidation being a necessity for catalytic turnover.[22,23]

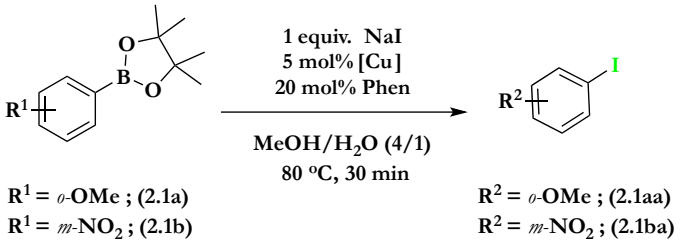


Table 2.3.5: Aerobic and anaerobic mechanistic investigations

Entry	Precursor	Product	O_2	Product[%][a]
1	2.1a	2.1aa	✓	74
2	2.1a	2.1aa	✗	<5
3	2.1b	2.1ba	✓	97
4	2.1b	2.1ba	✗	<5
5	2.1a	2.1aa	✓	51[b]
6	2.1a	2.1aa	✗	17[b]
7	2.1b	2.1ba	✓	78[b]
8	2.1b	2.1ba	✗	20[b]

[a] Yields were obtained *via* ^{1}H NMR analysis using *tert*-butyl methyl ether as an internal standard.
[b] 1 equiv. of $Cu(OCOCF_3)_2$, 1.2 equiv. 1,10-phenanthroline.

Furthermore, regarding reductive elimination from a high valent Cu(III) species **(2-III)**, both Ribas and Wang have previously demonstrated, that the Cu-catalysed nucleophilic iodination of arenes can proceed under mild conditions *via* Cu(III) intermediates.[25,26] These reactivity patterns support the mechanistic hypothesis of a Cu(III) reductive elimination. Finally, the use of stoichiometric copper under anaerobic conditions afforded low product conversion; this result indicates that the formation of a copper (III) species could be achieved *via* disproportionation and not *via* direct oxidation with O_2 (Table 2.3.5 entries 5-8).

2.3.2 Iodine-123 optimisation

Experiments employing iodine-123 were carried out in collaboration with Dr. Sean Preshlock, Dr. Stefan Verhoog and Thomas C. Wilson. For safety purposes, when handling ionising radiation, no less than two people were present during radiosynthesis. [^{123}I]NaI, was produced by GE Healthcare as no-carrier added [^{123}I]NaI in 0.05 M NaOH (**section 1.3.1**). Prior to radiosynthesis this solution was diluted in methanol until the total volume came to 200 μL and 5 μL aliquots containing approx. 4 MBq of [^{123}I]NaI were used per reaction.

Optimisation studies were attempted using electron rich **(2.1a)** and electron poor **(2.1b-2.3b)** model aryl boron precursors (**Table 2.3.6**). Employing Kabalka's technology resulted in greater radiochemical incorporation for **2.1a** (**Table 2.3.6**, entry 1) compared to **2.1b** (**Table 2.3.6**, entry 2).[14]

Cu_2O was employed for copper-mediated nucleophilic ^{123}I-iodination with successful iodine-123 incorporation accomplished for both **2.1a** and **2.1b** (**Table 2.3.6**, entries 5-8)‡.

‡ The Radiosynthetic experiments outlined in Table 2.3.6 entries 5-8 were conducted prior to optimisation studies detailed from pages 38-42.

Next, the optimised conditions for copper-mediated iodination using Cu(OCOCF3)2 as a copper source (detailed from pages 38-42) were translated to a radiosynthetic environment, giving **2.5a** in 68 ± 4% yield (**Table 2.3.6**, entry 9). Additional examination of the molar ratio of copper complex and ligand identified 2 mol% of Cu(OCOCF3)2 and 2 mol% of 1,10-phenanthroline as optimal for radiosynthesis (**Table 2.3.6**, entries 13-14). The efficacy of these conditions was further demonstrated by successful iodine-123 incorporation from an aryl boronic acid (**2.2b**) and trifluoroborate salt (**2.3b**) (**Table 2.3.6**, entries 15-16).

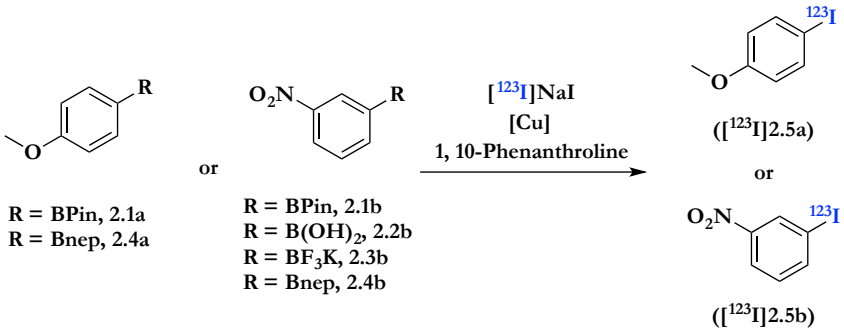


Table 2.3.6: Optimisation for the ^{123}I-iodination of aryl boron reagents

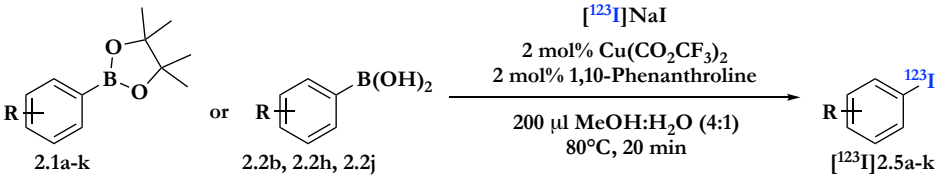
Entry[a]	Precursor	Cu Source	Cu mol%	Phen mol%	Product	RCC[b] (n = 2)[c]
1	2.1a	-[d]	n/a	n/a	2.5a	93% ± 5%
2	2.1b	-[d]	n/a	n/a	2.5b	0% ± 0%
3	2.4a	-[d]	n/a	n/a	2.5a	84%[e]
4	2.4b	-[d]	n/a	n/a	2.5a	0%[f]
5	2.1a	Cu_2O	140	600	2.5a	15% ± 5%
6	2.1b	Cu_2O	140	600	2.5b	29% ± 5%
7	2.1a	Cu_2O	140	n/a	2.5a	5% ± 1%
8	2.1a	Cu_2O	14	600	2.1a	29% ± 9%
9	2.1a	$Cu(OCOCF_3)_2$	5	20	2.5a	68 ± 4%
10	2.1a	$Cu(OCOCF_3)_2$	10	10	2.5a	79% ± 7%
11	2.1a	$Cu(OCOCF_3)_2$	5	5	2.5a	79% ± 15%

12	2.1b	$Cu(OCOCF_3)_2$	5	5	2.5b	82% ± 7%
13	**2.1a**	**$Cu(OCOCF_3)_2$**	**2**	**2**	**2.5a**	**87% ± 0%**
14	**2.1b**	**$Cu(OCOCF_3)_2$**	**2**	**2**	**2.5b**	**84% ± 6%**
15	**2.2b**	**$Cu(OCOCF_3)_2$**	**2**	**2**	**2.5b**	**73% ± 12%**
16	**2.3b**	**$Cu(OCOCF_3)_2$**	**2**	**2**	**2.5b**	**80% ± 2%**

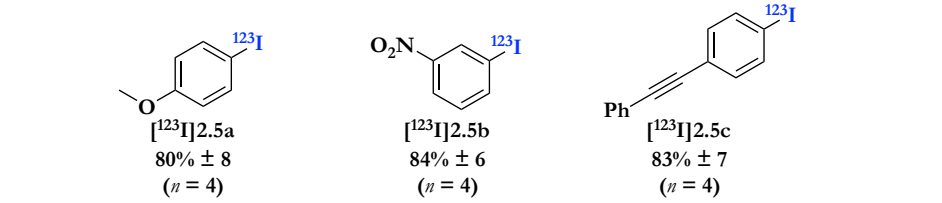
[a] Standard conditions: 1:1 [Cu]/1,10-phenanthroline in 200 µL of MeOH:H_2O (4:1) at 80 °C for 20 mins. [b]RCC = Radiochemical Conversion. [c]All reactions were repeated *n* times. [d]Conditions: Chloramine-T (1.8 equiv.), 200 µL of THF:H_2O (1:1) at rt for 20 mins. [e]RCY reported by G. W. Kabalka for **2-1a**. [f]RCY reported by G. W. Kabalka for **2.4b**. Pin = Pinacol. Nep = Neopentyl glycol.

2.4 Substrate Scope investigation

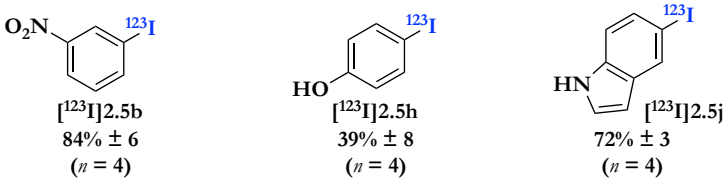
Eleven (hetero)aromatic compounds were tested using our newly optimised conditions (**Scheme 2.4.1 A and B**). Excellent RCCs were recorded for both electron poor and rich substrates. Unprotected phenol and indole moieties were well tolerated (**[^{123}I]2.5h** and **[^{123}I]2.5j**). However, RCCs suffered when employing *ortho*-substituted arenes [^{123}I]2.5e and **[^{123}I]2.5g**. Next, the reactivity of selected (hetero)aryl boronic acids **2.2b**, **2.2h**, **2.2j** was probed and moderate to high RCCs were obtained for the corresponding electron-poor **[^{123}I]2.5b**, electron-rich **[^{123}I]2.5h** and heterocyclic **[^{123}I]2.5j** products.



A. From the corresponding aryl boronic pinacol ester 2.1a-2.1k. All values quoted as RCC



B. From the corresponding aryl boronic acid 2.2b, 2.2h, 2.2j. All values quoted as RCC



Scheme 2.4.1: Substrate scope for copper-mediated ^{123}I-iodination of (hetero)arylboronic pinacol esters and acids

2.4.1 Calculation of radiochemical conversion

As stated in **section 1.4.2**, radiochemical reaction efficiency is quantified by either radiochemical conversion (RCC) or radiochemical yield (RCY). In **Scheme 2.4.1** RCC is utilised to report the quantity of radioiodinated product formed for all substrates. These RCC values were calculated using a combination of radio-TLC and radio-HPLC. The following section will detail the process utilised to quantify RCC for all products shown in **Scheme 2.4.1.**

Taking **[^{123}I]2.5i** as an example, 200 µl of 10% sodium thiosulfate was added to the reaction vial upon reaction completion. An aliquot of the mixture was removed, divided into two portions and subsequently used for radio-TLC and HPLC analysis. Radio-TLC enables product conversion to be directly determined. The reaction aliquot was placed on a TLC plate and run in a 1 : 1 mixture of ethyl acetate (EtOAc) : hexane. The TLC plate was then placed into a radio-TLC scanner and the spectra shown in **Figure 2.4.1** was produced. From integration of the areas under the two peaks a reaction conversion of 95% was calculated (**Figure 2.4.1**).

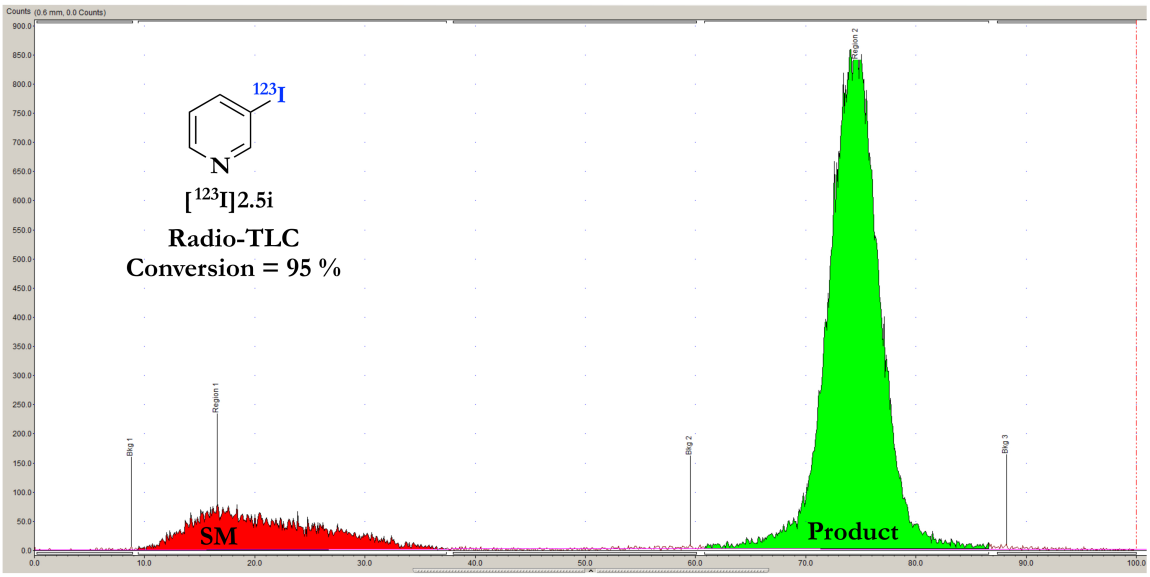


Figure 2.4.1: Radio-TLC of [^{123}I]5i

The radio-HPLC of **[^{123}I]2.5i** was used for both product identification and radiochemical purity evaluation (RCP = >99%) (**Figure 2.4.2**).

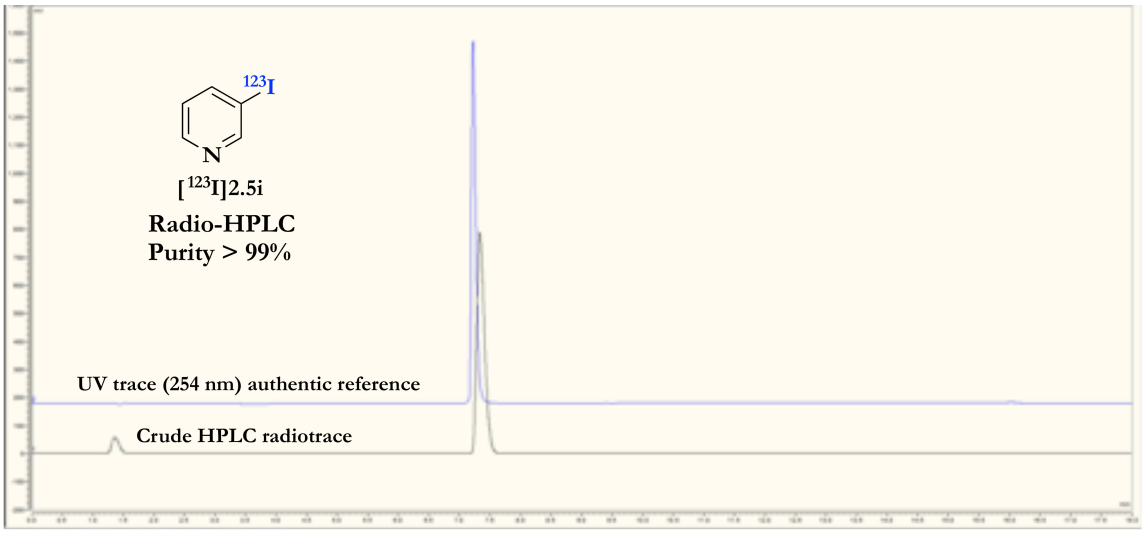


Figure 2.4.2: Radio-HPLC of [^{123}I]5i.

The reaction was run three additional times (n = 4) and each value obtained *via* radio-TLC was multiplied by the RCP (>99%, **Figure 2.4.2**) to give a RCC for each individual reaction. These values are summarised in **Table 2.4.1.**

Table 2.4.1: RCC determination for [^{123}I]5i

Reaction Number	Radio-TLC	Radiochemical Purity[%]	Radiochemical Conversion[%]
1	95%	>99%	95%
2	93%	-	93%
3	90%	>99%	90%
4	99%	-	99%
RCC and Standard Error of the Mean			94% ± 1%

The standard error of the mean was employed as error determination for the n = 4 reactions. This resulted in a RCC value of 94% ± 1% (n = 4) for **[^{123}I]2.5i**. The process was repeated for each substrate shown in **Scheme 2.4.1.**

2.5 Radiolabelling of clinically relevant SPECT radiotracers

To evaluate the efficacy of the copper-mediated ^{123}I-iodination, two clinically relevant SPECT radiotracers [^{123}I]IMPY (**[^{123}I]2.6**) and [^{123}I]DPA-713 (**[^{123}I]2.7**) were synthesised (**Figure 2.5.1**).

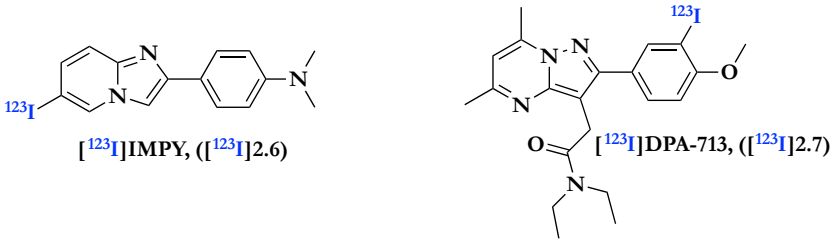
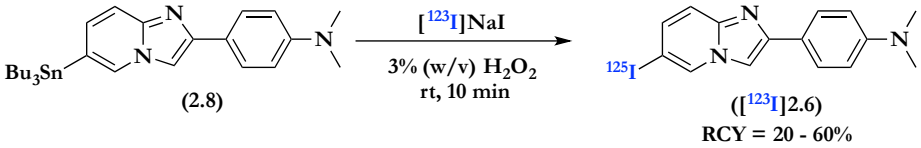


Figure 2.5.1: Structures of [^{123}I]2.6 and [^{123}I]2.7

2.5.1 Synthesis of [^{123}I]IMPY

[^{123}I]2.6 is a radiopharmaceutical that selectively binds to aggregated amyloid-β peptides (amyloid plaques) associated with the pathogenesis of Alzheimer's disease.[6] The synthesis of radioiodinated **IMPY**[§] was initially developed in 2003 by Kung[28] *via* ^{125}I-iododestannylation in 20-60% RCY (**Scheme 2.5.1**).



Scheme 2.5.1: [^{123}I]IMPY radiosynthesis *via* [^{123}I]iododestannylation

Accessing **[^{123}I]2.6** *via* copper mediated ^{123}I-iodination required the construction of a pinacol boronate precursor (**2.9**) and ^{127}I-iodinated reference (**2.6**). Synthesis of iodine-127 analogues of the desired radioiodinated product is a necessity for product identification *via* radio-HPLC (**Figure 2.5.2**).

§ Each isotope is made available as an aqueous solution of the iodide and hypoiodite in dilute sodium hydroxide (**section 1.3.1**).[27] Therefore, radioincorporation with one of the aforementioned isotopes theoretically facilitates the installation of all three isotopes.

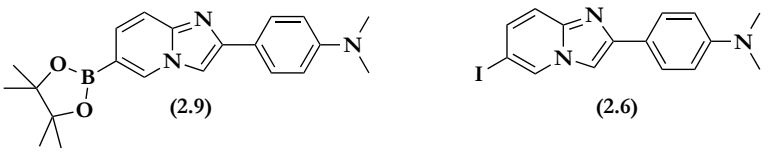
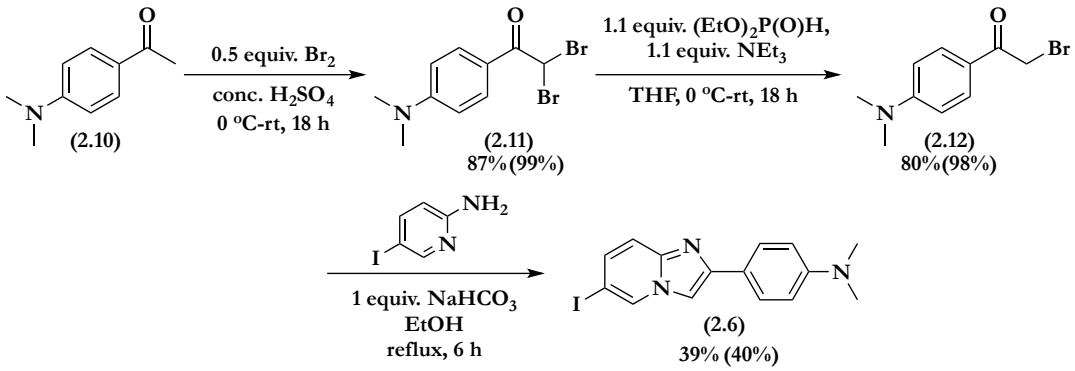


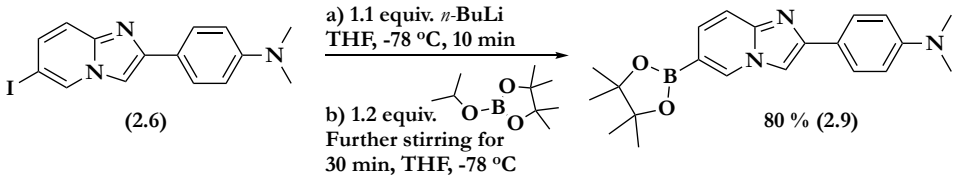
Figure 2.5.2: Chemical structure of 2.9 and 2.6

Implementation of the literature protocol outlined in **Scheme 2.5.2** resulted in the successful synthesis of **2.6**.[29,30] The α-dibromination of **2.10** using 0.5 equivalents of Br_2 and concentrated H_2SO_4, resulted in the formation of **2.11** in 87% yield. Phosphorous mediated reductive mono de-bromination and subsequent cyclisation proceeded as reported to give **2.6** in 39% yield (lit. 40%)[30] (**Scheme 2.5.2**).



Scheme 2.5.2: Synthesis of [^{127}I]IMPY (2.6)

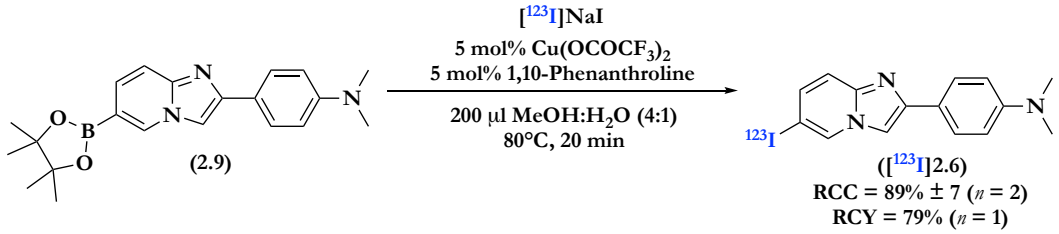
Next, facile construction of **2.9** was achieved *via* lithium halogen exchange reaction, using 2.5 M *n*-butyllithium (*n*-BuLi) and isopropoxy-tetramethyl-dioxaborolane (**Scheme 2.5.3**).



Scheme 2.5.3: Synthesis of 2.9 *via* lithium halogen exchange

The *n*-BuLi was added to the reaction flask containing **2.6** at -78 °C under argon. Isopropoxy-tetramethyl-dioxaborolane was subsequently added after 10 minutes.[31] The reaction was quenched with addition of ammonium chloride and **2.9** was isolated *via*

silica-gel column chromatography in 80% yield. Acquisition of **[^{123}I]2.6** was accomplished *via* copper-mediated nucleophilic ^{123}I-iodination of **2.9** (Scheme 2.5.4). Radiosynthesis commenced with addition of **2.9** (5 µmol) and [^{123}I]NaI (ca. 4 – 36 MBq, 5 - 15 µL MeOH approx.) to a V-vial. A solution of Cu(OCOCF3)2 (0.25 µmol) and 1,10-phenanthroline (0.25 µmol) in MeOH : H_2O (4 : 1, 200 µL) was subsequently added to the reaction and it was heated to 80 °C for 20 minutes.



Scheme 2.5.4: Synthesis of [^{123}I]2.6 *via* copper-mediated nucleophilic ^{123}I-iodination

To calculate the RCY for **[^{123}I]2.6**, 6 mL of H_2O was added to the V-vial. The contents were then loaded onto a C-18 SepPak Plus cartridge. Flushing the cartridge with 2 mL of H_2O, drying with air and subsequent elution with 2 mL of acetonitrile afforded **[^{123}I]2.6**. The RCY was then calculated by comparing the initial activity (MBq) to the percentage of activity (MBq) in the MeCN elute. To calculate RCP, an aliquot was removed for radio-HPLC analysis. The HPLC-trace obtained for **[^{123}I]2.6** can be seen in Figure 2.5.3. This protocol afforded **[^{123}I]2.6** in an improved RCY of 79% from **2.9** (lit. 20-60% RCY)[6].

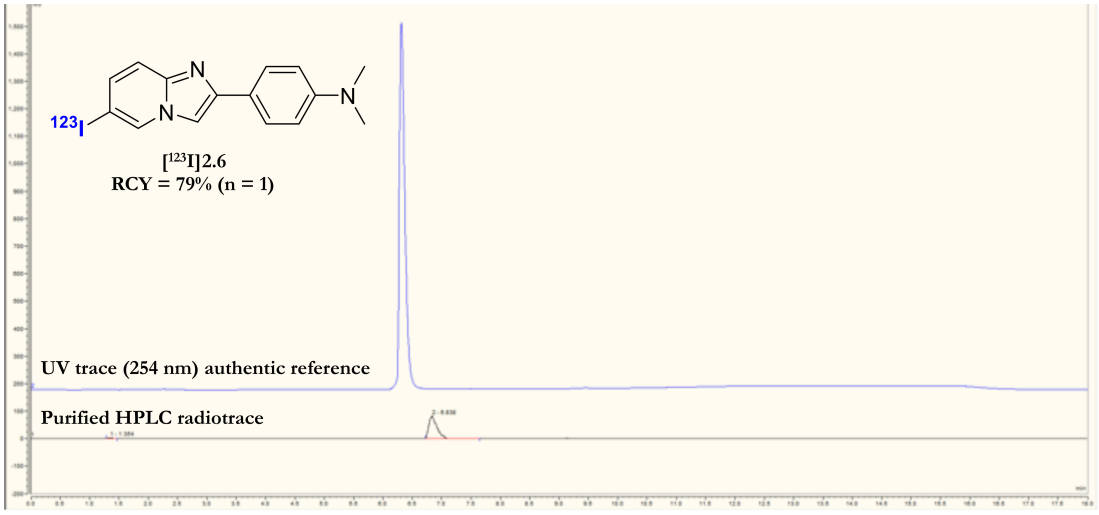
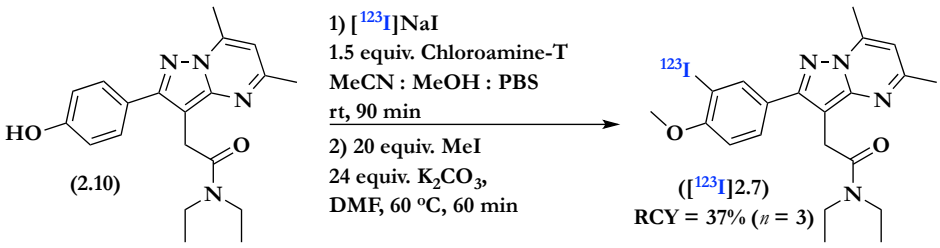


Figure 2.5.3: UV trace (254 nm) of 2.6 and radio-HPLC trace of [^{123}I]2.6.

2.5.2 Synthesis of [^{123}I]DPA-713

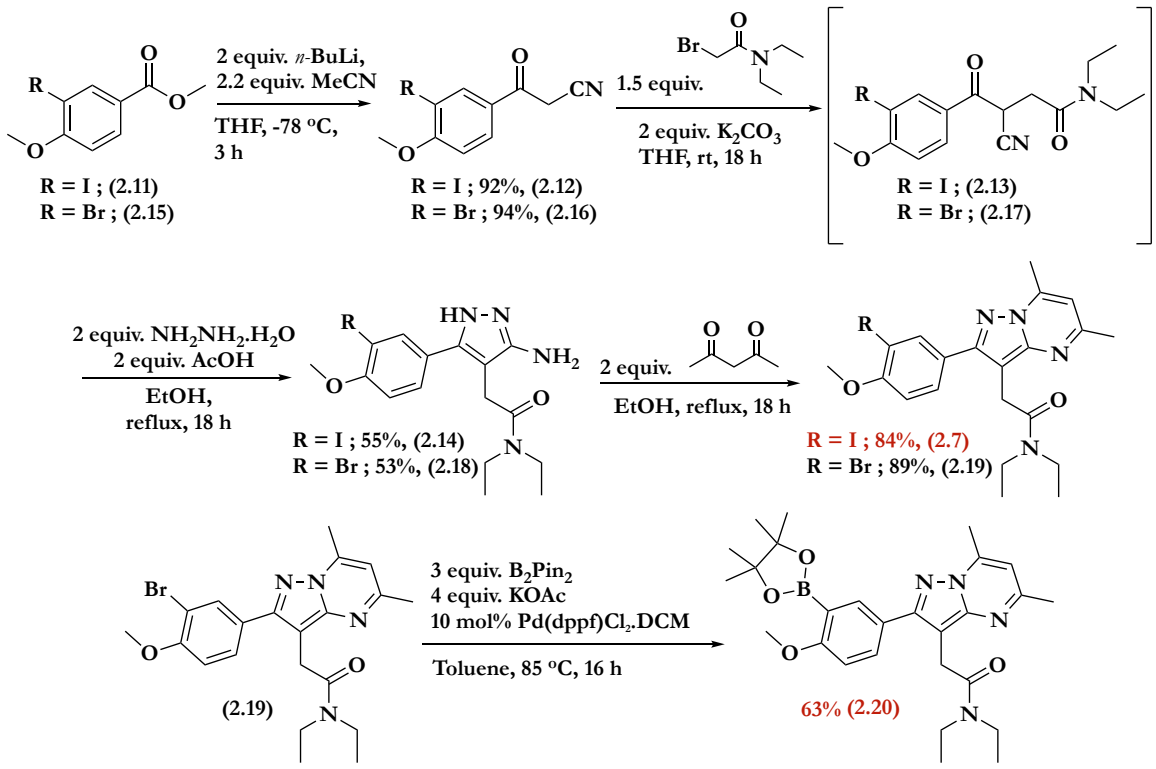
[^{123}I]DPA-713 (**[^{123}I]2.7**), is a selective radioligand for the translocator protein (TSPO) and has therefore been employed to image neurodegenerative diseases *in vivo*.[32,33] **[^{123}I]2.7** was previously synthesised in the Gouverneur group from **2.10**, *via* electrophilic iodination** and subsequent methylation in 37% RCY (Scheme 2.5.5).[32]



Scheme 2.5.5: Radiosynthesis of [^{123}I]2.7 *via* electrophilic iodination

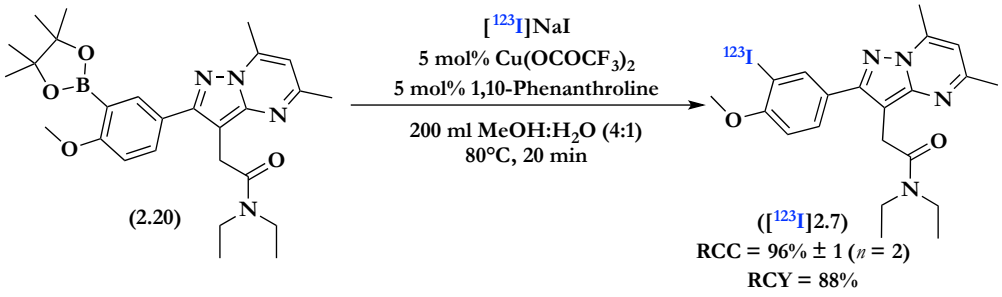
Synthesis of **[^{123}I]2.7** *via* copper-mediated ^{123}I-iodination, required the acquisition of iodine-127 reference **2.7** and boronate precursor **2.20**. Scheme 2.5.6 outlines the synthesis of target compounds **2.7** and **2.20**. Details of this synthetic protocol will be discussed in Chapter 4 of this thesis.

**[^{123}I]iodide and chloroamine-T form an '^{123}I^{+}' species *in situ*.[1]



Scheme 2.5.6: Synthesis of 2.7 and 2.20

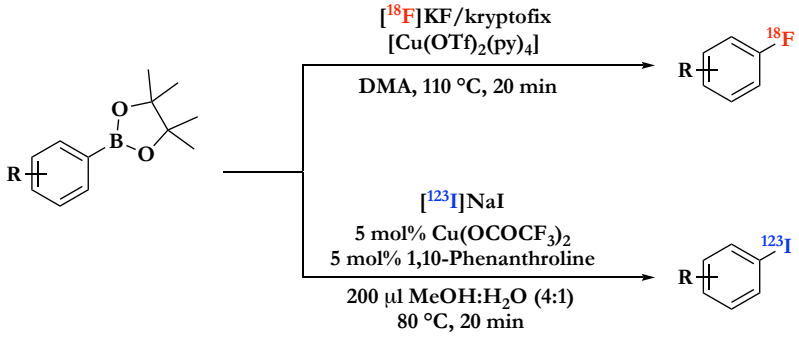
The copper-mediated nucleophilic ^{123}I-iodination was successfully implemented to synthesise [^{123}I]**2.7** in both high RCC (96% ± 1, n = 2) and RCY (88%, n = 1) (Scheme 2.5.7). This result demonstrates a significant improvement over the previously reported 2-step radiosynthetic protocol (Scheme 2.5.5).[32]



Scheme 2.5.7: Radiosynthesis of [^{123}I]2.7

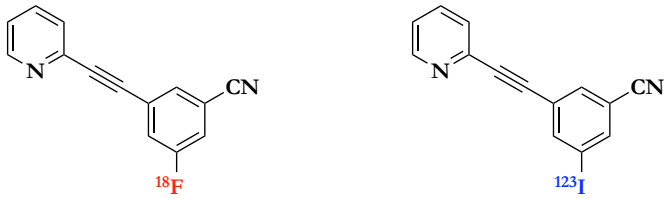
2.5.3 Divergent Radiohalogenation

In **section 2.5**, the efficacy of the copper-mediated nucleophilic ^{123}I-iodination was demonstrated by synthesising two clinically relevant SPECT tracers, **[^{123}I]2.6** and **[^{123}I]2.7**. The final aim of this project was to validate the use of an aryl boronic ester as a precursor for divergent radiohalogenation. It was envisaged that this radiosynthetic strategy could be realised by employing our previously disclosed copper-mediated nucleophilic ^{18}F-fluorination[15,16] in tandem with our novel copper-mediated nucleophilic ^{123}I-iodination (**Scheme 2.5.8**).



Scheme 2.5.8: Divergent radiohalogenation from a common aryl boronate precursor

Initially, two pairs of molecular candidates were selected for mutual radiosynthetic ^{18}F-fluorination and ^{123}I-iodination. The first pair of radioligands nominated, were [^{18}F]FPEB (**[^{18}F]2.21**) and [^{123}I]IPEB (**[^{123}I]2.22**), both previously utilised to image metabotropic glutamate receptors *in vivo* (**Figure 2.5.4**).[16,34,35]



[^{18}F]FPEB, ([^{18}F]2.21) **[^{123}I]IPEB, ([^{123}I]2.22)**

Figure 2.5.4: Molecular structures of [^{18}F]FPEB, ([^{18}F]2.21) and [^{123}I]IPEB, ([^{123}I]2.22)

The acquisition of pinacol boronate precursor **2.23** and reference compounds **2.22** and **2.21** was a prerequisite for the synthesis of **[^{123}I]2.22** and **[^{18}F]2.21** (**Figure 2.5.5**).

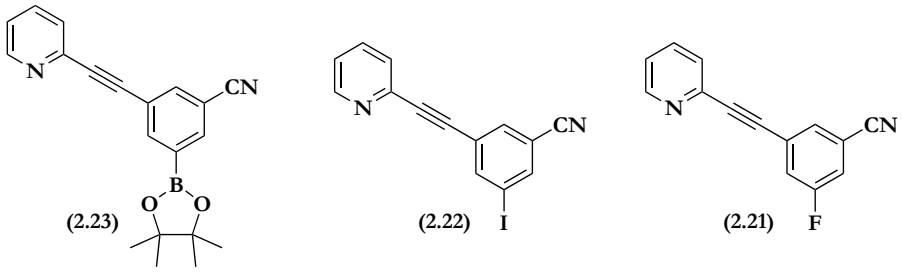
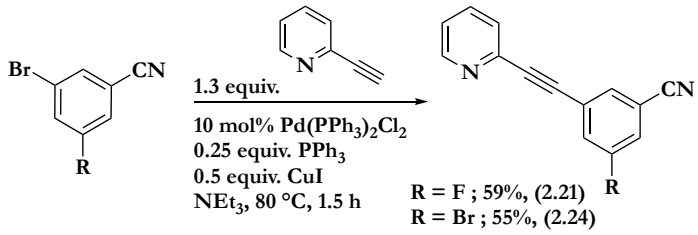


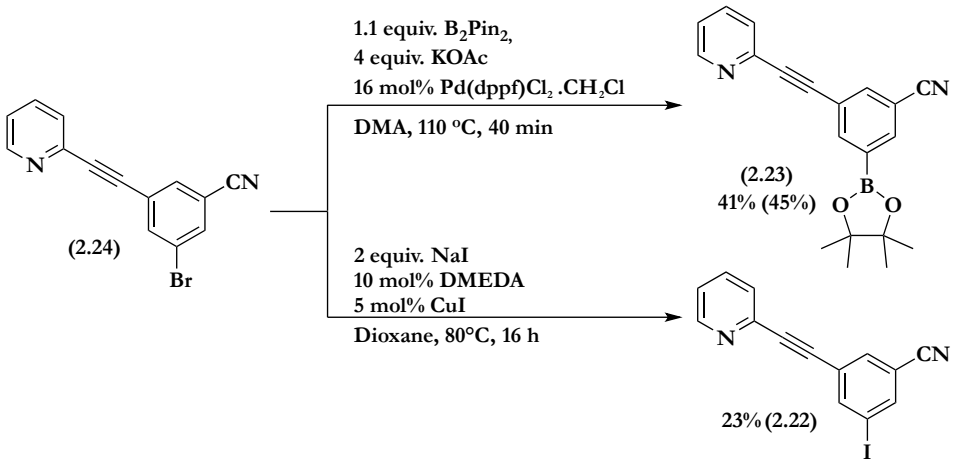
Figure 2.5.5: Molecular structures of synthetic targets 2.23, 2.22 and 2.21

Application of a reported literature protocol by Preshlock[16] enabled the facile construction of **2.21** in 59% yield (Scheme 2.5.9).



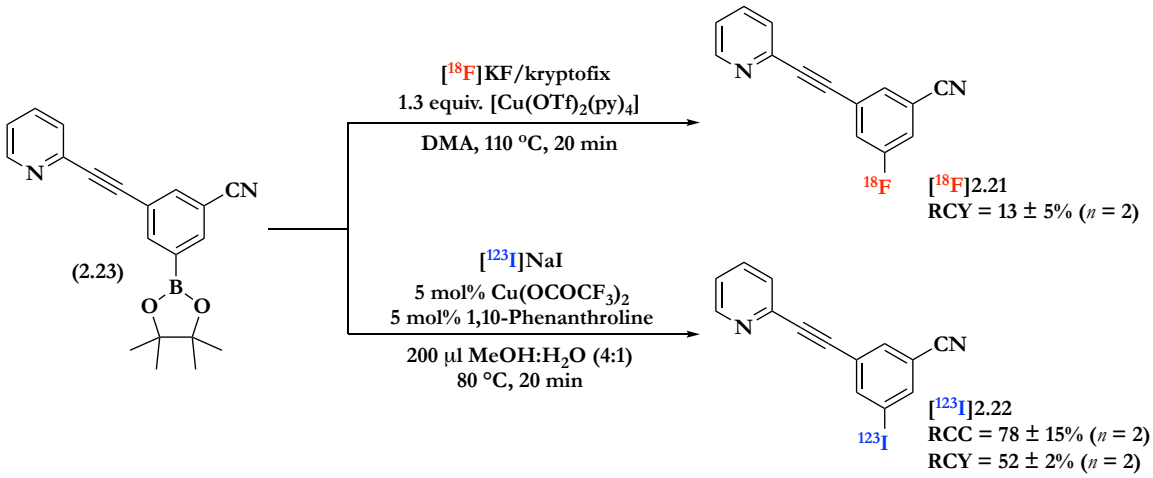
Scheme 2.5.9: Sonogashira reaction used to access both 2.21 and 2.24. Compound 2.21 was synthesised by Thomas C. Wilson.

Furthermore, brominated analogue **2.24** was synthesised in 55% yield using an identical synthetic procedure (Scheme 2.5.9). Subsequently, **2.24** was utilised to access **2.23** *via* Miyaura borylation and **2.22** *via* copper-catalysed aromatic Finkelstein reaction, in 41% and 23% yield respectively (Scheme 2.5.10).[16,36]



Scheme 2.5.10: Synthesis of boronate precursor 2.23 and ^{127}I-iodinated reference 2.22. Compound 2.22 was synthesised by Thomas C. Wilson

Next, **2.23** was subjected to both copper-mediated nucleophilic ^{18}F-fluorination and ^{123}I-iodination conditions, yielding **[^{18}F]2.21** (RCY = 13 ± 5%, *n* =2) and **[^{123}I]2.22** (RCY = 52 ± 2%, *n* =2) **(Scheme 2.5.11).**



Scheme 2.5.11: Demonstration of divergent radiohalogenation from common precursor 2.23

To calculate the RCY for both reactions, two different methods were utilised. Identical conditions to those detailed for **[^{123}I]2.6** in **section 2.5.1** were employed to isolate **[^{123}I]2.22**, i.e. *via* C-18 SepPak Plus cartridge. This protocol afforded **[^{123}I]2.22** in 52 ± 2% (*n* = 2) RCY. The purified radio-HPLC trace is shown in **Figure 2.5.6.**

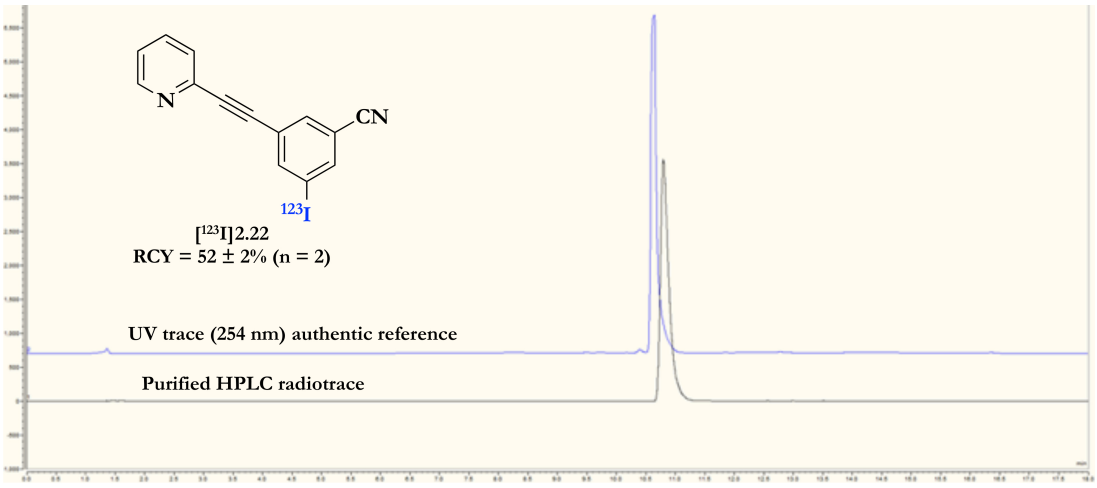


Figure 2.5.6: UV and purified HPLC radiotrace of [^{123}I]2.22

To calculate the RCY for **[^{18}F]2.21**, 1 mL of 40% MeCN/ 60% 25 mM-aqueous NH_4HCOO was added to the V-vial upon reaction completion. The mixture was subsequently

loaded directly onto a 2 mL HPLC loop and **[^{18}F]2.21** was isolated *via* semi-Preparative HPLC giving a RCY of 13 ± 5% (n = 2). The acquired radioactive HPLC trace is shown in **Figure 2.5.7.** As demonstrated from **Figure 2.5.6** and **Figure 2.5.7**, product purity employing the C-18 SepPak Plus cartridge (>99% purity for **[^{123}I]2.22**) was comparable to that attained using the semi-Preparative methodology (>99% purity for **[^{18}F]2.21**). This radiosynthetic protocol demonstrated for the first time the feasibility of divergent radiohalogenation from a common precursor, giving respectable RCYs for both products.

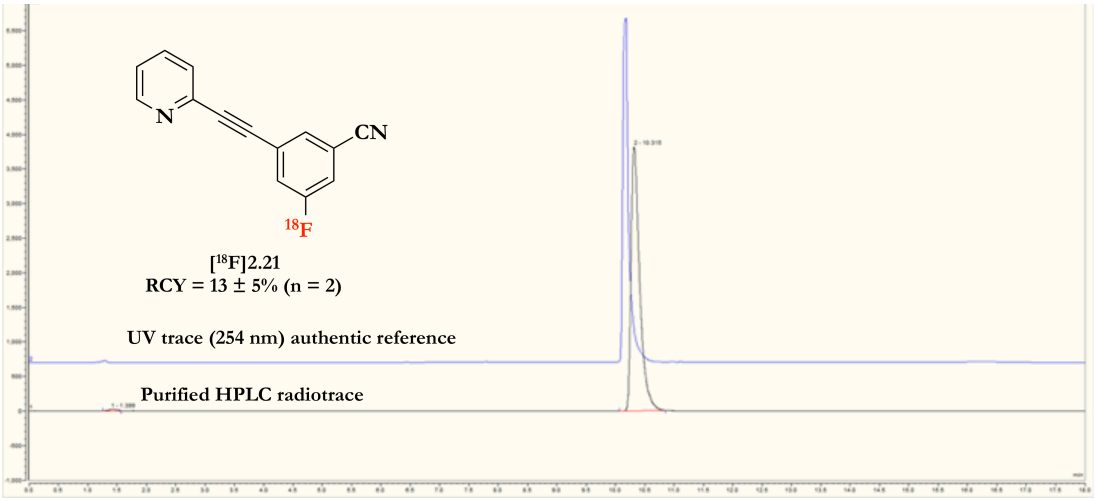


Figure 2.5.7: UV and purified HPLC radiotrace of [^{18}F]2.21

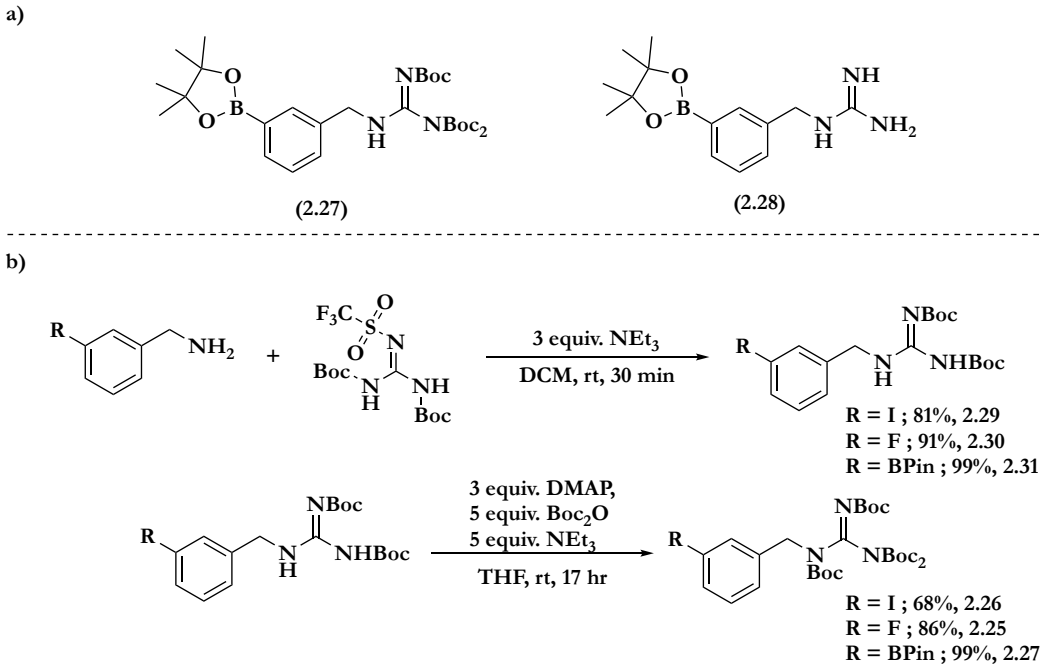
The second pair of molecular candidates nominated for divergent radiohalogenation were [^{18}F]MFBG (**[^{18}F]2.25**) and [^{123}I]MIBG (**[^{123}I]2.26**) (**Figure 2.5.8**). Both **[^{18}F]2.25** and **[^{123}I]2.26** have previously been employed for the targeted imaging of the norepinephrine transporter protein (NET), which is overexpressed in 90% of neuroblastomas.[34]



[^{18}F]MFBG, [^{18}F]2.25 **[^{123}I]MIBG, [^{123}I]2.26**

Figure 2.5.8: Molecular structure of [^{18}F]MFBG ([^{18}F]2.26) and [^{123}I]MIBG ([^{123}I]2.27).

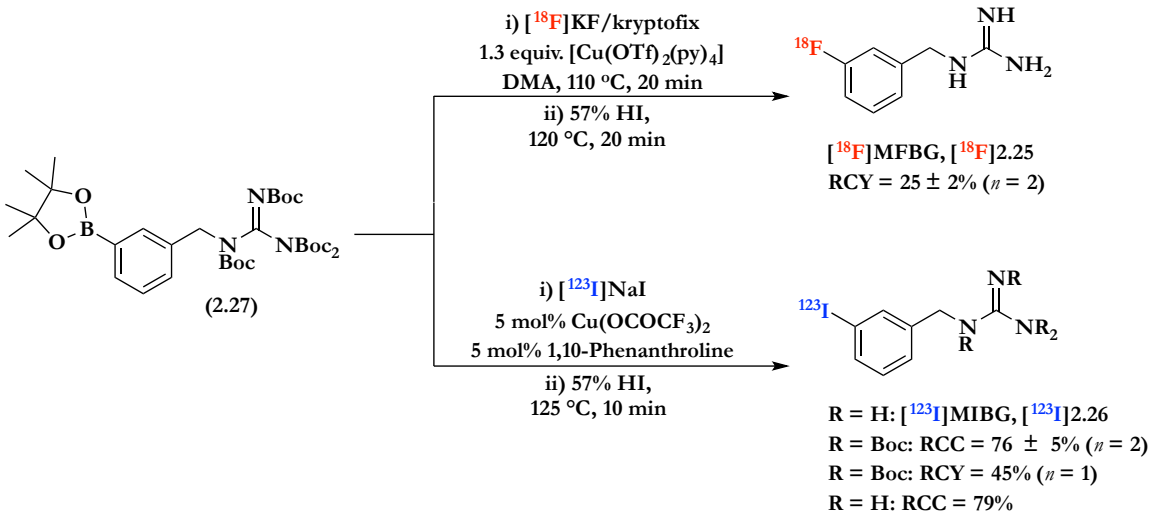
From previous experience in the Gouverneur group using the copper-mediated ^{18}F-fluorination of aryl boronates,[16] a Boc_2O protected aryl boronic ester **(2.27)** was elected as a common precursor for divergent radiosynthesis (**Scheme 2.5.12** a)). Employing compounds containing free amines, such as **2.28**, typically results in diminished RCYs, potentially owing to competitive C-N coupling.[37,38]



Scheme 2.5.12: a) Precursor 2.27 nominated for divergent radiohalogenation b) Synthesis of 2.27, 2.25, 2.26 performed by Thomas C. Wilson

2.27 and radiosynthetic references [^{19}F]MFBG **(2.25)** and [^{127}I]MIBG **(2.26)** were collectively synthesised according to the procedure shown in **Scheme 2.5.12** b).

Subsequently, **2.27** was subjected to both copper-mediated ^{18}F-fluorination and ^{123}I-iodination conditions, followed by deprotection with hydrogen iodide (HI). This resulted in the formation of **[^{18}F]2.26** and **[^{123}I]2.27** in 25 ± 2% (n = 2) and 45% (n = 1) RCY respectively. Therefore, demonstrating the efficacy of this protocol for divergent radiohalogenation.



Scheme 2.5.13: Demonstration of divergent radiohalogenation from common precursor 2.27

2.6 Conclusions

In conclusion, this chapter has outlined the first copper-mediated nucleophilic ^{123}I-iodination of aryl pinacol boronic esters and acids. The reaction is well tolerated toward both electron rich and poor (hetero)aromatics. The protocol was successfully applied to the radiosynthesis of four clinically relevant SPECT tracers [^{123}I]DPA-713, [^{123}I]IMPY, [^{123}I]MIBG and [^{123}I]IPEB, all isolated with moderate to high RCYs. Furthermore, the concept of divergent radiohalogenation has been validated *via* reaction of a common aryl boron precursor with either [^{18}F]fluoride or [^{123}I]iodide in the presence of a copper complex. This was exemplified with the successful radiolabelling of [^{18}F]FPEB/[^{123}I]IPEB and [^{18}F]MFBG/[^{123}I]MIBG.

2.7 References

(1) Seevers, R. H.; Counsell, R. E. *Chem. Rev.* **1982**, *82*, 575–590.
(2) Pimlott, S. L.; Sutherland, A. *Chem. Soc. Rev.* **2011**, *40* (1), 149–162.
(3) Br cke, T.; Kornhuber, J.; Angelberger, P.; Asenbaum, S.; Frassine, H.; Podreka, I. *J. Neural Transm.* **1993**, *94* (2), 137–146.
(4) O'Brien, J. T.; Colloby, S. J.; Pakrasi, S.; Perry, E. K.; Pimlott, S. L.; Wyper, D. J.; McKeith, I. G.; Williams, E. D. *J. Neurol. , Neurosurg. Psychiatry* **2006**, *78* (4), 356–362.
(5) Khalil, M. M.; Tremoleda, J. L.; Bayomy, T. B.; Gsell, W. *Int. J. Molecular Imaging* **2011**, (4), 1–15.
(6) Newberg, B. A.; Wintering, N. A.; Plössi, K.; Hochold, J.; Stabin, G. M.; Watson, M.; Skovronsky, D.; Clark, C. M.; Kung, M.-P.; Kung, H. F. *J. Nucl. Med.* **2006**, *47*, 748–754.
(7) Kil, K.-E.; Zhu, A.; Zhang, Z.; Choi, J.-K.; Kura, S.; Gong, C.; Brownell, A.-L. *ACS Med. Chem. Lett.* **2014**, *5* (6), 652–656.
(8) Kimbrough, R. D. *Environmental Health Perspectives* **1976**, *14*, 51–56.
(9) Racys, D. T.; Sharif, S. A. I.; Pimlott, S. L.; Sutherland, A. *J. Org. Chem.* **2016**, *81* (3), 772–780.
(10) Cant, A. A.; Champion, S.; Bhalla, R.; Pimlott, S. L.; Sutherland, A. *Angew. Chem. Int. Ed.* **2013**, *52* (30), 7829–7832.
(11) Akula, M. R.; Zhang, J. H.; Kabalka, G. W. J. *Labelled Compd. Radiopharm.* **2001**, *44*, 260–261.
(12) Kabalka, G. W.; Mereddy, A. R. *Nucl. Med. Biol.* **2004**, *31* (7), 935–938.
(13) Akula, M. R.; Yao, M.-L.; Kabalka, G. W. *J. Labelled Compd. Radiopharm.* **2010**, *54* (3), 132–134.
(14) Kabalka, G. W.; Akula, M. R.; Zhang, J. *Nucl. Med. Biol.* **2002**, *29*, 841–843.
(15) Tredwell, M.; Preshlock, S. M.; Taylor, N. J.; Gruber, S.; Huiban, M.; Passchier, J.; Mercier, J.; Génicot, C.; Gouverneur, V. *Angew. Chem. Int. Ed.* **2014**, *53* (30), 7751–7755.
(16) Preshlock, S.; Calderwood, S.; Verhoog, S.; Tredwell, M.; Huiban, M.; Hienzsch, A.; Gruber, S.; Wilson, T. C.; Taylor, N. J.; Cailly, T.; Schedler, M.; Collier, T. L.; Passchier, J.; Smits, R. X.; Mollitor, J.; Hoepping, A.; Mueller, M.; Génicot, C.; Mercier, J. X. L.; Gouverneur, V. X. R. *Chem. Commun.* **2016**, *52*, 8361–8364.
(17) Kabalka, G. W.; Yao, M.-L. *J. Organomet. Chem.* **2009**, *694* (11), 1638–1641.
(18) Partridge, B. M.; Hartwig, J. F. *Org. Lett.* **2013**, *15* (1), 140–143.
(19) Xu, J.; Wang, X.; Shao, C.; Su, D.; Cheng, G.; Hu, Y. *Org. Lett.* **2010**, *12* (9), 1964–1967.
(20) Lam, P.; Bonne, D.; Vincent, G.; Clark, C.; Combs, A. *Tetrahedron Lett.* **2003**, 1691–1694.
(21) Evans, D.; Katz, J.; West, T. *Tetrahedron Lett.* **1998**, *39*, 2937–2940.
(22) King, A. E.; Brunold, T. C.; Stahl, S. S. *J. Am. Chem. Soc.* **2009**, *131* (14), 5044–5045.
(23) Vantourout, J. C.; Miras, H. N.; Isidro-Llobet, A.; Sproules, S.; Watson, A. J. B. *J. Am. Chem. Soc.* **2017**, jacs.6b12800–jacs.6b12813.
(24) King, A. E.; Ryland, B. L.; Brunold, T. C.; Stahl, S. S. *Organometallics* **2012**, *31* (22), 7948–7957.
(25) Yao, B.; Wang, Z.-L.; Zhang, H.; Wang, D.-X.; Zhao, L.; Wang, M.-X. *J. Org. Chem.* **2012**, *77* (7), 3336–3340.
(26) Casitas, A.; Ribas, X. *Chem. Sci.* **2013**, *4* (6), 2301–2318.
(27) Adam, M. J.; Wilbur, D. S. *Chem. Soc. Rev.* **2005**, *34* (2), 153–11.

(28) Zhuang, Z.-P.; Kung, M.-P.; Wilson, A.; Lee, C.-W.; Plössl, K.; Hou, C.; Holtzman, D. M.; Kung, H. F. *J. Med. Chem.* **2003**, *46* (2), 237–243.
(29) Diwu, Z.; Beachdel, C.; Klaubert, D. H. *Tetrahedron Lett.* **1998**, *39*, 4987–4990.
(30) Choi, J.-S.; Braymer, J. J.; Park, S. K.; Mustafa, S.; Chae, J.; Lim, M. H. *Metallomics* **2011**, *3* (3), 284–289.
(31) Reich, H. J.; Phillips, N. H.; Reich, I. L. *J. Am. Chem. Soc.* **1985**, *107* (13), 4101–4102.
(32) O'Brien, E. R.; Kersemans, V.; Tredwell, M.; Checa, B.; Serres, S.; Soto, M. S.; Gouverneur, V.; Leppert, D.; Anthony, D. C.; Sibson, N. R. *J. Nucl. Med.* **2014**, *55* (2), 275–280.
(33) Anthony, D. C.; Dickens, A. M.; Seneca, N.; Couch, Y.; Campbell, S.; Checa, B.; Kersemans, V.; Warren, E. A.; Tredwell, M.; Sibson, N. R.; Gouverneur, V.; Leppert, D. *Ann. Clin. Transl. Neurol.* **2014**, *1* (9), 659–669.
(34) Zhang, H.; Huang, R.; Pillarsetty, N.; Thorek, D. L. J.; Vaidyanathan, G.; Serganova, I.; Blasberg, R. G.; Lewis, J. S. *Eur. J. Nucl. Med. Mol. Imaging* **2013**, *41* (2), 322–332.
(35) Hamill, T. G.; Krause, S.; Ryan, C.; Bonnefous, C.; Govek, S.; Seiders, T. J.; Cosford, N. D. P.; Roppe, J.; Kamenecka, T.; Patel, S.; Gibson, R. E.; Sanabria, S.; Riffel, K.; Eng, W.; King, C.; Yang, X.; Green, M. D.; O'malley, S. S.; Hargreaves, R.; Burns, H. D. *Synapse* **2005**, *56* (4), 205–216.
(36) Klapars, A.; Buchwald, S. L. *J. Am. Chem. Soc.* **2002**, *124* (50), 14844–14845.
(37) Qiao, J.; Lam, P. *Synthesis* **2010**, *2011* (06), 829–856.
(38) Taylor, N. J.; Emer, E.; Preshlock, S.; Schedler, M.; Tredwell, M.; Verhoog, S.; Mercier, J.; Génicot, C.; Gouverneur, V. *J. Am. Chem. Soc.* **2017**, *139* (24), 8267–8276.

Chapter 3

Access to ^{18}F-aryl prosthetic groups *via* copper-mediated nucleophilic ^{18}F-fluorination.

3.1 Introduction

The indirect incorporation of [^{18}F]fluoroarenes *via* prosthetic group conjugation is an indispensable tool for labelling macromolecules not amenable to direct ^{18}F-fluorination.[1] For biomolecules sensitive to the severe reaction conditions frequently necessitated for ^{18}F-fluorination, a conjugation agent can be labelled with fluorine-18 and successively coupled to the desired macromolecular target (Figure 3.1.1 b)). Figure 3.1.1 c) displays some commonly utilised [^{18}F]fluoroaromatic prosthetic groups.

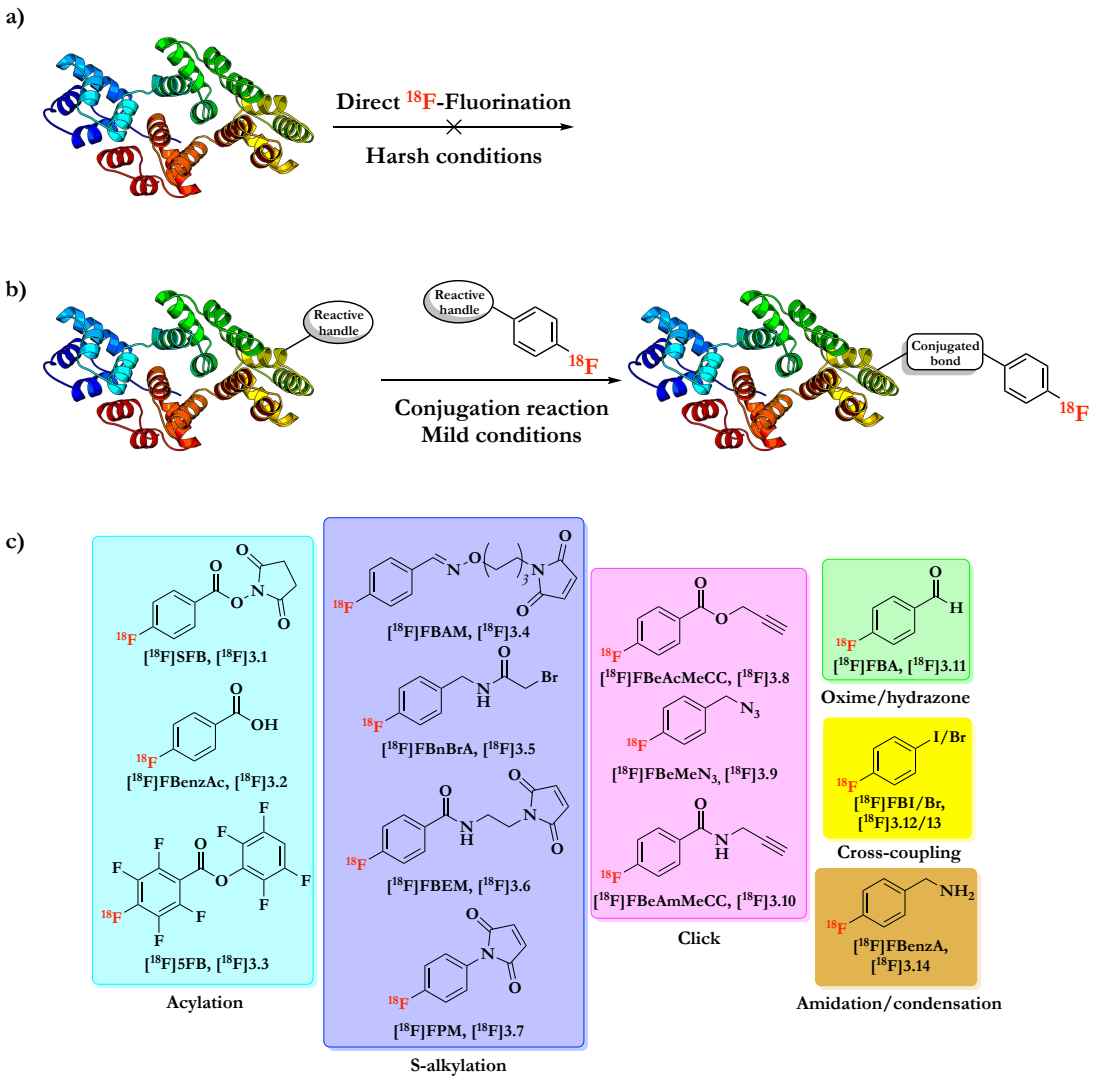
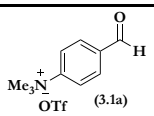
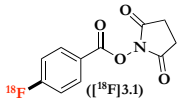
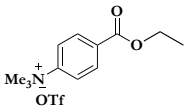
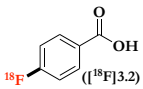
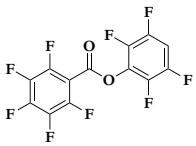
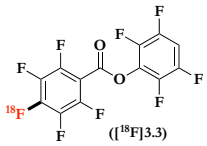
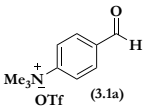
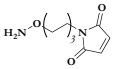
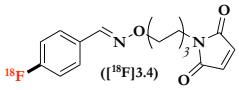
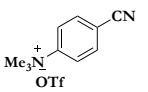
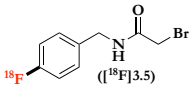
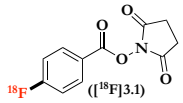
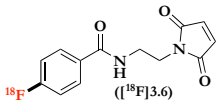
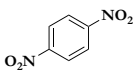
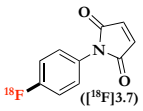


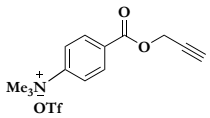
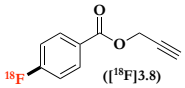
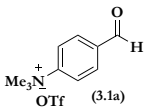
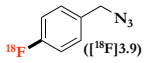
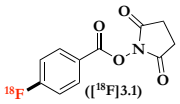
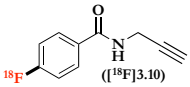
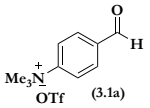
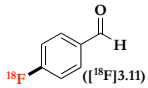
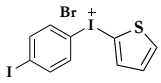
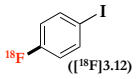
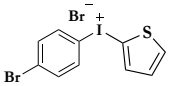
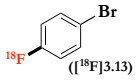
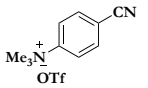
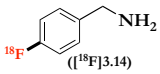
Figure 3.1.1: a) Macromolecule that is not amenable to direct ^{18}F-fluorination b) Successful ^{18}F-labelling of a (un)modified macromolecule *via* indirect prosthetic group conjugation c) Common ^{18}F-labelled aryl prosthetic groups

Typically these synthons are employed for acylation, thiol-alkylation, click chemistry, metal mediated cross-coupling, amidation/condensation reactions and oxime/hydrazone formation.[2]

Although ^{18}F-aryl prosthetic groups are widely employed, many established radiosynthetic procedures require elaborate, multi-step synthetic post-labelling protocols prior to further synthesis or conjugation.[2-6] This is a consequence of traditional synthetic methods toward [^{18}F]fluoroaromatic compounds being reliant on the use of activated aryl groups to achieve good radiochemical yields (RCYs).[7-9] Table 3.1.1 discloses a summary of frequently cited synthetic protocols for the most common ^{18}F-aryl synthons.

Table 3.1.1: Frequently cited radiosynthetic syntheses of common ^{18}F-aryl prosthetic groups.

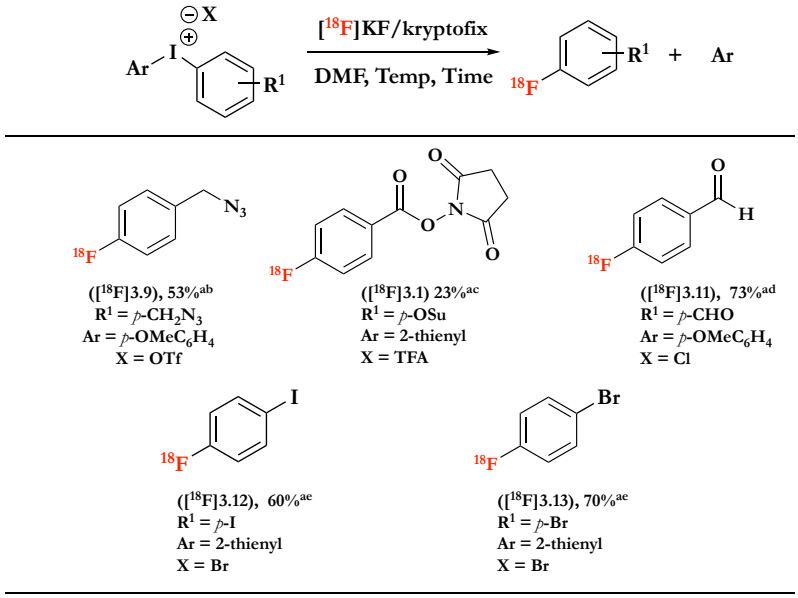
Entry	SM	Reagents	Product	Time [min]	Yield [%]
1	 (3.1a)	1) [^{18}F]KF/kryptofix, DMF, 120 °C 2) $KMnO_4$, NaOH, 120 °C 3) DSC, pyridine, MeCN, 150 °C	 ([^{18}F]3.1)	115	30-35[a10]
2		1) [^{18}F]KF/kryptofix, DMSO, 90 °C 2) 2 M NaOH, 90 °C	 ([^{18}F]3.2)	25	85[b11]
3		1) $Bu_4N^+[^{18}F]F^-$, DMSO, mw irradiation	 ([^{18}F]3.3)	16	32[b12]
4	 (3.1a)	1) [^{18}F]KF/kryptofix, DMF, 120 °C 2)  MeOH, 1 M HCl, 50 °C	 ([^{18}F]3.4)	69	29[a13,14]
5		1) [^{18}F]KF/kryptofix, DMSO, 180 °C 2) $LiAlH_4$, THF, 120 °C 3) $BrCOCH_2Br$, H_2O/DCM, 25 °C	 ([^{18}F]3.5)	90	20-30[a15]
6	 ([^{18}F]3.1)	1)-3), 3.1a-[^{18}F]3.1 4) MeCN, DIPEA 40 °C 	 ([^{18}F]3.6)	150	5[a16]
7		1) [^{18}F]CsF, DMSO, 160 °C 2) 10% Pd/C, 50% H_3PO_2, THF, 65 °C 3) Maleic anhydride, THF 65 °C 4) NaOAc/Ac_2O, Benzene, 100 °C	 ([^{18}F]3.7)	100	15[a17]

8		1) [^{18}F]KF/kryptofix DMSO, 120 °C		15	58[b18]
9		1) [^{18}F]KF/kryptofix DMSO, 120 °C 2) $NaBH_4/H_2O$ C-18 sep-pak 3) aq. HBr, C-18 sep-pak, 50 °C 4) Amberlite-N_3, DMF, rt		75	34[a19]
10		1)-3), 3.15-[^{18}F]3.1 4) Propargyl amine NEt_3, THF, 50 °C		98	27[a20]
11		1) [^{18}F]KF/kryptofix DMSO, 160 °C		10	74[b21]
12		1) [^{18}F]KF/kryptofix DMF, 130 °C		15	60[b22]
13		1) [^{18}F]KF/kryptofix DMF, 130 °C		10	70[b22]
14		1) [^{18}F]KF/kryptofix DMSO, 95 °C 2) $NaBH_4/Co(OAc)_2$, $THF\text{-}H_2O$, rt		30	80[b23]

[a] Radiochemical Yield (RCY).[b] Radiochemcial Conversion (RCC).

It is evident from Table 3.1.1 that the range of [^{18}F]fluoroaromatic compounds available *via* simple one-step S_NAr is limited. Thus to access most prosthetic groups, downstream synthetic manipulations are required, and the overall synthetic route to each prosthetic group is different.

Attempts have been made to both simplify and generalise these radiosynthetic protocols,[24-27] most notably through the use of unsymmetrical diaryliodonium salts, first discovered in 1995 by Pike.[28] This methodology has facilitated the radiosynthesis of a host of [^{18}F]fluoroaromatic synthons in a single synthetic step (Scheme 3.1.1).[22,29,30] However, this radiochemistry is not without its limitations, which to date have prevented wider implementation throughout the field of prosthetic group chemistry: multi-step preparation of the starting material is required, including oxidising conditions for precursor synthesis and diaryliodoniums are susceptible to photo-initiated decomposition *via* homolysis of the aryl iodine bond.[31,32]

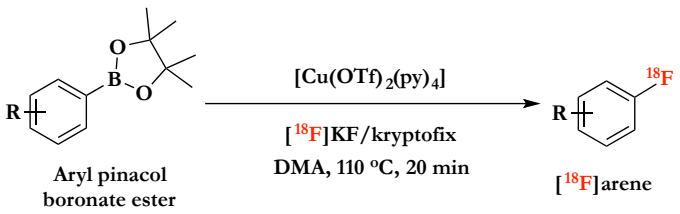


[a]RCC. [b]180 °C, 3 mins.[29] [c]Argon atmosphere, TEMPO, 130 °C, 5 mins.[30] [d]180 °C, 5 mins.[29] [e]130 °C, 10-15 mins.[22]

Scheme 3.1.1: Single-step prosthetic group synthesis *via* unsymmetrical diaryliodonium salts

Triarylsulfonium salts[33] and diarylsulfoxides[34] have also been employed for fluorine-18 aryl prosthetic group synthesis, however both methodologies are not broadly applicable, as yields suffer in the presence of commonly used activating groups.

To address these issues, we sought to apply the copper-mediated nucleophilic ^{18}F-fluorination of arenes Scheme 3.1.2.[35,36] We envisioned that this would enable a unified, one-step route to various commonly used ^{18}F-aryl prosthetic groups, where reactivity was largely independent of aryl ring electronic properties.



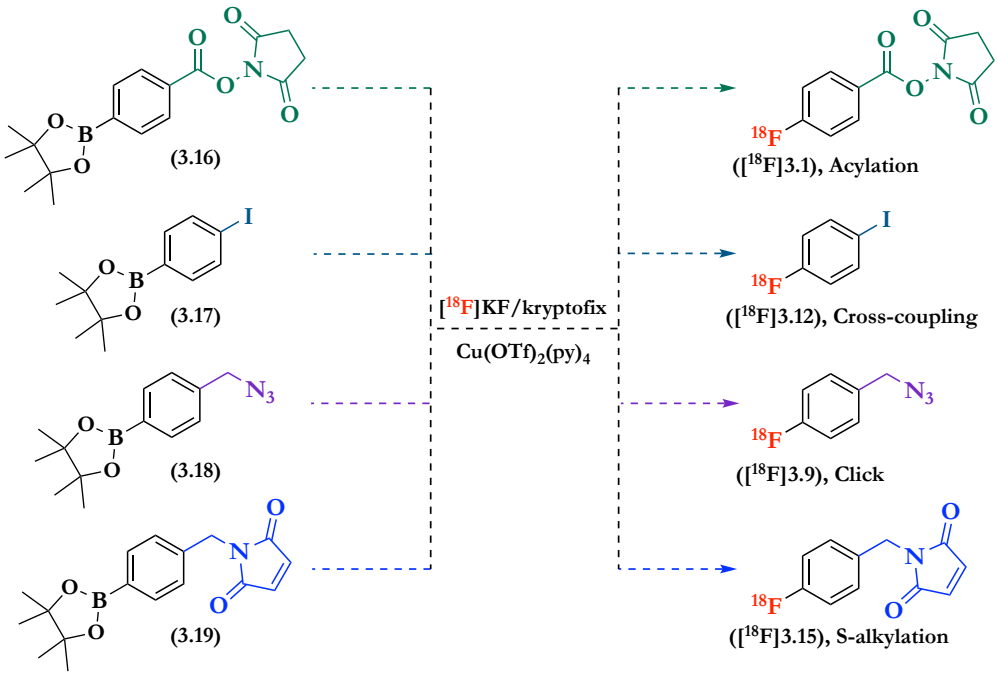
Scheme 3.1.2: Copper-mediated nucleophilic ^{18}F-fluorination of arenes

We reasoned that such an approach would decrease the number of radiosynthetic steps and thus lower the synthesis time for many common ^{18}F-aryl prosthetic groups. Importantly, the copper-mediated nucleophilic ^{18}F-fluorination methodology is known to possess broad substrate scope and high functional group tolerance, which would

potentially facilitate radio-labelling of electron-rich/deficient aryl motifs in the presence of air.

3.2 Preliminary investigations

Our study began by identifying prospective aryl boronic esters comprising the most frequently used functional groups for prosthetic group conjugation. We elected to synthesise the following starting materials (Scheme 3.2.1)**: 3.16** for acylation, **3.17** for metal-mediated cross-coupling, **3.18** for click chemistry, and **3.19** for thiol-alkylation.



Scheme 3.2.1: Proposed single step copper-mediated nucleophilic ^{18}F-fluorination toward the construction of four ^{18}F-aryl prosthetic groups

It was envisaged that the pinacol boronate ester (BPin) precursors shown in **Scheme 3.2.1** could be labelled in a single radiosynthetic step *via* copper-mediated nucleophilic ^{18}F-fluorination. This methodology would enable the conversion of the proposed starting materials **(3.16-3.19)**, to their corresponding ^{18}F-radiolabeled prosthetic groups under a common set of reaction conditions.

Accessing each ^{18}F-radiolabeled prosthetic group initially required the acquisition of the corresponding BPin precursor and the ^{19}F-fluorinated HPLC reference needed for verification of product identity during radiosynthesis (Figure 3.2.1).

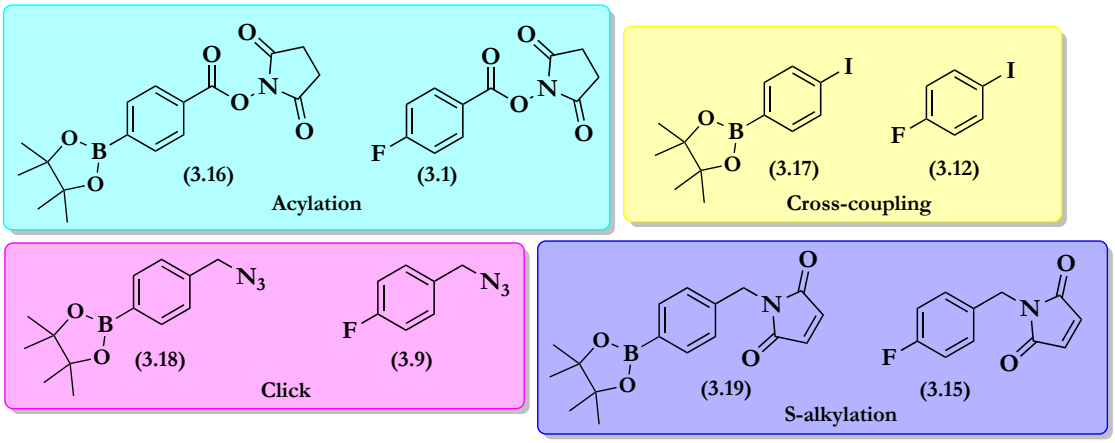
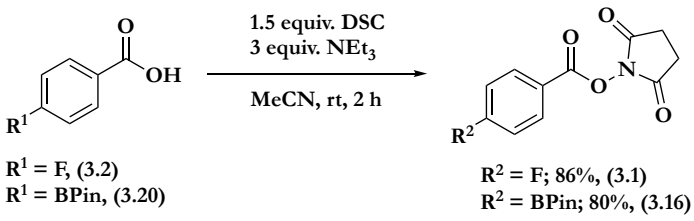


Figure 3.2.1: Precursors required for ^{18}F-labeled prosthetic group radiosynthesis

3.2.1 Synthesis of boronate precursors and ^{19}F prosthetic group analogues

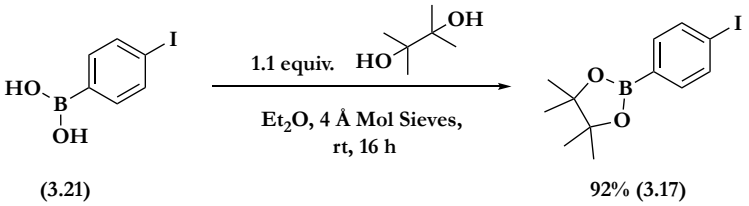
Owing to the prevalence of cross-coupling reactions in synthetic organic chemistry, many arylboranes and arylhalides are commercially available. As a consequence, molecular candidates **3.12** and **3.19** were available to purchase from chemical vendors.

Synthetic targets **3.1** and **3.16** were synthesised *via* esterification of the parent benzoic acid utilising disuccinimidyl carbonate (DSC) and triethylamine (NEt_3) (Scheme 3.2.2).[37] Both compounds were isolated *via* silica gel column chromatography in 86% and 80% yield, respectively.



Scheme 3.2.2: Synthesis of ^{19}F-fluorinated reference (3.1) and BPin precursor (3.16) of [^{18}F]3.1

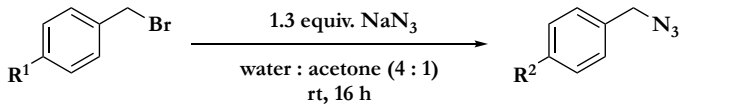
Construction of **3.17** was achieved *via* condensation of 4-iodophenyl-boronic acid **(3.21)** with pinacol over 4 Å molecular sieves for 16 hours.[38] Simple filtration afforded **3.17** in 92% yield (Scheme 3.2.3).



(3.21) **92% (3.17)**

Scheme 3.2.3: Synthesis of BPin precursor 3.17

Substitution of benzyl bromide derivatives **3.22** and **3.23** with sodium azide (NaN_3) enabled the formation of synthetic targets **3.9** and **3.19** in >95% yield (Scheme 3.2.4).[38]

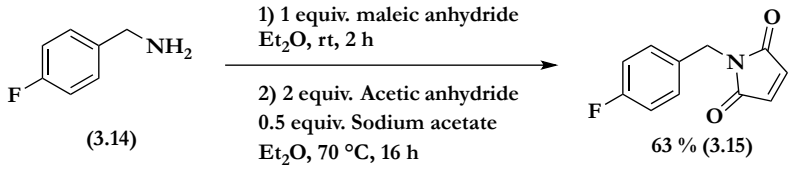


R^1 = F, (3.22)
R^1 = BPin, (3.23)

R^2 = F; 90%, (3.9)
R^2 = BPin; >95%, (3.19)

Scheme 3.2.4: Synthesis of 3.9 and 3.19 *via* S_N2 reaction

Facile construction of **3.15** was realised by employing the literature procedure outlined in Scheme 3.2.5.[39] Reaction of 4-fluorobenzylamine **(3.14)** with maleic anhydride, acetic anhydride and sodium acetate in diethyl ether, under reflux for 16 hours, resulted in the formation of **3.15** in 63% yield.



(3.14) **63 % (3.15)**

Scheme 3.2.5: Synthesis of ^{19}F-fluorinated reference 3.15

3.3 ^{18}F-labelling of aryl prosthetic groups

Experiments employing fluorine-18 were carried out in collaboration with Dr. Stefan Verhoog. For safety purposes, when handling ionising radiation, no less than two people were present during radiosynthesis.

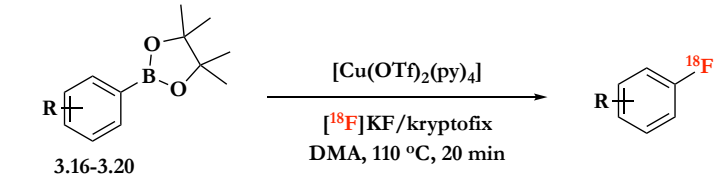
From previous investigations in the Gouverneur group,[36] two sets of reaction conditions were utilised for the copper-mediated prosthetic group radiofluorination: (**A**) 0.02 mmol of aryl pinacol boronate reagent and 0.03 mmol of $Cu(OTf)_2(py)_4$ in DMA for electron poor substrates and (**B**) 0.02 mmol of aryl pinacol boronate reagent and 0.02 mmol of $Cu(OTf)_2(py)_4$ in DMA for electron-rich substrates.

The general reaction procedure was as follows: a small aliquot (25-30 MBq, 10–50 μL) of a solution of ^{18}F-KF/K_{222} in anhydrous MeCN was dispensed into a V-vial containing $Cu(OTf)_2(py)_4$ (0.03 or 0.02 mmol), aryl pinacol boronate (0.02 mmol) and a magnetic stirrer bar. Air was flushed through the reaction vial using a syringe, and then 300 μL of solvent DMA was added *via* syringe. The sealed vial was then heated at 110 °C for 20 minutes. The reaction was quenched by addition of water (200 μL). An aliquot of the reaction mixture was removed for analysis by radio-TLC and radio-HPLC for determination of reaction conversion and product identification, respectively. Radiochemical conversion (RCC) for each substrate was calculated by multiplying the conversion obtained from radio-TLC by the radiochemical purity (RCP) determined from the radio-HPLC (analogous to Section 2.4.1).

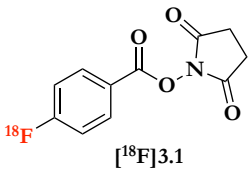
Employing the above protocol afforded four ^{18}F-aryl prosthetic groups in a single radiosynthetic step under a common set of reaction conditions (Table 3.3.1). Modest to high RCCs were obtained for all substrates. As proposed, this methodology enabled a unified, single-step radiosynthesis of the elected ^{18}F-aryl prosthetic groups from bench-stable starting materials. This result improves operational ease for

prosthetic group radiosynthesis by eliminating the need for unique and often challenging multi-step reaction sequences.

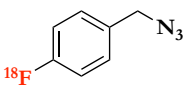
Table 3.3.1: Radiosynthesis of ^{18}F-aryl prosthetic groups



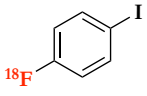
3.16-3.20



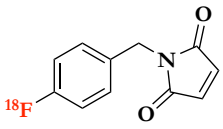
[^{18}F]3.1
61% ± 6 (n = 4)[a]



[^{18}F]3.9
47% ± 2 (n = 4)[b]



[^{18}F]3.12
64% ± 5 (n = 4)[a]



[^{18}F]3.15
74% ± 3 (n = 4)[b]

All values reported as RCC. [a]Conditions: 0.02 mmol of SM and 0.03 mmol of $Cu(OTf)_2(py)_4$. [b]Conditions: 0.02 mmol of SM and 0.02 mmol of $Cu(OTf)_2(py)_4$.

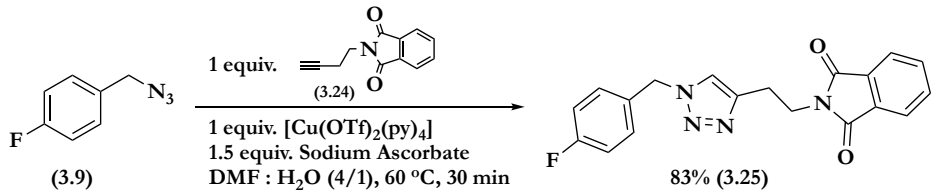
3.4 Post labelling conjugation

To demonstrate the feasibility of the copper-mediated ^{18}F-fluorination of aryl prosthetic groups, three post-labelling conjugation reactions were performed: (1) the copper-catalysed alkyne azide cycloaddition (CuAAC), (2) a thiol-alkylation coupling, and (3) an acylation coupling reaction.

3.4.1 Copper-catalysed alkyne azide cycloaddition

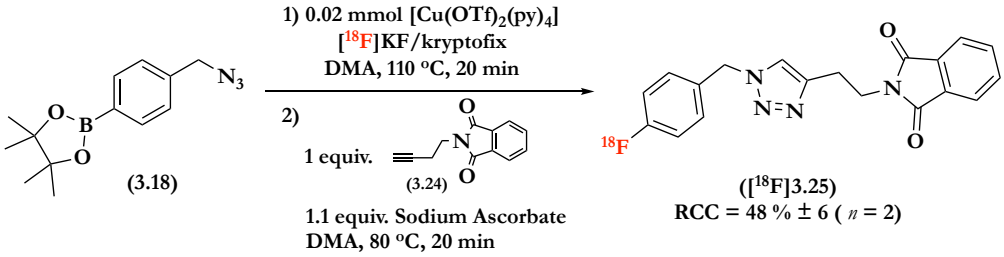
The CuAAC forming 1,2,3-triazoles is a chemoselective chemical transformation employed prevalently for the conjugation of ^{18}F-labelled prosthetic groups.[40,41]

Phthalimide **3.24** was elected as coupling partner for the CuAAC. Initally, **3.24** was utilised to obtain fluorine-19 reference compound **3.25**, which was required for radiosynthetic product identification (Scheme 3.4.1).



Scheme 3.4.1: Synthesis of 3.25 *via* copper catalysed alkyne-azide cycloaddition

Thereafter, the radiosynthesis of **[^{18}F]3.25** *via* one-pot two-step CuAAC reaction followed. Upon formation of **[^{18}F]3.9** (section 3.3), 1.1 equivalents of sodium ascorbate in 200 µL of H_2O and 1 equivalent of **3.24** in 100 µL of DMA was added to the reaction vial *via* syringe. The reaction was heated at 80 °C for 20 minutes and subsequently quenched with 1 mL of H_2O. An aliquot was removed for analysis by radio-HPLC and radio-TLC. The RCC for the one-pot CuAAC was calculated to be 48% ± 6 (n = 2) over two radiosynthetic steps. Figure 3.4.1 shows the radio-HPLC trace of **[^{18}F]3.25** overlaid with the UV trace of reference compound **3.25**, confirming product identity.



Scheme 3.4.2: One-pot two-step copper catalysed alkyne azide cycloaddition

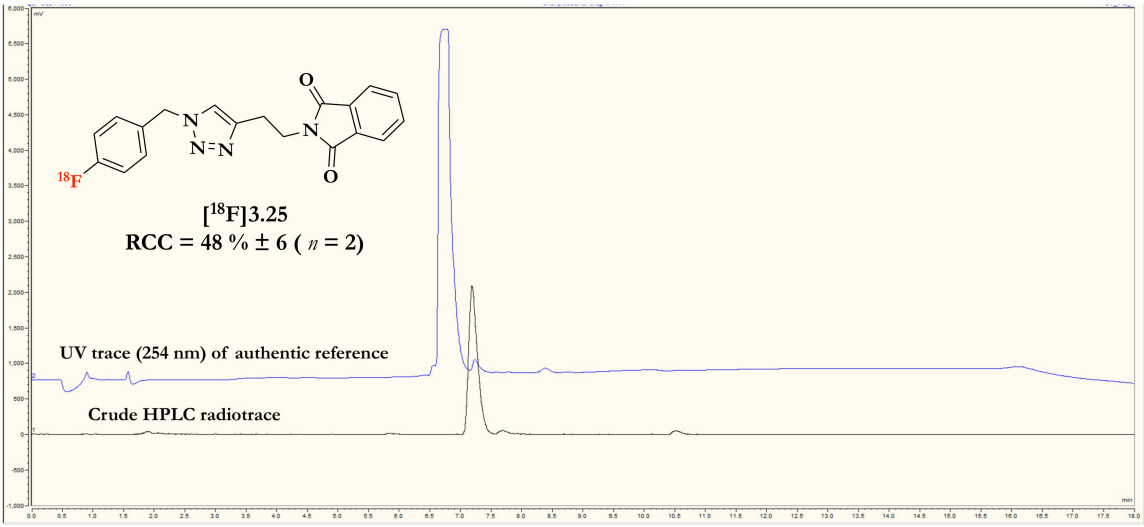
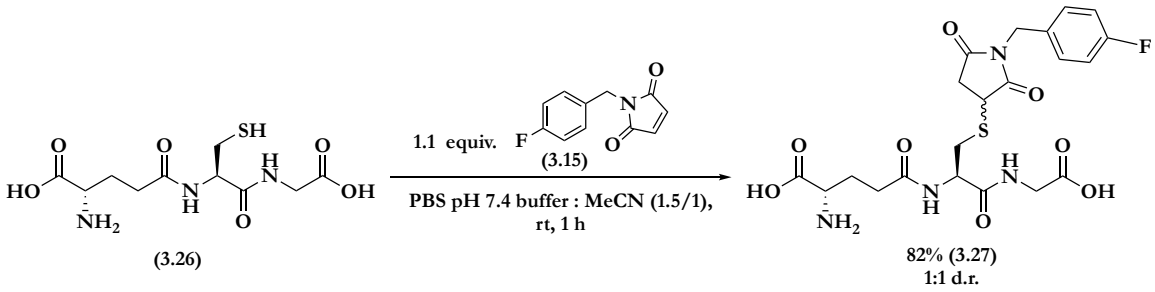


Figure 3.4.1: Radio-HPLC of [^{18}F]3.25

3.4.2 Thiol-alkylation with [^{18}F]3.15

The thiol-alkylation of cysteine containing peptides or proteins with ^{18}F-maleimide prosthetic groups, is a chemoselective labelling technique that frequently affords ^{18}F-labelled thioether conjugated products, in high RCYs under mild reaction conditions.[6]

To evaluate the efficacy of **[^{18}F]3.15** as a prosthetic group, cysteine-containing tripeptide glutathione **(3.26),** was elected as coupling partner for thiol-alkylation. Reference compound **3.27** was synthesised in 82% yield prior to radiosynthesis (Scheme 3.4.3) and purification was achieved *via* simple extraction with H_2O following solvent removal and addition of 1 mL of dichloromethane to the reaction vial.



Scheme 3.4.3: Construction of reference compound 3.27 *via* thiol-alkylation

Subsequently, **[^{18}F]3.15** was prepared from 135–1187 MBq of dried [^{18}F]fluoride, resulting in 32–379 MBq of isolated product with a RCY of 33% ± 7 (n = 3) in a total synthesis time of 30–40 minutes from aqueous [^{18}F]fluoride (Table 3.4.1). To calculate the RCY for **[^{18}F]3.15**, 10 mL of H_2O was added to the V-vial after 20 minutes. The contents were then loaded onto a C-18 SepPak Plus cartridge. Flushing the cartridge with 2 mL of H_2O, drying with air and subsequent elution with 2 mL of MeCN afforded **[^{18}F]3.15**. The RCY was then calculated by comparing the initial activity (MBq) to the percentage of activity (MBq) in the MeCN elute (Table 3.4.1).

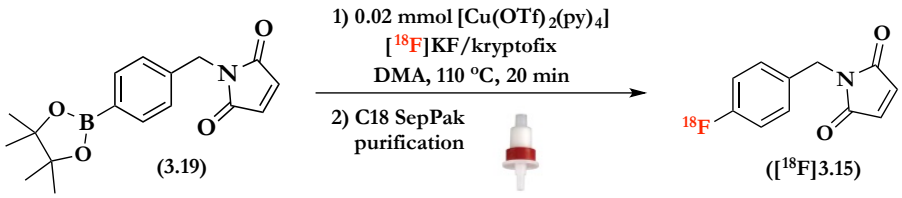


Table 3.4.1: Isolation of [^{18}F]3.15 *via* C18 SepPak purification

Entry	Starting Activity (MBq)	Isolated Activity (MBq)	RCP[%]	RCY[%]
1	134.9	32.2	98	23
2	1178	379	99	32
3	469	196	99	42
RCY and Standard Error of the Mean			33% ± 7 (n = 3)	

Aliquots (150-400 µl) of the 2 mL MeCN solution containing **[^{18}F]3.15** were utilized for the ensuing alkylation with **3.26**. Full conversion to **[^{18}F]3.27** was observed under all conditions trialed (Table 3.4.2). A RCC of 99% ± 0 (n = 2) was calculated for **[^{18}F]3.27**. Figure 3.4.2 displays the radio-HPLC trace of **[^{18}F]3.27**, used for product identification and RCC determination.

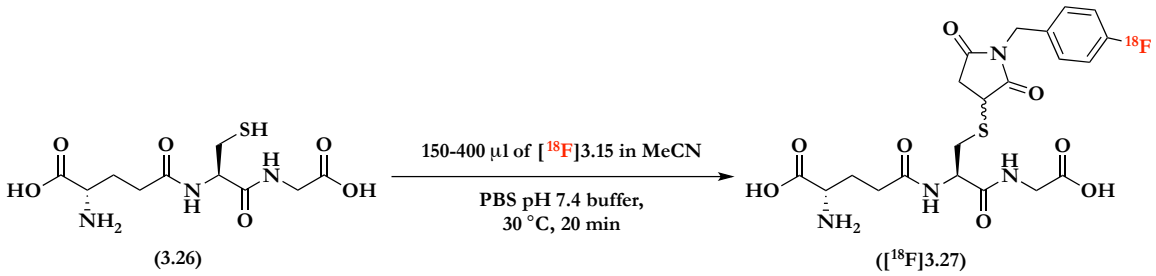


Table 3.4.2: Formation of [^{18}F]3.27 *via* S-alkylation

Entry	GSH[µmol]	Buffer[µl]	RCC[%]
1	6	500	>99%[ab]
2	3	500	>99%[ab]
3	3	1000	>99%[ab]

[a]Small aliquots (150-400 µl) of the 2 mL MeCN solution containing **[^{18}F]3.15** after C18 SepPak purification were used.[b](n = 2).

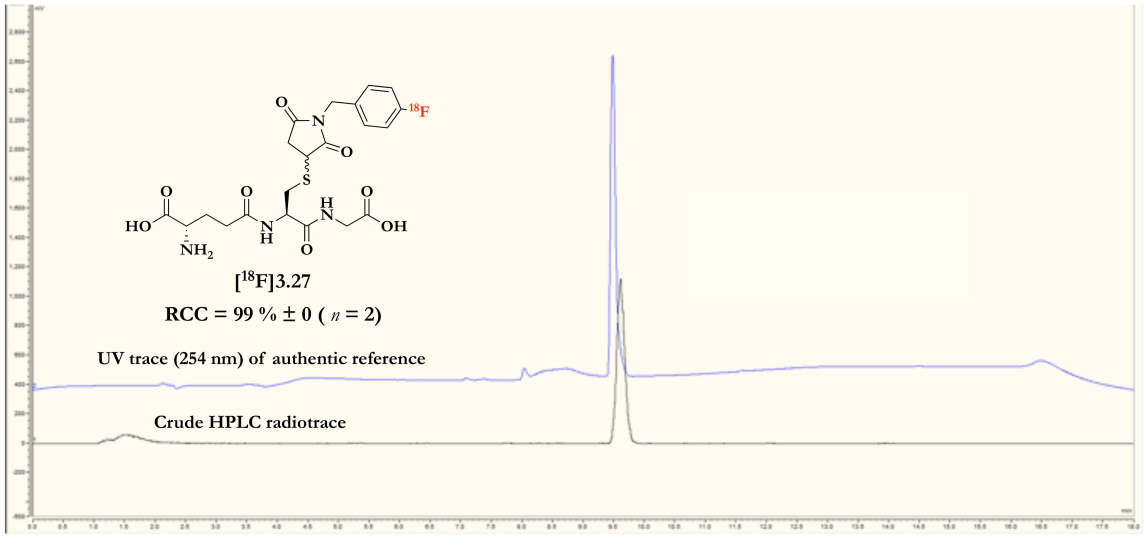
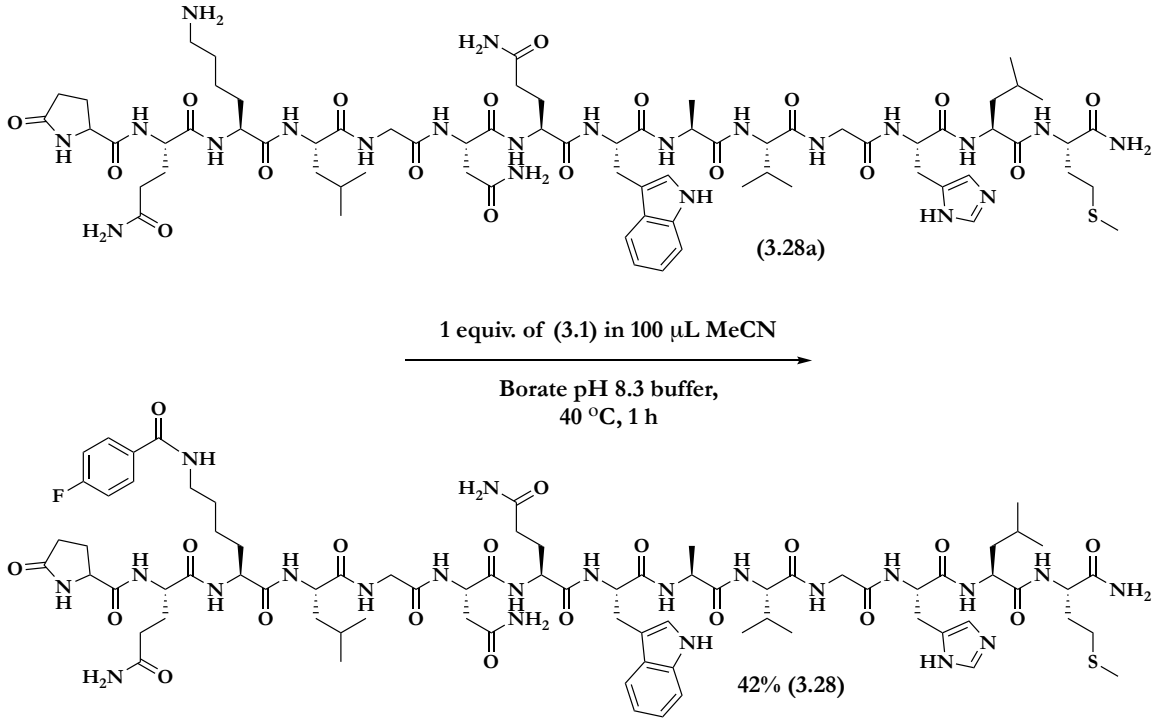


Figure 3.4.2: Radio-HPLC of [^{18}F]3.27

3.4.3 Acylation with [^{18}F]3.1

Acylation of biomolecules using **[^{18}F]3.1** is the most prevalent transformation utilised for the indirect incorporation of fluorine-18 *via* prosthetic group conjugation.[2,6] [Lys^3]-bombesin a 14-mer neuropeptide, which binds the gastrin-releasing receptor (GRPR)* with high-affinity, was nominated as coupling partner for site-selective acylation with **[^{18}F]3.1.** Initially, reference compound **3.28** was synthesised *via* acylation of [Lys^3]-bombesin **(3.28a)** with **3.1** in 42% yield (Scheme 3.4.4). Purification of **3.28** was achieved by semi-preparative HPLC using a Phenomenex C-18 luna semi-prep column.

* GRPR is overexpressed on a plethora of tumor cells, including prostate and breast tumor cells.[42]



Scheme 3.4.4: Synthesis of reference compound 3.28 *via* acylation

Thereafter, **[^{18}F]3.1** was prepared from dried [^{18}F]fluoride and three different purification protocols were trialed prior to conjugation with **3.28a**. The results are summarised in Table 3.4.3. For operational simplicity, purification *via* Oasis WAX cartridge (WAX = Weak Anion Exchange) was advocated **(**Table 3.4.3 entry 2). This methodology enabled successful removal of side-products and facilitated rapid isolation of **[^{18}F]3.1** in high RCP (97%). To calculate the RCY for **[^{18}F]3.1** using this protocol **(**Table 3.4.3 entry 2), 10 mL of H_2O was added to the V-vial after 20 minutes. The contents were then loaded onto the Oasis WAX cartridge. Flushing the cartridge with 2 mL of H_2O, drying with air and subsequent elution with 2 mL of MeCN afforded **[^{18}F]3.1**. The RCY was then calculated by comparing the initial activity (MBq) to the percentage of activity (MBq) in the MeCN elute.

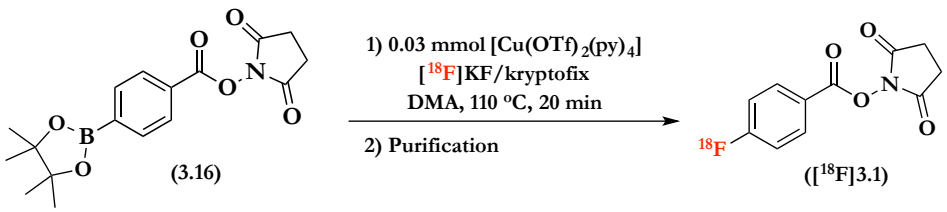
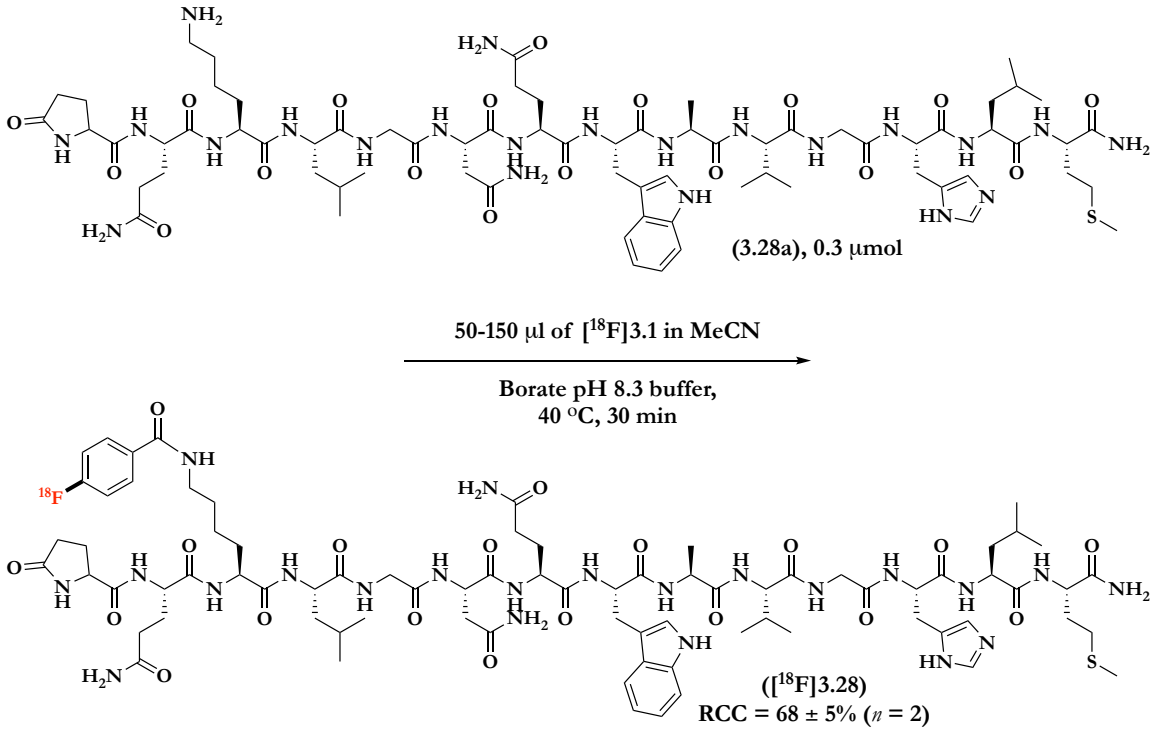


Table 3.4.3: Isolation of [^{18}F]3.1

Entry	Purification Method	Synthesis Time[min]	RCP[%]	RCY[%]
1	Water C18	62	91	26 ± 4[a]
2	**Oasis WAX**	**65**	**97**	**18 ± 4[b]**
3	Prep-HPLC	105	>98	11[c]

[a](n = 3).[b](n = 2).[c](n = 1)

Subsequently, the 2 mL MeCN solution containing **[^{18}F]3.1** was concentrated to approx. 1 mL under a stream of N_2 at 70 °C and an aliquot (50-150 µL) utilised for the succeeding acylation with [Lys^3]-bombesin **(3.28a).** Full conversion of **[^{18}F]3.1** was observed and a RCC of 68 ± 5% (n = 2) was calculated for **[^{18}F]3.28** (Scheme 3.4.5).



Scheme 3.4.5: Radiosynthesis of [^{18}F]3.28 *via* acylation

Figure 3.4.3 depicts the radio-HPLC trace of **[^{18}F]3.28**, used for product identification and RCC determination. Of the two additional peaks observed in the crude radio-HPLC of **[^{18}F]3.28**, the peak at 18.8 minutes (closest to **[^{18}F]3.28** reference) was identified as 4-[^{18}F]fluorobenzoic acid *via* spiking experiment, however the identity of the peak at 16.1 minutes is still to be established.

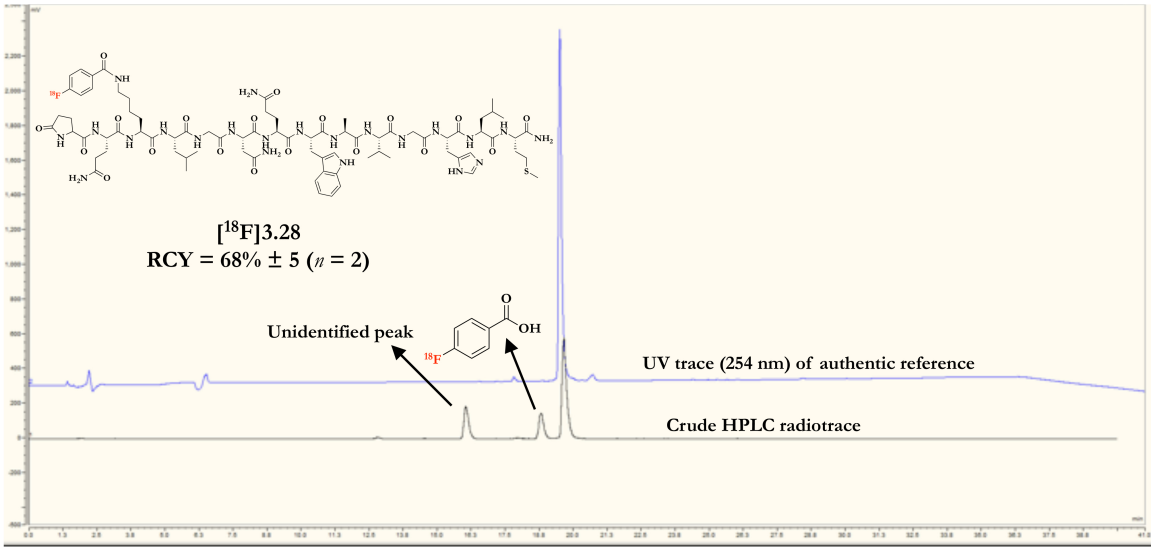
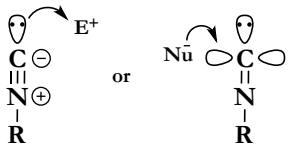


Figure 3.4.3: Radio-HPLC of [^{18}F]3.28 used for product identification and RCC determination

Having demonstrated that the copper-mediated ^{18}F-fluorination of arenes could be utilised to access ^{18}F-labelled prosthetic groups and perform post-labelling conjugation transformations, we next questioned whether this methodology could be employed to create a novel ^{18}F-labelled aryl synthon.

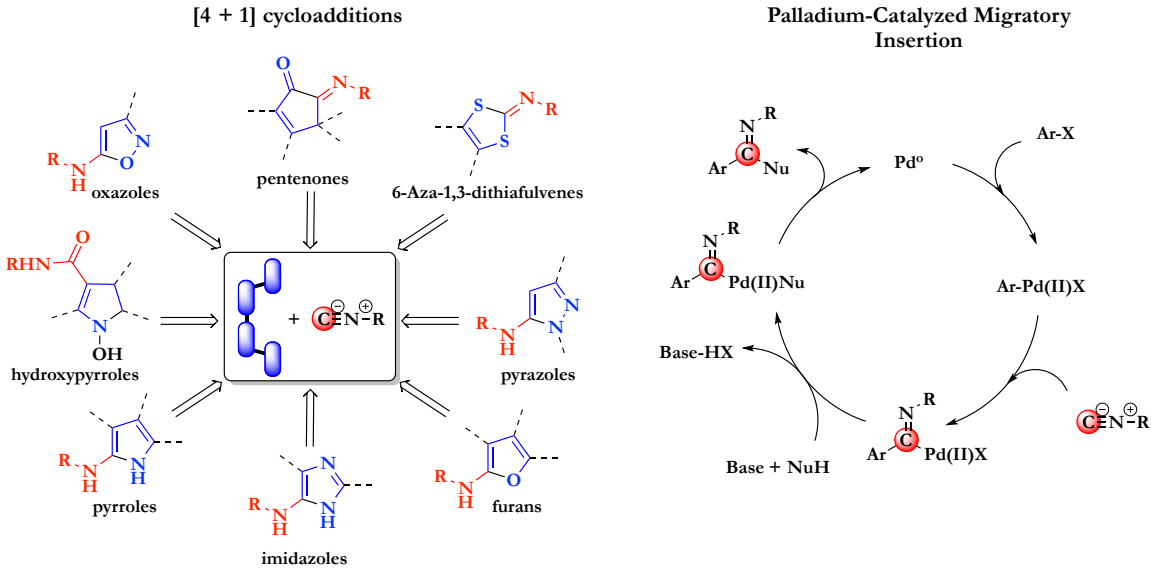
3.5 ^{18}F-Labelling of aryl isocyanide

Owing to their unique divalent stability at carbon, isocyanides (formally known as isonitriles) possess a unique reactivity profile.[43]



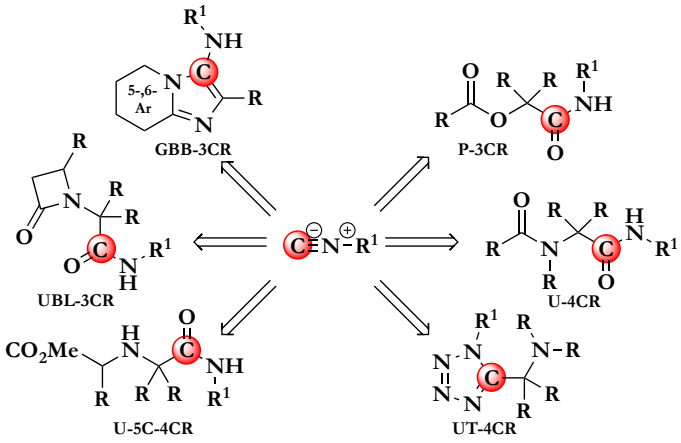
Scheme 3.5.1: Ambiphilic reactivity of isocyanide

A plethora of significant chemical transformations have been developed exploiting the inimitable nature of isocyanides, including [4 + 1] cycloadditions and palladium-catalyzed migratory insertions (Scheme 3.5.2).[43-47]



Scheme 3.5.2: Demonstration of Isocyanide based [4 + 1] cycloadditions and Pd-Catalyzed Migratory Insertions

Arguably, the most useful and ubiquitous synthetic protocols employing isonitriles are the isocyanide based multi-component reactions (IMCRs).[48] These convergent reactions enable the rapid construction of architecturally complex molecular scaffolds from simple starting materials (Scheme 3.5.3) Their application has been successful in drug discovery, resulting in the development of a host of potent chemical probes and compound libraries.[49,50]

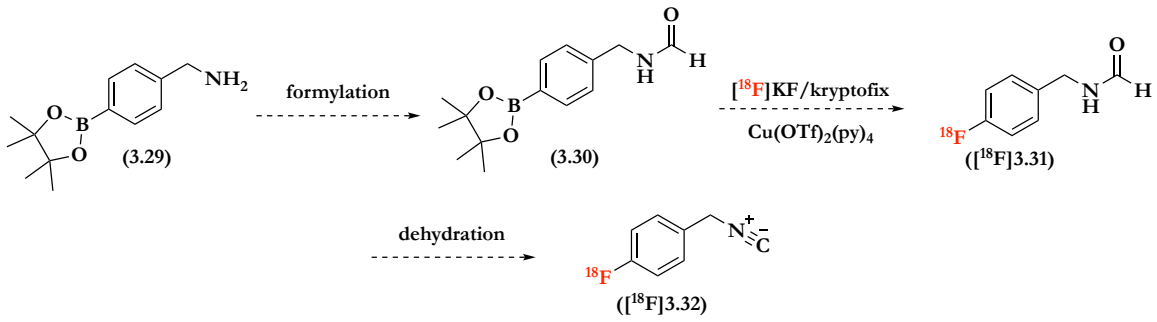


Scheme 3.5.3: Isocyanide based multi-component reactions (IMCRs)

Despite the abundance of isocyanide-containing compounds and the benefit they would have on the field of synthetic radiochemistry (allowing for the construction of complex structures/heterocycles in a single radiosynthetic step), a thorough literature search failed to identify a single viable method for accessing an ^{18}F-labelled isonitrile prosthetic group. Therefore we sought to develop a prosthetic group of this nature by employing the aforementioned copper-mediated nucleophilic ^{18}F-fluorination of arenes.[35]

3.5.1 Preliminary investigations

The dehydration of *N*-formamides with di/triphosgene[51,52] or phosphoryl chloride ($POCl_3$)[53] was used as inspiration for our synthetic efforts toward ^{18}F-labelled aryl isocyanide **[^{18}F]3.32**. The proposed synthetic pathway to **[^{18}F]3.32** is shown in Scheme 3.5.4.



Scheme 3.5.4: Proposed synthetic pathway toward [^{18}F]3.32

It was postulated that radiosynthesis of **[^{18}F]3.32** could be realised in 3 synthetic steps. Precursor **3.30** would be accessed *via* formylation of commercially available **3.29**, subsequent copper-mediated nucleophilic ^{18}F-fluorination of **3.30** would yield **[^{18}F]3.31** and a final post-labelling dehydration of **[^{18}F]3.31** would potentially afford **[^{18}F]3.32** (Scheme 3.5.4).

3.5.1.1 Synthetic efforts toward 3.30

Initial studies began with the attempted synthesis of **3.30** *via* formylation of commercially available **3.29.** Table 3.5.1 discloses the conditions attempted for formation of **3.30**. Unfortunately, recovery of starting material **3.29** was observed under all parameters tested.

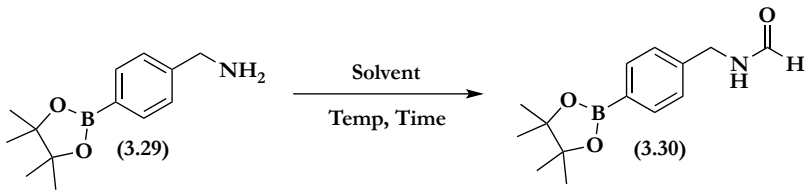
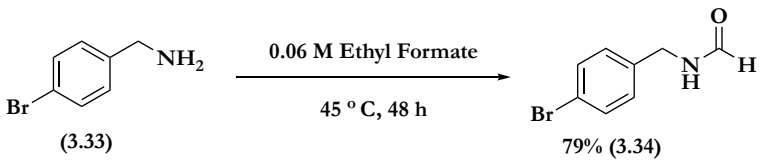


Table 3.5.1: Attempted synthesis of 3.30

Entry	Time[hr]	Temp[° C]	Solvent	Yield[%][a]
1	48	45	Ethyl Formate	0
2	48	60	Ethyl Formate	0
3	16	80	Formic Acid	0

[a]Reaction conducted on 0.05 mmol scale at 0.04 M solvent concentration.

As a consequence, formylation of commercially available **3.33** with ethyl formate was tested, resulting in formation of **3.34** in 79% yield (Scheme 3.5.5).[54]



Scheme 3.5.5: Formylation of 3.33

Next, Miyaura borylation[55] was trialled on **3.34** (Table 3.5.2). Formation of **3.30** was observed for all conditions examined. However, a catalytic loading of 10 mol% was needed for full consumption of **3.34** (entries 5-6). This was a requirement to aid facile product purification *via* silica gel column chromatography.

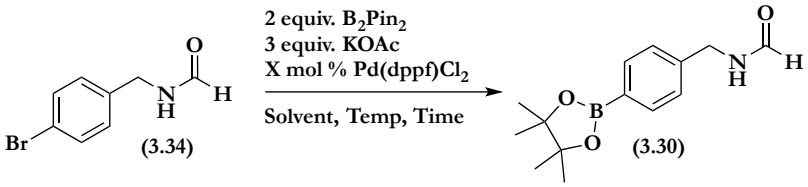


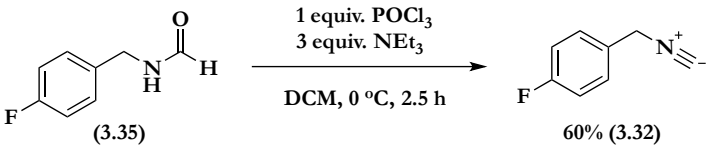
Table 3.5.2: Optimisation of Miyaura Borylation

Entry	Pd(dppf)Cl$_2$ [mol %]	Solvent	Temp[° C]	Time[hr]	Conversion[%]	Yield[%]
1	5	Toluene	85	24	70	65[a]
2	5	DMF	85	24	75	70[a]
3	5	Toluene	110	24	75	68[a]
4	5	DMF	110	24	80	75[a]
5	**10**	**Toluene**	**85**	**24**	**100**	**84[b]**
6	**10**	**DMF**	**85**	**24**	**100**	**87[b]**

[a] Yields obtained *via* ^{1}H NMR analysis using an internal standard. [b]Isolated yield.

3.5.1.2 Synthesis of 3.32 a reference for ^{18}F incorporation

To identify ^{18}F radiosynthetic products, ^{19}F analogues must be synthesised to provide a direct reference for ^{18}F incorporation *via* radio-HPLC. Therefore, $POCl_3$ dehydration of **3.35** was examined, enabling formation of ^{19}F reference **3.32** in 60% yield *via* silica gel column chromatography (Scheme 3.5.6).



Scheme 3.5.6: Formation of 3.32 *via* $POCl_3$ mediated dehydration

3.5.1.3 Optimisation of dehydration parameters for isocyanide formation

Our next aim was to trial various dehydration conditions for formation of **3.32**. The ideal radiosynthetic protocol to form [^{18}F]**3.32** would entail a rapid dehydration of

precursor **[^{18}F]3.31** under mild reaction conditions. Table 3.5.3 depicts the optimisation conducted. In order to emulate the constraints of a radiosynthetic environment, all reactions shown in Table 3.5.3 were quenched after 30 minutes.

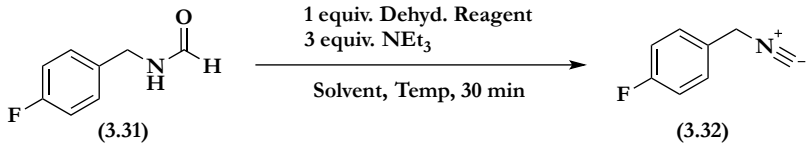


Table 3.5.3: Dehydration optimisation forming 3.32

Entry	Dehyd. Reagent	Solvent	Temp[° C]	Yield[%][a]
1	**$POCl_3$**	**DCE**	**25**	**42**
2	**Triphosgene**	**DCE**	**25**	**45[b]**
3	**$POCl_3$**	**MeCN**	**25**	**39**
4	**Triphosgene**	**MeCN**	**25**	**43[b]**
5	$POCl_3$	DCE	25	34[c]
6	Triphosgene	DCE	25	37[d]
7	$POCl_3$	DCE	75	17
8	$POCl_3$	MeCN	85	15
9	Triphosgene	DCE	75	20[b]
10	Triphosgene	MeCN	85	18[b]
11	TCT	DCE	75	0
12	*p*-TSCl	DCE	25	17[e]
13	CCl_4	DCE	25	<5[f]
14	CCl_4	DCE	60	21[f]

[a]Yields obtained *via* ^{19}F NMR analysis using an internal standard. [b] 0.5 equiv. of triphosgene. [c]2 equiv. of $POCl_3$ and 6 equiv. of NEt_3. [d]1 equiv. of triphosgene and 6 equiv. of NEt_3. [e]3 equiv. of DABCO as base.[56] [f]2 equiv. of triphenylphosphine (PPh_3) added to reaction.[57]

The use of both $POCl_3$ and triphosgene at room temperature proved optimal (entries 1-4). Attempted synthesis with known dehydrating reagents 2,4,6-trichloro[1,3,5]triazine cyanuric chloride (TCT),[58,59] *p*-toluene sulfonyl chloride (*p*-TSCl),[56] and carbon tetrachloride (CCl_4)[57] failed to return **3.32** in satisfactory yield (entries 11-14).

3.5.2 Use of 3.32 for proposed post-labelling conjugation

Our next objective was to investigate potential post-labelling conjugation reactions employing **3.32**. Two transformations were proposed: a one-pot Ugi reaction[60] and an isocyanide-tetrazine [4 + 1] cycloaddition.[44]

Taking inspiration from a recently disclosed study by Dömling,[60] a one-pot dehydration and subsequent Ugi reaction was attempted employing **3.31** as starting material (Table 3.5.4) It was hypothesised that this synthetic strategy would increase operational ease during radiosynthesis, allowing for a one-pot radioconvergent synthesis to be achieved from a stable and benign benzyl formamide precursor (**3.31**).

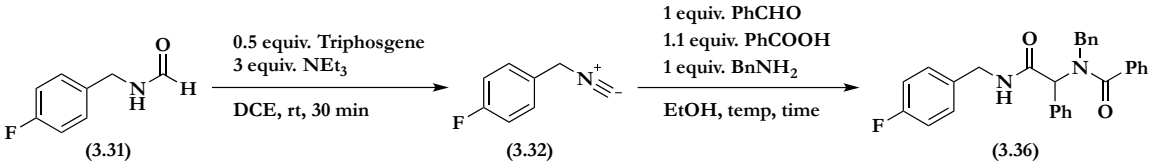


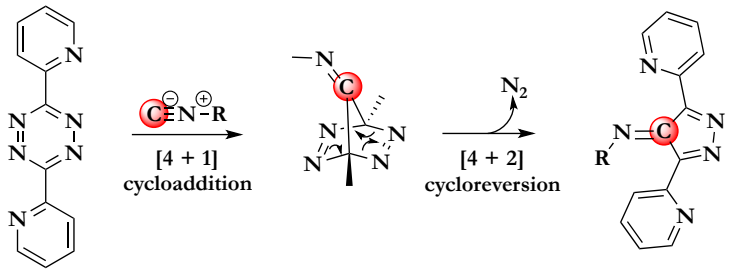
Table 3.5.4: Optimisation of one-pot Ugi-reaction

Entry	**3.32** [equiv.]	Conc.[M]	Temp[° C]	Time[hr]	Conversion[%][a]
1	1	0.5	25	18	32
2	1	0.5	50	18	48
3	1	0.5	80	18	58
4	1	0.5	80	0.5	19
5	1	1	80	0.5	44
6	**0.2**	**0.5**	**80**	**0.5**	**87**

[a]Conversion to **3.36** from **3.32** obtained *via* ^{19}F NMR analysis using an internal standard.

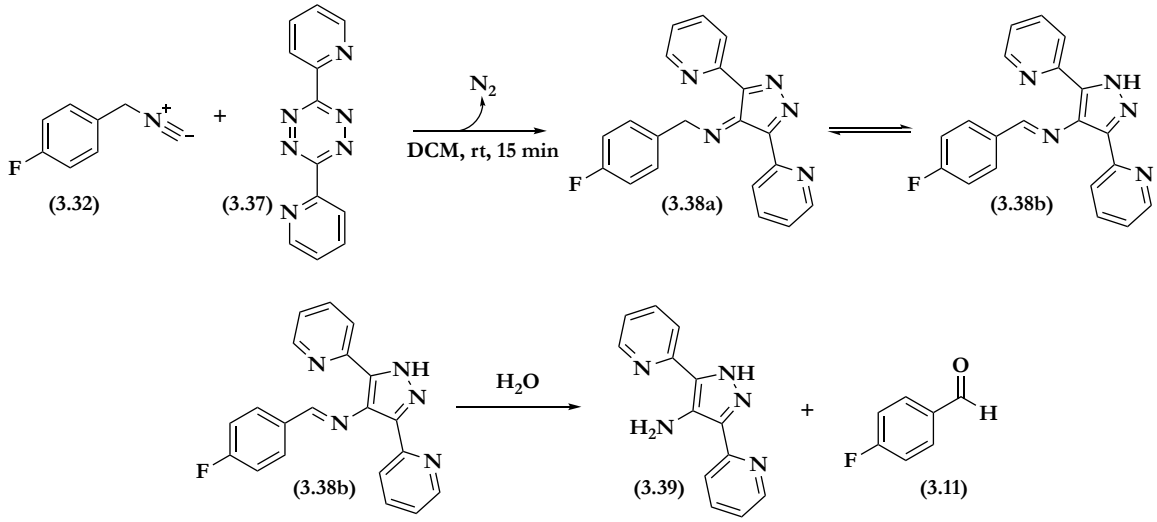
Reaction temperature, time and solvent concentration were varied in an effort to optimise the one-pot Ugi reaction (Table 3.5.4). We discovered that the multi-component step of the reaction is highly dependent on temperature and concentration. Reducing the stoichiometry of **3.32** had a beneficial effect on formation of **3.36** (entry 6). This observation boded well for translation of this methodology to a radiochemical setting.

The isocyanide-tetrazine [4 + 1] cycloaddition reaction is a transformation that has recently been employed for biocompatible ligation in aqueous media and is the first example of its kind using isocyanides (Scheme 3.5.7).[44]



Scheme 3.5.7: Isocyanide-tetrazine [4 + 1] cycloaddtion reaction

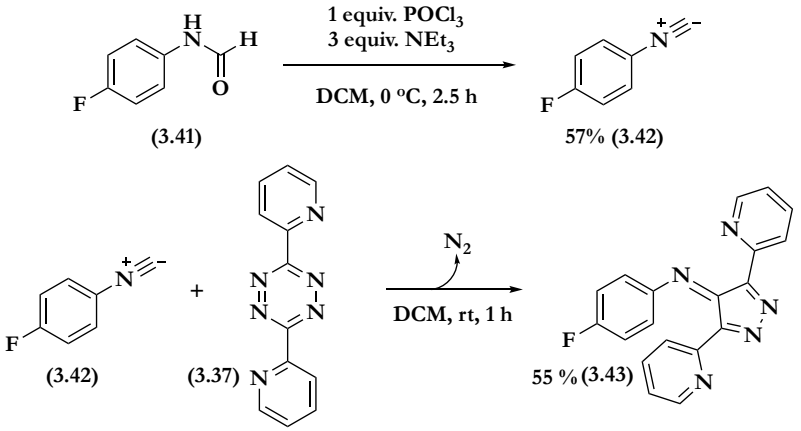
Isocyanide-tetrazine [4 + 1] cycloaddition was performed utilising **3.32.** Unfortunately, upon reaction of primary isocyanide **3.32** with **3.37**, the expected cycloaddition product **3.38b** could not be isolated. This is potentially due to hydrolysis of **3.38b**, forming aminopyrazole **3.39** and 4-fluorobenzaldehyde **(3.11)** (Scheme 3.5.8).[44,61]



Scheme 3.5.8: Isocyanide-tetrazine [4 + 1] cycloaddition of 3.32 and 3.37

Interestingly, structural modification of the isonitrile reaction partner **(3.42)** enabled successful formation of cycloaddition adduct **3.43** (Scheme 3.5.9). 1-Fluoro-4-isocyanobenzene **(3.42)** was synthesised *via* $POCl_3$ dehydration of **3.41** and subjected to [4 +1] cycloaddition with **3.37.** The desired product **(3.43)** was isolated in 55% yield after

one hour stirring in DCM at room temperature (Scheme 3.5.9). The release of nitrogen was less vigorous for this reaction, potentially owing to the attenuated nucleophilicity of **3.42** in comparison to **3.32.**

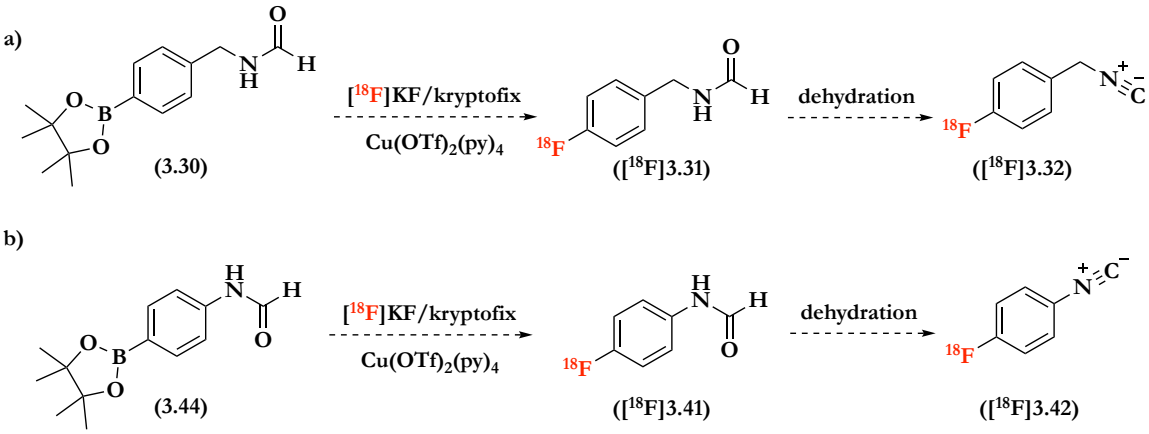


Scheme 3.5.9: Successful isocyanide-tetrazine [4 + 1] cycloaddition reaction from 3.42

3.5.3 Attempted radiosynthesis of ^{18}F-aryl isocyanide

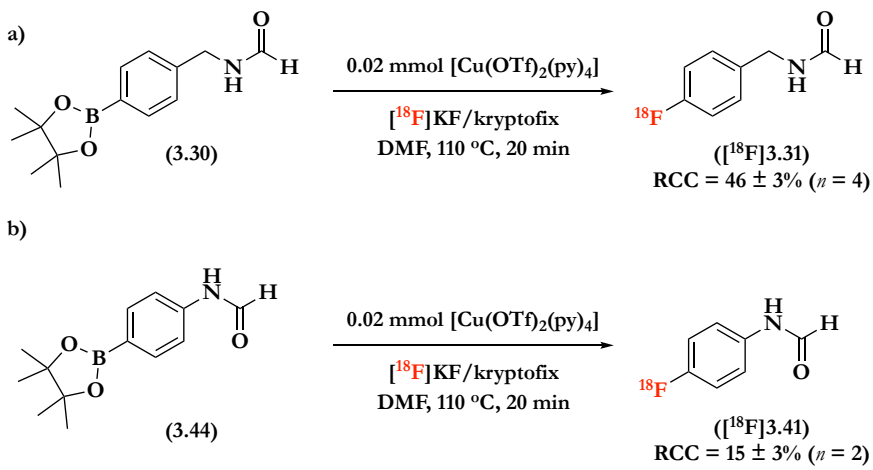
Experiments employing fluorine-18 were carried out in collaboration with Dr. Sean Preshlock. For safety purposes, when handling ionising radiation, no less than two people were present during radiosynthesis.

^{18}F-Aryl isocyanides **[^{18}F]3.31** and **[^{18}F]3.42** were nominated for radiosynthesis. This would initially require the construction of both **[^{18}F]3.31** and **[^{18}F]3.41,** followed by subsequent post-labelling dehydration (Scheme 3.5.10).



Scheme 3.5.10: Proposed radiosynthesis of elected targets [^{18}F]3.32 and [^{18}F]3.42

The radiosynthesis of **[^{18}F]3.31** and **[^{18}F]3.41** was successful under copper-mediated ^{18}F-fluorination conditions as illustrated in Scheme 3.5.11. The general reaction procedure was as follows: an aliquot of dried [^{18}F]KF/K_{222} residue in anhydrous MeCN was dispensed into a V-vial containing $Cu(OTf)_2(py)_4$ (0.02 mmol), **3.30/3.44** (0.02 mmol) and a magnetic stirrer bar. Air was flushed through the reaction vial, and 300 µL of DMF was added *via* syringe. The sealed vial was then heated at 110 °C for 20 minutes. The reaction was quenched by addition of water (200 µL). An aliquot was removed for analysis by radio-TLC and HPLC for radiochemical conversion and product identification. This methodology afforded **[^{18}F]3.31** and **[^{18}F]3.41** in 46% ± 3 (n = 4) and 15% ± 3 (n = 4) RCC, respectively.



Scheme 3.5.11: Radiosynthesis of [^{18}F]3.31 and [^{18}F]3.41

Next, isocyanide formation was attempted from **[^{18}F]3.31** and **[^{18}F]3.41.** A batch-scale synthesis of **[^{18}F]3.31** and **[^{18}F]3.41** ensued, whereby, a 5 mL vial containing a dried [^{18}F]KF/$K_{2.2.2}$ complex was purged with 30 mL of air using a syringe and then a solution of **3.30/3.44** (0.02 mmol) and Cu(OTf)2(py)4 (14 mg, 0.02 mmol) in anhydrous DMF (400 µL) was added. The mixture was heated at 120 °C for 20 minutes in a sealed vial with stirring. The reaction solution was diluted with 8 mL de-ionized H_2O and loaded onto an Oasis HLB Plus LP Extraction Cartridge. Flushing the cartridge with 2 mL of H_2O, drying with air and subsequent elution with 2 mL of MeCN afforded **[^{18}F]3.31/[^{18}F]3.41**

in 11% ± 4 (*n* = 2) and 6% ± 2 (*n* = 2) RCY, respectively. Aliquots (20-40 µl) of the 2 mL MeCN solution containing either **[^{18}F]3.31** or **[^{18}F]3.41** were utilised for post-labelling dehydration optimisation studies (Table 3.5.5).

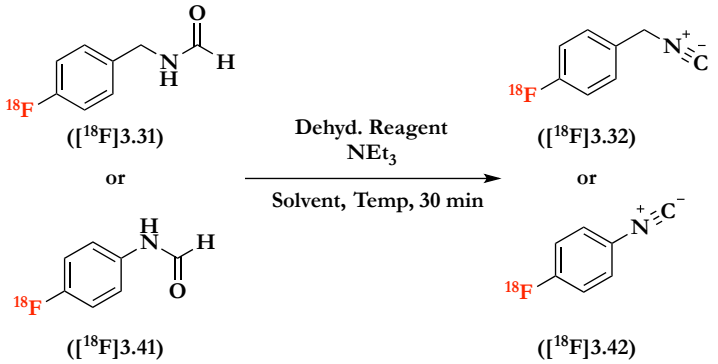


Table 3.5.5: Attempted radiosynthesis of [^{18}F]3.32 and [^{18}F]3.42 *via* post-labelling dehydration

Entry	S.M	Dehyd. Reagent	Solvent	Temp[° C]	RCC[%]
1	[^{18}F]3.31	Triphosgene[a]	DCE	25	-
2	[^{18}F]3.31	Triphosgene[a]	MeCN	25	-
3	[^{18}F]3.31	Triphosgene[b]	DCE	25	-
4	[^{18}F]3.31	Triphosgene[af]	DCE	25	-
5	[^{18}F]3.31	$POCl_3$[c]	DCE	25	-
6	[^{18}F]3.31	$POCl_3$[c]	MeCN	25	-
7	[^{18}F]3.31	Triphosgene[d]	DCE	25	-
8	[^{18}F]3.31	$POCl_3$[e]	DCE	25	-
9	[^{18}F]3.31	Triphosgene[a]	DCE	60	-
10	[^{18}F]3.41	Triphosgene[a]	DCE	25	-
11	[^{18}F]3.41	Triphosgene[a]	MeCN	25	-
12	[^{18}F]3.41	Triphosgene [b]	DCE	25	-
13	[^{18}F]3.41	$POCl_3$[c]	DCE	25	-
14	[^{18}F]3.41	$POCl_3$[c]	MeCN	25	-
14	[^{18}F]3.41	Triphosgene[d]	DCE	25	-
16	[^{18}F]3.41	Triphosgene[a]	DCE	60	-

[a]0.5 equiv. of triphosgene and 3 equiv. of NEt_3. [b]0.5 equiv. of triphosgene and 3 equiv. of DIPEA. [c] 1 equiv. of $POCl_3$ and 3 equiv. of NEt_3. [d]3 equiv. of triphosgene and 10 equiv. of NEt_3. [e]6 equiv. of $POCl_3$ and 10 equiv. of NEt_3.[f]Reaction run for 1 hr.

A solution of dehydrating reagent in 100 μL of DCE/MeCN and a solution of NEt_3 in 100 μL of DCE/MeCN was added *via* syringe to the V-vial containing either **[^{18}F]3.31** or **[^{18}F]3.41.** The sealed vial was stirred for 30 minutes before being quenched by addition of ethanol/water, (3:1, 200 μL). An aliquot of the reaction mixture was removed for analysis by radio-TLC and radio-HPLC for determination of reaction conversion and product identification, respectively. Unfortunately, under all reaction parameters trialed, radiosynthesis of **[^{18}F]3.32** and **[^{18}F]3.42** could not be realised. Increase in equivalents of dehydrating reagent, temperature and reaction time all failed to yield the desired radiosynthetic products. This outcome may be due to the absence of an inert atmosphere used during radiosynthesis to facilitate ease of operation.

3.6 Conclusion and future work

In conclusion, this chapter has outlined the successful synthesis of four popular ^{18}F-aryl prosthetic groups in a single radio-synthetic step from bench stable starting materials. Three post-labelling conjugation reactions were successfully implemented: (1) the copper-catalysed alkyne azide cycloaddition (CuAAC), (2) a thiol-alkylation coupling and (3) an acylation coupling reaction.

Attempts to synthesise an ^{18}F-arylisocyanide *via* copper-mediated ^{18}F-fluorination were unsuccessful. In the future, further radiosynthetic optimisation employing different dehydration conditions may facilitate access to this important motif.

3.7 References

(1) Miller, P. W.; Long, N. J.; Vilar, R.; Gee, A. D. *Angew. Chem. Int. Ed.* **2008**, *47* (47), 8998–9033.
(2) Kuhnast, B.; Dolle, F. *Curr. Radiopharmaceuticals* **2010**, *3*, 174–201.
(3) Vaidyanathan, G.; Zalutsky, M. R. *Nat. Protoc.* **2006**, *1* (4), 1655–1661.
(4) Guenther, K. J.; Yoganathan, S.; Garofalo, R.; Kawabata, T.; Strack, T.; Labiris, R.; Dolovich, M.; Chirakal, R.; Valliant, J. F. *J. Med. Chem.* **2006**, *49* (4), 1466–1474.
(5) Dissoki, S.; Hagooly, A.; Elmachily, S.; Mishani, E. *J. Labelled Compd. Radiopharm.* **2011**, *54* (11), 693–701.
(6) Miller, P. W.; Long, N. J.; Vilar, R.; Gee, A. D. *Angew. Chem. Int. Ed.* **2008**, *47* (47), 8998–9033.
(7) Terrier, F. *Chem. Rev.* **1982**, *82* (2), 77–152.
(8) Fernández, I.; Frenking, G.; Uggerud, E. *J. Org. Chem.* **2010**, *75* (9), 2971–2980.
(9) Tredwell, M.; Gouverneur, V. *Angew. Chem. Int. Ed.* **2012**, *51* (46), 11426–11437.
(10) Vaidyanathan, G.; Zalutsky, M. R. *Nat. Protoc.* **2006**, *1* (4), 1655–1661.
(11) Sutcliffe-Goulden, J.; O'Doherty, M.; Marsden, P.; Hart, I.; Marshall, J.; Bansal, S. *Eur. J. Nucl. Med. Mol. Imaging* **2002**, *29* (6), 754–759.
(12) Herman, L. W.; Fischman, A. J.; Tompkins, R. G.; Hanson, R. N.; Byon, C.; Strauss, H. W.; Elmaleh, D. R. *Nucl. Med. Biol.* **1994**, *21* (7), 1005–1010.
(13) Berndt, M.; Pietzsch, J.; Wuest, F. *Nucl. Med. Biol.* **2007**, *34* (1), 5–15.
(14) Hultsch, C.; Berndt, M.; Bergmann, R.; Wuest, F. *Appl. Radiat. Isotopes* **2007**, *65* (7), 818–826.
(15) de Vries, E. F. J.; Vroegh, J.; Elsinga, P. H.; Vaalburg, W. *Appl. Radiat. Isotopes* **2003**, *58* (4), 469–476.
(16) Cai, W.; Zhang, X.; Wu, Y.; Chen, X. *J. Nucl. Med.* **2006**, *45*, 1172–1180.
(17) Shiue, C. Y.; Wolf, A. P.; Hainfield, J. F. *J. Labelled Compd. Radiopharm.* **1998**, *26*, 287–289.
(18) Vaidyanathan, G.; White, B. J.; Zalutsky, M. R. *Curr. Radiopharm.* **2009**, *2* (12), 63–74.
(19) Thonon, D.; Kech, C.; Paris, J.; Lemaire, C.; Luxen, A. *Bioconjugate Chem.* **2009**, *20* (4), 817–823.
(20) Ramenda, T.; Bergmann, R.; Wuest, F. *Lett. Drug Des. Discovery* **2007**, *4* (4), 279–285.
(21) Haka, M. J.; Kilbourn, M. R.; Watkins, G. L.; Tooronigan, S. A. *J. Labelled Compd. Radiopharm.* **1988**, *7* (27), 823–833.
(22) Ross, T. L.; Ermert, J.; Hocke, C.; Coenen, H. H. *J. Am. Chem. Soc.* **2007**, *129* (25), 8018–8025.
(23) Koslowsky, I.; Mercer, J.; Wuest, F. *Org. Biomol. Chem.* **2010**, *8* (20), 4730–4736.
(24) Tang, G.; Tang, X.; Wang, X. *J. Labelled Compd. Radiopharm.* **2010**, *53* (8), 543–547.
(25) Calderwood, S.; Collier, T. L.; Gouverneur, V.; Liang, S. H.; Vasdev, N. *J. Fluorine Chem.* **2015**, *178*, 249–253.
(26) Lee, E.; Hooker, J. M.; Ritter, T. *J. Am. Chem. Soc.* **2012**, *134* (42), 17456–17458.
(27) Kügler, F.; Ermert, J.; Kaufholz, P.; Coenen, H. *Molecules* **2015**, *20* (1), 470–486.
(28) Pike, V. W.; Aigbirhio, F. I. *J. Chem. Soc., Chem. Commun.* **1995**, No. 21, 2215–2.
(29) Chun, J.-H.; Pike, V. W. *Eur. J. Org. Chem.* **2012**, *2012* (24), 4541–4547.
(30) Carroll, M. A.; Carrol; Ran, Y. *Espacenet*. November 19, 2009.
(31) Carroll, M. A.; Nairne, J.; Smith, G.; Widdowson, D. A. *J. Fluorine Chem.* **2007**, *128* (2), 127–132.
(32) Chun, J.-H.; Pike, V. W. *Org. Biomol. Chem.* **2013**, *11* (37), 6300–6307.

(33) Mu, L.; Fischer, C. R.; Holland, J. P.; Becaud, J.; Schubiger, P. A.; Schibli, R.; Ametamey, S. M.; Graham, K.; Stellfeld, T.; Dinkelborg, L. M.; Lehmann, L. *Eur. J. Org. Chem.* **2012**, *2012* (5), 889–892.
(34) Chun, J.-H.; Morse, C. L.; Chin, F. T.; Pike, V. W. *Chem. Commun.* **2013**, *49* (21), 2151–2153.
(35) Tredwell, M.; Preshlock, S. M.; Taylor, N. J.; Gruber, S.; Huiban, M.; Passchier, J.; Mercier, J.; Génicot, C.; Gouverneur, V. *Angew. Chem. Int. Ed.* **2014**, *53* (30), 7751–7755.
(36) Preshlock, S.; Calderwood, S.; Verhoog, S.; Tredwell, M.; Huiban, M.; Hienzsch, A.; Gruber, S.; Wilson, T. C.; Taylor, N. J.; Cailly, T.; Schedler, M.; Collier, T. L.; Passchier, J.; Smits, R. X.; Mollitor, J.; Hoepping, A.; Mueller, M.; Génicot, C.; Mercier, J. X. L.; Gouverneur, V. X. R. *Chem. Commun.* **2016**, *52*, 8361–8364.
(37) Poty, S.; Désorgère, P.; Goze, C.; Boschetti, F.; Dhuys, T.; Schols, D.; Cawthorne, C.; Archibald, S. J.; Maecke, H. R.; Denat, F. *Dalton Trans.* **2015**, *44*, 5004–5016.
(38) White, J. R.; Price, G. J.; Schiffers, S.; Raithby, P. R.; Plucinski, P. K.; Frost, C. G. *Tetrahedron Lett.* **2010**, *51* (30), 3913–3917.
(39) Puerto Galvis, C. E.; Kouznetsov, V. V. *Org. Biomol. Chem.* **2013**, *11* (3), 407–411.
(40) Glaser, M.; Robins, E. G. *J. Labelled Compd. Radiopharm.* **2009**, *52* (10), 407–414.
(41) Gill, H. S.; Marik, J. *Nat. Protoc.* **2011**, *6* (11), 1718–1725.
(42) Patel, O.; Shulkes, A.; Baldwin, G. S. *Biochimica et Biophysica Acta (BBA) - Reviews on Cancer* **2006**, *1766* (1), 23–41.
(43) Tobisu, M.; Chatani, N. *Chem. Lett.* **2011**, *40* (4), 330–340.
(44) Stöckmann, H.; Neves, A. A.; Stairs, S.; Brindle, K. M.; Leeper, F. J. *Org. Biomol. Chem.* **2011**, *9* (21), 7303–7303.
(45) Vlaar, T.; Ruijter, E.; Maes, B. U. W.; Orru, R. V. A. *Angew. Chem. Int. Ed.* **2013**, *52* (28), 7084–7097.
(46) Lygin, A. V.; de Meijere, A. *Angew. Chem. Int. Ed.* **2010**, *49* (48), 9094–9124.
(47) Kaur, T.; Wadhwa, P.; Bagchi, S.; Sharma, A. *Chem. Commun.* **2016**, *52*, 6958–6976.
(48) Dömling, A.; Ugi, I. *Angew. Chem. Int. Ed.* **2000**, 3168–3210.
(49) Akritopoulou-Zanze, I. *Curr. Opin. Chem. Biol.* **2008**, *12* (3), 324–331.
(50) Wilson, R. M.; Stockdill, J. L.; Wu, X.; Li, X.; Vadola, P. A.; Park, P. K.; Wang, P.; Danishefsky, S. J. *Angew. Chem. Int. Ed.* **2012**, *51* (12), 2834–2848.
(51) Skorna, G.; Ugi, I. *Angew. Chem. Int. Ed.* **1977**, *16*, 259–260.
(52) Eckert, Von, H.; Forster, B. *Angew. Chem.* **1987**, *99*, 927–928.
(53) Obrecht, R.; Herrmann, R.; Ugi, I. *Synthesis* **1985**, 400–401.
(54) Gerack, C. J.; McElwee-White, L. *Chem. Commun.* **2012**, *48* (92), 11310–11313.
(55) Ishiyama, T.; Murata, M.; Miyaura, N. *J. Org. Chem.* **1995**, 7508–7510.
(56) Guchhait, S. K.; Priyadarshani, G.; Chaudhary, V.; Seladiya, D. R.; Shah, T. M.; Bhogayta, N. P. *RSC Adv.* **2013**, *3* (27), 10867–10868.
(57) Appel, R.; Kleinstuck, R.; Ziehn, K.-D. *Angew. Chem. Int. Ed.* **1971**, *10*, 132–132.
(58) Wittmann, R. *Angew. Chem.* **1961**, *6* (73), 219–220.
(59) Porcheddu, A.; Giacomelli, G.; Salaris, M. *J. Org. Chem.* **2005**, *70* (6), 2361–2363.
(60) Neochoritis, C. G.; Stotani, S.; Mishra, B.; Dömling, A. *Org. Lett.* **2015**, *17* (8), 2002–2005.
(61) Imming, V. P.; Mohr, R.; Müller, E.; Overheu, W.; Seitz, G. *Angew. Chem.* **1982**, *4* (94), 291.

Chapter 4

^{18}F-DPA 713 a novel second generation radioligand for PET imaging of neuroinflammation

4.1 Introduction

The translocator protein (TSPO), first discovered in 1977,[1] is a five transmembrane domain protein localised predominantly on the outer mitochondrial membrane.[2]

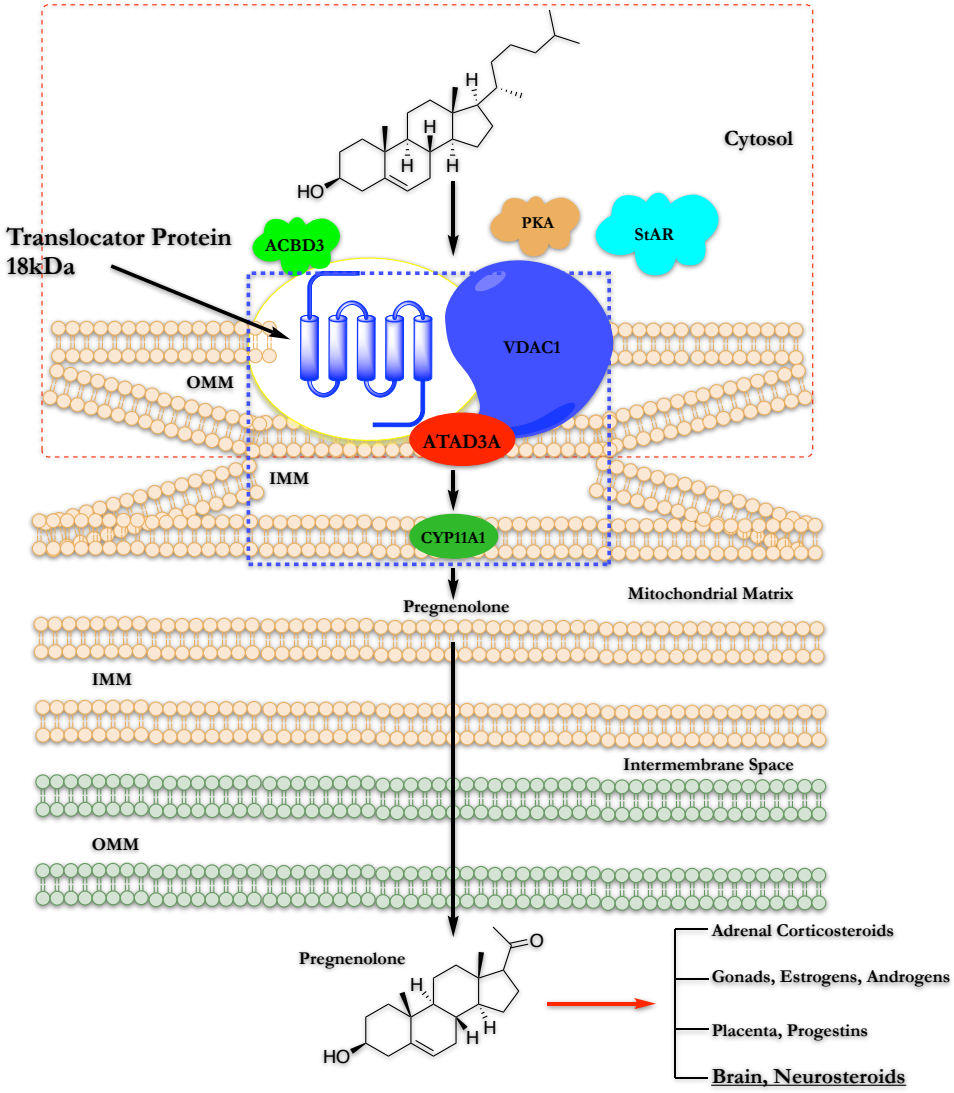


Figure 4.1.1: Cholesterol translocation facilitated by TSPO; TSPO is particularly enriched at contact sites between the inner and outer mitochondrial membrane and is a member of both the transduceosome (red margin) and metabolon (blue margin) protein complexes. The transduceosome facilitates the import of cholesterol from the cytosol to the mitochondria, while the metabolon complex directs cholesterol toward Cytochrome P450scc enzyme CYP11A1, enabling cleavage of the cholesterol side chain, which is the first enzymatic step in steroidal synthesis.[3,4]

TSPO is thought to be implicated in the translocation of cholesterol and porphyrins from the outer to the inner membrane of the mitochondria, this being the rate-determining step for steroidogenesis and neurosteroidogenesis.[5-7] (Figure 4.1.1). Therefore, TSPO is highly expressed in steroidogenic tissues such as the gonads, adrenal glands, placenta and the brain.[8] The activity of TPSO is relevant to other cellular processes, such as apoptosis[9] and the TSPO gene is highly conserved in animals.[10] Furthermore, TSPO is up-regulated in activated glial cells, which are essential to the central nervous system (CNS).[11-13] Glial up-regulation of TSPO is a major characteristic of neurodegenerative diseases.[14] As a result, a plethora of TSPO-specific radioligands have been designed and utilised as markers for gliosis* detection in the brain.[15]

4.2 TSPO Specific Radioligands

First synthesised in 1984 by Camsonne,[16] [^{11}C]PK11195 (**[^{11}C]4-1**) is the most widely utilised TSPO-specific radioligand for Positron Emission Tomography (PET) (Figure 4.2.1 a). However, **[^{11}C]4-1** displays poor signal-to-noise ratio and high non-specific cerebral binding, which limits accurate quantification.[17,18] A multitude of second-generation TSPO specific radiolabelled compounds, such as [^{11}C]PBR28 **([^{11}C]4-2)**, [^{18}F]GE-180 **([^{18}F]4-3)**, [^{11}C]DAA1106 **([^{11}C]4-4**) and [^{11}C]DPA-713 **([^{11}C]4-5**), have therefore been developed (Figure 4.2.1 b).[19-28] Although these second-generation radioligands show improved signal-to-noise ratios in PET, some display substantial heterogeneity in their binding potentials due to inter-subject variability of TSPO in humans.[29] A rs6971† polymorphism, which induces an amino acid substitution from alanine to threonine (Ala^{147}-Thr^{147}) in the TSPO protein sequence, is responsible for such differences in affinity. This leads to three distinct binding classes: high-affinity binders (*HABs, major*

*A non-specific reactive alteration of glial cells, in response to central nervous system damage.
†A single nucleotide polymorphism (SNP) located on exon 4 of the TSPO gene.

genotype, Ala/Ala amino acid in 147 position of TSPO), mixed-affinity binders (*MABs, Ala/Thr amino acid)* and low-affinity binders (*LABs, minor genotype, Thr/Thr amino acid).* Both HABs and LABs express a single binding site for TSPO with either high or low affinity respectively, whilst MABs express both binding sites. A study conducted in 2012 by Owen[30] reported the following substitution prevalence amongst Caucasian subjects: 49% = HABs, 42% = MABs, and 9% = LABs, with substitution occurrence varying across ethnic groups. Therefore, an ideal TSPO radiotracer would possess high binding affinity (*K*i) for TSPO and no discrepancy in binding affinity between HAB and LAB populations.

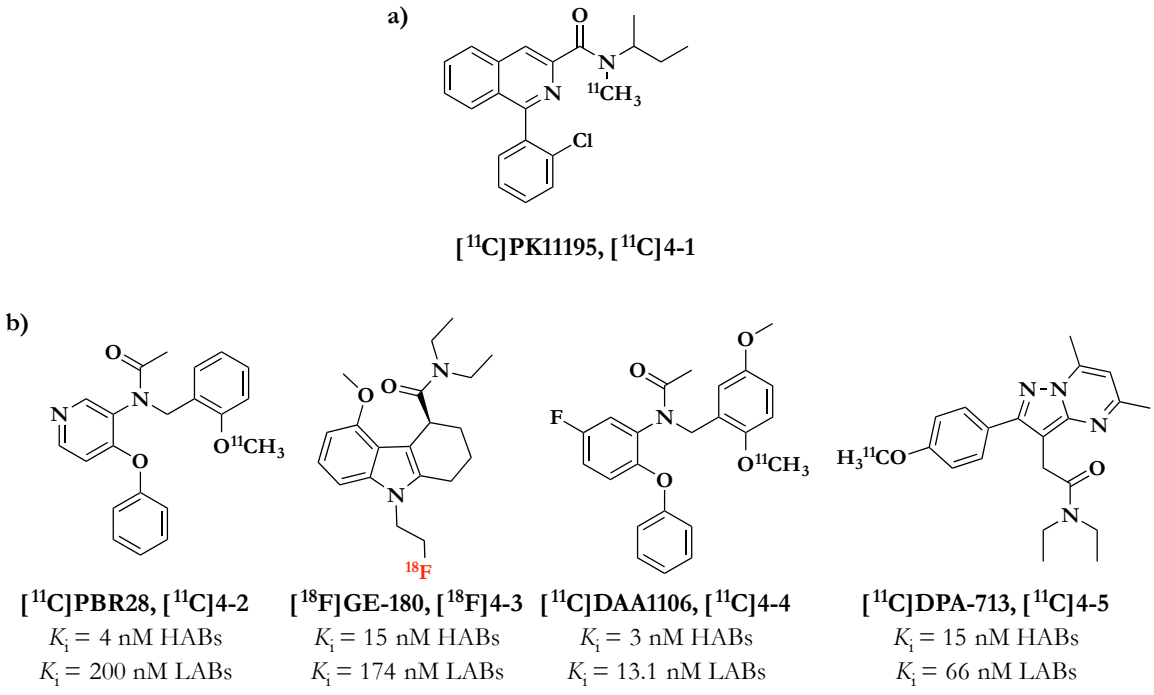
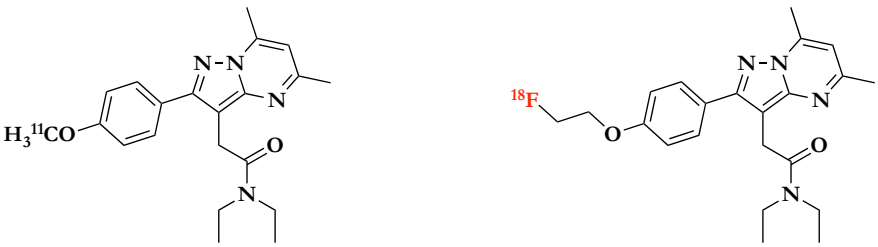


Figure 4.2.1: a) First-generation TSPO radiotracer [^{11}C]4-1 b) Second-generation TSPO radiotracers [^{11}C]4-2, [^{18}F]4-3, [^{11}C]4-4‡ and [^{11}C]4-5.[29]

Certain second-generation chemical probes such as **[^{18}F]4-3** may appear to have a high affinity for TSPO in animal models (K_i = 0.67 nM measured from rat tissue[32]), but in human samples the discrepancy in binding affinity observed between HABs and LABs

‡ A fluorine-18 variant of DAA1106 has been previously synthesised in the Gouverneur group.[31]

(15 nM vs. 174 nM, approx. 12 fold, Figure 4.2.1 b)) prevent it from being widely adopted in clinics§.[33] The difference in K_i between HABs and LABs for **[[11]C]4-5** is much lower (approx. 4 fold, Figure 4.2.1 b)), making it an attractive prospect for imaging TSPO in human volunteers.[34,35] However, owing to the short half-life (≈ 20 min) of [11]C positron emitting radioisotopes, a plethora of [18]F-labelled analogues of **[[11]C]4-5** have been synthesised. The most prominent of these derivatives is the [18]F-ethyl ether variant, [[18]F]DPA-714 **([[18]F]4-6)** (Figure 4.2.2).[36] Fluorine-18 incorporation imparts a longer half-life of 109.7 minutes, this enables higher-resolution images to be obtained and permits the transport of a radiotracer to hospitals or academic institutes which do not have direct access to a cyclotron **(section 1.2)**.[37]



[[11]C]DPA-713, [[11]C]4-5
K_i = 4.7 nM (rat membrane)

[[18]F]DPA-714, [[18]F]4-6
K_i = 7.0 nM (rat membrane)

Figure 4.2.2: Structures of [[11]C]DPA-713 ([[11]C]4-5) and [[18]F]DPA-714 ([[18]F]4-6).

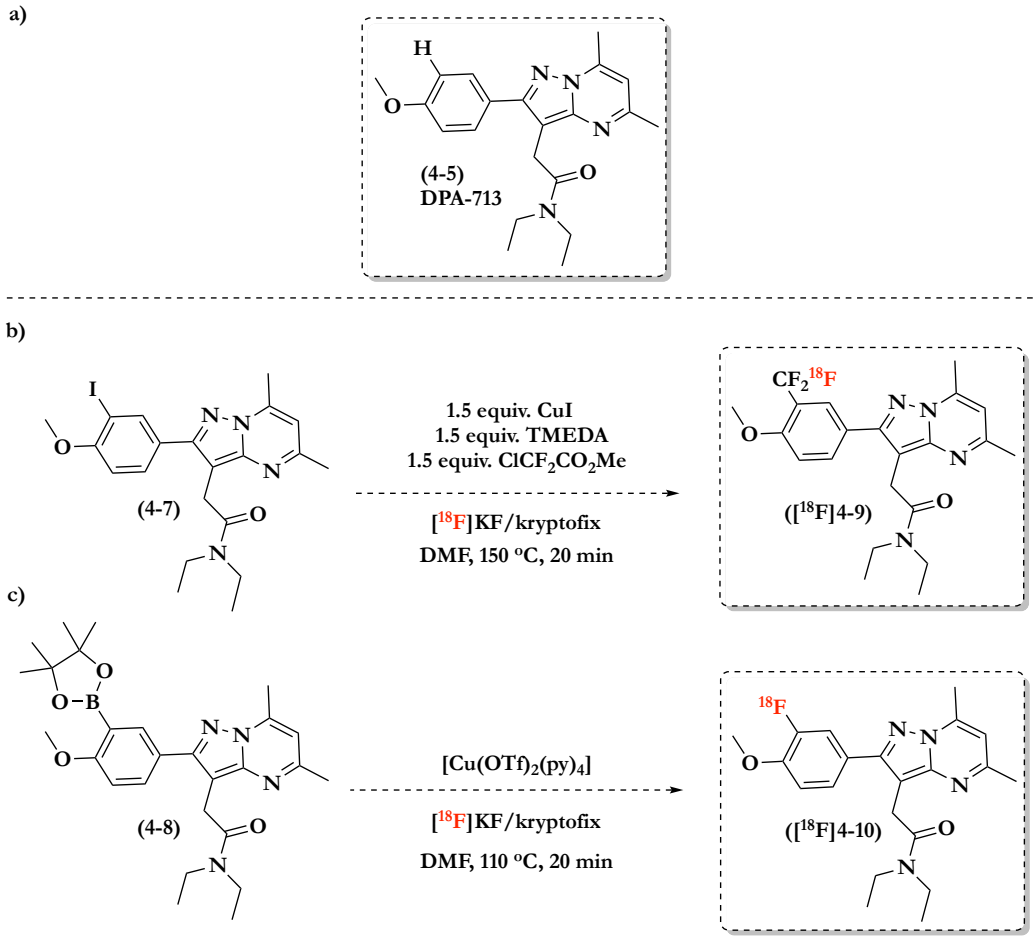
[[18]F]4-6 possesses similar *in vitro* binding affinity for TSPO compared to **[[11]C]4-5**; K_i = 7.0 nM vs. 4.7 nM, quantified from rat kidney membranes (Figure 4.2.2).[36] However, **[[18]F]4-6** exhibits lower specific binding *in vivo*, as observed in numerous PET animal models.[38,39] This observation may be due to the direct metabolism of **[[18]F]4-6** by cytochrome P-450, yielding radiometabolites which pass through the blood brain barrier (BBB), lowering overall PET image quality.[39] Furthermore, a study by Golla[40] conducted in human volunteers, demonstrated that no significant increase in regional tracer binding could be discerned between volunteers with Alzhiemer's disease and

§ This represents a challenge for quantitative PET studies using **[[18]F]4-3**, the existence of patients with varying affinity for **[[18]F]4-3** means that the difference in PET signal across subjects cannot be interpreted directly as differences in receptor density.[29]

healthy controls using **[^{18}F]4-6**. This observation indicates that **[^{18}F]4-6** may not be a suitable tracer for human TSPO studies.

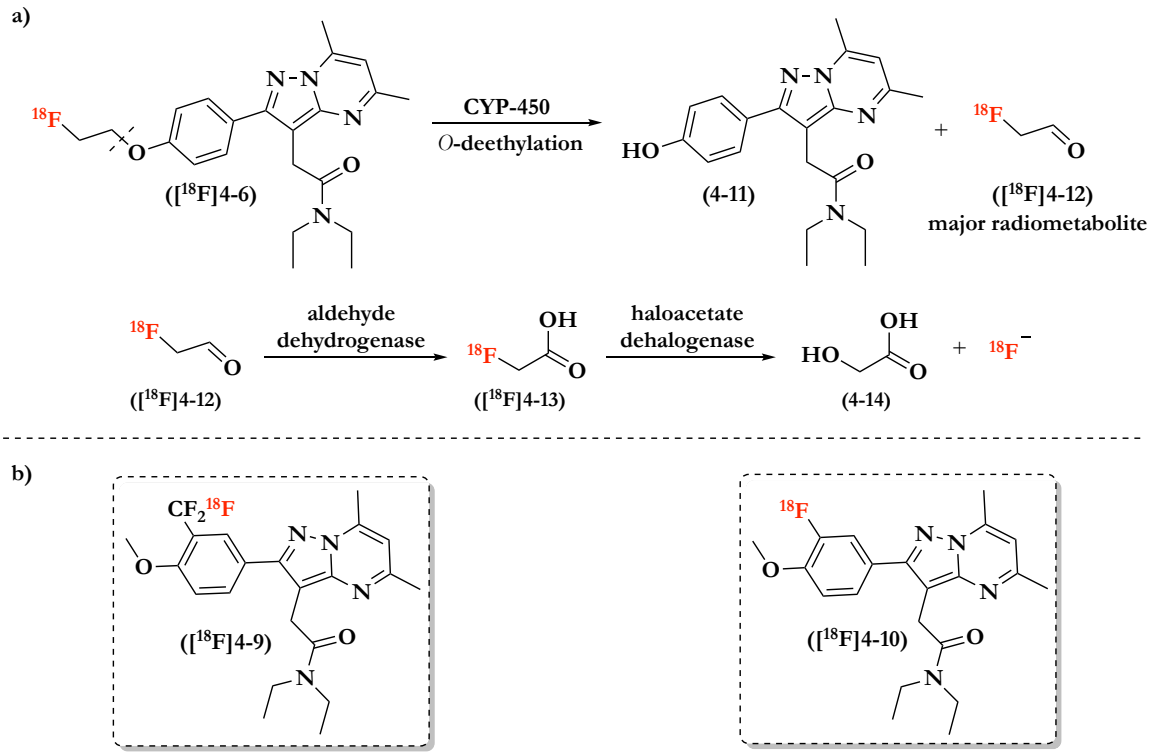
4.3 Aim of study

With the advent of novel methodology developed in the Gouverneur group for direct aromatic ^{18}F-trifluoromethylation[41] and ^{18}F-fluorination,[31] it was our aim to develop a novel fluorine-18 variant of DPA-713 **(4-5)**, that would potentially bind TSPO with high affinity and demonstrate favourable stability *in vivo* (Scheme 4.3.1).



Scheme 4.3.1: a) Structure of DPA-713 (4-5). b) Proposed ^{18}F-trifluoromethylation forming [^{18}F]4-9. c) Proposed ^{18}F-fluorination forming [^{18}F]4-10.

We reasoned that positioning the [18]F-fluorine label directly on the aromatic ring of **4-5**, would potentially improve metabolic stability in comparison to **[[18]F]4-6**; formation of **[[18]F]4-12** is considered to be the major [18]F-labelled radiometabolite of **[[18]F]4-6** (Scheme 4.3.2 a) and b)).[42] Subsequently, this may potentially reduce the observed non-specific binding associated with **[[18]F]4-6**, improving overall tracer performance.



Scheme 4.3.2: a) Metabolism of [[18]F]4-6 *via* CYP-450 *O*-deethylation yielding [[18]F]fluoroacetaldehyde ([[18]F]4-12). Subsequent metabolism of [[18]F]4-12 may give [[18]F]fluoride *in vivo*.[39,42] b) Structures of proposed DPA-713 analogues.

If direct [18]F-fluorination and [18]F-trifluoromethylation of **4-5** proved to be successful, both compounds would be tested in a clinically relevant animal model of neuroinflammation to assess their performance against other available TSPO tracers.

4.4 Synthetic strategy

3-Iodo-DPA-713 **(4-7)** was selected as a viable precursor to [^{18}F]CF$_3$DPA-713 **([^{18}F]4-9)** (Figure 4.4.1). It was postulated that a subsequent Miyaura borylation of **4-7** would yield **4-8**, required for radiosynthesis of [^{18}F]DPA-713 **([^{18}F]4-10)** (Figure 4.4.1 b)). To access **4-7**, a stepwise synthetic strategy was devised; this approach will be further detailed in **section 4.4.1.**

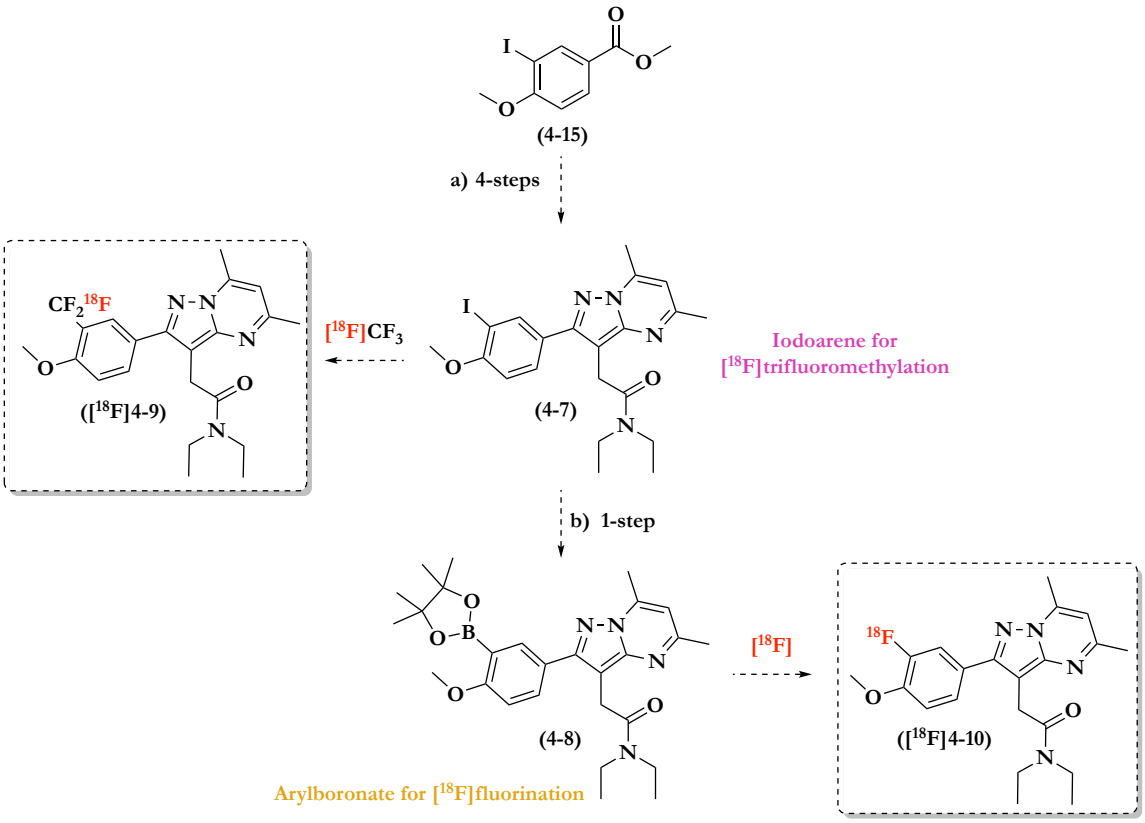
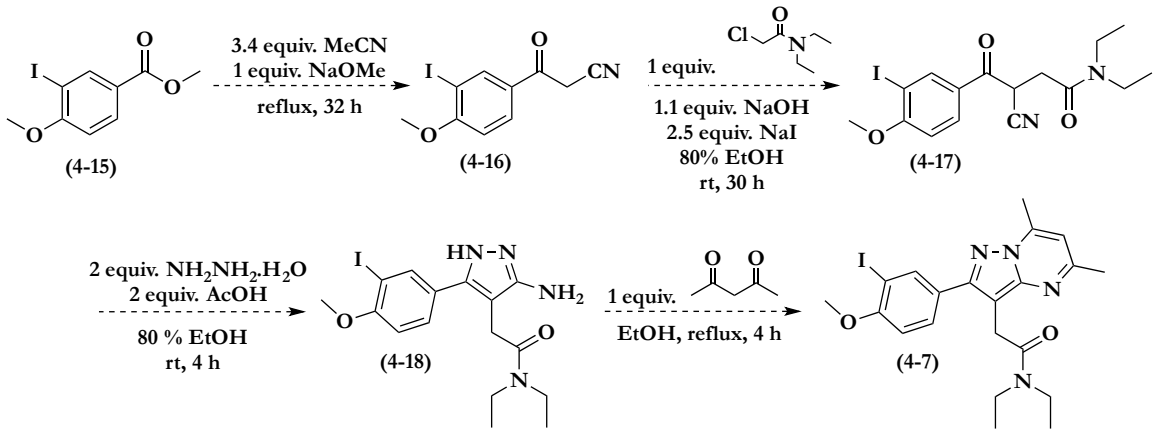


Figure 4.4.1: Synthetic strategy toward [^{18}F]4-9 and [^{18}F]4-10

4.4.1 Strategy for synthesis of 3-iodo-DPA-713

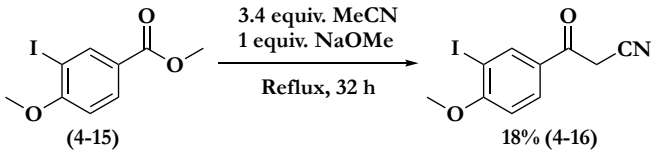
The successful synthesis of DPA-713 **(4-5)** reported by Reynolds[43] was used as inspiration for our synthetic efforts toward **4-7**. The proposed synthetic pathway to **4-7** is shown in Scheme 4.4.1, commencing from commercially available methyl 3-iodo-methoxybenzoate **(4-15).**[**]



Scheme 4.4.1: Proposed synthetic pathway toward 4-7.

4.5 Synthetic efforts toward 3-iodo-DPA-713

Initially, alkylation of **4-15** was examined, using acetonitrile (MeCN) as the nucleophile and sodium methoxide (NaOMe) as base (Scheme 4.5.1). The desired product 3-(3-iodo-4-methoxyphenyl)-3-oxopropanenitrile **(4-16)** was isolated in an unsatisfactory 18% yield. As a result, examination and optimisation of the reaction parameters was investigated.



Scheme 4.5.1: Synthesis of (4-16)

[**]Late stage functionalisation of DPA-713 (**4-5)** was also attempted,[43] details in chapter 5.

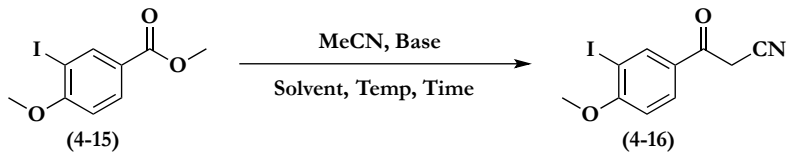


Table 4.5.1: Optimisation studies for the synthesis of 4-16

Entry	Base	Solvent	Nucleophile	Temp[°C]	Time[hr]	Yield[%][a]
1	2 eq. LiHMDS	MeCN	5 eq. MeCN	-10	18	22
2	2 eq. LiHMDS	MeCN	5 eq. MeCN	-78	18	14
3	1.5 eq. NaH	THF	3 eq. MeCN	0	48	31
4	2 eq. NaH	THF	3 eq. MeCN	0	48	45
5	**2 eq. *n*-BuLi**	**THF**	**3 eq. MeCN**	**-78**	**3**	**92**

[a]Determined by ^{1}H NMR analysis using ethylene carbonate as an internal standard.

Table 4.5.1 details the optimisation process on **4-15**. The use of *n*-Butyllithium (*n*-BuLi) as base proved optimal (entry 5); full conversion to **4-16** was observed after 3 hours at -78 °C. Silica gel column chromatography was not required, and the product was obtained in a 92% yield following acidification with 1 M HCl, extraction with EtOAc and a brine wash. Other bases employed such as lithium bis(trimethylsilyl)amide (LiHMDS), and sodium hydride (NaH) were less effective (entries 1-4). Thus a trend of increasing base strength, yielding greater formation of **4-16** was observed. ††

The ensuing alkylation of **4-16** initially suffered from poor reactivity (Table 4.5.2 entry 1).[45] Formation of **4-17** was not observed *via* LC/MS or ^{1}H NMR. Therefore, an evaluation of the reaction parameters was undertaken (Table 4.5.2). Heating to reflux, varying the iodide source and exploration of microwave irradiation[46] all proved to be unsuccessful (entries 2-6). Gratifyingly the use of a more electrophilic reaction partner (**4-20**)[47] and K_2CO_3 in both EtOH[48] and THF gave the desired product **(4-17)** in 42% and 86% yield respectively (entries 8-9).

†† LiHMDS; pK_a of conjugate acid ≈ 26, NaH; pK_a of conjugate acid ≈ 42, *n*-BuLi; pK_a of conjugate acid ≈ 50.[44]

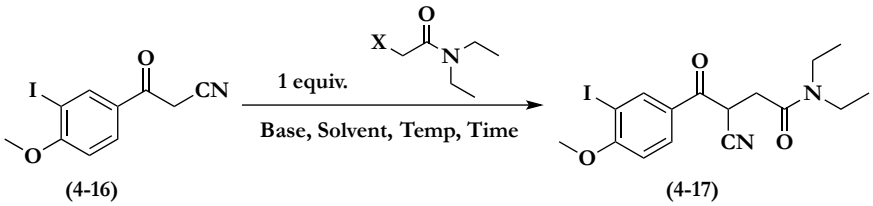


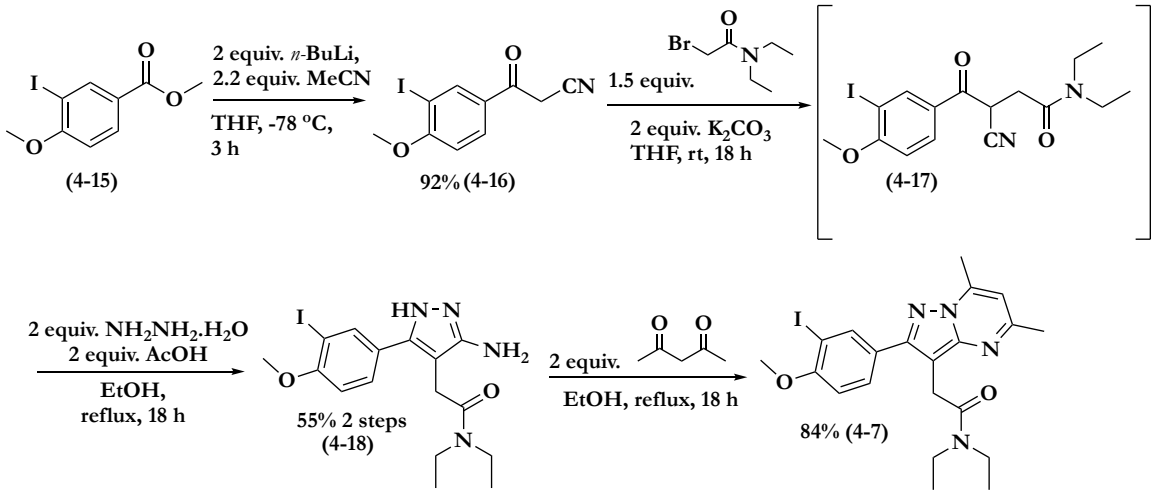
Table 4.5.2: Optimisation studies for synthesis of 4-17

Entry	X	Additive[a]	Base[b]	Solvent	Temp [°C]	Time [hr]	Yield [%][d]
1	Cl	NaI	NaOH	EtOH	rt	30	0
2	Cl	NaI	NaOH	EtOH	85	18	11
3	Cl	NaI	NaOH	EtOH	mw 80[c]	1.5	17
4	Cl	KI	NaOH	EtOH	mw 80[c]	1.5	31
5	Cl	KI	NaOH	EtOH	rt	48	0
6	Cl	KI	NaOH	EtOH	85	18	12
7	Cl	-	K_2CO_3	EtOH	rt	18	0
8	Br	-	K_2CO_3	EtOH	rt	18	42[e]
9	**Br**	**-**	**K_2CO_3**	**THF**	**rt**	**18**	**86[e]**

[a]2.5 equiv. [b]2 equiv. [c]Microwave irradiation 80 Watts.

[d] Determined by ^{1}H NMR analysis using ethylene carbonate as an internal standard. [e]Isolated yield.

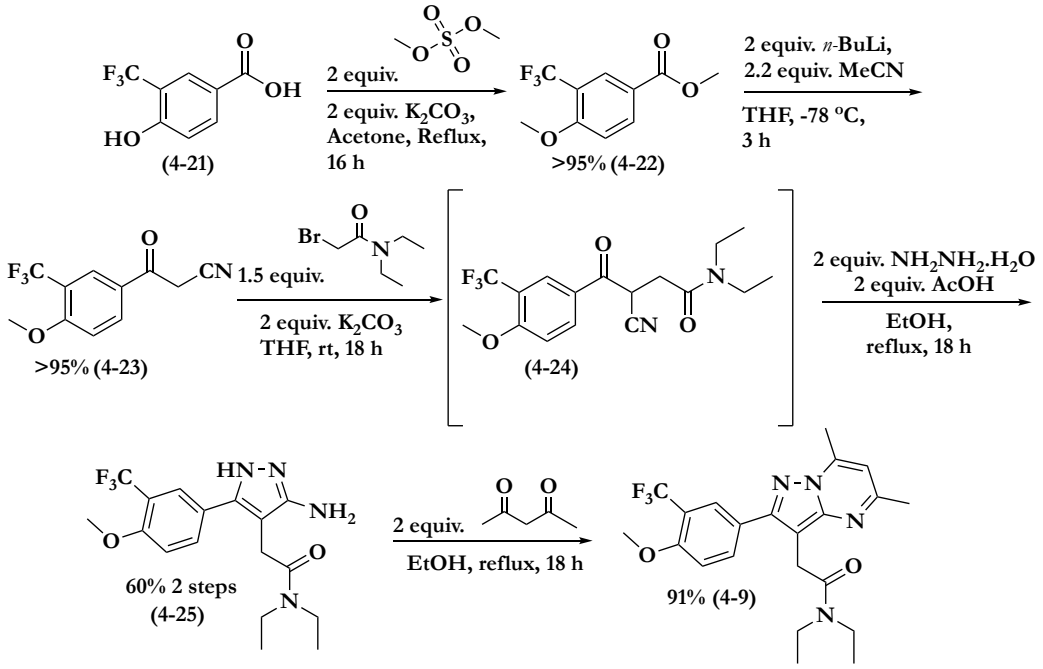
Subsequently, cyclisation of **4-17** was induced using hydrazine hydrate, leading to formation of iodo-aminopyrazole **4-18** in 55% yield (calculated over 2 steps, Scheme 4.5.2). This was succeeded by a double condensation reaction employing 2,4-pentadione, to form target compound **4-7** in 84% yield (Scheme 4.5.2).



Scheme 4.5.2: Synthesis of iodoarene precursor 4-7 for ^{18}F-trifluoromethylation

4.5.1 Synthesis of [^{19}F]CF_3DPA-713 reference for fluorine-18 incorporation

The identification of fluorine-18 radiosynthetic products requires the acquisition of fluorine-19 analogues to provide a direct reference for ^{18}F incorporation *via* radio-HPLC (refer to **section 4.7**). Taking inspiration from the synthetic strategy devised for **4-7** (Scheme 4.5.2), facile construction of [^{19}F]CF_3DPA-713 (**4-9**) ensued. **4-9** was synthesised in 50% yield over 5 synthetic steps (Scheme 4.5.3). Since 3-trifluoromethoxybenzoate (**4-22**) is not available commercially, it was accessed *via* methylation of **4-21** with dimethyl sulfate in >95% yield.[49]



Scheme 4.5.3: Synthesis of fluorinated reference 4-9

4.6 Synthesis of aryl boronate precursor for [18]F-fluorination

Our next aim was to prepare the corresponding aryl boronic ester **(4-8)** from 3-iodo-DPA-713 (**4-7**). To achieve this transformation, Miyaura borylation[50] conditions were applied to **4-7**. The execution of this Miyaura coupling required extensive investigation. Table 4.6.1 depicts a summary of the optimisation conducted.

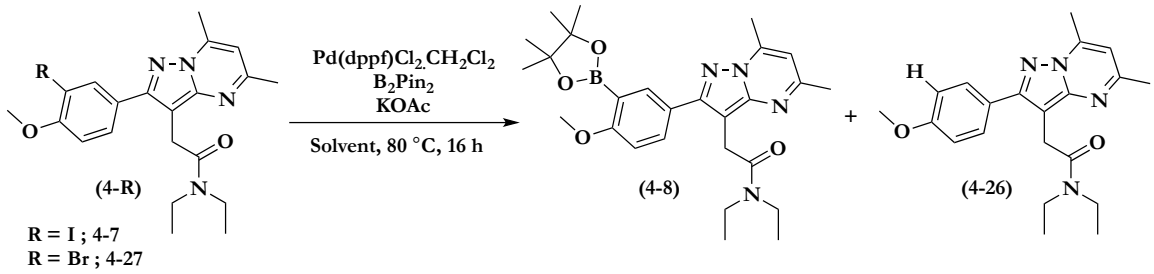


Table 4.6.1: Suzuki-Miyaura borylation forming 4-8

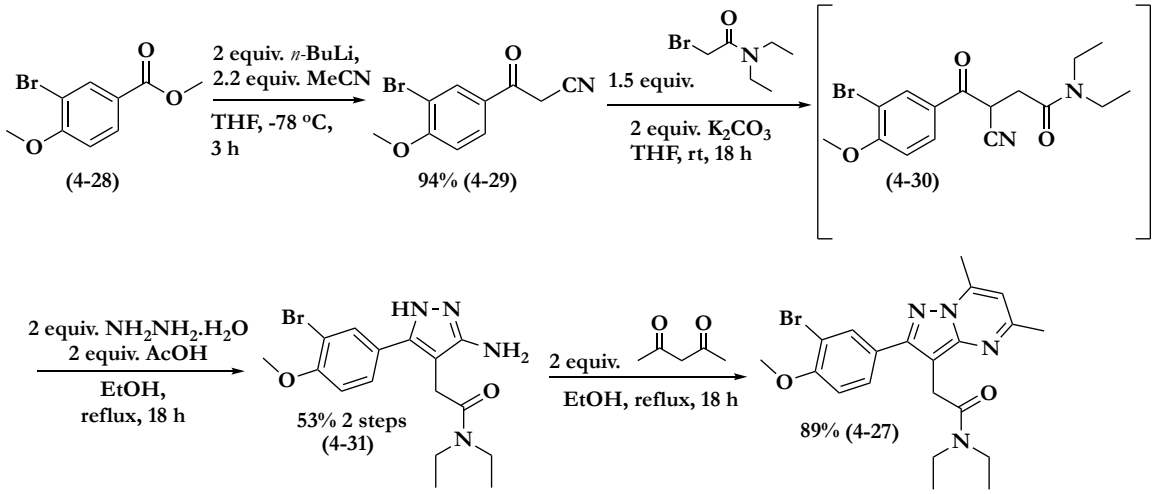
Entry	R	B_2Pin_2[eq.]	KOAc[eq.]	Cat.[eq.]	Solvent	**4-8** : **4-26**[%][c]
1	I	1.5	3	0.03	DMF	24 : 15
2	I	1.5	3	0.03	Toluene	31 : 11
3	I	2	3	0.05	DMF	36 : 22
4	I	2	3	0.05	Toluene	32 : 16
5	I	3	4	0.1	Toluene	63 : 15
6[a]	I	3	4	0.1	Toluene	66 : 17
7[b]	I	3	4	0.1	Toluene	52 : 14
8	**Br**	**3**	**4**	**0.1**	**Toluene**	**63 : 0**
9	Br	3	4	0.1	DMF	67 : 8

[a]Reaction run at 120 °C. [b]$PdCl_2(PPh_3)_2$ used as catalyst. [c] Determined by ^{1}H NMR analysis using ethylene carbonate as an internal standard.

The quantity of B_2Pin_2 and KOAc employed was extremely important for product formation, with three and four equivalents furnishing the best results respectively (entries 5-9). Importantly, the choice of halogen tethered to **4-R** played a crucial role in this transformation. Using **4-7** as coupling partner resulted in significant formation of

protiated product **4-26**‡‡ (entries 1-7). Under these conditions, product isolation could not be achieved *via* silica gel chromatography, since retention factors of product (**4-8**), starting material (**4-7**) and protiated side-product (**4-26**) were identical under all solvent conditions examined.

Synthesis of 3-bromo-DPA-713 **(4-27)** (Scheme 4.6.1) and subsequent Miyaura borylation with B_2Pin_2 in toluene (Table 4.6.1, entry 8), afforded **4-8** in 63% yield. Significantly, formation of the protiated product **4-26** was diminished under these conditions.



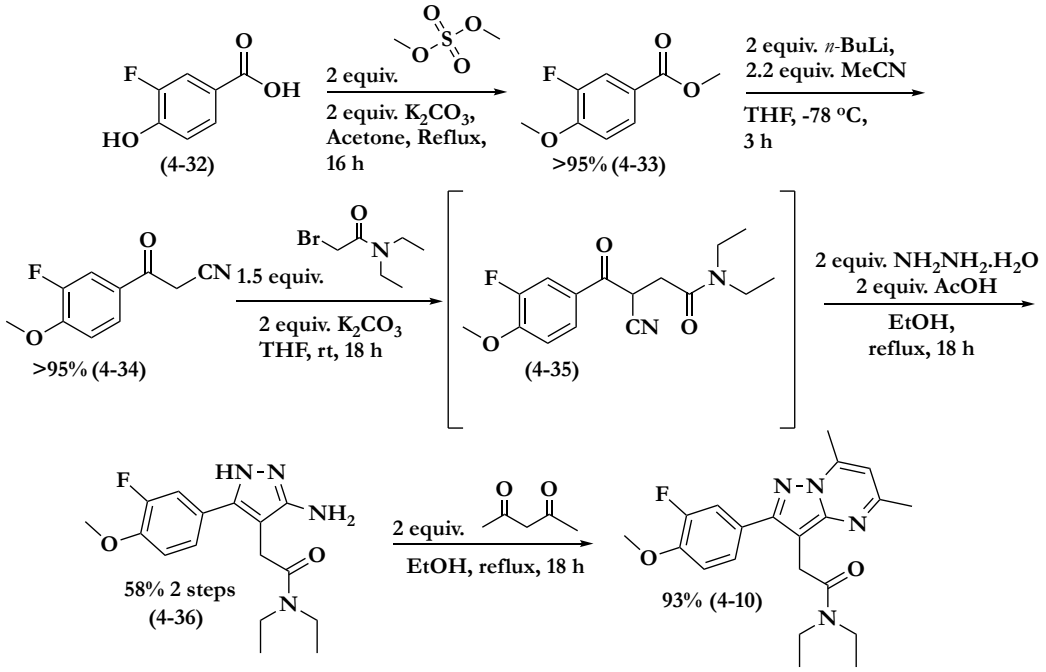
Scheme 4.6.1: Synthesis of 3-bromo-DPA-713 (4-27)

The variation in reactivity observed between aryl-iodide (**4-7**) and aryl-bromide (**4-27**) for the Miyaura borylation may be due to the formation of different catalytic intermediates during the course of the reaction. Post oxidative addition, the electron donating *ortho*-OMe group may promote dissociation of iodine from the palladium complex, forming a cationic palladium species; this pathway being less-favoured for the aryl-bromide (**4-27**).[51,52] Palladium-mediated hydrohalogenation has been shown to proceed *via* a cationic palladium intermediate and the cationic reaction pathway for palladium-mediated borylation is promoted in polar solvents and by electron donating

‡‡ Aromatic protons at 7.79 (d, J = 8.9 Hz, 2H) and 7.00 ppm (d, J = 8.9 Hz, 2H) identified in crude ^{1}H NMR.

substituents.[51,53,54] These findings corroborate with the observation that protiated product formation (**4-26**) is increased in DMF in comparison to toluene and increased for **4-7** in comparison to **4-27** (Table 4.6.1).

Next, [^{19}F]DPA-713 (**4-10**), required for radiosynthetic product identification of [^{18}F]**4-10** was synthesised. The synthetic route shown in Scheme 4.6.2 afforded **4-10** in 49% yield over 5 synthetic steps.

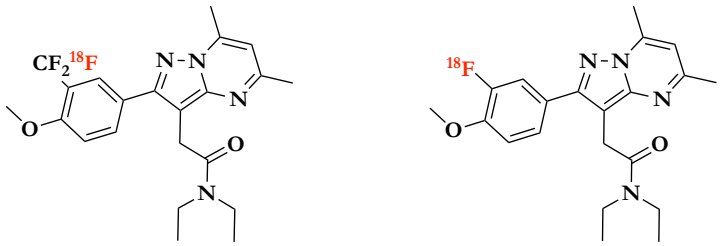


Scheme 4.6.2: Synthesis of fluorinated reference 4-10

4.7 Radiochemistry

Experiments employing fluorine-18 were carried out in collaboration with Dr. Sean Preshlock. For safety purposes, when handling ionising radiation, no less than two people were present during radiosynthesis.

This section details the radiosynthesis of **[^{18}F]4-9** and **[^{18}F]4-10** *via* ^{18}F-trifluoromethylation and ^{18}F-fluorination respectively.



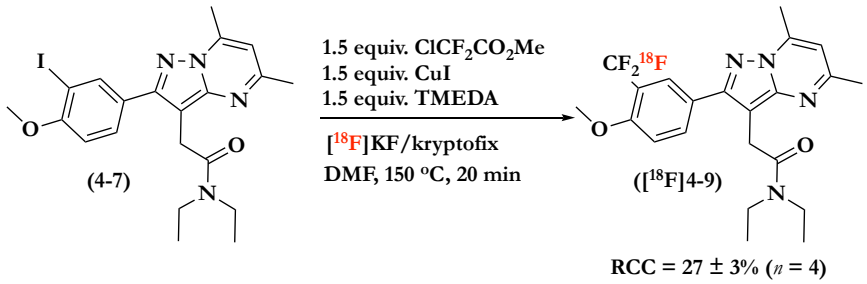
[^{18}F]CF$_3$DPA-713, ([^{18}F]4-9) **[^{18}F]DPA-713, ([^{18}F]4-10)**

Figure 4.7.1: Structures of [^{18}F]4-9 and [^{18}F]4-10.

4.7.1 ^{18}F-Trifluoromethylation

The ^{18}F-trifluoromethylation of **4-7** was carried-out using the literature conditions on a 20–30 MBq scale.[41] 20–30 MBq of dried [^{18}F]KF/K$_{222}$ in MeCN (10–40 µL) was dispensed into a V-vial containing 1.5 equivalents of CuI. Next, 1.5 equivalents of methyl chlorofluoroacetate, TMEDA and **4-7** in DMF were then added *via* syringe. The reaction was heated at 150 °C for 20 minutes (Scheme 4.7.1). To calculate the radiochemical conversion (RCC), the reaction mixture was quenched with water, and an aliquot was removed for analysis by radio-TLC and radio-HPLC. The conversion of [^{18}F]KF to **[^{18}F]4-9** was determined by radio-TLC, comparing the baseline radioactivity (unreacted [^{18}F]fluoride) with the activity of **[^{18}F]4-9** found at a higher R_f value. The RCC was then calculated by multiplying the reaction conversion by the radiochemical

purity (RCP) of the product, which was previously determined by radio-HPLC[§§]. The reaction was repeated four times and a RCC of 27 ± 3% (n = 4) was obtained (Scheme 4.7.1).



Scheme 4.7.1: Radiosynthesis of [[18]F]4-9

Thereafter, a batch scale synthesis of **[[18]F]4-9** was performed starting from 3-3.6 GBq of [[18]F]fluoride. This resulted in 0.320–0.450 GBq of isolated **[[18]F]4-9** with a radiochemical yield (RCY) of 12 ± 2% (n = 3). RCY was determined by isolation of **[[18]F]4-9** *via* semi-preperative HPLC, eluting with 50% MeCN/50% isocratic at 4 mL/min.

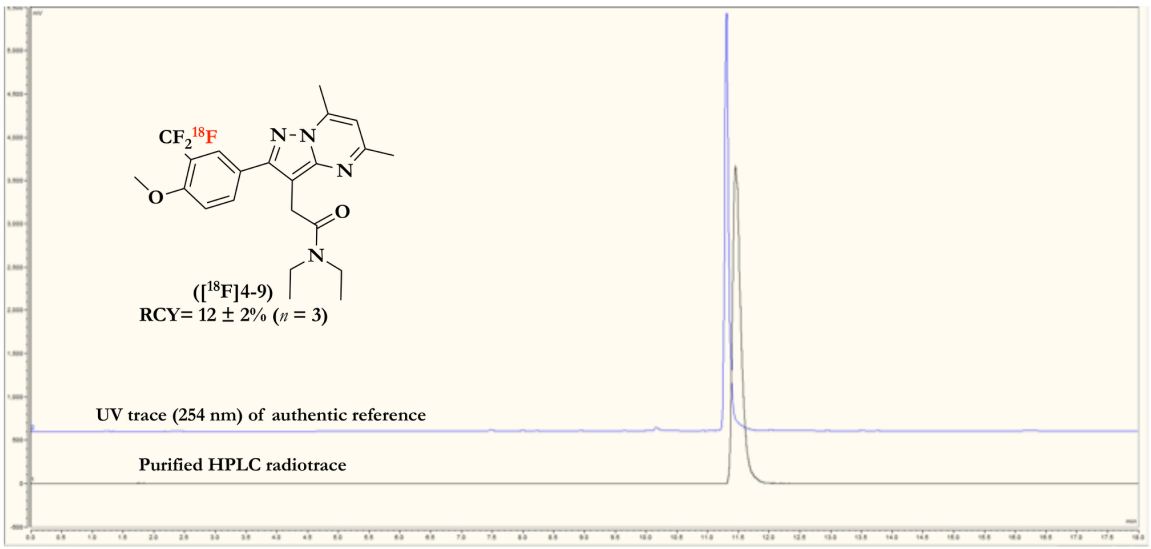
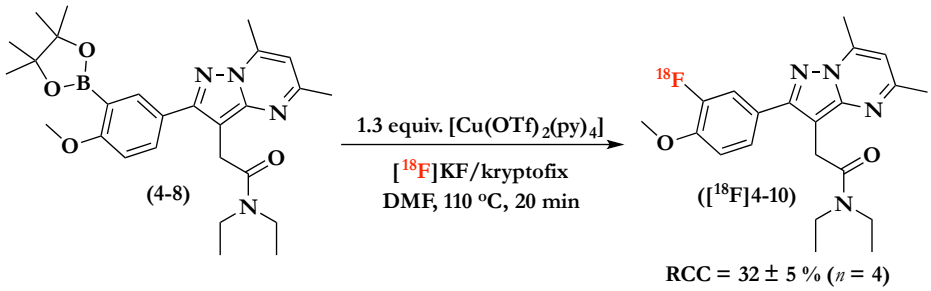


Figure 4.7.2: Purified batch scale HPLC chromatograph of [[18]F]4-9

§§ Analogous to the RCC calculation described in section 2.4.1

4.7.2 ^{18}F-Fluorination

^{18}F-Fluorination of **4-8** was successfully carried out on a 20–30 MBq scale. Aliquots of dried [^{18}F]KF/K_{222} in MeCN (20–30 MBq, 10–40 µL) were dispensed into a V-vial containing 1.3 equivalents of $Cu(OTf)_2(py)_4$, **4-8** and a magnetic stirrer bar. DMF was added to the reaction and the vial was heated at 110 °C for 20 minutes. The RCC was calculated *via* radio-TLC, using the same method discussed in **section 4.7.1**. The ^{18}F-fluorination of **4-8** was repeated four times resulting in a RCC of 32 ± 5% (n = 4) (Scheme 4.7.2).



Scheme 4.7.2: Radiosynthesis of [^{18}F]4-10

From Figure 4.7.3 it is evident that both the UV trace of **4-10** and fluorine-18 crude radiotrace align, thus confirming the identity of **[^{18}F]4-10.**

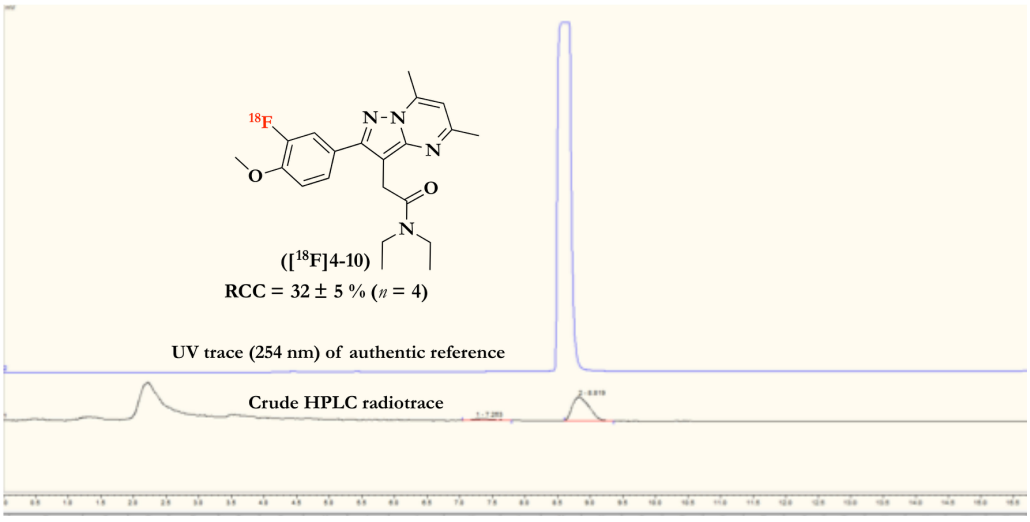
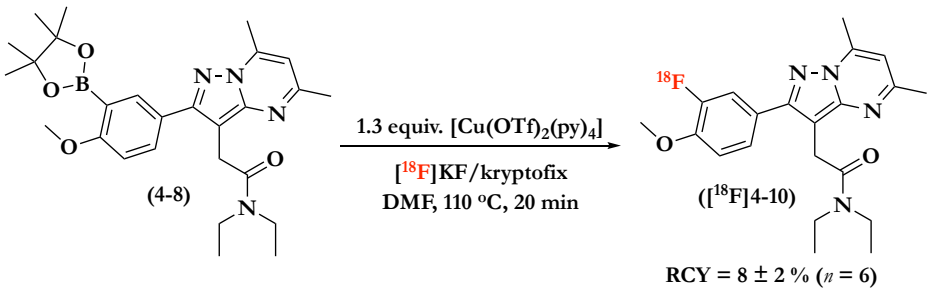


Figure 4.7.3: Radio-HPLC of [^{18}F]4-10 used for product identification

Subsequently, a batch scale synthesis of **[^{18}F]4-10** was conducted, commencing with 3.3–5.24 GBq of aqueous [^{18}F]fluoride. However, the increasing quantity of K_2CO_3 required for successful elution of [^{18}F]fluoride from the QMA cartridge resulted in reduced yields of **[^{18}F]4-10.** As a consequence, an eluting solution used previously by Katsifis,[55] containing kryptofix 222/$K_2C_2O_4$/K_2CO_3 in a ratio of 6 : 1 : 0.1 was employed.[55] The reduced basicity of Katsifis' solution proved optimal and **[^{18}F]4-10** was prepared in 8% ± 2% (n = 6) RCY, with a total synthesis time of 68–78 min from aqueous [^{18}F]fluoride (Scheme 4.7.3).



Scheme 4.7.3: RCY for batch scale synthesis of [^{18}F]4-10

The product was identified and purified *via* semi-prep radio-HPLC, chromatograph shown in Figure 4.7.4.

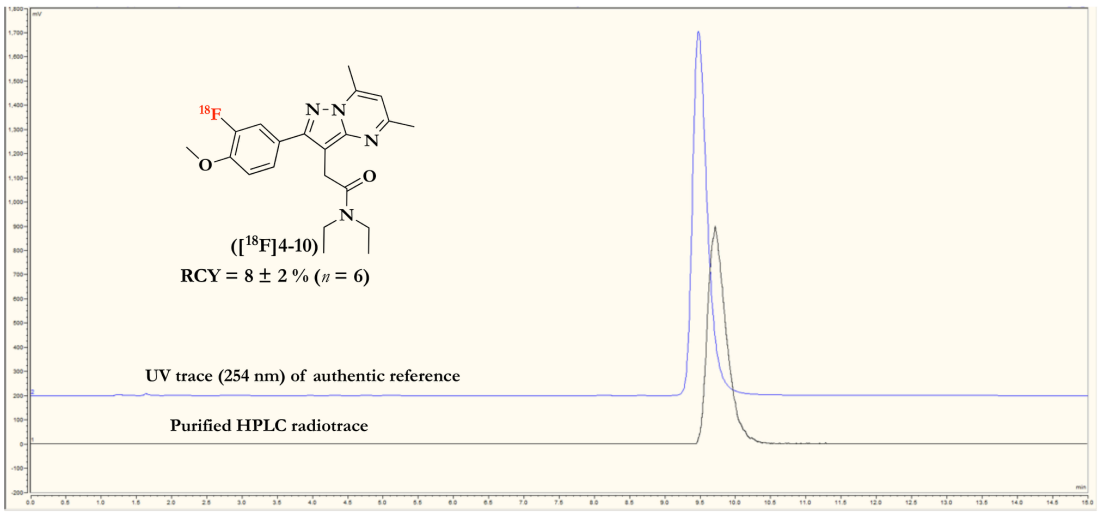


Figure 4.7.4: Purified batch scale HPLC chromatograph of [^{18}F]4-10

4.8 Biological Studies

This work was carried out in collaboration with Prof. Daniel Anthony and Dr. Alex Dickens.

Multiple Sclerosis (MS) is primarily an inflammatory disease of the CNS, where focal lymphocytic infiltration leads to damage of myelin (demyelination) and axons resulting in neurodegeneration.[56,57] Neuronal damage of the MS brain is concomitant with microglial activation; axonal injury arises in both MS lesions and within normal appearing white matter, exclusive to regions of activated microglia.[58] As stated in **Section 4.1**, augmented expression of TSPO is a hallmark of neuroinflammation[15,59] due to the activation of microglia and astrocytes.[60,61] Therefore we sought to test **[^{18}F]4-9** and **[^{18}F]4-10** in a clinically relevant animal model of MS to assess their performance against other available TSPO tracers.

4.8.1 Statistical Analysis

The digital images discussed in the following sections were analysed in image J (NIH) using a set size region of interest, which was placed in the ipsi and contralateral striatum. The average intensity in the region of interest (ROI) was then converted to a binding per mm^2 and the background radiation was subtracted. A binding potential ($\mathbf{B_{pnd}}$) was then generated using the following formula:

$$\mathbf{B_{pnd} = ((PSL/cm^2)_{(Lesion)} - (PSL/cm^2)_{(Contralateral)})/(PSL/cm^2)_{(Contralateral)}}$$

The top three binding potential values were used from each brain and averaged. This data was then used for subsequent analysis in Prism (v7 Graph Pad). Student's t-tests were used to determine if there was a difference in the means when two groups were present.

4.8.2 Autoradiography of LPS induced neuroinflammation using [^{18}F]4-9

Initially an *in vivo* evaluation of **[^{18}F]4-9** was conducted in a rat model of neuroinflammation induced *via* lipopolysaccharide (LPS).[62,63] LPS is an endotoxin from gram-negative bacteria that damages dopaminergic (DA) neurons *via* microglial activation and subsequent production of neurotoxic co-factors.[64]

To induce inflammation, the rats were placed onto a stereotaxic frame, and the skull was exposed. The brain of the animal was then exposed *via* a burr hole, which was drilled through the skull. A finely-drawn glass cannula was inserted into the left striatum. LPS in saline was then injected over five minutes, followed by a two-minute rest period, to allow diffusion into the brain prior to the removal of the capillary. A saline control group was also included in the study. Twenty-four hours after the intracerebral injection, the animals were injected intravenously with 30 MBq of **[^{18}F]4-9** in pure EtOH,*** prepared *via* batch scale synthesis (**section 4.7.1**). To allow for complete binding of **[^{18}F]4-9**, the animals were killed by decapitation after 40 minutes. This is the maximum time point of binding for TSPO ligands PK11195 **(4-1)** and GE-180 **(4-3).**[65] The rodent brain was removed and cryosections from the striatum (20 µM) were collected on a positively charged slide. The sections were dried and left overnight, and images were acquired at a resolution of 100 µm² on a typhoon scanner.

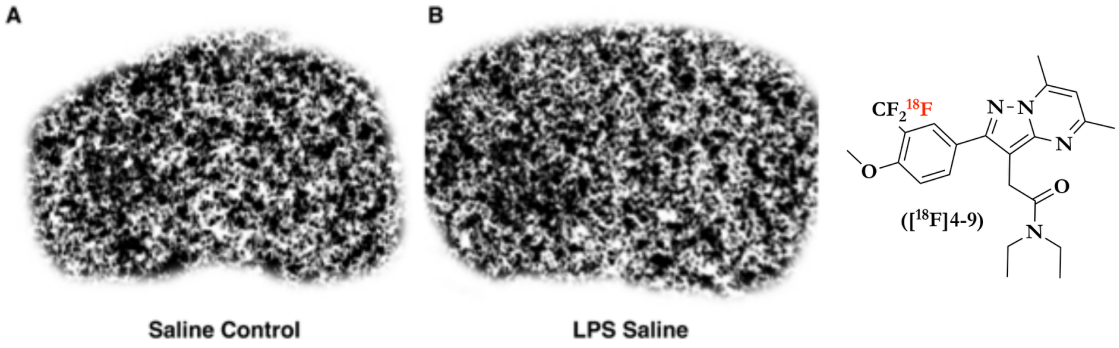


Figure 4.8.1: Autoradiographic cross section of rat brain injected with 30 MBq of [^{18}F]4-9 a) Saline control & b) LPS saline

*** **[^{18}F]4-9** was not soluble in saline solution

Figure 4.8.1 details autoradiographic images of a) the saline control group and b) the LPS model of neuroinflammation collected for *in vivo* evaluation of **[^{18}F]4-9**. Unfortunately, no observed increase in uptake of **[^{18}F]4-9** around the lesion ($\mathbf{B_{pnd}}$ = 0.01 ± 0.02) in the rat brain was detected. A possible explanation for this result is the low solubility of **[^{18}F]4-9**, which may result in poor drug delivery and low brain uptake of the radiotracer.

4.8.3 Autoradiography of LPS-induced neuroinflammation using [^{18}F]4-10

An LPS model of neuroinflammation, similar to that used in **section 4.8.2** was induced in male adult C57Bl6 mice, to test the binding potential of **[^{18}F]4-10**. **[^{18}F]4-10** was synthesised on a batch scale (**section 4.7.2**) and subsequently injected (control: 14.1 MBq ± 0.3, LPS: 15.0 MBq ± 0.3) *via* a tail vein cannula. The injection of LPS into the striatum of mice caused a moderate increase in binding of **[^{18}F]4-10** ($\mathbf{B_{pnd}}$ = 0.37 ± 0.03; Figure 4.8.2 B) compared to saline-injected animals at day one (Figure 4.8.2 A + B). Interestingly, three days following the intracerebral injection of LPS, the binding of **[^{18}F]4-10** had increased (p = 0.0007, n = 3) suggesting a higher level of TSPO expression ($\mathbf{B_{pnd}}$ = 0.60 ± 0.03; Figure 4.8.2 C). Given the increased binding of **[^{18}F]4-10** observed in the LPS model of neuroinflammation, we aimed to test **[^{18}F]4-10** in a more clinically relevant animal model of MS.

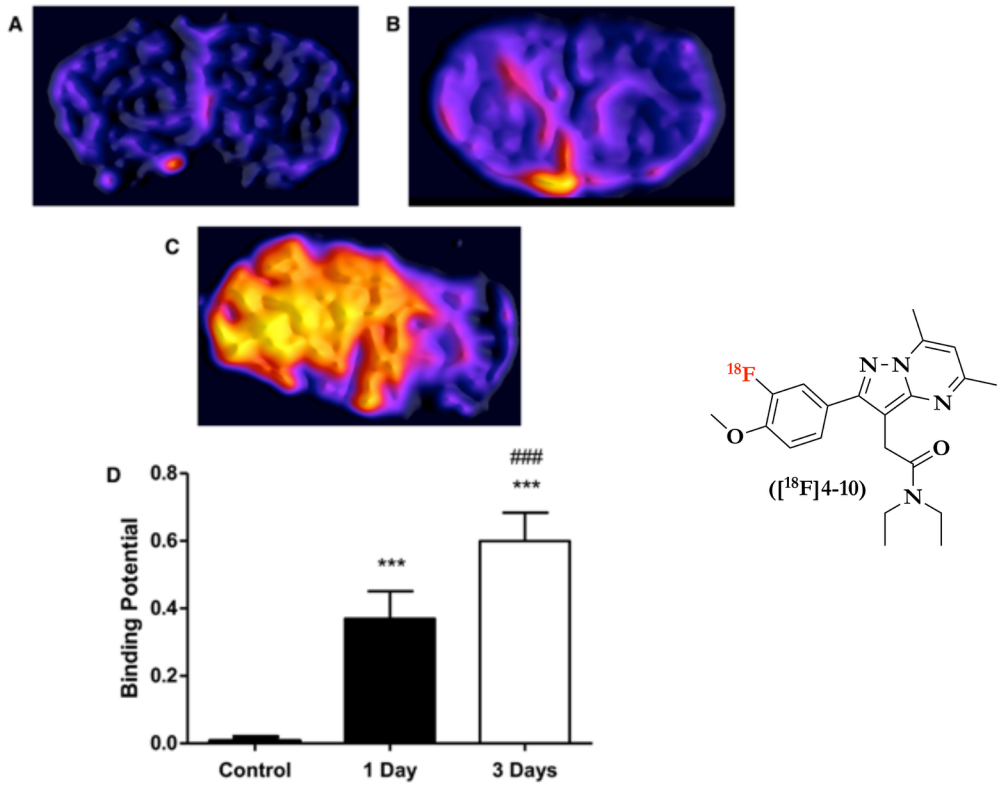


Figure 4.8.2: TSPO expression in mice increases following the injection of LPS into the striatum. A = Control. B= [^{18}F]4-10 binding at day 1. C = [^{18}F]4-10 binding at day 3. D = Binding Potential.

4.8.4 [^{18}F]4-10 binds to the TSPO expression surrounding a focal MS-like lesion in mice

An *in vivo* evaluation of **[^{18}F]4-10** was conducted in a focal MOG-EAE (fMOG-EAE) model of MS. Experimental allergic encephalomyelitis (EAE) is an inflammatory demyelinating disease of the central nervous system and is utilised as an animal model for human MS, sharing many clinical and pathophysiological characteristics.[66] Induction of EAE is possible in rodents *via* exposure to antigens, such as spinal cord homogenate (SCH), myelin basic protein (MBP), myelin proteolipid protein (MPL) and myelin oligodendrocyte glycoprotein (MOG), in conjunction with an adjuvant to elicit an enhanced immune response.[67] In the fMOG-EAE animal model, a focal demyelinating lesion is generated, with blood-brain barrier (BBB) breakdown, microglial & astrocyte activation, recruitment of monocytes and of T and B cells, and

loss of axons, mirroring human MS.[68,69] A peripheral injection of MOG in complete Freud's adjuvant and subsequent intracerebral injection of heat-killed Bacillus Calmette–Guérin (BCG) resulted in the development of a fMOG-EAE lesion in the mice (**section 5.4.5 for details**). The lesion had similar characteristics to an fMOG-EAE lesion generated in rats with activation of microglia and astrocytes in the brain tissue surrounding the core.[70,71] This activation has been shown to increase the expression of TSPO around the lesions.[72]

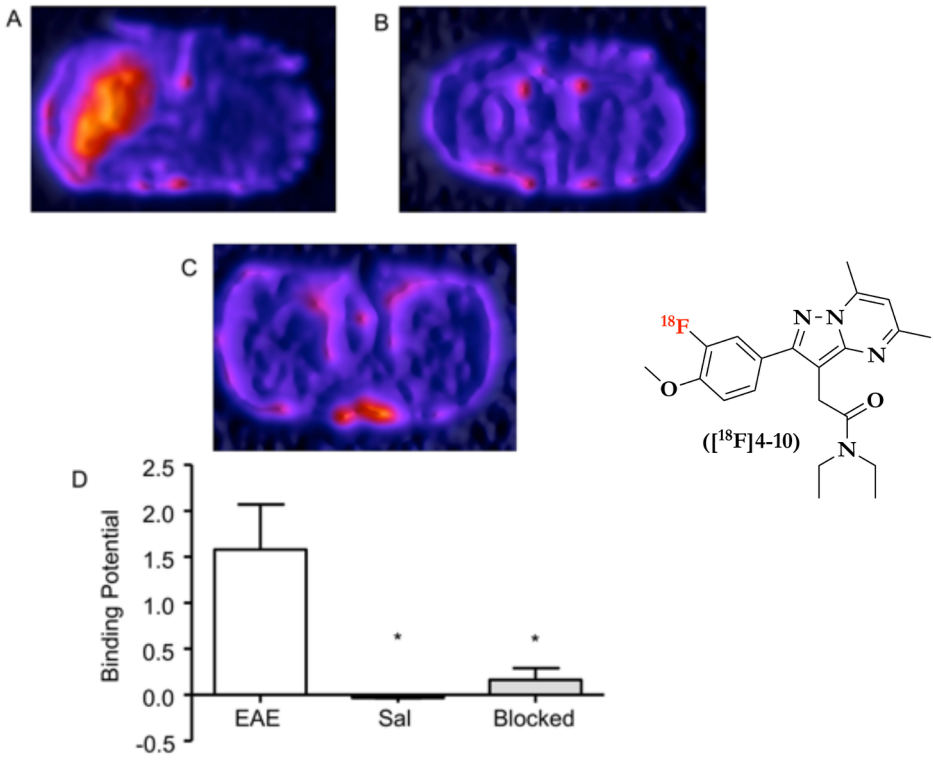
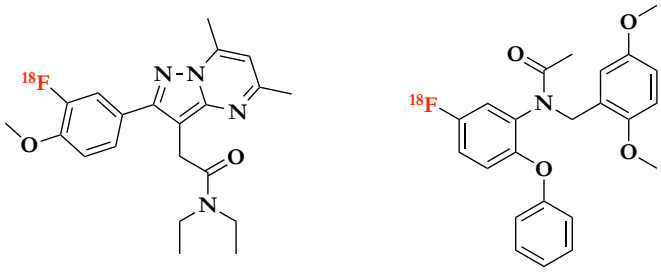


Figure 4.8.3: [^{18}F]4-10 binds specifically to the TSPO receptor around a fEAE lesion in mice. Representative ex-vivo digital autoradiography images (A, B, C): A) Taken from an animal with a fEAE lesion, B) a control animal and C) animal with fEAE lesion where the binding is blocked with unlabelled PK11195. D) Quantitation demonstrating an increase in binding of [^{18}F]4-10 (B_{pnd} = 1.58 ± 0.49) at the site of a fEAE lesion compared to the control animals (B_{pnd} = -0.03 ± 0.01). Pre-injecting the animal with cold PK11195 blocked the binding of the radiotracer [^{18}F]4-10 (B_{pnd} = 0.16 ± 0.12). Data are mean ± SEM of n = 3 mice per group. * p < 0.05 compared to lesioned animal.

The increase in TSPO expression in our animals could be observed by the increase ($p < 0.05$, $n = 3$) in uptake of **[^{18}F]4-10** around the lesion ($\mathbf{B_{pnd}}$ = 1.58 ± 0.49, Figure 4.8.3 A + D). Such an increase in binding of **[^{18}F]4-10** was not observed in the control animals ($\mathbf{B_{pnd}}$ = -0.03 ± 0.01, Figure 4.8.3 B + D). To assess the specificity of **[^{18}F]4-10** for TSPO, *in-vivo* autoradiography blocking experiments were also performed. The TSPO specific ligand, PK11195 **(4-1)** was injected *via* tail vein cannula 20 minutes prior to the injection of **[^{18}F]4-10** (16.5 MBq ± 0.4) at a concentration approximately 1000 times greater than **[^{18}F]4-10**. The pre-injection of unlabelled **4-1** blocked the majority of the radiotracer binding ($p < 0.05$, $n = 3$) around the lesion ($\mathbf{B_{pnd}}$ = 0.16 ± 0.12, Figure 4.8.3 C). Complete blockade of the radiotracer is rare due to the sensitivity of digital autoradiography imaging, however, the reduction in signal was comparable to that of [^{18}F]GE-180 **(4-3)**.[65] The data suggests that **[^{18}F]4-10** binds specifically to TSPO surrounding an MS-like lesion in mice.

4.8.5 [^{18}F]4-10 has a greater binding affinity for TSPO in the brains of mice

We sought to assess the performance of **[^{18}F]4-10** against another prominent TSPO tracer [^{18}F]DAA1106 (**[^{18}F]4-4**).[15]

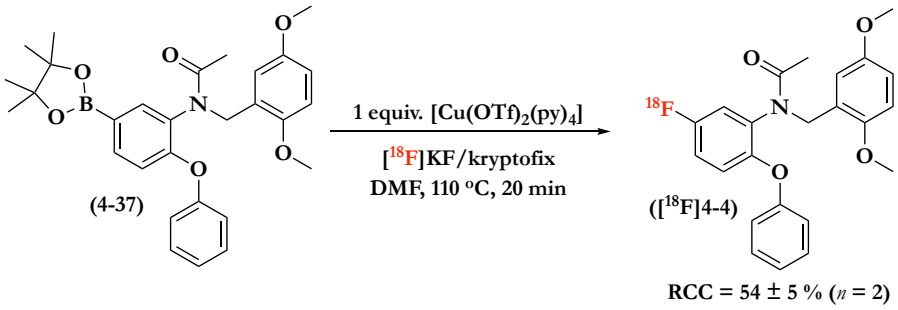


[^{18}F]4-10 **[^{18}F]4-4**

Figure 4.8.4: Chemical structures of [^{18}F]4-10 and [^{18}F]4-4

[^{18}F]4-4 was synthesised from **4-37**†††, starting from 30 MBq of dried [^{18}F]KF/K_{222} in MeCN (Scheme 4.8.1). The radiosynthetic protocol employed was identical to that used for **[^{18}F]4-10** (Section 4.7.2).

††† Full synthesis of **4-37** described in Experimental Chapter 5



Scheme 4.8.1: Radiosynthesis of [^{18}F]4-4

Purification and isolation of **[^{18}F]4-4** (0.3 MBq) was achieved *via* preparative-HPLC. For *in vitro* studies comparing **[^{18}F]4-10** to **[^{18}F]4-4** (n = 3), adjacent sections were incubated with 0.02 MBq/mL of **[^{18}F]4-4** for a period of 1 hour. Following incubation with the radioactivity, all slides were washed twice with TRIS-HCl buffer. The sections were dried and placed in an imaging cassette and the images were collected on a typhoon scanner.

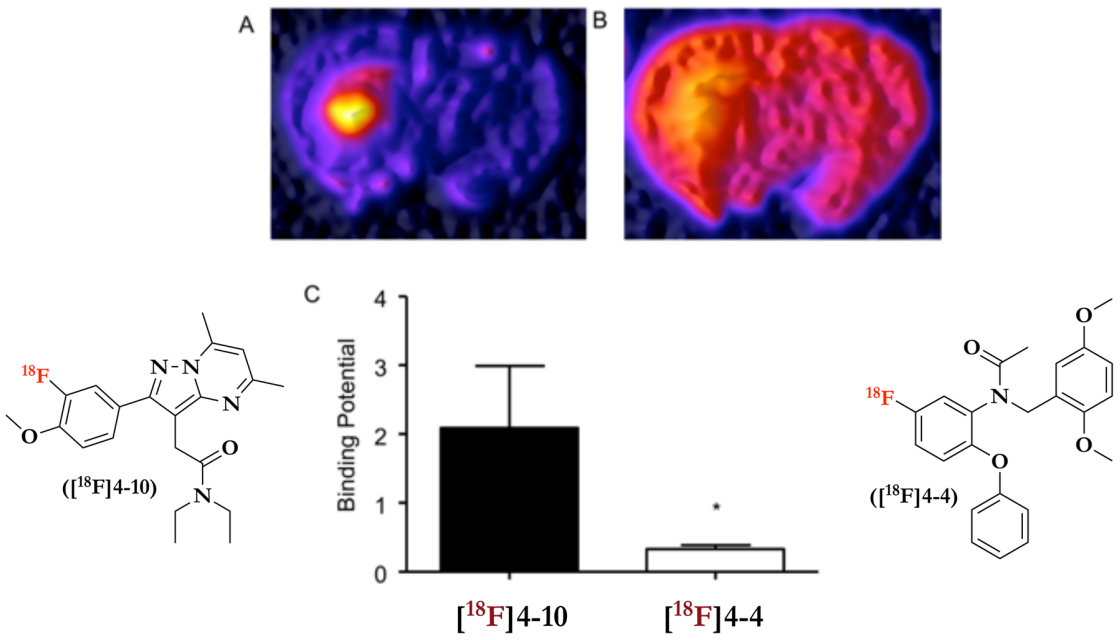


Figure 4.8.5: [^{18}F]4-10 has a greater binding affinity for the TSPO protein in the brains of mice. ***In-vitro*** **representative digital autoradiography images (A+B) taken from sequential sections imaged with [^{18}F]4-10 (A) and [^{18}F]4-4 (B). (C) The binding potential of [^{18}F]4-10 in the lesion is increased compared to [^{18}F]4-4.**

It is evident from Figure 4.8.5 (A + B) that **[^{18}F]4-10** has a greater binding affinity ($p = 0.028$, $n = 3$) for TSPO in the brains of mice. Most notably, the increase in background binding when using **[^{18}F]4-4** is quite apparent from Figure 4.8.5 B. Figure 4.8.5 C also demonstrates the binding potential of **[^{18}F]4-10** ($\mathbf{B_{pnd}} = 2.09 \pm 0.52$) in the lesion is increased compared to **[^{18}F]4-4** ($\mathbf{B_{pnd}} = 0.33 \pm 0.03$).

4.9 Conclusions and future work

In conclusion, this chapter has outlined the synthesis of two ^{18}F analogues of the Translocator Protein (TSPO) ligand N,N-diethyl-2-(4-methoxyphenyl)-5,7-dimethylpyrazolo[1,5-a]pyrimidine-3-acetamide-713 (DPA-713): [^{18}F]DPA-713 (**[^{18}F]4-10**) and [^{18}F]CF_3DPA-713 (**[^{18}F]4-9**). Both compounds have been tested in clinically relevant animal models of neuroinflammation. More specifically, **[^{18}F]4-10** was tested in a clinically relevant animal model of MS (fMOG-EAE lesion) where a marked increase in the uptake of **[^{18}F]4-10** around the lesion was observed. Its performance was also assessed against [^{18}F]DAA1106 (**[^{18}F]4-4**), another prominent TSPO tracer. In this instance, **[^{18}F]4-10** demonstrated a greater binding affinity for the TSPO protein in the brains of mice.

In the future, studies employing human MS tissue would be beneficial for elucidating the discrepancy in binding between HABs and LABs for this newly developed radiotracer.

4.10 References

(1) Braestrup, C.; Squires, R. F. *Proc. Natl. Acad. Sci.* **1977**, *74* (9), 3805–3809.

(2) Banister, S. D.; Wilkinson, S. M.; Hanani, R.; Reynolds, A. J.; Hibbs, D. E.; Kassiou, M. *Tetrahedron Lett.* **2012**, *53* (29), 3780–3783.

(3) McEnery, M.; Snowman, A.; Trifiletti, R.; Snyder, S. H. *Proc. Natl. Acad. Sci.* **1992**, *89* (8), 3170–3174.

(4) Papadopoulos, V.; Aghazadeh, Y.; Fan, J.; Campioli, E.; Zirkin, B.; Midzak, A. *Molecular and Cellular Endocrinology* **2015**, *408* (C), 90–98.

(5) Lacapère, J.-J.; Papadopoulos, V. *Steroids* **2003**, *68* (7-8), 569–585.

(6) Papadopoulos, V.; Liu, J.; Culty, M. *Molecular and Cellular Endocrinology* **2007**, *265-266*:59–64.

(7) Guo, Y.; Kalathur, R. C.; Liu, Q.; Kloss, B.; Bruni, R.; Ginter, C.; Kloppmann, E.; Rost, B.; Hendrickson, W. A. *Science* **2015**, *347* (6221), 551–555.

(8) Rupprecht, R.; Papadopoulos, V.; Rammes, G.; Baghai, T. C.; Fan, J.; Akula, N.; Groyer, G.; Adams, D.; Schumacher, M. *Nat. Rev. Drug Discov.* **2010**, *9*, 971–988.

(9) Veenman, L.; Gavish, M. *Curr. Mol. Med.* **2012**, *12* (4), 398–412.

(10) Papadopoulos, V.; Baraldi, M.; Guilarte, T. R.; Knudsen, T. B.; Lacapère, J.-J.; Lindemann, P.; Norenberg, M. D.; Nutt, D.; Weizman, A.; Zhang, M.-R.; Gavish, M. *Trends Pharmacol. Sci.* **2006**, *27* (8), 402–409.

(11) Kuhlmann, A. C.; Guilarte, T. R. *J. Neurochem.* **2002**, *74* (4), 1694–1704.

(12) Maeda, J.; Higuchi, M.; Inaji, M.; Ji, B.; Haneda, E.; Okauchi, T.; Zhang, M.-R.; Suzuki, K.; Suhara, T. *Brain Research* **2007**, *1157*, 100–111.

(13) Cosenza-Nashat, M.; Zhao, M. L.; Suh, H. S.; Morgan, J.; Natividad, R.; Morgello, S.; Lee, S. C. *Neuropathol. Appl. Neurobiol.* **2009**, *35* (3), 306–328.

(14) Girard, C.; Liu, S.; Adams, D.; Lacroix, C.; Sinéus, M.; Boucher, C.; Papadopoulos, V.; Rupprecht, R.; Schumacher, M.; Groyer, G. *J. Neuroendocrinol.* **2011**, *24* (1), 71–81.

(15) Chen, M.-K.; Guilarte, T. R. *J. Pharm. Therapeutics* **2008**, *118* (1), 1–17.

(16) Camsonne, R.; Crouzel, C.; Comar, D.; M, M.; C, P.; Sastre, J.; MA, M.; Syrota, A. *J. Labelled Compd. Radiopharm.* **1984**, *21*, 985–991.

(17) Belloli, S.; Moresco, R. M.; Matarrese, M.; Biella, G.; Sanvito, F.; Simonelli, P.; Turolla, E.; Olivieri, S.; Cappelli, A.; Vomero, S.; Galli-Kienle, M.; Fazio, F. *Neurochem. Int.* **2004**, *44* (6), 433–440.

(18) Lockhart, A.; Davis, B.; Matthews, J. C.; Rahmoune, H.; Hong, G.; Gee, A.; Earnshaw, D.; Brown, J. *Nucl. Med. Biol.* **2003**, *30* (2), 199–206.

(19) O'Brien, E. R.; Kersemans, V.; Tredwell, M.; Checa, B.; Serres, S.; Soto, M. S.; Gouverneur, V.; Leppert, D.; Anthony, D. C.; Sibson, N. R. *J. Nucl. Med.* **2014**, *55* (2), 275–280.

(20) Damont, A.; Roeda, D.; Dollé, F. *J. Labelled Compd. Radiopharm.* **2013**, *56* (3-4), 96–104.

(21) Pimlott, S. L.; Sutherland, A. *Chem. Soc. Rev.* **2011**, *40* (1), 149–162.

(22) Wickstrøm, T.; Clarke, A.; Gausemel, I.; Horn, E.; Jørgensen, K.; Khan, I.; Mantzilas, D.; Rajanayagam, T.; In 't Veld, D.-J.; Trigg, W. *J. Labelled Compd. Radiopharm.* **2013**, *57* (1), 42–48.

(23) Briard, E.; Hong, J.; Musachio, J. L.; Zoghbi, S. S.; Fujita, M.; Imaizumi, M.; Cropley, V.; Innis, R. B.; Pike, V. W. *J. Labelled Compd. Radiopharm.* **2005**, *48*, S71.

(24) Imaizumi, M.; Briard, E.; Zoghbi, S. S.; Gourley, J. P.; Hong, J.; Musachio, J. L.; Gladding, R.; Pike, V. W.; Innis, R. B.; Fujita, M. *Synapse* **2007**, *61* (8), 595–605.

(25) Wang, M.; Yoder, K. K.; Gao, M.; Mock, B. H.; Xu, X.-M.; Saykin, A. J.; Hutchins, G. D.; Zheng, Q.-H. *Bioorg. Med. Chem. Lett.* **2009**, *19* (19), 5636–5639.

(26) Wilson, A. A.; Garcia, A.; Parkes, J.; McCormick, P.; Stephenson, K. A.; Houle, S.; Vasdev, N. *Nucl. Med. Biol.* **2008**, *35* (3), 305–314.
(27) Briard, E.; Zoghbi, S. S.; Siméon, F. G.; Imaizumi, M.; Gourley, J. P.; Shetty, H. U.; Lu, S.; Fujita, M.; Innis, R. B.; Pike, V. W. *J. Med. Chem.* **2009**, *52* (3), 688–699.
(28) Chauveau, F.; Boutin, H.; Van Camp, N.; Dollé, F.; Tavitian, B. *Eur. J Nucl. Med. Mol. Imaging* **2008**, *35* (12), 2304–2319.
(29) Owen, D. R. J.; Gunn, R. N.; Rabiner, E. A.; Bennacef, I.; Fujita, M.; Kreisl, W. C.; Innis, R. B.; Pike, V. W.; Reynolds, R.; Matthews, P. M.; Parker, C. A. *J. Nucl. Med.* **2011**, *52* (1), 24–32.
(30) Owen, D. R.; Yeo, A. J.; Gunn, R. N.; Song, K.; Wadsworth, G.; Lewis, A.; Rhodes, C.; Pulford, D. J.; Bennacef, I.; Parker, C. A.; StJean, P. L.; Cardon, L. R.; Mooser, V. E.; Matthews, P. M.; Rabiner, E. A.; Rubio, J. P. *J. Cereb. Blood Flow Metab.* **2012**, *32* (1), 1–5.
(31) Tredwell, M.; Preshlock, S. M.; Taylor, N. J.; Gruber, S.; Huiban, M.; Passchier, J.; Mercier, J.; Génicot, C.; Gouverneur, V. *Angew. Chem. Int. Ed.* **2014**, *53* (30), 7751–7755.
(32) Wadsworth, H.; Jones, P. A.; Chau, W.-F.; Durrant, C.; Fouladi, N.; Passmore, J.; O'Shea, D.; Wynn, D.; Morisson-Iveson, V.; Ewan, A.; Thaning, M.; Mantzilas, D.; Gausemel, I.; Khan, I.; Black, A.; Avory, M.; Trigg, W. *Bioorg. Med. Chem. Lett.* **2012**, *22* (3), 1308–1313.
(33) Fan, Z.; Calsolaro, V.; Atkinson, R. A.; Femminella, G. D.; Waldman, A.; Buckley, C.; Trigg, W.; Brooks, D. J.; Hinz, R.; Edison, P. *J. Nucl. Med.* **2016**, *57* (11), 1753–1759.
(34) Endres, C. J.; Pomper, M. G.; James, M.; Uzuner, O.; Hammoud, D. A.; Watkins, C. C.; Reynolds, A.; Hilton, J.; Dannals, R. F.; Kassiou, M. *J. Nucl. Med.* **2009**, *50* (8), 1276–1282.
(35) Coughlin, J. M.; Wang, Y.; Munro, C. A.; Ma, S.; Yue, C.; Chen, S.; Airan, R.; Kim, P. K.; Adams, A. V.; Garcia, C.; Higgs, C.; Sair, H. I.; Sawa, A.; Smith, G.; Lyketsos, C. G.; Caffo, B.; Kassiou, M.; Guilarte, T. R.; Pomper, M. G. *Neurobiol. Dis.* **2015**, *74* (C), 58–65.
(36) James, M. L.; Fulton, R. R.; Vercoullie, J.; Henderson, D. J.; Garreau, L.; Chalon, S.; Dollé, F.; Costa, B.; Selleri, S.; Guilloteau, D.; Kassiou, M. *J. Nucl. Med.* **2008**, *49* (5), 814–822.
(37) Miller, P. W.; Long, N. J.; Vilar, R.; Gee, A. D. *Angew. Chem. Int. Ed.* **2008**, *47* (47), 8998–9033.
(38) Doorduin, J.; Klein, H. C.; Dierckx, R. A.; James, M.; Kassiou, M.; de Vries, E. F. J. *Mol. Imaging. Biol.* **2009**, *11* (6), 386–398.
(39) Peyronneau, M.-A.; Saba, W.; Goutal, S.; Damont, A.; Dollé, F.; Kassiou, M.; Bottlaender, M.; Valette, H. *Drug Metab. Dispos.* **2013**, *41* (1), 122–131.
(40) Golla, S. S. V.; Boellaard, R.; Oikonen, V.; Hoffmann, A.; van Berckel, B. N. M.; Windhorst, A. D.; Virta, J.; Haaparanta-Solin, M.; Luoto, P.; Savisto, N.; Solin, O.; Valencia, R.; Thiele, A.; Eriksson, J.; Schuit, R. C.; Lammertsma, A. A.; Rinne, J. O. *J. Cereb. Blood Flow Metab.* **2015**, *35* (5), 766–772.
(41) Huiban, M.; Tredwell, M.; Mizuta, S.; Wan, Z.; Zhang, X.; Collier, T. L.; Gouverneur, V.; Passchier, J. *Nat. Chem.* **2013**, *5*, 941–944.
(42) Keller, T.; Krzyczmonik, A.; Forsback, S.; Picón, F. R. L.; Kirjavainen, A. K.; Takkinen, J.; Rajander, J.; Cacheux, F.; Damont, A.; Dollé, F.; Rinne, J. O.; Haaparanta-Solin, M.; Solin, O. *Mol. Imaging Biol.* **2017**, *19* (5), 736–745.
(43) Reynolds, A.; Hanani, R.; Hibbs, D.; Damont, A.; Da Pozzo, E.; Selleri, S.; Dollé, F.; Martini, C.; Kassiou, M. *Bioorg. Med. Chem. Lett.* **2010**, *20* (19), 5799–5802.

(44) Dempsey, B.; Serjeant, E. P. *Ionisation constants of organic acids in aqueous solution.*; Dempsey, B., Serjeant, E. P., Eds.; Oxford; Pergamon Press, 1979; Vol. 18, pp 1–989.
(45) Reynolds, A.; Hanani, R.; Hibbs, D.; Damont, A.; Da Pozzo, E.; Selleri, S.; Dollé, F.; Martini, C.; Kassiou, M. *Bioorg. Med. Chem. Lett.* **2010**, *20* (19), 5799–5802.
(46) Tang, D.; McKinley, E. T.; Hight, M. R.; Uddin, M. I.; Harp, J. M.; Fu, A.; Nickels, M. L.; Buck, J. R.; Manning, H. C. *J. Med. Chem.* **2013**, *56* (8), 3429–3433.
(47) Riches, S. L.; Saha, C.; Filgueira, N. F.; Grange, E.; McGarrigle, E. M.; Aggarwal, V. K. *J. Am. Chem. Soc.* **2010**, *132* (22), 7626–7630.
(48) Romanov-Michailidis, F.; Besnard, C.; Alexakis, A. *Org. Lett.* **2012**, *14* (18), 4906–4909.
(49) Ogura, T.; Usuki, T. *Tetrahedron* **2013**, *69* (13), 2807–2815.
(50) Ishiyama, T.; Murata, M.; Miyaura, N. *J. Org. Chem.* **1995**, 7508–7510.
(51) Lam, K. C.; Marder, T. B.; Lin, Z. *Organometallics* **2010**, *29* (7), 1849–1857.
(52) Baudoin, O.; Guénard, D.; Guéritte, F. *J. Org. Chem.* **2000**, *65* (26), 9268–9271.
(53) Ahmadi, Z.; McIndoe, J. S. *Chem. Commun.* **2013**, *49* (98), 11488–3.
(54) Kawamorita, S.; Ohmiya, H.; Iwai, T.; Sawamura, M. *Angew. Chem. Int. Ed.* **2011**, *50* (36), 8363–8366.
(55) Katsifis, A.; Hamacher, K.; Schnitter, J.; Stöcklin, G. *Appl. Radiat. Isot.* **1993**, *7* (44), 1015–1020.
(56) Compston, A.; Coles, A. *The Lancet* **2002**, *359* (9313), 1221–1231.
(57) Compston, A.; Coles, A. *The Lancet* **2008**, *372* (9648), 1502–1517.
(58) Howell, O. W.; Rundle, J. L.; Garg, A.; Komada, M.; Brophy, P. J.; Reynolds, R. *J Neuropathol. Exp. Neurol.* **2010**, *69* (10), 1017–1033.
(59) Benavides, J.; Fage, D.; Carter, C.; Scatton, B. *Brain Research* **1987**, 167–172.
(60) Banati, R. B. *Glia* **2002**, *40* (2), 206–217.
(61) Lavisse, S.; Guillermier, M.; Hérard, A.-S.; Petit, F.; Delahaye, M.; Van Camp, N.; Ben Haim, L.; Lebon, V.; Remy, P.; Dollé, F.; Delzescaux, T.; Bonvento, G.; Hantraye, P.; Escartin, C. *J. Neurosci.* **2012**, *32* (32), 10809–10818.
(62) Gao, H.-M.; Jiang, J.; Wilson, B.; Zhang, W.; Hong, J.-S.; Bin Liu. *J. Neurochem.* **2002**, *81*, 1285–1297.
(63) Lee, J.; Lee, Y.; Yuk, D.; Choi, D.; Ban, S.; Oh, K.; Hong, J. *J. Neuroinflammation* **2008**, *5* (1), 37–14.
(64) Qin, L.; Wu, X.; Block, M. L.; Liu, Y.; Breese, G. R.; Hong, J.-S.; Knapp, D. J.; Crews, F. T. *Glia* **2007**, *55* (5), 453–462.
(65) Dickens, A. M.; Vainio, S.; Marjamaki, P.; Johansson, J.; Lehtiniemi, P.; Rokka, J.; Rinne, J.; Solin, O.; Haaparanta-Solin, M.; Jones, P. A.; Trigg, W.; Anthony, D. C.; Airas, L. *J. Nucl. Med.* **2014**, *55* (3), 466–472.
(66) Bittner, S.; Afzali, A. M.; Wiendl, H.; Meuth, S. G. *JoVE* **2014**, No. 86, 1–5.
(67) Petrovsky, N.; Aguilar, J. C. *Immunol. Cell Biol.* **2004**, *82*, 488–496.
(68) Kerschensteiner, M.; Bareyre, F. M.; Buddeberg, B. S.; Merkler, D.; Stadelmann, C.; Brück, W.; Misgeld, T.; Schwab, M. E. *J. Exp. Med.* **2004**, *200* (8), 1027–1038.
(69) Merkler, D. *Brain* **2006**, *129* (8), 1972–1983.
(70) Anthony, D. C.; Miller, K. M.; Fearn, S.; Townsend, M. J.; Opdenakker, G.; Wells, G. M. A.; Clements, J. M.; Chandler, S.; Gearing, A. J. H.; Perry, V. H. *J. Neuroimmunol.* **1998**, *87*, 62–72.
(71) Serres, S.; Anthony, D. C.; Jiang, Y.; Campbell, S. J.; Broom, K. A.; Khrapitchev, A.; Sibson, N. R. *NMR Biomed.* **2009**, 1014–1024.
(72) Airas, L.; Dickens, A. M.; Elo, P.; Marjamäki, P.; Johansson, J.; Eskola, O.; Jones, P. A.; Trigg, W.; Solin, O.; Haaparanta-Solin, M.; Anthony, D. C.; Rinne, J. *J. Nucl. Med.* **2015**, *56* (2), 305–310.

Chapter 5

Experimental Data

5 Experimental Data

5.1 General Experimental

Commercial reagents and solvents were purchased from Acros Organics, Alfa Aesar, Apollo Scientific, Fisher Scientific, Fluorochem or Sigma-Aldrich and, unless otherwise stated, used as received. Anhydrous solvents were purified by expression through an activated alumina column built according to the procedures described by Pangborn and Grubbs.[1]

All reactions were performed in oven-dried apparatus with magnetic stirring under an inert atmosphere of argon or nitrogen unless otherwise indicated. All solvents were dried on a column of alumina prior to use. Thin layer chromatography (TLC) was performed using Merck aluminium-foil baked plates precoated with Kieselgel 60 F_{245}. The products were visualised using UV fluorescence (254 nm) and/or potassium permanganate stain. Flash column chromatography was performed over Merck silica gel C60 (40-60 m) using eluent systems as described for each experiment.

^{1}H, ^{13}C and ^{19}F NMR spectra were recorded on Bruker DPX200, DPX250 or AVIII400 and AVII500 spectrometers. ^{1}H NMR and ^{13}C NMR spectra are reported as chemical shifts (δ) in parts per million (ppm) relative to the solvent peak using the Bruker internal referencing procedure (edlock). ^{19}F NMR spectra are referenced relative to $CFCl_3$ in $CDCl_3$. Coupling constants (*J*) are reported in units of Hertz (Hz) to the nearest 0.1 Hz. Multiplicities are reported as observed in the spectra with the following abbreviations are used to describe multiplets: s (singlet), d (doublet), t (triplet), q (quartet), sext (sextet), sept (septet), m (multiplet) and br. s (broad singlet).

Low Resolution Mass Spectra (LRMS, *m/z*) were recorded on a H2Os LCT Premier spectrometer using positive (ESI^+) or negative (ESI^-) electrospray ionisation. High resolution mass spectra (HRMS, *m/z*) were recorded on a Bruker MicroTOF spectrometer using positive (ESI^+) or negative electrospray ionisation (ESI^-) or on a Micromass GCT spectrometer using field ionisation (FI^+) or chemical ionization (CI^+).

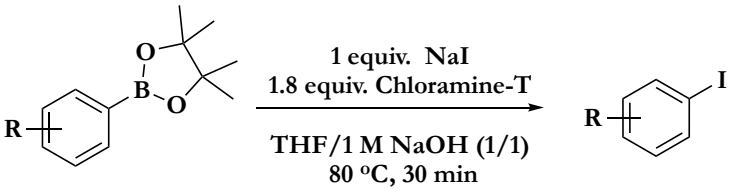
Infrared (IR) spectra were recorded as neat compound or in a solution using a Bruker Tensor 27 FT-IR spectrometer. Absorptions are reported in wavenumbers (cm^{-1}). Melting points (MP) of solids were measured using a Leica Griffin III apparatus and are uncorrected.

The following characterisation data are provided for each novel compound: ^1H NMR spectra, ^{13}C NMR spectra, IR spectra and HRMS. ^{19}F NMR spectra are also provided for those compounds containing ^{19}F nuclei. MP are provided for solids. The following characterisation data are provided for known compounds: ^1H NMR spectra, ^{13}C NMR spectra and ^{19}F NMR spectra where applicable. This data is consistent with the cited literature values. All compounds used for which a preparative procedure does not appear were commercially available or synthesised by persons named in this thesis. IUPAC names were obtained using the ACD I-Lab 2.0 service.

5.2 Chapter 2: Radiosynthesis of SPECT tracers *via* copper mediated ^{123}I-iodination of (hetero)aryl boron reagents.

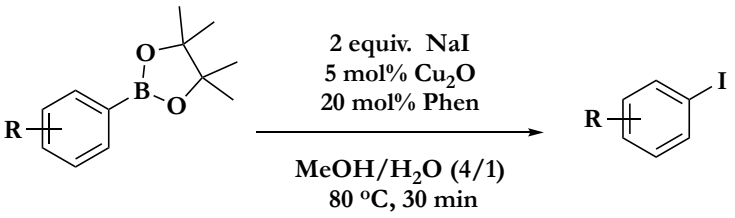
5.2.1 General Procedures:

General Procedure 2A:



A round bottom flask, under normal atmosphere, containing THF/1M NaOH (1/1) (2. 5 mL, 0.02 M) was charged with the chosen aromatic 4,4,5,5-tetramethyl-dioxaborolane (0.05 mmol, 1 equiv.), NaI (0.05 mmol, 1 equiv.) and chloramine-T (0.09 mmol, 1.8 equiv.) The mixture was stirred for 30 minutes at 80 °C and upon cooling to room temperature the contents of the reaction vessel were concentrated *in vacuo*. H_2O (5 mL) was added and extraction was performed with DCM (3 x 10 mL). The organic layers were dried with $MgSO_4$ and subsequently concentrated. Yields were obtained *via* ^{1}H NMR analysis using *tert*-butyl methyl ether (0.05 mmol, 1 equiv.) as an internal standard.[2] Refer to **Table 2.3.1** and **Table 2.3.4**.

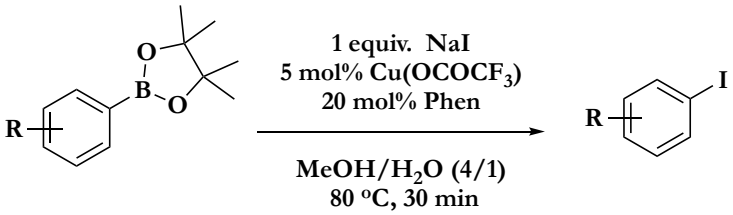
General procedure 2B:



A round bottom flask, under normal atmosphere, containing MeOH/H_2O (4/1) (2. 5 mL, 0.02 M) was charged with the chosen aromatic 4,4,5,5-tetramethyl-dioxaborolane (0.05 mmol, 1 equiv.), NaI (0.1 mmol, 2 equiv.), Cu_2O (5 mol%) and 1,10-phenanthroline (20 mol%). The mixture was heated for 30 minutes at 80 °C and upon cooling down to room temperature, H_2O (5 mL) was added and extraction was performed with DCM (3

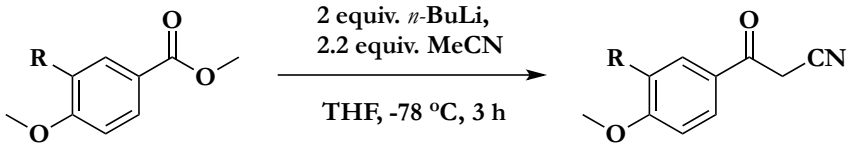
x 10 mL). The organic layers were dried with $MgSO_4$ and concentrated *in vacuo*. Yields were obtained *via* ^{1}H NMR analysis using *tert*-butyl methyl ether (0.05 mmol, 1 equiv.) as an internal standard.[3] Refer to **Table 2.3.1** and **Table 2.3.4**.

General Procedure 2C:



A round bottom flask, under normal atmosphere, containing MeOH/H_2O (4/1) (2. 5 mL, 0.02 M) was charged with the chosen aromatic 4,4,5,5-tetramethyl-dioxaborolane (0.05 mmol, 1 equiv.), NaI (0.05 mmol, 1 equiv.), $Cu(OCOCF_3)$ (5 mol%) and 1,10-phenanthroline (20 mol%). The mixture was heated for 30 minutes at 80 °C and upon cooling down to room temperature, H_2O (5 mL) was added and extraction was performed with DCM (3 x 10 mL). The organic layers were dried with $MgSO_4$ and concentrated *in vacuo*. Yields were obtained *via* ^{1}H NMR analysis using *tert*-butyl methyl ether (0.05 mmol, 1 equiv.) as an internal standard. Refer to **Table 2.3.4**.

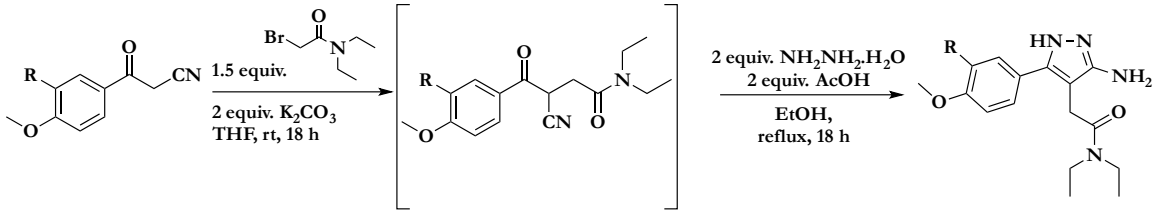
General Procedure 2D:



Under argon at – 78 °C, a solution of MeCN (13.2 mmol, 2.2 equiv.) in THF (10 mL) was added drop-wise over a period of 20 minutes to a solution of *n*-butyllithium (12 mmol, 2 equiv. 2.5 M in *n*-hexane) in 5 mL of THF. The mixture was left to stir at -78 °C for one hour before the chosen benzoate (6 mmol, 1 equiv. in 10 mL THF) was added over a period of 15 minutes. After one hour the reaction was warmed to – 45 °C and the stirring continued until complete consumption of starting material was observed *via* TLC. The reaction was quenched using 2 M aq. HCl (50 mL), diluted with EtOAc (50

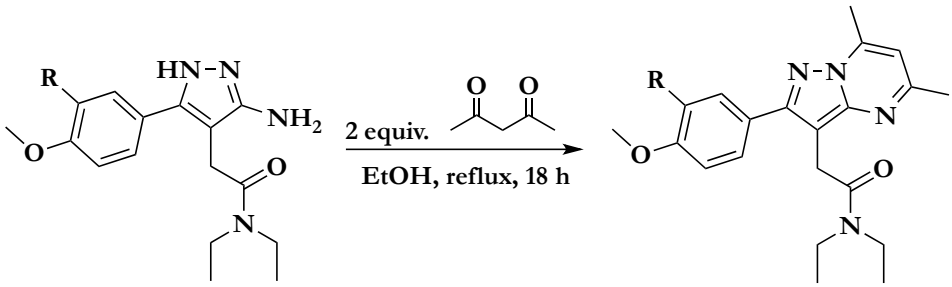
mL) and the layers were separated. The organic layer was washed with brine (4 x 40 mL), dried with $MgSO_4$ and concentrated to afford the expected 3-(4-methoxyphenyl)-3-oxopropanenitrile derivative.

General Procedure 2E:



K_2CO_3 (8 mmol, 2 equiv.) was added to a reaction vessel containing the chosen 3-(4-methoxyphenyl)-3-oxopropanenitrile derivative (4 mmol, 1 equiv.) in THF (30 mL). Subsequently, 2-bromodiethylacetamide (6 mmol, 1.5 equiv.) was added drop-wise and the reaction was left to stir overnight. The reaction was quenched using 1 M aq. HCl (50 mL), followed by dilution with EtOAc (60 mL) and the layers were separated. The mixture was washed with brine (4 x 50 mL) dried and concentrated *in vacuo*. The crude sample was flushed through a short plug of silica using EtOAc/cyclohexane (2/8 to 4 /6) as the eluent to give an oil. This oil was dissolved in EtOH (30 mL), treated with hydrazine monohydrate (8 mmol, 2 equiv.), glacial acetic acid (8 mmol, 2 equiv.) and was heated to reflux for 18 hours. The solvent was evaporated under reduced pressure and diluted with EtOAc before being washed with saturated Na_2CO_3 (3 x 50 mL). The organic layer was dried with $MgSO_4$ and concentrated i*n vacuo* prior to purification *via* silica gel flash column chromatography using MeOH/DCM (3/7) as the eluent to afford the expected pyrazolo[1,5-*a*]pyrimidin-3-yl]acetamide derivative.

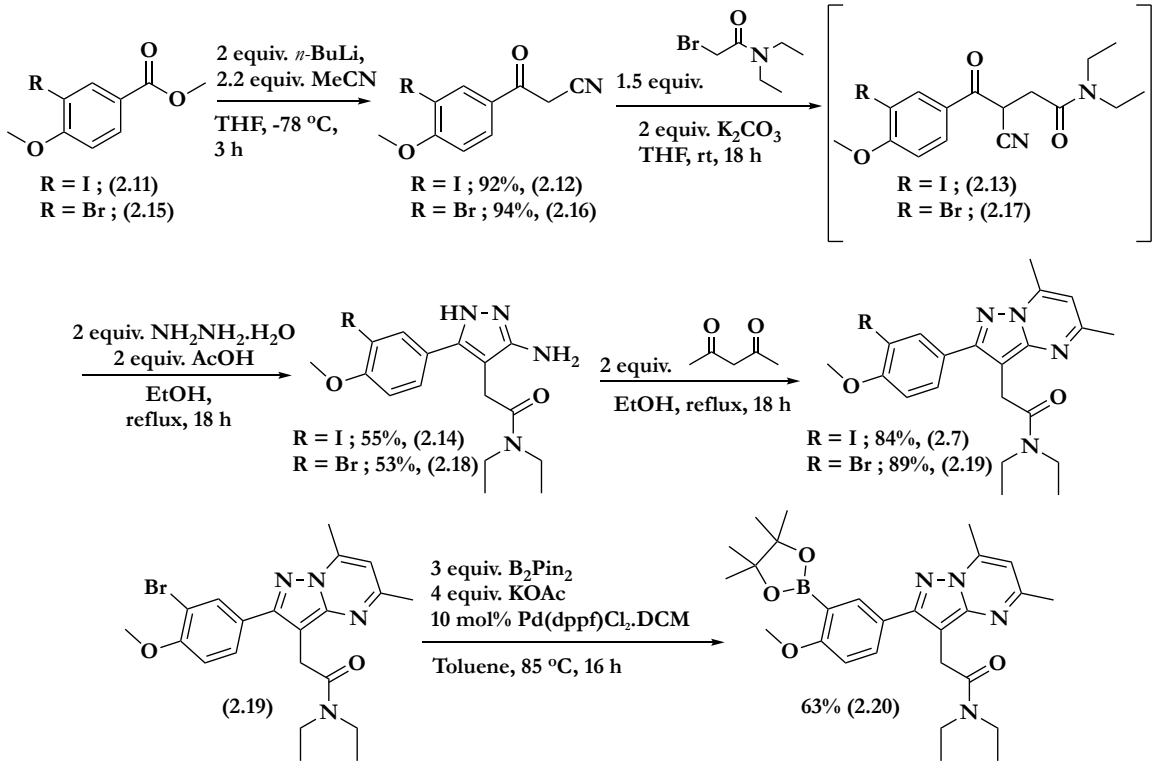
General Procedure 2F:



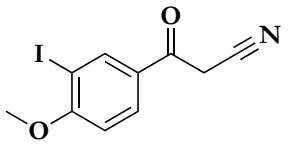
2,4-Pentanedione (4 mmol, 2 equiv.) was added to a solution of the chosen pyrazolo[1,5-*a*]pyrimidin-3-yl]acetamide derivative (2 mmol, 1 equiv.) in 10 mL of EtOH. The reaction mixture was heated at reflux for 18 hours. Upon cooling to ambient temperature, the solvent was removed in *vacuo*. The crude material was purified *via* silica gel flash column chromatography using MeOH/DCM (1/9) as the eluent to give the expected DPA-713 analogue.

5.2.2 Substrates

Synthesis of DPA-713 derivatives:



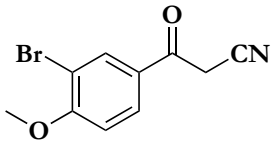
3-(3-Iodo-4-methoxyphenyl)-3-oxopropanenitrile (2.12):



Synthesised following general procedure 2D, yielding **2.12** (1.66 g, 5.52 mmol, 92%) as a white solid.

Mp: 128 – 130 °C; **^{1}H NMR** (400 MHz, $CDCl_3$): δ = 8.32 (d, *J* = 2.0 Hz, 1H, Ar*H*), 7.92 (dd, *J* = 8.5, 2.0 Hz, 1H, Ar*H*), 6.89 (d, *J* = 8.5 Hz, 1H, Ar*H*), 4.02 (s, 2H, COCH_2CN), 3.98 (s, 3H, OCH_3); **^{13}C NMR** (101 MHz, $CDCl_3$): δ = 184.4, 163.0, 140.2, 130.9, 128.8, 113.7, 110.4, 86.5, 56.9, 29.1; **IR** (*ν*, cm^{-1}): 2941, 2269, 1707, 1583, 1256, 1203, 935, 818, 662; **HRMS** (ESI) for $C_{10}H_8O_2N^{127}I$ $[M + Na]^+$ requires m/z 323.9492, found 323.9490.

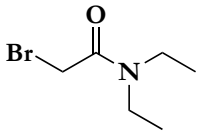
3-(3-Bromo-4-methoxyphenyl)-3-oxopropanenitrile (2.15):



Synthesised following general procedure 2D, yielding **2.15** (1.43 g, 5.63 mmol, 94%) as a yellow solid.

Mp: 110 – 112°C; **^{1}H NMR** (400 MHz, $CDCl_3$): δ = 8.11 (s, 1H, Ar*H*), 7.88 (d, *J* = 8.7 Hz, 1H, Ar*H*), 6.98 (d, *J* = 8.7 Hz, 1H, Ar*H*), 4.05 (s, 2H, COCH_2CN), 3.99 (s, 3H, OCH_3); **^{13}C NMR** (101 MHz, $CDCl_3$): δ = 184.7, 160.9, 133.9, 129.9, 128.2, 113.8, 112.6, 111.5, 56.8, 29.2; **IR** (*ν*, cm^{-1}): 980, 2915, 2255, 1687, 1589, 1285, 1202, 966, 828, 818, 774, 676; **HRMS** (ESI) for $C_{10}H_7O_2N^{79}Br$ $[M-H]^+$ requires m/z 251.9665 found 251.9674.

2-Bromo-*N*,*N*-diethylacetamide:

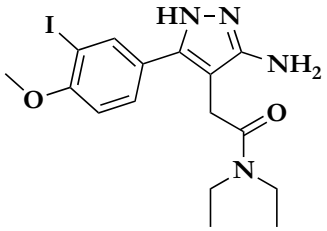


Freshly distilled diethylamine (2 mL, 19.8 mmol) was slowly added to a solution of bromoacetyl bromide (860 L, 9.90 mmol) in 50 mL DCM at -78 °C. The mixture was allowed to warm to room temperature and left to stir for one hour. 25 mL of H_2O was added and the reaction mixture was extracted with DCM (3 x 40 mL). The combined organic layers were dried with $MgSO_4$ and concentrated, yielding the title compound as a white solid (1.9 g, 9.8 mmol, 98%).

^{1}H NMR (400 MHz; $CDCl_3$): δ = 3.86 (s, 2H, BrCH_2), 3.41 (qd, *J* = 7.2, 2.6 Hz, 4H, CH_2NCH_2), 1.27 (t, *J* = 7.2 Hz, 3H, CH_2CH_3), 1.16 (t, *J* = 7.2 Hz, 3H, CH_2CH_3); **^{13}C NMR** ($CDCl_3$, 101 MHz): δ = 165.9, 42.9, 40.5, 26.4, 14.4, 12.5.

Data consistent with literature values.[4]

2-(3-Amino-5-(3-iodo-4-methoxyphenyl)-1*H*-pyrazol-4-yl)-*N*,*N*-diethylacetamide (2.14):

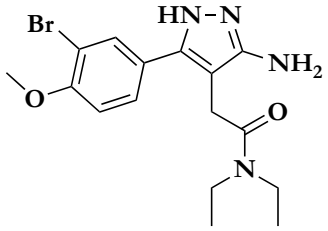


Synthesised following general procedure 2E, yielding **2.14** (940 mg, 2.19 mmol, 55%) as a yellow powder.

Mp: 87 – 89°C; **^{1}H NMR** (400 MHz, $CDCl_3$): δ = 7.78 (d, *J* = 2.1 Hz, 1H, Ar*H*), 7.34 (dd, *J* = 8.4, 2.1 Hz, 1H, Ar*H*), 6.81 (d, *J* = 8.5 Hz, 1H, Ar*H*), 5.97 (br.s, 2H, NH_2), 3.89 (s, 3H, OCH_3), 3.46 (s, 2H, CH_2CO), 3.33 (q, *J* = 7.1 Hz, 2H, NCH_2CH$_3$), 3.12 (q, *J* = 7.1 Hz, 2H, NCH_2CH$_3$), 1.09 (t, *J* = 7.1 Hz, 3H, CH_2CH_3), 0.98 (t, *J* = 7.1 Hz, 3H, CH_2CH_3). (Signal due to pyrazole

NH is not observed); **^{13}C NMR** (101 MHz, $CDCl_3$): δ = 170.3, 158.2, 153.8, 141.7, 138.6, 129.2, 125.2, 111.9, 97.7, 86.2, 56.5, 42.5, 40.7, 28.3, 14.3, 13.1; **IR** (*ν*, cm^{-1}): 3210, 2968, 1610, 1506, 1432, 1251, 1046, 814; **HRMS** (ESI) for $C_{16}H_{22}O_2N_4{}^{127}I$ $[M+H]^+$ requires m/z = 429.0782, found 429.0779.

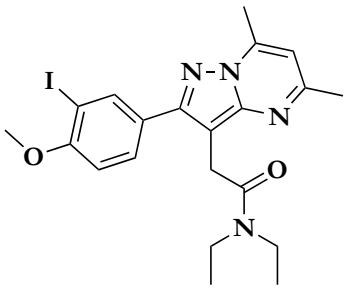
2-(3-Amino-5-(3-bromo-4-methoxyphenyl)-1*H*-pyrazol-4-yl)-*N*,*N*-diethylacetamide (2.16):



Synthesised following general procedure 2E, yielding **2.16** (810 mg, 2.12 mmol, 53%) as a yellow powder.

Mp: 84 – 86 °C; **^{1}H NMR** (400 MHz, $CDCl_3$): δ = 7.53 (d, *J* = 2.1 Hz, 1H, Ar*H*), 7.27 (dd, *J* = 8.5, 2.1 Hz, 1H, Ar*H*), 6.83 (d, *J* = 8.5 Hz, 1H, Ar*H*), 3.89 (s, 3H, OCH_3), 3.45 (s, 2H, CH_2CO), 3.32 (q, *J* = 7.1 Hz, 2H, NCH_2CH$_3$), 3.10 (q, *J* = 7.1 Hz, 2H, NCH_2CH$_3$), 1.07 (t, *J* = 7.1 Hz, 3H, CH$_2$CH_3), 0.96 (t, *J* = 7.1 Hz, 3H, CH$_2$CH_3) (Signal due to pyrazole NH and NH_2 are not observed); **^{13}C NMR** (400 MHz, $CDCl_3$): δ = 170.4, 155.7, 153.3, 142.3, 132.5, 128.2, 125.1, 111.9, 111.7, 97.2, 56.3, 42.4, 40.7, 28.0, 14.4, 13.2; **IR** (*ν*, cm^{-1}): 3542, 2915, 1615, 1595, 1469, 1428, 1229, 1107, 971, 832, 747; **HRMS** (ESI) for $C_{16}H_{21}{}^{79}BrN_4O_2$ $[M+H]^+$ requires m/z 379.0775, found 379.0770.

***N*,*N*-Diethyl-2-(2-(3-iodo-4-methoxyphenyl)-5,7-dimethylpyrazolo[1,5-*a*]pyrimidin-3-yl)acetamide (2.7):**

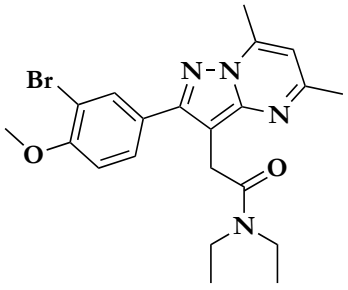


Synthesised following general procedure 2F, yielding **2.7** (827 mg, 1.68 mmol, 84% yield) as a yellow powder.

Mp: 151 – 152 °C. **^{1}H NMR** (400 MHz, $CDCl_3$): 8.19 (d, *J* = 2.1 Hz, 1H, Ar*H*), 7.87 (dd, *J* = 8.5, 2.1 Hz, 1H, Ar*H*), 6.90 (d, *J* = 8.5 Hz, 1H, Ar*H*), 6.52 (s, 1H, Ar*H*), 3.92 (s, 2H, CH_2CO), 3.91 (s, 3H, OCH_3), 3.52 (q, *J* = 7.1 Hz, 2H, NCH_2CH$_3$), 3.42 (q, *J* = 7.1 Hz, 2H, NCH_2CH$_3$), 2.74 (s, 3H, NCCH_3), 2.55 (s, 3H, NCCH_3), 1.24 (t, *J* = 7.1 Hz, 3H, CH$_2$CH_3), 1.13 (t, *J* = 7.1 Hz, 3H, CH$_2$CH_3); **^{13}C-NMR** (101 MHz, $CDCl_3$): δ 169.7, 158.2, 157.6, 153.4, 139.2, 130.0, 128.3, 110.6, 108.3, 100.9, 100.0, 86.0, 56.4, 42.3, 40.7, 28.0, 24.5, 16.9, 14.4, 13.2.

Data consistent with literature values.[5]

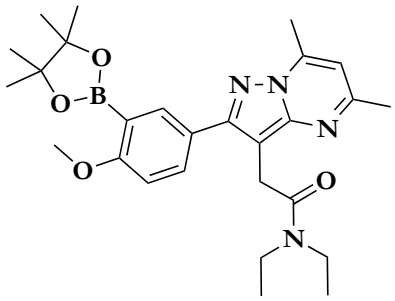
2-(2-(3-Bromo-4-methoxyphenyl)-5,7-dimethylpyrazolo[1,5-*a*]pyrimidin-3-yl)-*N*,*N*-diethyl acetamide (2.19):



Synthesised following general procedure 2F, yielding **2.19** (792 mg, 1.78 mmol, 89%) as a yellow powder.

Mp: 145 – 146 °C; **^{1}H NMR** (400 MHz, $CDCl_3$): δ = 7.99 (d, *J* = 2.1 Hz, 1H, Ar*H*), 7.84 (dd, *J* = 8.5, 2.1 Hz, 1H, Ar*H*), 6.97 (d, *J* = 8.5 Hz, 1H, Ar*H*), 6.51 (s, 1H, Ar*H*), 3.93 (s, 3H, OCH_3), 3.91 (s, 2H, CH_2CO), 3.52 (q, *J* = 7.1 Hz, 2H, NCH_2CH$_3$), 3.41 (q, *J* = 7.1 Hz, 2H, NCH_2CH$_3$), 2.73 (s, 3H, NCCH_3), 2.53 (s, 3H, NCCH_3), 1.23 (t, *J* = 7.1 Hz, 3H, CH$_2$CH_3), 1.12 (t, *J* = 7.1 Hz, 3H, CH$_2$CH_3); **^{13}C NMR** (101 MHz, $CDCl_3$): δ = 169.9, 157.8, 156.0, 153.6, 147.9, 144.9, 133.3, 129.1, 127.9, 111.9, 111.8, 108.5, 101.1, 56.4, 42.5, 40.8, 28.1, 24.8, 17.0, 14.5, 13.2; **IR** (*ν*, cm^{-1}): 2980, 1638, 1554, 1225, 1052, 945, 907, 845, 787, 763; **HRMS** (ESI) for $C_{21}H_{24}{}^{79}BrN_4O_2$ [M-H]$^-$ requires m/z 443.1088, found 443.1081.

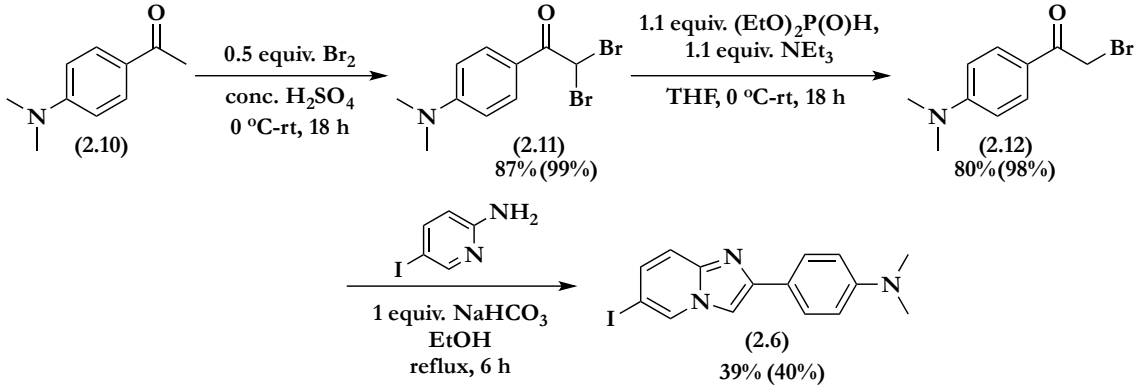
***N*,*N*-Diethyl-2-(2-(4-methoxy-3-(4,4,5,5-tetramethyl-1,3,2-dioxaborolan-2-yl)phenyl)-5,7-dimethylpyrazolo[1,5-*a*]pyrimidin-3-yl)acetamide (2.20):**



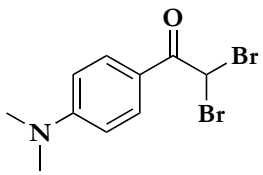
To a 10 mL round bottom flask under argon, charged with 2 mL of toluene was added *N*,*N*-diethyl-2-[2-(3-bromo-4-methoxyphenyl)-5,7-dimethylpyrazolo[1,5-*a*]pyrimidin-3-yl]acetamide **(2.19)** (177 mg, 0.4 mmol), Pd(dppf)Cl_2.CH_2Cl_2 (32 mg, 0.04 mmol), potassium acetate (157 mg, 1.6 mmol) and bis(pinacolato)diboron (305 mg, 1.2 mmol). The reaction was left to stir at 85 °C for 18 hours. The reaction was allowed to cool and the solvent removed in *vacuo* before addition of EtOAc (5 mL). The mixture was filtered through a short plug of celite, evaporated and subjected to silica gel flash column chromatography using using acetone/DCM (1/9 to 2/8) as the eluent. Crystallisation followed by filtration from petroleum ether and diethylether afforded **2.20** as a white solid (123 mg, 0.25 mmol, 63%).

Mp: 120 - 122 °C; **^{1}H NMR** (400 MHz, $CDCl_3$): δ = 8.03 (d, *J* = 2.3 Hz, 1H, Ar*H*), 7.89 (dd, *J* = 8.6, 2.3 Hz, 1H, Ar*H*), 6.94 (d, *J* = 8.6 Hz, 1H, Ar*H*), 6.49 (s, 1H, Ar*H*), 3.90 (s, 2H, CH_2CO), 3.87 (s, 3H, OCH_3), 3.46 (q, *J* = 7.2 Hz, 2H, NCH_2CH$_3$), 3.39 (q, *J* = 7.1 Hz, 2H, NCH_2CH$_3$), 2.75 (s, 3H, NCCH_3), 2.52 (s, 3H, NCCH_3), 1.36 (s, 12H, B(OCCH_3CH_3)$_2$), 1.18 (t, *J* = 7.2 Hz, 3H, CH$_2$CH_3), 1.10 (t, *J* = 7.1 Hz, 3H, CH$_2$CH_3); **^{13}C NMR** (400 MHz, $CDCl_3$): δ = 170.0, 164.4, 157.3, 155.1, 147.7, 144.7, 136.9, 133.2, 125.8, 110.5, 108.1, 100.9, 83.4, 56.0, 42.3, 40.7, 28.1, 24.9, 24.7, 17.0, 14.4, 13.1 (Signal due to carbon bearing the boron was not observed); **IR** (*ν*, cm^{-1}): 2974, 1649, 1585, 1398, 1249, 1140, 1067, 1024, 859, 759. **HRMS** (ESI) for $C_{27}H_{38}{}^{11}BN_4O_4$ $[M+H]^+$ requires m/z 493.2978, found 493.2978.

Synthesis of (6-Iodo-2-(4'-dimethylamino-)phenyl-imidazo[1,2-*a*]pyridine), IMPY (2.6):



2,2-Dibromo-1-(4-(dimethylamino)phenyl)ethan-1-one (2.11):



Prepared according to literature procedure.[6]

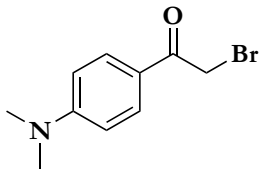
Bromine (1.1 mL, 9.0 mmol) was added dropwise to a solution of 1-(5-(dimethylamino)phenyl-2-yl)ethanone **(2.10)** (2.9 g, 18 mmol) in concentrated H_2SO_4 (95%, 18 mL) at 0 °C. The reaction mixture was stirred overnight at room temperature

and subsequently poured into ice H_2O and neutralized with 3% NaOH. The aqueous phase was extracted with EtOAc (3 x 70 mL). The organic layers were combined, washed with brine (3 x 70 mL), dried and concentrated *in vacuo*. Purification of the crude product by silica gel flash column chromatography using EtOAc/hexanes (1/9) afforded 2,2-dibromo-1-(5-(dimethylamino)pyridin-2-yl)ethanone **(2.11)** as a yellow solid (5.00 g, 15.6 mmol, 87%).

^{1}H NMR (400 MHz, $CDCl_3$): δ = 7.96 – 7.92 (m, 2H, Ar*H*), 6.67 (s, 1H, C*H*Br_2), 6.65 – 6.61 (m, 2H, Ar*H*), 3.07 (s, 6H, N(CH_3)$_2$); **^{13}C NMR** (101 MHz, $CDCl_3$): δ = 184.3, 154.3, 132.4, 117.7, 110.9, 77.5, 77.2, 76.8, 40.7, 40.2.

Data consistent with literature values.[6]

2-Bromo-1-(4-(dimethylamino)phenyl)ethan-1-one (2.12):



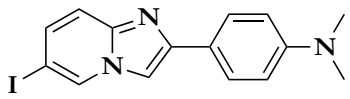
Prepared according to literature procedure.[6]

To a solution of 2,2-dibromo-1-(5-(dimethylamino)pyridin- 2-yl)ethanone **(2.11)** (3.0 g, 9.3 mmol) in 50 mL of anhydrous THF was added triethylamine (1.4 mL, 10 mmol) and diethyl phosphite (1.3 mL, 10 mmol) at 0 °C. The reaction was stirred overnight at room temperature. The mixture was diluted with EtOAc and the aqueous phase further extracted with EtOAc (3 x 70 mL). The combined organic layers were washed with brine (3 x 50 mL), dried and concentrated *in vacuo*. Purification of the crude product *via* silica gel flash column chromatography using EtOAc/hexanes (1/9) afforded **2.12** as a green solid (1.8 g, 7.5 mmol, 80%).

^{1}H NMR (400 MHz, $CDCl_3$): δ = 7.98 (d, *J* = 4.4 Hz, 2H, Ar*H*), 6.97 (d, = 4.4 Hz, 2H, Ar*H*), 4.80 (s, 2H, CH_2Br), 3.10 (s, 6H, N(CH_3)$_2$); **^{13}C NMR** (101 MHz, $CDCl_3$): δ = 189.6, 154.2, 132.0, 121.6, 110.9, 40.3, 31.3.

Data consistent with literature values.[6]

4-(6-Iodoimidazo[1,2-*a*]pyridin-2-yl)-*N*,*N*-dimethylaniline (2.6):



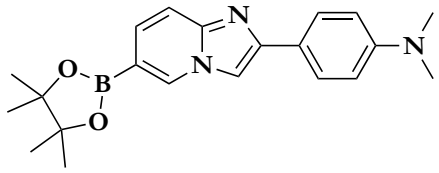
Prepared according to literature procedure.[7]

A mixture of 2-bromo-1-(4-(dimethylamino)phenyl)ethan-1-one **(2.12)** (484 mg, 2 mmol) and 2-amino-5-iodopyridine (440 mg, 2 mmol) in EtOH (25 mL) was stirred at reflux for 2 hours. The mixture was allowed to cool and $NaHCO_3$ (250 mg) was then added. Subsequently the mixture was stirred at reflux for 4 hours before being cooled and the precipitate was filtered and washed with cold EtOH giving 4-(6-iodoimidazo[1,2-*a*]pyridin-2-yl)-*N*,*N*-dimethylaniline **(2.6)** as a green solid (280 mg, 0.77 mmol, 39% yield).

Mp: 230 – 232 °C.**^{1}H NMR** (400 MHz, $CDCl_3$): δ = 7.90 (s, 1H, Ar*H*), 7.39 – 7.37 (m, 3H, Ar*H*), 6.96 (d, *J* = 9.3 Hz, 1H, Ar*H*), 6.85 (dd, *J* = 9.3, 1.4 Hz, 1H, Ar*H*), 6.36 – 6.34 (m, 2H, Ar*H*), 2.58 (s, 6H, N(CH_3)$_2$).**^{13}C NMR** (126 MHz, $CDCl_3$): δ = 150.5, 147.0, 144.1, 131.8, 130.0, 127.0, 121.2, 118.0, 112.4, 106.2, 74.4, 40.4; **IR** (*ν*, cm^{-1}): 2981, 2360, 1615, 1512, 1383, 1196, 950, 820, 671; **HRMS** (ESI) for $C_{15}H_{14}IN_3$ $[M+H]^+$ requires m/z 364.0305, found 364.0312.

Data consistent with literature values.[7]

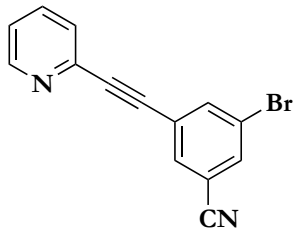
***N*,*N*-Dimethyl-4-(6-(4,4,5,5-tetramethyl-1,3,2-dioxaborolan-2-yl)imidazo[1,2-*a*]pyridin-2-yl)aniline (2.9):**



To a solution of 4-(6-iodoimidazo[1,2-*a*]pyridin-2-yl)-*N*,*N*-dimethylaniline **(2.6)** (73 mg, 0.2 mmol) in THF (2 mL) at - 78 °C was added 2.5 M *n*-BuLi (96 µL, 0.24 mmol). After 10 minutes 2-isopropoxy-4,4,5,5-tetramethyl-1,3,2-dioxaborolane (53 µL, 0.26 mmol) was added drop-wise. The reaction was left to stir for 30 minutes before addition of NH_4Cl (10 mL). The aqueous layer was extracted with DCM (3 x 20 mL), washed with brine (3 x 20 mL), dried and concentrated *in vacuo*. The reaction was subjected to silica gel flash column chromatography using MeOH/DCM (2/8) as the eluent affording **2.9** as an off white solid (58 mg, 1.6 mmol, 80% yield).

Mp: 219 – 222 °C. **^{1}H NMR** (400 MHz, $CDCl_3$): δ = 8.51 (s, 1H, Ar*H*), 7.85 (d, *J* = 8.7 Hz, 2H, Ar*H*), 7.70 (s, 1H, Ar*H*), 7.57 (d, *J* = 9.0 Hz, 1H, Ar*H*), 7.43 (d, *J* = 9.0 Hz, 1H, Ar*H*), 6.79 (d, *J* = 8.7 Hz, 2H, Ar*H*), 3.00 (s, 6H, N(CH_3)$_2$), 1.37 (s, 12H, B(OCCH_3CH_3)$_2$); **^{13}C NMR** (126 MHz, $CDCl_3$): δ = 149.4, 145.7, 145.2, 131.5, 127.6, 126.0, 120.6, 115.0, 111.4, 105.2, 83.2, 39.5, 23.9 (Signal due to carbon bearing the boron was not observed); **IR** (*ν*, cm^{-1}): 2980, 2360, 1614, 1538, 1493, 1383, 1271, 965, 948, 820; **HRMS** (ESI) for $C_{21}H_{26}BN_3O_2$ $[M+H]^+$ requires m/z 364.2191, found 364.2183.

3-Bromo-5-(pyridine-2-ylethynyl)benzonitrile (2.24):



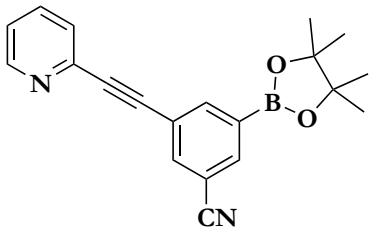
Prepared according to literature procedure.[8]

A Schlenk tube containing 2-ethynylpyridine (0.5 mL, 5.0 mmol), 3,5-dibromobenzonitrile (3.9 g, 15.0 mmol), trans-dichlorobis(triphenyl-phosphine)palladium (350 mg, 0.5 mmol), CuI (475 mg, 2.5 mmol) and PPh_3 (262 mg, 1.0 mmol) in triethylamine (14.0 mL, 99.9 mmol) was heated at 80 °C for 1.5 hours. After cooling to room temperature the resulting reaction mixture was diluted with sat. NH_4Cl (100 mL) and extracted with diethyl ether (3 x 80 mL). The combined organic layers were dried over Na_2SO_4, filtered and concentrated *in vacuo*. The residue was dissolved in hexane/EtOAc (4/1) and filtered through a small silica-gel column and concentrated *in vacuo*. The crude product was purified by crystallisation from hot hexane/EtOAc (placed in the freezer) to afford the product as an off white solid (770 mg, 2.75 mmol, 55%).

^{1}H NMR (400 MHz, $CDCl_3$): δ = 8.65 (ddd, J = 5.0, 1.8, 1.0 Hz, 1H, Ar*H*), 7.95 (dd, J = 1.8, 1.5 Hz, 1H, Ar*H*), 7.80 – 7.76 (m, 2H, Ar*H*), 7.73 (td, J = 7.7, 1.8 Hz, 1H, Ar*H*), 7.54 (dt, J = 7.8, 1.1 Hz, 1H, Ar*H*), 7.31 (ddd, J = 7.8, 5.0, 1.1 Hz, 1H, Ar*H*); **^{13}C NMR** (126 MHz, $CDCl_3$): δ = 150.1, 141.9, 138.9, 136.5, 134.2, 133.9, 127.6, 125.7, 123.8, 123.0, 116.7, 114.3, 91.8, 84.8.

Data consistent with literature values.[8]

3-(Pyridin-2-ylethynyl)-5-(4,4,5,5-tetramethyl-1,3,2-dioxaborolan-2-yl)benzonitrile (2.23):



Prepared according to literature procedure.[8]

To a 25 mL round bottom flask under argon, charged with 7 mL of *N,N*-dimethylacetamide, was added 3-bromo-5-(pyridin-2-ylethynyl)benzonitrile **(2.24)** (640.0 mg, 2.26 mmol), $Pd(dppf)Cl_2.CH_2Cl_2$ (110.8 mg, 0.14 mmol), potassium acetate (887.0 mg, 9.04 mmol) and bis(pinacolato)diboron (631 mg, 2.49 mmol). The reaction was left to stir at 110 °C for 40 minutes, cooled to room temperature, diluted with H_2O (100 mL), and extracted with EtOAc (4 x 35 mL). The combined organic extracts were washed with brine (30 mL x 3), dried with $MgSO_4$ and concentrated *in vacuo*. The resulting residue was dissolved in diethyl ether/hexane (5/1) and filtered through a small silica-gel column. The filtrate was concentrated *in vacuo* and the residue was purified by crystallization from hot acetonitrile (placed in the freezer) to afford the product as an off white solid (306 mg, 0.93 mmol, 41%).

^{1}H NMR (400 MHz, CD_2Cl_2): δ = 8.62 – 8.54 (m, 1H, Ar*H*), 8.19 (s, 1H, Ar*H*), 8.04 (t, *J* = 1.4 Hz, 1H, Ar*H*), 7.91 (t, *J* = 1.5 Hz, 1H, Ar*H*), 7.69 (td, *J* = 7.7, 1.8 Hz, 1H, Ar*H*), 7.53 (dd, *J* = 7.7, 1.5 Hz, 1H, Ar*H*), 7.28 (ddd, *J* = 7.5, 4.9, 1.4 Hz, 1H, Ar*H*), 1.31 (s, 12H, $B(OCC\mathit{H_3}C\mathit{H_3})_2$); **^{13}C NMR** (126 MHz, CD_2Cl_2): δ = 150.6, 143.1, 142.3 138.4, 137.4, 136.6, 127.8, 123.7, 123.6, 118.3, 113.1, 91.0, 86.4, 85.2, 25.0 (signal due to carbon bearing boron was not observed).

Data consistent with literature values.[8]

5.2.3 Radiochemistry

General Information and Procedures

Sodium [^{123}I]Iodide Preparation:

Sodium [^{123}I]iodide was produced by GE Healthcare as no-carrier added [^{123}I]sodium iodide in 0.05 M NaOH. In each case this solution was diluted in methanol until the total volume came to 200 µL.

Analysis [^{123}I]Iodide:

For all reactions, an aliquot was removed for analysis by radioTLC and radioHPLC.

All radiochemical conversions quoted are decay corrected and are calculated by radio-TLC, taking into account the radiochemical purity observed by radio-HPLC.

HPLC analysis was performed with a Dionex Ultimate 3000 dual channel HPLC system equipped with shared autosampler, parallel UV-detectors and with Flowram analogue output.

Radio-TLC was performed on Merck Kiesegel 60 F254 plates. Analysis was performed using a LabLogic NaI/PMT-radiodetectors.

HPLC gradient A: water/acetonitrile, 1 mL/min, Waters Nova-Pak C18 Column, 4 µm, 3.9 x 150 mm
0-1 min (5% MeCN) isocratic

1-10 min (5% MeCN to 95% MeCN) linear increase

10-14 min (95% MeCN) isocratic

14-15 min (95% MeCN to 5% MeCN) linear decrease

15-17 min (5% MeCN) isocratic

HPLC gradient B: water/acetonitrile containing 0.1 mg/mL TFA, 1 mL/min, Waters Nova-Pak C18 Column, 4 μm, 3.9 x 150 mm
0-2 min (5% MeCN containing 0.1 mg/mL TFA) isocratic

1-10 min (5% MeCN containing 0.1 mg/mL TFA to 95% MeCN containing 0.1 mg/mL TFA) linear increase

10-14 min (95% MeCN containing 0.1 mg/mL TFA) isocratic

14-15 min (95% MeCN containing 0.1 mg/mL TFA to 5% MeCN containing 0.1 mg/mL TFA) linear decrease

15-17 min (5% MeCN containing 0.1 mg/mL TFA) isocratic

General procedure for the ^{123}I-Iodination of Aryl Bpin or B(OH)$_2$ substrates (2.1a–k and 2.2b, h and j):

To a V-vial containing a magnetic stirrer bar, arylBPin (15 μmol) or arylBOH)$_2$ (15 μmol) and [^{123}I]NaI (ca. 4 MBq, 5 μL MeOH approx.) was added Cu(OCOCF$_3$)$_2$ (0.30 μmol), 1,10-phenanthroline (0.30 μmol) in MeOH/H$_2$O (4/1, 200 μL) from a stock solution. The reaction vial was then heated to 80 °C for 20 minutes. The reaction was quenched by addition of 10 mol% sodium thiosulfate (200 μL) and MeCN (100 μL). An aliquot was removed for analysis by radio-TLC and HPLC to calculate the radiochemical conversion (RCC) and purity respectively.

Procedure for the ^{123}I-Iodination of ArylBPin Tracers: [^{123}I]DPA-713 [^{123}I]IMPY, Boc Protected [^{123}I]MIBG and [^{123}I]IPEB ([^{123}I]2.6, [^{123}I]2.7, [^{123}I]2.27, [^{123}I]2.22):

The optimised method started with the preparation of a V-vial containing a magnetic stirrer bar and [^{123}I]NaI (ca. 4 MBq, 5 μL MeOH approx.) to which arylBPin (5 μmol), Cu(OCOCF$_3$)$_2$ (0.25 μmol), 1,10-phenanthroline (0.25 μmol) in MeOH/H$_2$O (4/1, 200 μL). The reaction vial was then heated to 80 °C for 20 minutes. The reaction was quenched by addition of 10 mol% sodium thiosulfate (400 μL) and MeCN (100 μL). An aliquot was removed for analysis by thin-layer chromatography (radio-TLC) and high performance

liquid chromatography (radio-HPLC) to calculate the radiochemical conversion and purity respectively.

Procedure for the ^{123}I-Iodination and determination of RCY of ArylBPin Tracers: [^{123}I]DPA-713, [^{123}I]IMPY, and [^{123}I]IPEB (([^{123}I]2.6, [^{123}I]2.7, [^{123}I]2.22):

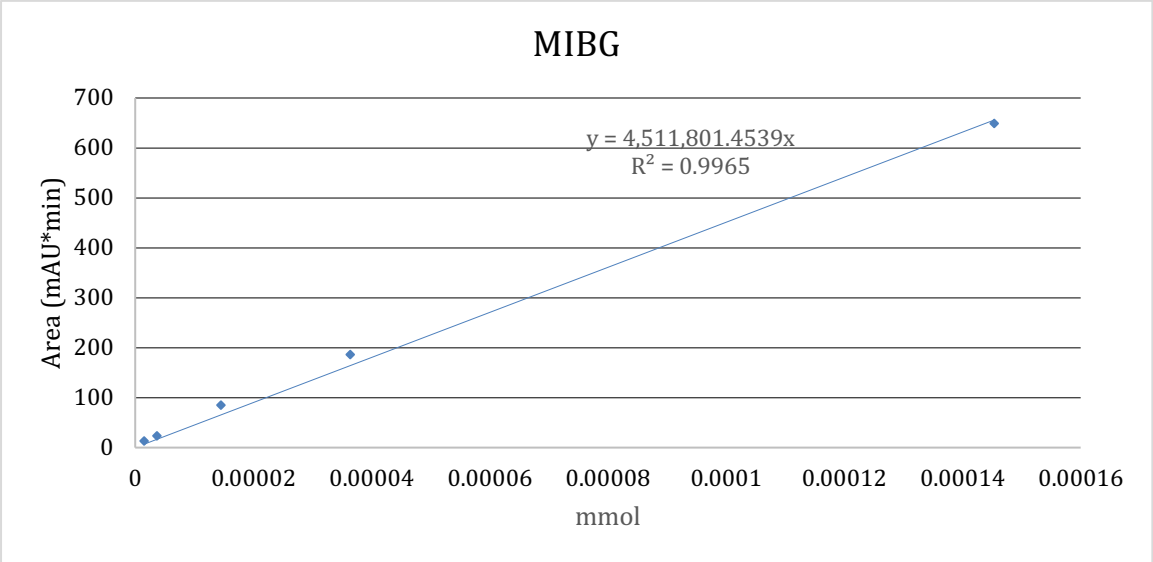
The optimised method started with the preparation of a V-vial containing a magnetic stirrer bar, arylBPin (5 μmol) and [^{123}I]NaI (ca. 4 – 36 MBq, 5 - 15 μL MeOH approx.) to which $Cu(OCOCF_3)_2$ (0.25 μmol), 1,10-phenanthroline (0.25 μmol) in MeOH/H_2O (4/1, 200 μL). The reaction vial was then heated to 80 °C for 20 minutes. The reaction was diluted in H_2O (6 mL) and loaded onto a C-18 SepPak Plus cartridge. This was then flushed with H_2O (2 mL) and air (2 mL) followed by elution of the ^{123}I-iodinated product with MeCN (2 mL). The radiochemical yield was then calculated as a percentage of activity (MBq) found in the MeCN elute compared to the starting activity (MBq). An aliquot was removed for analysis by HPLC to calculate the radiochemical purity.

Procedure for the ^{123}I-iodination, deprotection and determination of RCY of [^{123}I]MIBG ([^{123}I]2.26):

The optimised method started with the preparation of a V-vial containing a magnetic stirrer bar, arylBPin (5 μmol) and [^{123}I]NaI (ca. 3 – 7 MBq, 5 μL MeOH approx.) to which $Cu(OCOCF_3)_2$ (0.25 μmol), 1,10-phenanthroline (0.25 μmol) in 4/1 MeOH/H_2O (200 μL). The reaction vial was then heated to 80 °C for 20 minutes. The reaction was diluted in H_2O containing 10% MeOH (6 mL) and loaded onto a C-18 SepPak Plus cartridge and flushed with H_2O/MeOH (9/1, 6 mL). [^{123}I[MIBG was then eluted with DCM (2 x 1 mL) followed by air (2 x 1 mL). At this point the radiochemical yield was calculated as a percentage of activity (MBq) found in the DCM elute compared to the starting activity (MBq). The DCM elute was subsequently removed at 50 °C under a stream of N_2. Once dry 300 μL of 57% HI was added and the reaction stirred for 10 minutes at 125 °C. After

10 minutes, an aliquot was removed for analysis by high performance liquid chromatography (radio-HPLC) to calculate the conversion of the deprotection step and the purity respectively.

Specific Activity



Run	MIBG (mg/mL)	Inject Volume (uL)	Mass/inject (mg)	mmol/inject	Area (mAU*min)
1	0.01	40	0.0004	1.45407E-06	13.4771
2	0.1	10	0.001	3.63517E-06	23.7597
3	0.1	40	0.004	1.45407E-05	84.464
4	1	10	0.01	3.63517E-05	185.6973
5	1	40	0.04	0.000145407	648.4869

	SA (GBq/umol)	Activity (MBq)	mmol	Area (mAU*min)
Calculation	**19.78860287**	0.6	3.03205E-08	0.1368
	14.11702583	0.25	1.77091E-08	0.0799

Radiochemical Conversion:

To determine the radiochemical conversion (RCC) the reaction mixture was quenched with 10% sodium thiosulfate, after which an aliquot is analysed by radio-TLC and radio-HPLC. The conversion of [^{123}I]NaI can be determined by radio-TLC, choosing a suitable eluent and comparing the activity on the base-line, from unreacted [^{123}I]NaI, with the activity from the ^{123}I-containing organic material at higher R_f. The RCC can then be determined by taking into account the purity of the ^{123}I-containing product. This is usually determined as the average of at least two experiments, with the error defined as the standard deviation of the mean and is corrected for decay of ^{123}I.

Equation used for the calculation of the standard error of mean:

$$Mean = \bar{x} = \frac{1}{n}\sum_{i=1}^{n} x_i = \frac{1}{n}(x_1 + x_2 + \cdots + x_n)$$

$$Standard\ Deviation\ (of\ the\ population) = \sigma = \sqrt{\frac{1}{n}\sum_{i=1}^{n}(x_i - \bar{x})^2}$$

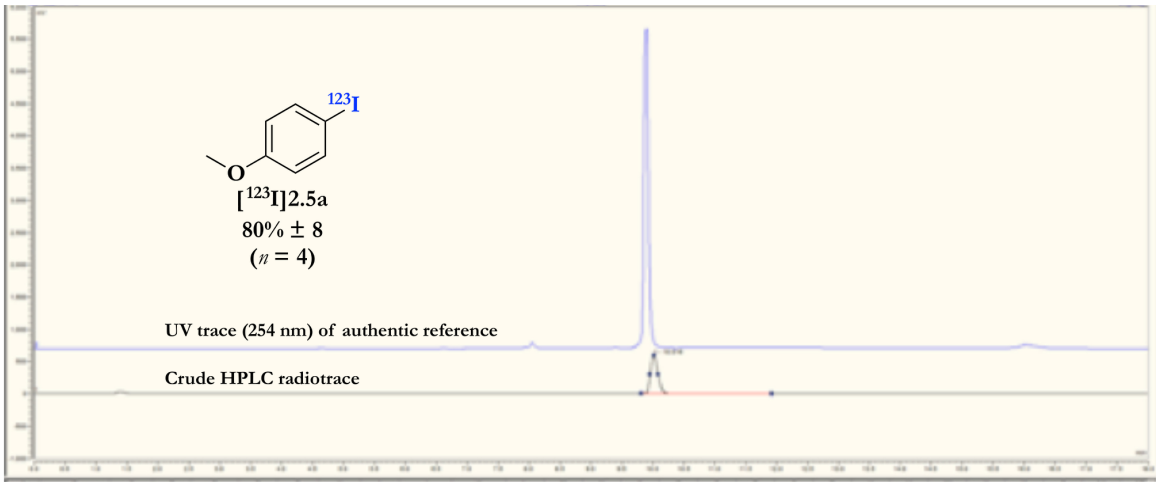
$$Standard\ Error\ of\ the\ Mean = \frac{\sigma}{\sqrt{n}}$$

HPLC Traces for small-scale reactions:

The solid blue line indicates the UV trace for cold reference material and the solid black line is the crude radio-HPLC trace. All samples were run using HPLC gradient A unless otherwise specified. In each case, a table presenting all individual radiochemical conversions is presented. For each pair of reactions, only one HPLC run is carried out for which the purity of the second reaction is then assumed to be equal.

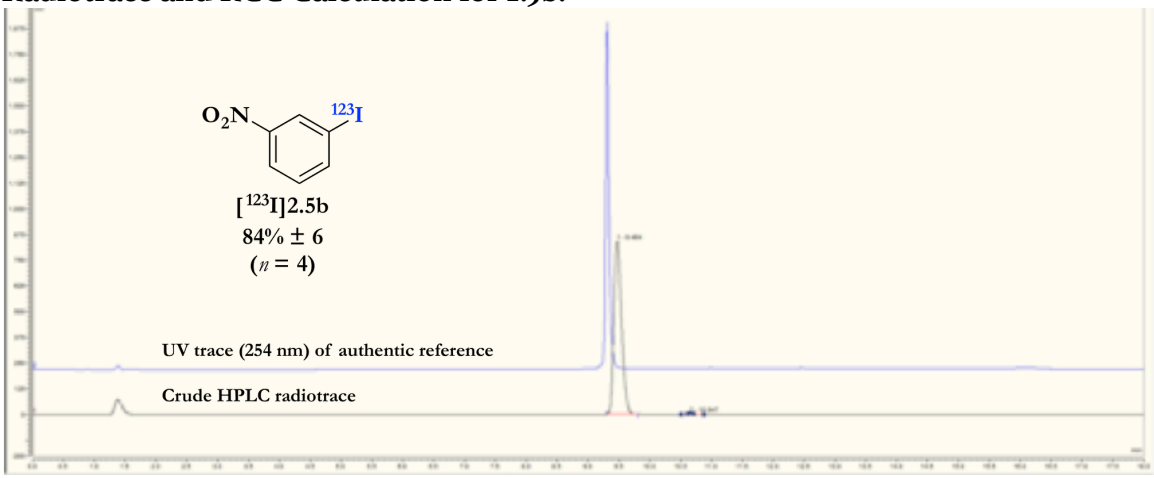
HPLC Traces Derived from Boron Pinacol Ester Starting Material (2.1a – 2.1k):

Radiotrace and RCC Calculation for 2.5a:



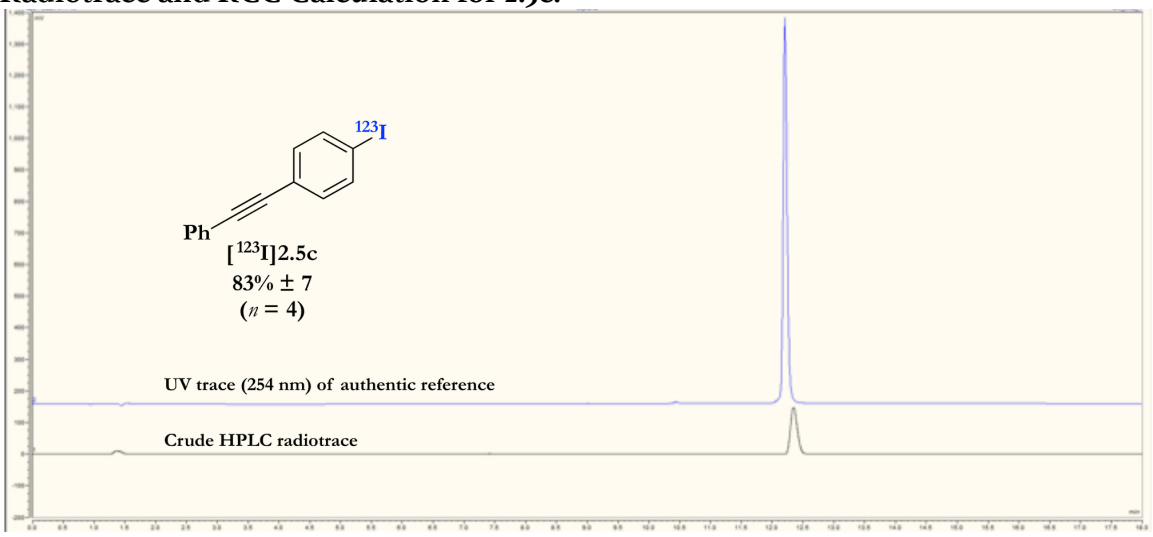
Reaction Number	Radio-TLC (%)	Radiochemical Purity (%)	Radiochemical Conversion (%)
1	56%	>99%	56%
2	89%	-	89%
3	87%	>99%	87%
4	87%	-	87%
RCC and Standard Error of the Mean			80% ± 8%

Radiotrace and RCC Calculation for 2.5b:



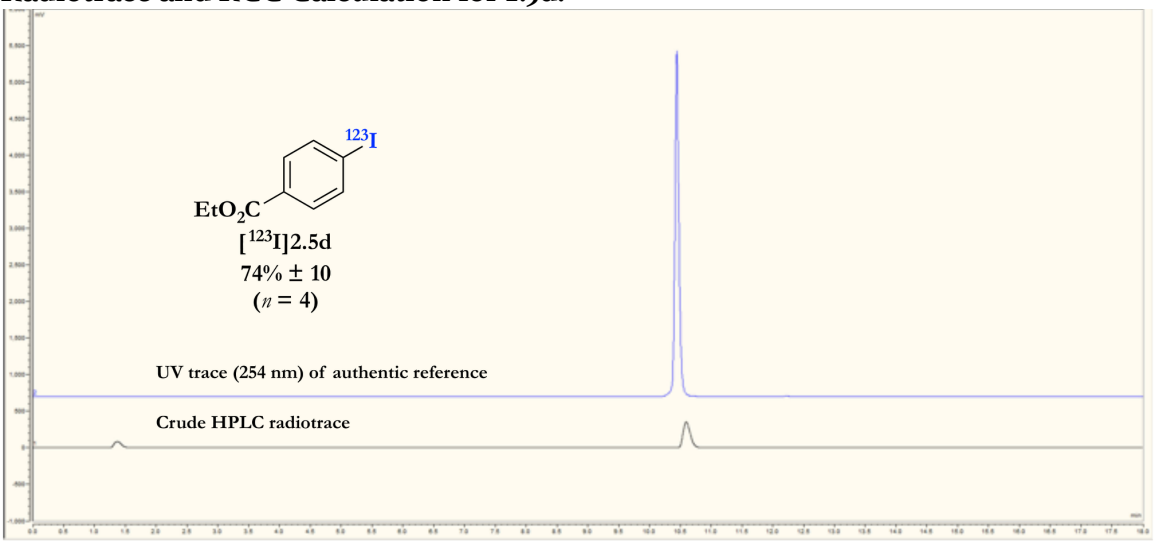
Reaction Number	Radio-TLC (%)	Radiochemical Purity (%)	Radiochemical Conversion (%)
1	67%	>99%	67%
2	89%	-	89%
3	97%	>99%	97%
4	84%	-	84%
RCC and Standard Error of the Mean			84% ± 6%

Radiotrace and RCC Calculation for 2.5c:



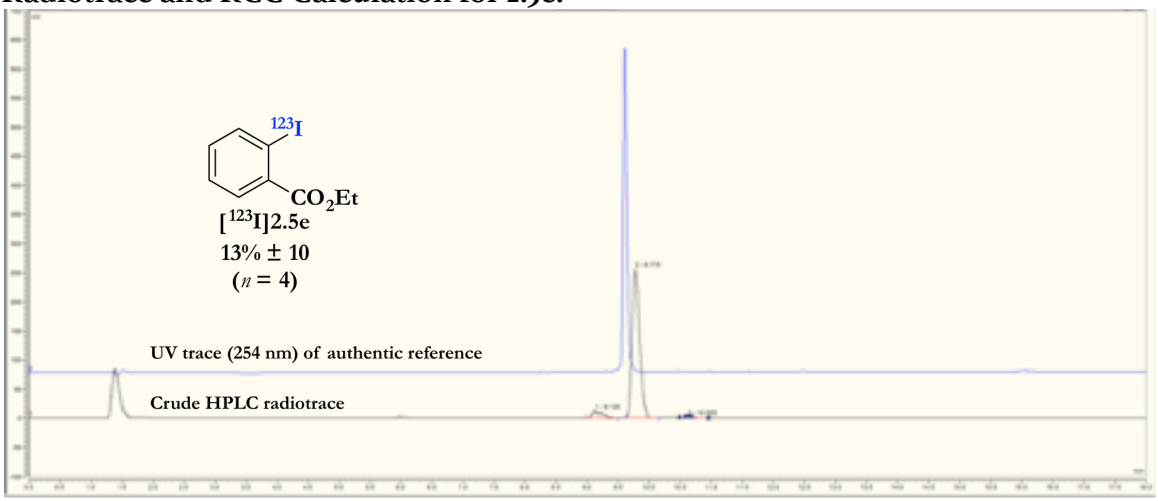
Reaction Number	Radio-TLC	Radiochemical Purity	RCC
1	81%	>99%	81%
2	65%	-	65%
3	93%	>99%	93%
4	93%	-	93%
RCC and Standard Error of the Mean			78% ± 15%

Radiotrace and RCC Calculation for 2.5d:



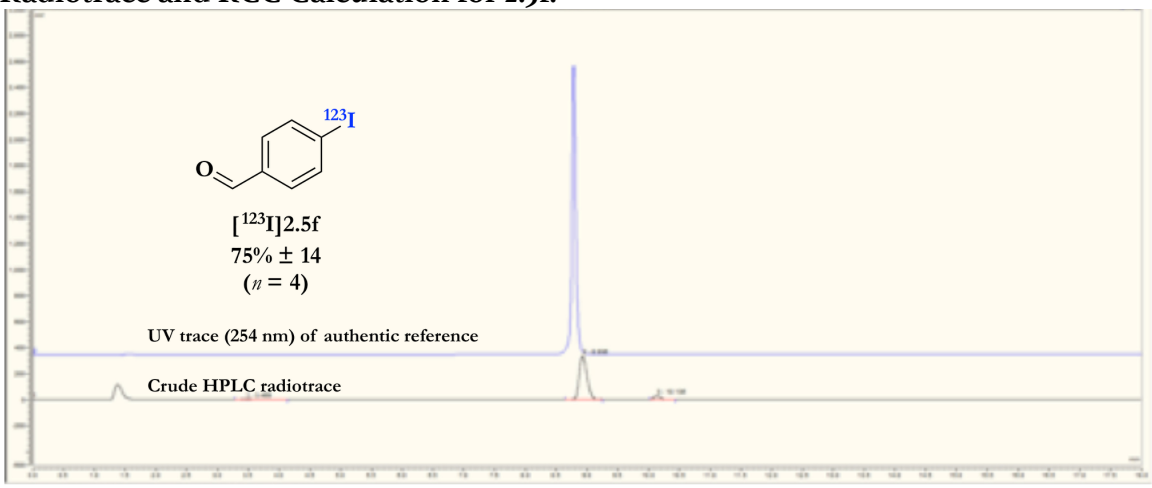
Reaction Number	Radio-TLC (%)	Radiochemical Purity (%)	Radiochemical Conversion (%)
1	46%	>99%	46%
2	92%	-	92%
3	72%	>99%	72%
4	87%	-	87%
RCC and Standard Error of the Mean			74% ± 10%

Radiotrace and RCC Calculation for 2.5e:



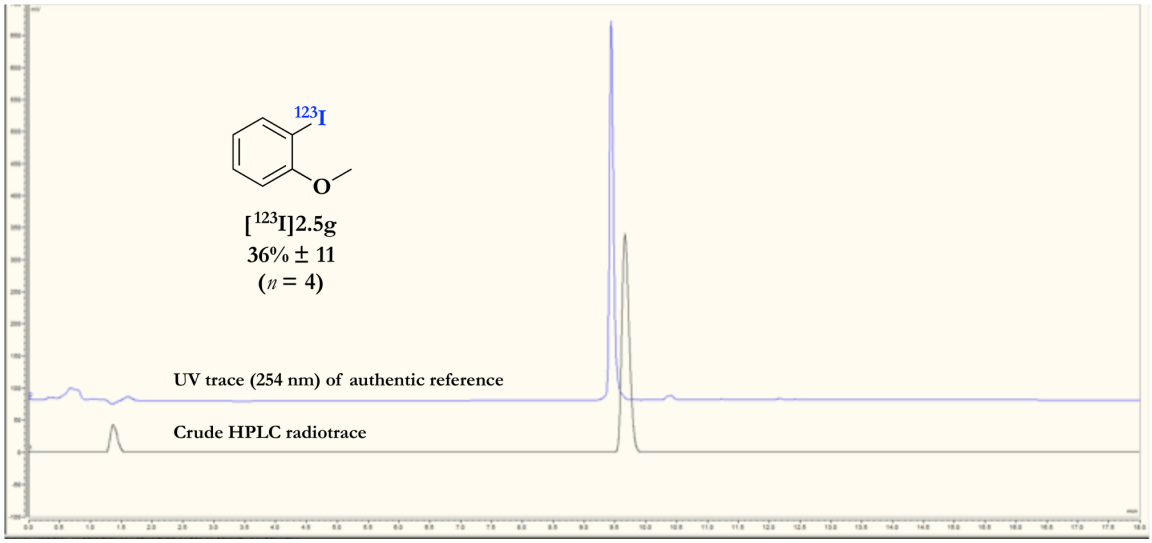
Reaction Number	Radio-TLC (%)	Radiochemical Purity (%)	Radiochemical Conversion (%)
1	0%	>99%	0%
2	5%	-	5%
3	46%	94%	43%
4	2%	-	2%
RCC and Standard Error of the Mean			13% ± 10%

Radiotrace and RCC Calculation for 2.5f:



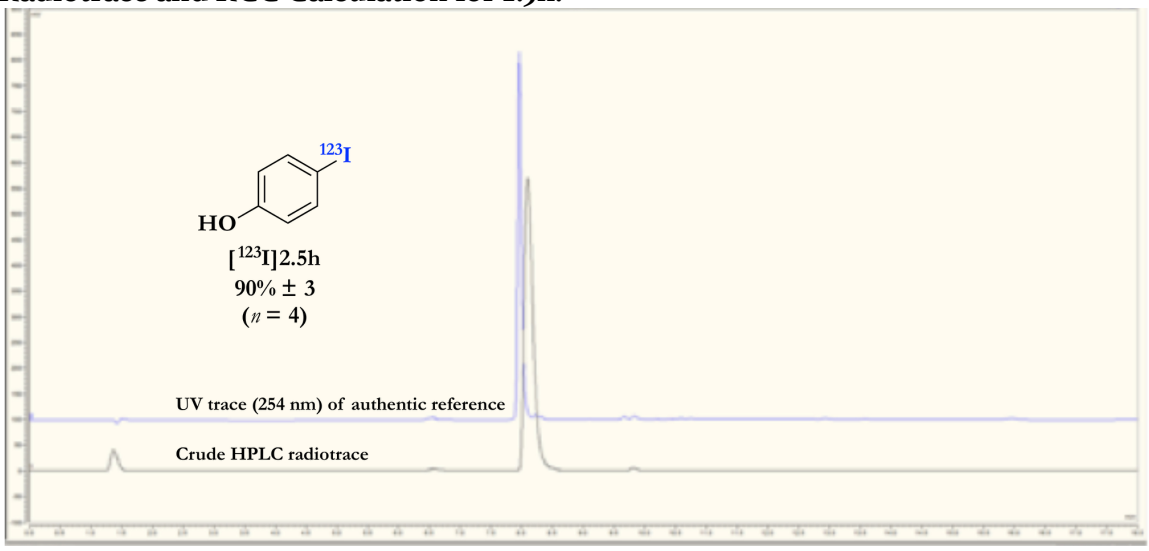
Reaction Number	Radio-TLC (%)	Radiochemical Purity (%)	Radiochemical Conversion (%)
1	37%	91%	33%
2	92%	-	83%
3	98%	93%	91%
4	99%	-	92%
RCC and Standard Error of the Mean			75% ± 14%

Radiotrace and RCC Calculation for 2.5g:



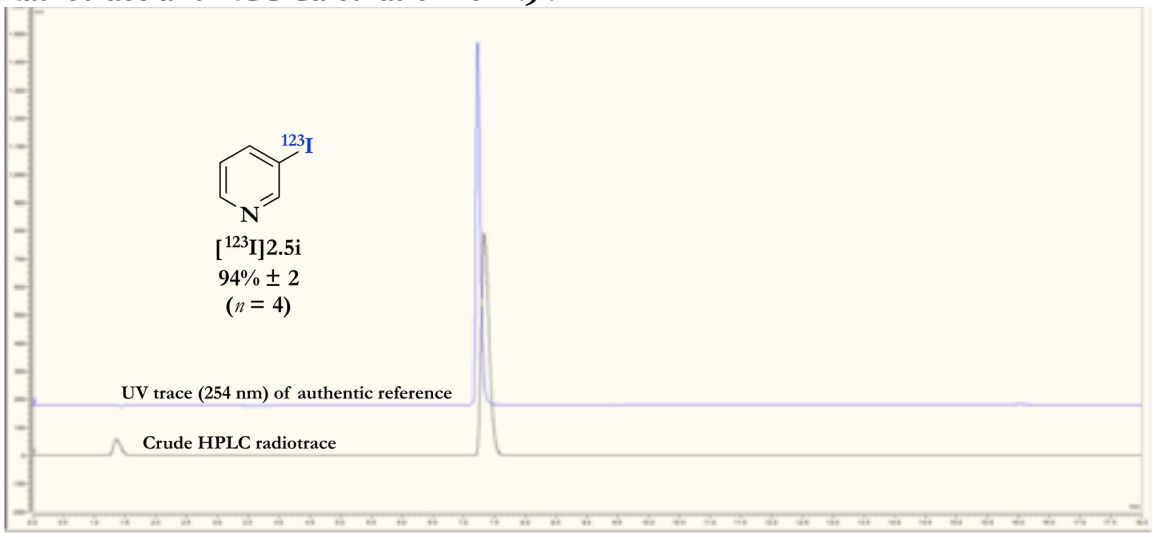
Reaction Number	Radio-TLC (%)	Radiochemical Purity (%)	Radiochemical Conversion (%)
1	70%	98%	69%
2	33%	-	32%
3	19%	>99%	19%
4	23%	-	23%
RCC and Standard Error of the Mean			36% ± 11%

Radiotrace and RCC Calculation for 2.5h:



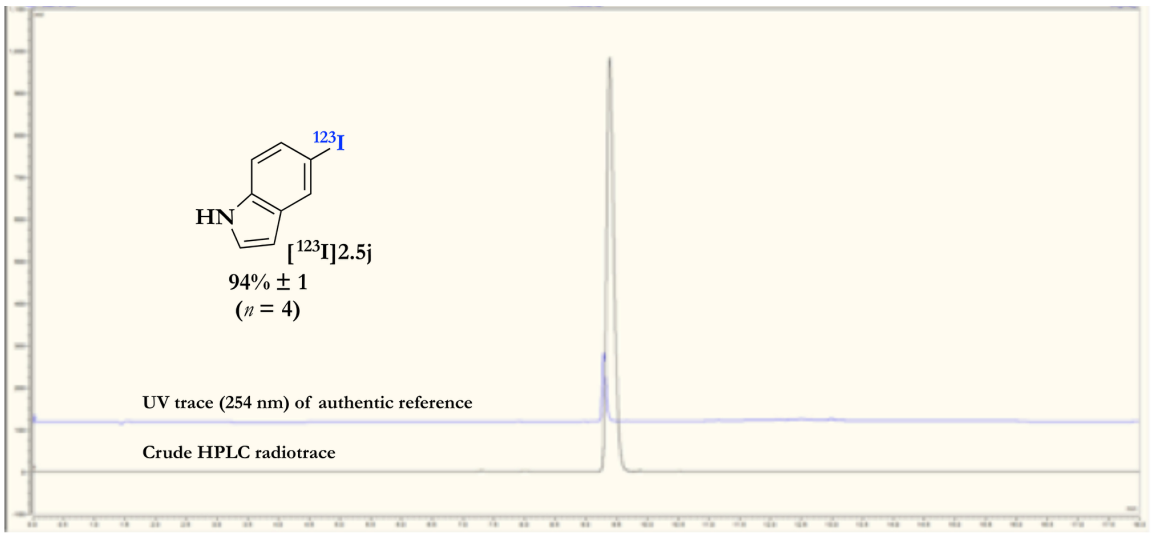
Reaction Number	Radio-TLC (%)	Radiochemical Purity (%)	Radiochemical Conversion (%)
1	85%	>99%	85%
2	90%	-	90%
3	91%	98%	89%
4	98%	-	96%
RCC and Standard Error of the Mean			88% ± 3%

Radiotrace and RCC Calculation for 2.5i:



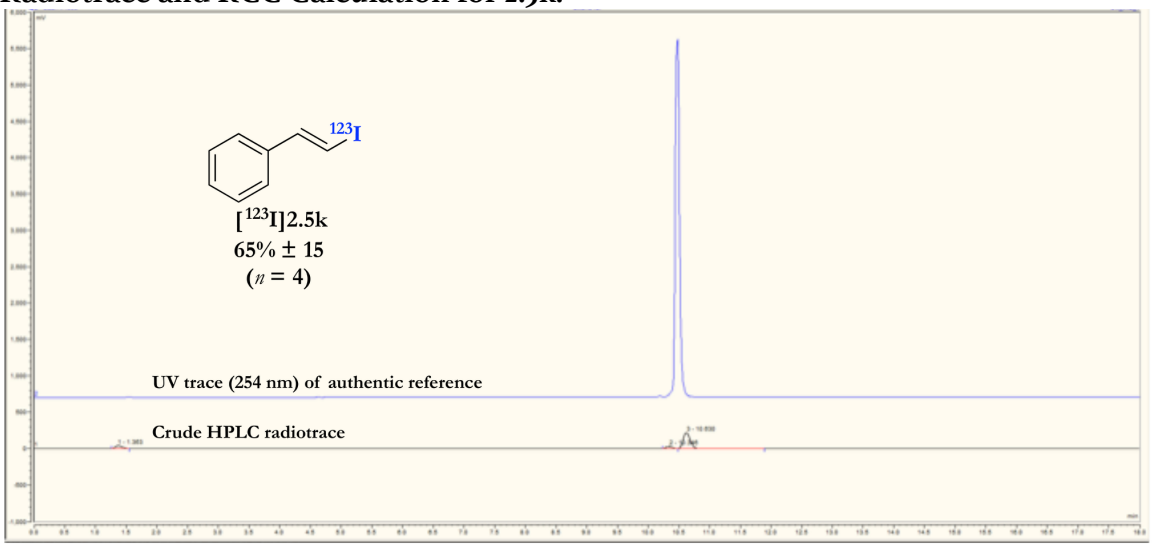
Reaction Number	Radio-TLC (%)	Radiochemical Purity (%)	Radiochemical Conversion (%)
1	95%	>99%	95%
2	93%	-	93%
3	90%	>99%	90%
4	99%	-	99%
RCC and Standard Error of the Mean			94% ± 1%

Radiotrace and RCC Calculation for 2.5j:



Reaction Number	Radio-TLC (%)	Radiochemical Purity (%)	Radiochemical Conversion (%)
1	92%	>99%	92%
2	93%	-	93%
3	94%	>99%	94%
4	95%	-	95%
RCC and Standard Error of the Mean			94% ± 1%

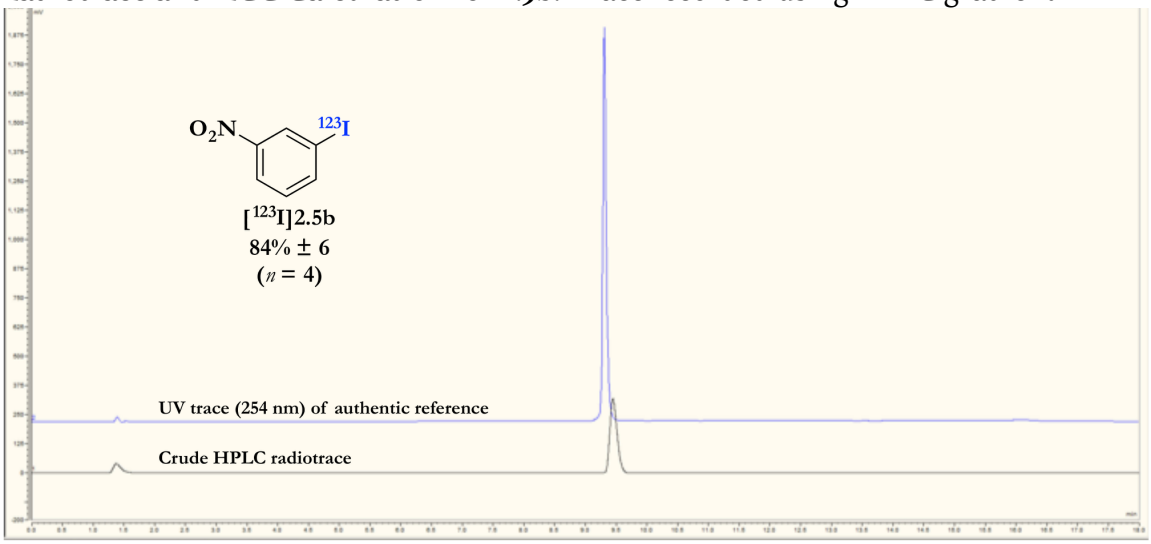
Radiotrace and RCC Calculation for 2.5k:



Reaction Number	Radio-TLC (%)	Radiochemical Purity (%)	Radiochemical Conversion (%)
1	89%	90%	80%
2	54%	-	49%
3	75%	92%	69%
4	84%	-	77%
RCC and Standard Error of the Mean			65% ± 15%

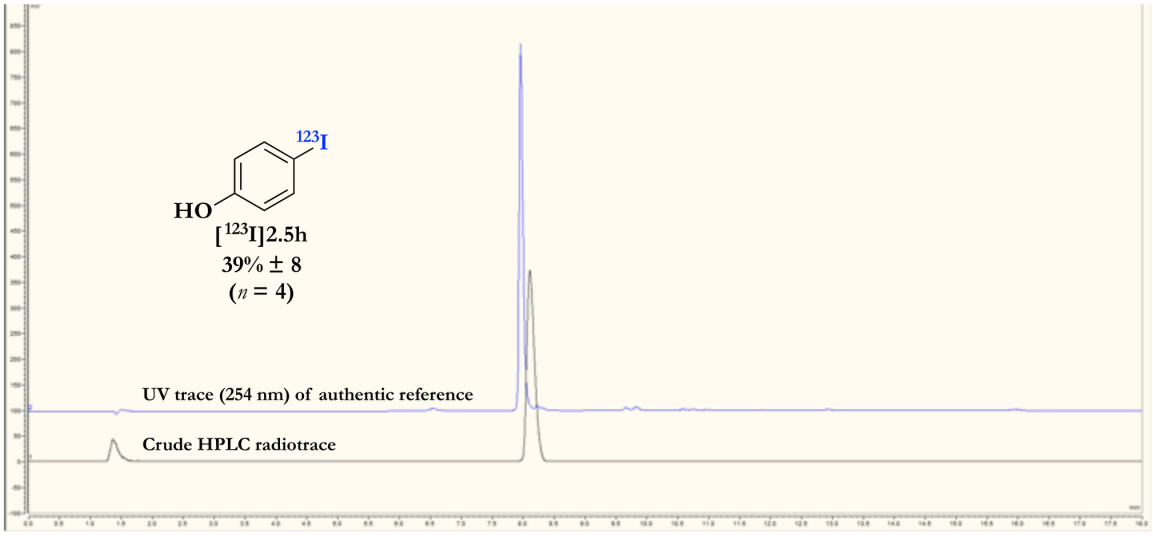
HPLC Traces Derived from Boronic Acid Starting Material (2.2b, 2.2h, 2.2j)

Radiotrace and RCC Calculation for 2.5b: Trace recorded using HPLC gradient B



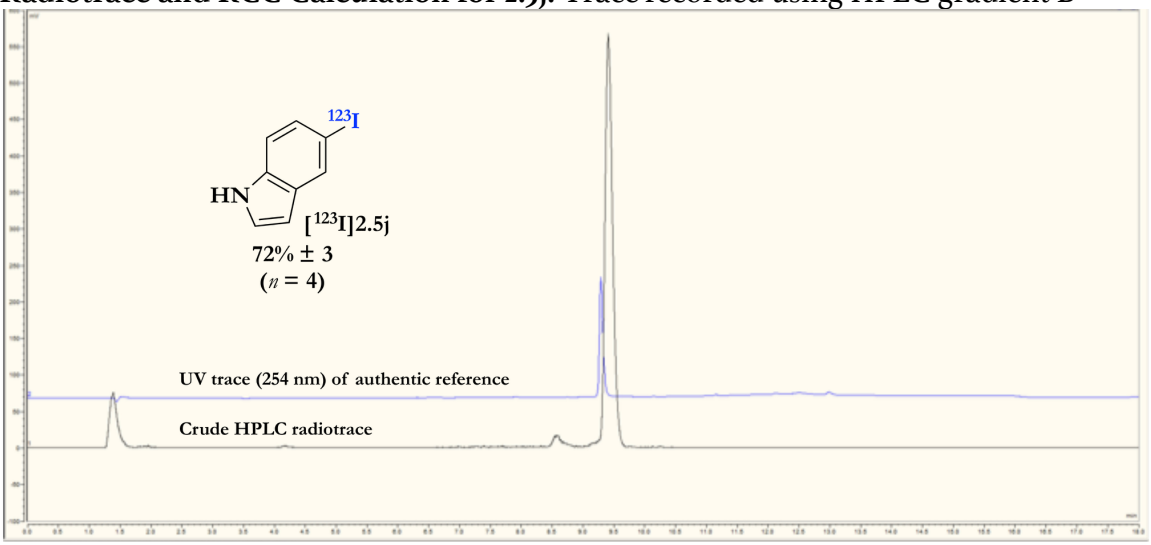
Reaction Number	Radio-TLC (%)	Radiochemical Purity (%)	Radiochemical Conversion (%)
1	60%	>99%	60%
2	85%	-	85%
3	35%	>99%	35%
4	40%	-	40%
RCC and Standard Error of the Mean			63% ± 15%

Radiotrace and RCC Calculation for 2.5h: Trace recorded using HPLC gradient B



Reaction Number	Radio-TLC (%)	Radiochemical Purity (%)	Radiochemical Conversion (%)
1	35%	>99%	35%
2	63%	-	63%
3	29%	>99%	29%
4	28%	-	28%
RCC and Standard Error of the Mean			39% ± 8%

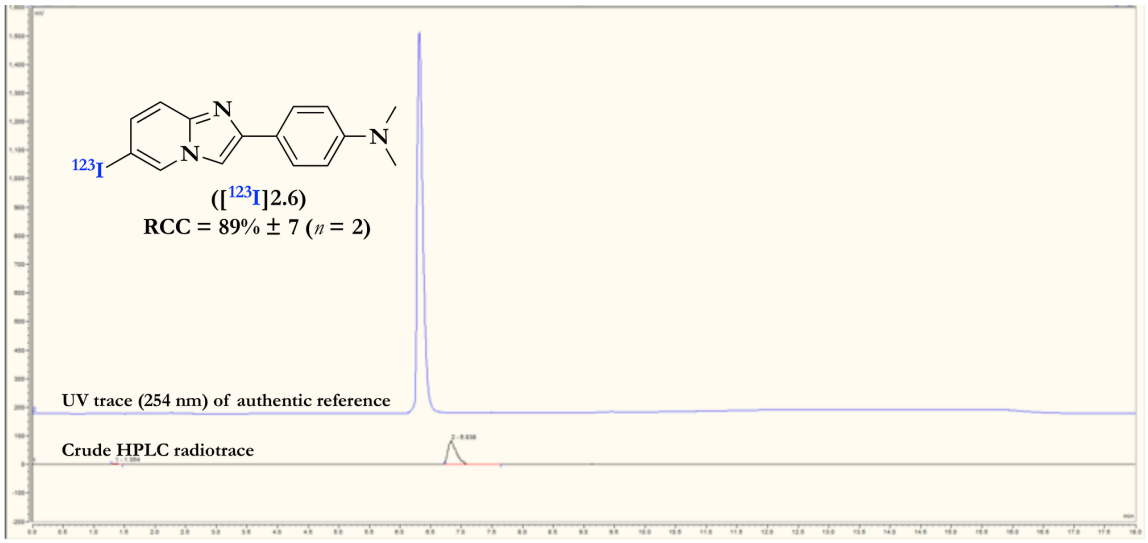
Radiotrace and RCC Calculation for 2.5j: Trace recorded using HPLC gradient B



Reaction Number	Radio-TLC (%)	Radiochemical Purity (%)	Radiochemical Conversion (%)
1	70%	96%	67%
2	77%	-	74%
3	75%	86%	65%
4	64%	-	55%
RCC and Standard Error of the Mean			72% ± 3%

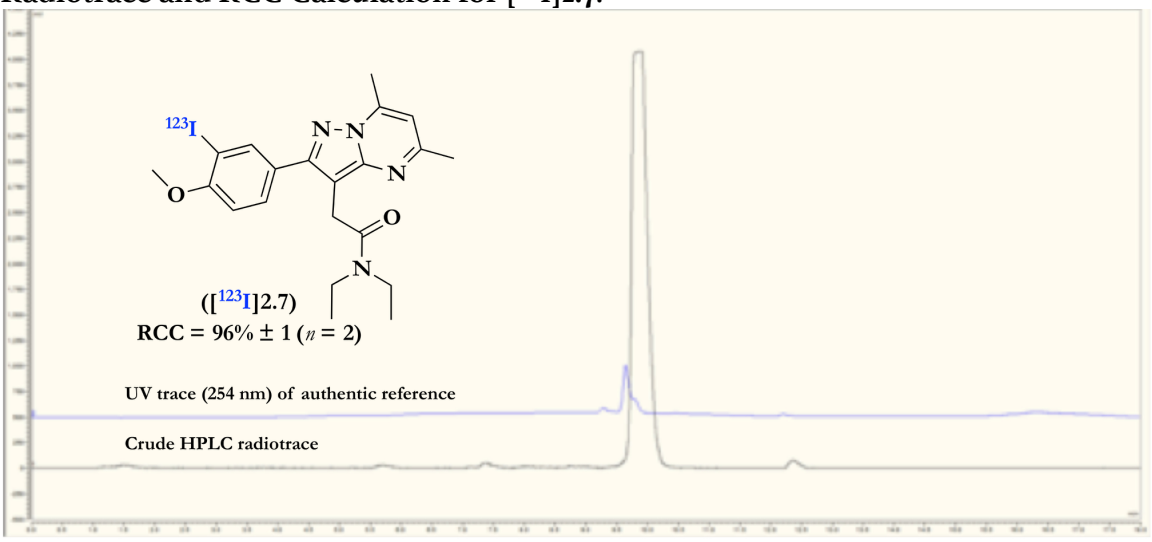
HPLC Traces of SPECT Traces (all traces taken using HPLC gradient A unless otherwise specified)

Radiotrace and RCC Calculation for [^{123}I]2.6: Trace recorded using HPLC gradient B



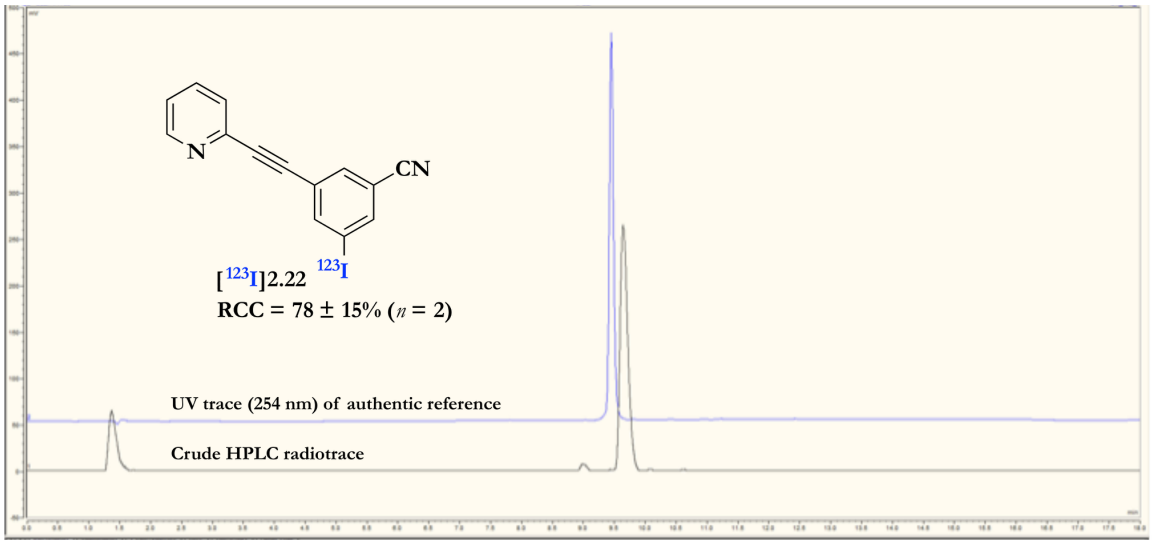
Reaction Number	Radio-TLC (%)	Radiochemical Purity (%)	Radiochemical Conversion (%)
1	82%	>99%	82%
2	95%	-	95%
RCC and Standard Error of the Mean			89% ± 7%

Radiotrace and RCC Calculation for [^{123}I]2.7:



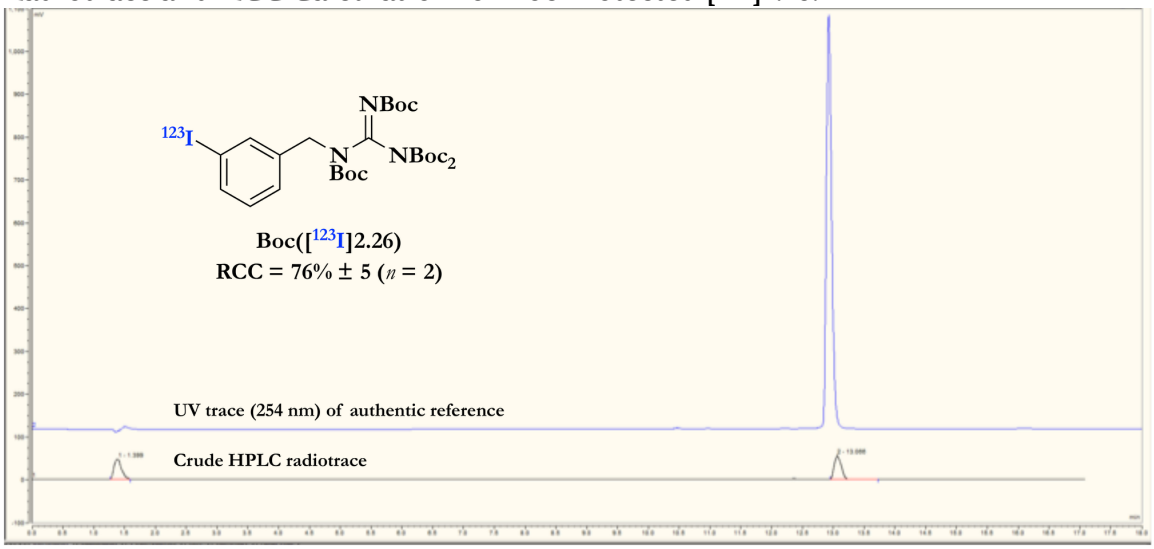
Reaction Number	Radio-TLC (%)	Radiochemical Purity (%)	Radiochemical Conversion (%)
1	95%	>99%	95%
2	97%	-	97%
RCC and Standard Error of the Mean			98% ± 1%

Radiotrace and RCC Calculation for [^{123}I]2.22:



Reaction Number	Radio-TLC (%)	Radiochemical Purity (%)	Radiochemical Conversion (%)
1	64%	>98%	63%
2	94%	-	92%
RCC and Standard Error of the Mean			78% ± 15%

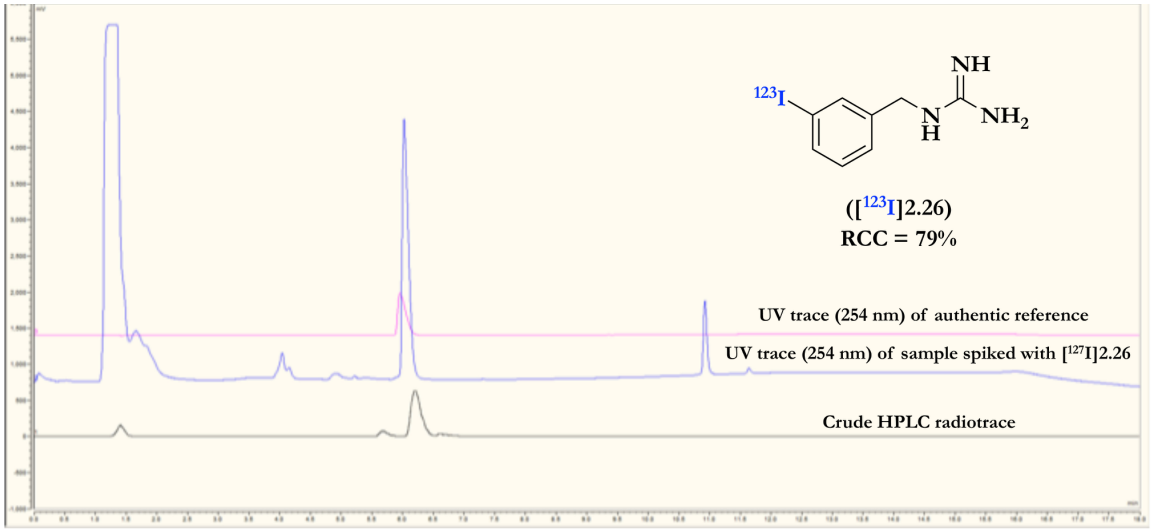
Radiotrace and RCC Calculation for Boc Protected [^{123}I]2.26:



Reaction Number	Radio-TLC (%)	Radiochemical Purity (%)	Radiochemical Conversion (%)
1	82%	>99%	80%
2	72%	-	71%
RCC and Standard Error of the Mean			76% ± 5%

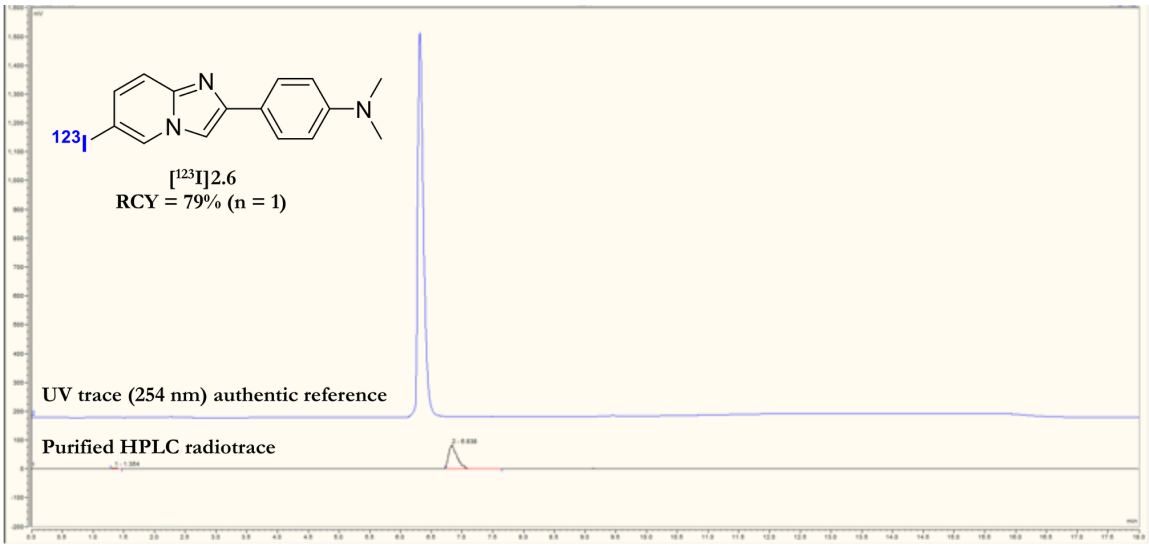
Radiotrace and RCC for [^{123}I]2.26:

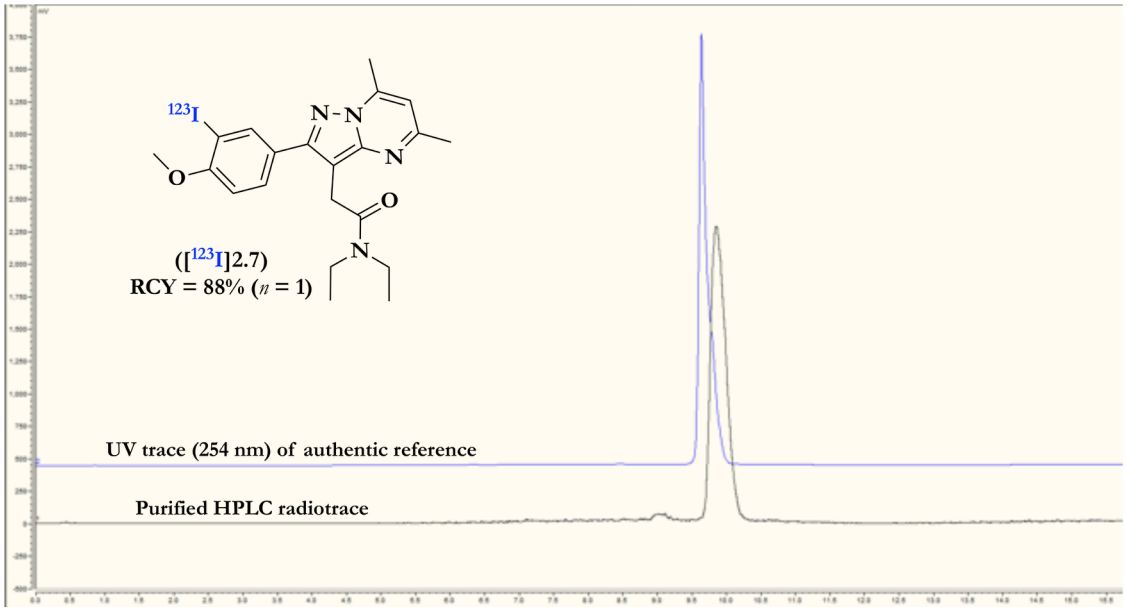
The product injected onto an analytical column overlaid with a UV spectra spiked with an authentic reference sample. Trace carried out using HPLC gradient B.

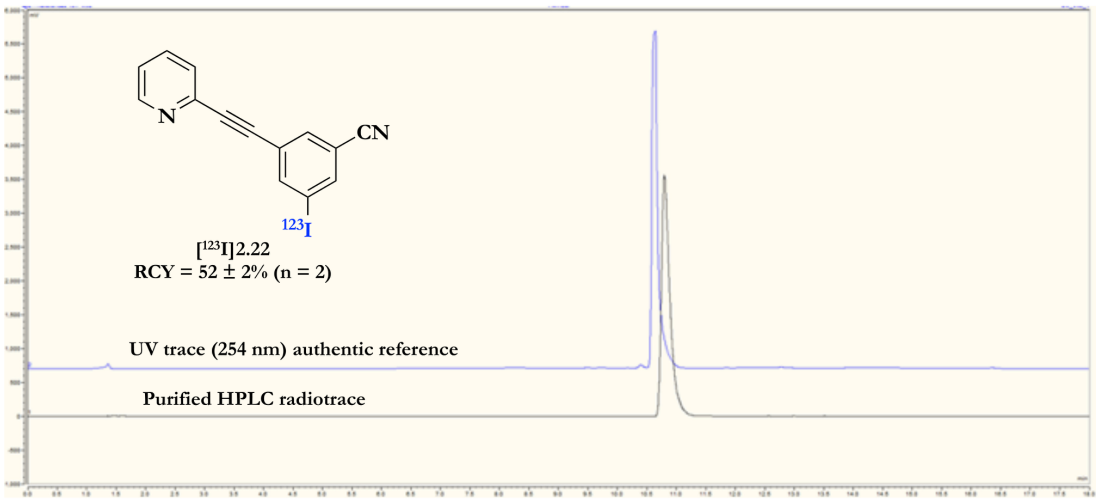


Starting Activity (MBq)	MeOH Flush Activity (MBq)	H_2O Flush Activity (MBq)	RCP (%)	RCY* (%) (Protected Species)	Deprotection Condition	RCC(%) [^{123}I]2.26
8.1	3.6	1.1	-	44	57% HI (300 µL), 125 °C, 10 mins	79

Isolated Radiotraces:



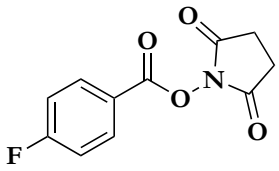



N
CN
123I
[123I]2.22
RCY = 52 ± 2% (n = 2)
UV trace (254 nm) authentic reference
Purified HPLC radiotrace

5.3 Chapter 3: Access to ^{18}F aryl prosthetic groups *via* copper-mediated ^{18}F nucleophilic fluorination.

5.3.1 Substrate Synthesis

2,5-dioxopyrrolidin-1-yl 4-fluorobenzoate (3.1):

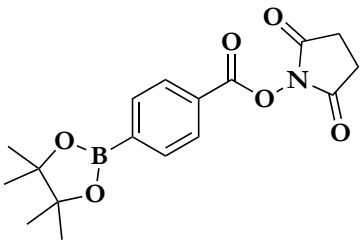


A solution of 4-fluorobenzoic acid (280 mg, 2 mmol), disuccinimidyl carbonate (512 mg, 2 mmol) and triethylamine (0.28 mL, 2 mmol) in 10 mL of acetonitrile was stirred for 2 hours at room temperature. After reaction completion the reaction mixture was concentrated *in vacuo* giving a residue that was purified *via* silica gel flash column chromatography using ethyl acetate/cyclohexane (1/9) as eluent to yield **3.1** as a white solid (408 mg, 1.72 mmol, 86%).

^{1}H-NMR (400 MHz, $CDCl_3$): δ 8.16-8.11 (m, 2H, Ar*H*), 7.23-7.13 (m, 2H, Ar*H*), 2.87 (s, 4H, N(COCH_2)$_2$). **^{13}C-NMR** (101 MHz, $CDCl_3$): δ 169.2, 166.7 (d, *J* = 257.6 Hz), 160.9, 133.4 (d, *J* = 9.5 Hz), 121.4 (d, *J* = 3.0 Hz), 116.3 (d, *J* = 22.4 Hz), 25.9. **^{19}F-NMR** (377 MHz, $CDCl_3$): δ -101.25

Data consistent with literature values.[9]

2,5-Dioxopyrrolidin-1-yl-4-(4,4,5,5-tetramethyl-1,3,2-dioxaborolan-2-yl)benzoate (3.16):

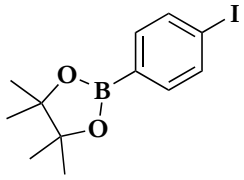


A solution of 4-(4,4,5,5-tetramethyl-1,3,2-dioxaborolan-2-yl)benzoic acid (496 mg, 2 mmol), disuccinimidyl carbonate (512 mg, 2 mmol) and triethylamine (0.28 mL, 2 mmol) in 10 mL of acetonitrile was stirred for 2 hours at room temperature. After reaction completion the reaction mixture was concentrated *in vacuo* giving a residue that was purified *via* silica gel flash column chromatography using ethyl acetate/cyclohexane (1/9) as eluent, yielding **3.16** as a white solid (552 mg, 1.61 mmol, 80%).

^{1}H-NMR (400 MHz, $CDCl_3$): δ 8.11-8.09 (m, 2H, Ar*H*), 7.93-7.91 (m, 2H, Ar*H*), 2.90 (s, 4H, N(COCH_2)$_2$), 1.35 (s, 12H, B(OCCH_3CH_3)$_2$). **^{13}C-NMR** (101 MHz, $CDCl_3$): δ 169.2, 161.9, 134.9, 129.4, 127.1, 84.4, 25.6, 24.8. (Signal due to carbon bearing the boron was not observed).

Data consistent with literature values.[10]

2-(4-Iodophenyl)-4,4,5,5-tetramethyl-1,3,2-dioxaborolane (3.17):

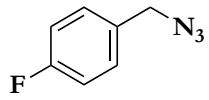


(4-Iodophenyl)boronic acid (500 mg, 2.03 mmol) and 2,3-dimethylbutane-2,3-diol (265 mg, 2.23 mmol) were placed into a 100 mL Schlenk tube containing 4 Å molecular sieves and 20 mL of anhydrous diethyl ether. The reaction was left to stir overnight at room temperature under nitrogen. The solution was filtered through a short pad of Celite® and the solvent removed *in vacuo* to give **3.17** as a white solid (607 mg, 1.84 mmol, 92% yield).

^{1}H-NMR (400 MHz, $CDCl_3$): δ 7.69 (d, *J* = 8.3 Hz, 2H, Ar*H*), 7.48 (d, *J* = 8.3 Hz, 2H, Ar*H*), 1.30 (s, 12H, B(OCCH_3CH_3)$_2$).**^{13}C-NMR** (101 MHz, $CDCl_3$): δ 137.1, 136.5, 99.0, 84.3, 25.1. (Signal due to carbon bearing the boron was not observed).

Data consistent with literature values.[11]

1-(Azidomethyl)-4-fluorobenzene (3.9):

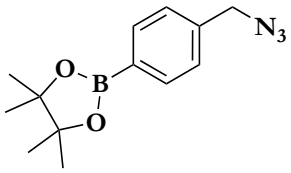


To a solution of 1-(bromomethyl)-4-fluorobenzene (473 mg, 2.5 mmol) in a mixture of water/acetone (1/4, 50 mL) was added sodium azide (250 mg, 3.75 mmol). The reaction mixture was left to stir overnight at room temperature and was subsequently concentrated *in vacuo.* 50 mL of DCM was added to the reaction vessel and the organic layer separated. The remaining aqueous layer was further extracted with DCM (3 x 30 mL) and the combined organic layers were dried over $MgSO_4$. The solvent was removed under reduced pressure yielding **3.9** as a pale yellow oil (340 mg, 2.25 mmol, 90%).

^{1}H-NMR (400 MHz, $CDCl_3$): δ 7.32-7.27 (m, 2H, Ar*H*), 7.11-7.06 (m, 2H, Ar*H*), 4.32 (s, 2H, C*H*$_2$N$_3$). **^{13}C-NMR** (101 MHz, $CDCl_3$): δ 162.9 (d, *J* = 247.8 Hz), 131.2 (d, *J* = 3.1 Hz,), 130.0 (d, *J* = 9.4 Hz), 115.8 (d, *J* = 22.3 Hz), 54.1. **^{19}F-NMR** (377 MHz, $CDCl_3$): δ -113.57.

Data consistent with literature values.[12]

2-(4-(Azidomethyl)phenyl)-4,4,5,5-tetramethyl-1,3,2-dioxaborolane (3.19):



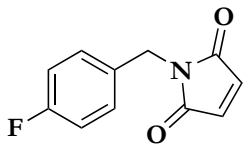
To a solution of 2-(4-(bromomethyl)phenyl)-4,4,5,5-tetramethyl-1,3,2-dioxaborolane (1 g, 3.4 mmol) in a mixture of water/acetone (1/4, 50 mL) was added sodium azide (330 mg, 5 mmol). The reaction mixture was left to stir overnight at room temperature and was subsequently concentrated *in vacuo.* 50 mL of DCM was added to the reaction vessel and the organic layer separated. The remaining aqueous layer was further extracted with DCM (3 x 30 mL) and the combined organic layers were dried over $MgSO_4$ and

the solvent was removed under reduced pressure to yield **3.19** as a clear solid (858 mg, 3.31 mmol, >95%).

^{1}H-NMR (400 MHz, $CDCl_3$): δ 7.85 (d, *J* = 8.2 Hz, 2H, Ar*H*), 7.33 (d, *J* = 8.2 Hz, 2H, Ar*H*), 4.34 (s, 2H, CH_2N_3), 1.36 (s, 12H, B(OCCH_3CH_3)$_2$). **^{13}C-NMR** (101 MHz, $CDCl_3$): δ 138.2, 135.2, 127.3, 83.8, 54.6, 24.8. (Signal due to carbon bearing the boron was not observed).

Data consistent with literature values.[13]

1-(4-Fluorobenzyl)-1*H*-pyrrole-2,5-dione (3.15):

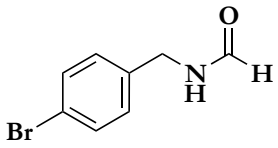


Fluorobenzylamine (0.37 mL, 3.2 mmol) in anhydrous diethyl ether (10 mL) was added to a cooled solution of maleic anhydride (314 mg, 3.2 mmol) in 5mL of anhydrous diethyl ether. The resulting solid was filtered after 1.5 hours, washed with cold ether and mixed with acetic anhydride (1.5 mL) and sodium acetate (131 mg, 1.6 mmol). The mixture was left to stir at 70 °C overnight and alkalinised with 2M Na_2CO_3, extracted with DCM (3 x 30 mL) dried and concentrated *in vacuo*. The crude material was subjected to silica gel flash column chromatography using ethyl acetate/cyclohexane (1/9) as eluent yielding **3.15** as a white solid (410 mg, 1.99 mmol, 63%). **^{1}H-NMR** (400 MHz, $CDCl_3$): δ 7.32 (td, *J* = 6.0, 2.6 Hz, 2H, Ar*H*), 7.00-6.96 (m, 2H, Ar*H*), 6.70 (s, 2H, *H*C=C*H*), 4.63 (s, 2H, CH_2N). **^{13}C-NMR** (101 MHz, $CDCl_3$): δ 170.5, 162.6 (d, *J* = 246.4 Hz), 134.4, 132.2 (d, *J* = 3.5 Hz), 130.5 (d, *J* = 8.2 Hz), 115.7 (d, *J* = 21.3 Hz), 40.9. **^{19}F-NMR** (377 MHz, $CDCl_3$): δ -114.22.

Data consistent with literature values.[14,15]

.

***N*-(4-Bromobenzyl)formamide (3.34):**

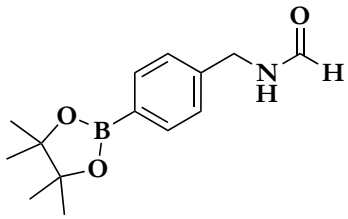


To a 100 mL round bottom flask charged with ethyl formate (25 mL) was added (4-bromophenyl)methanamine (2.4 mL, 19 mmol). The reaction was left to stir for 24 hours at 45 °C. After this time the mixture was concentrated *in vacuo* then purified *via* silica gel flash column chromatography using ethyl acetate/cyclohexane (2/3-1/0) as eluent, yielding **3.34** as a pale yellow solid (3.2 g, 15 mmol, 79%).

Major isomer given: ^{1}**H-NMR** (400 MHz, $DMSO_{d6}$): δ 8.54 (br.s, 1H, N*H*), 8.21 (s, 1H, C*H*O), 7.41-7.32 (m, 2H, Ar*H*), 7.29-7.20 (m, 2H, Ar*H*), 4.32 (d, *J* = 6.0 Hz, 2H, CH_2NH). ^{13}C-**NMR** (101 MHz, $DMSO_{d6}$): δ 162.5, 137.5, 131.4, 129.0, 120.1, 40.3.

Data consistent with literature values.[16]

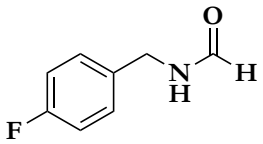
***N*-(4-(4,4,5,5-Tetramethyl-1,3,2-dioxaborolan-2-yl)benzyl)formamide (3.30):**



To a 25 mL round bottom flask under argon, containing 10 mL of toluene was added **3.34** (1 g, 4.67 mmol), Pd(dppf)Cl_2.CH_2Cl_2 (380 mg, 0.46 mmol), potassium acetate (1.35 g, 14.04 mmol) and bis(pinacolato)diboron (2.37 g, 9.34 mmol). The reaction was left to stir at 85 °C for 18 hours. The reaction was allowed to cool to room temperature and the solvent removed in *vacuo* before addition of ethyl acetate (5 mL). The mixture was filtered through a short plug of Celite®, evaporated and subjected to silica gel flash column chromatography using ethyl acetate/cyclohexane (2/3 to 1/0) as the eluent. This afforded **3.30** as a red solid (1.02 g, 3.92 mmol, 84%).

Mp: 160-162 °C. **^{1}H-NMR** (400 MHz, $CDCl_3$): δ 8.25 (s, 1H, C*H*O), 7.78 (d, *J* = 8.1 Hz, 2H, Ar*H*), 7.28 (d, *J* = 8.1 Hz, 2H, Ar*H*), 6.03 (br.s, 1H, N*H*), 4.49 (d, *J* = 5.9 Hz, 2H, CH_2NH), 1.34 (s, 12H, B(OCCH_3CH_3)$_2$). **^{13}C-NMR** (101 MHz, $CDCl_3$): δ 161.0, 140.6, 135.2, 127.0, 83.8, 42.1, 24.8. (Signal due to carbon bearing the boron was not observed). IR *ν* 3650, 3289, 2980, 2360, 1663, 1359, 1143, 1088, 962, 858. **HRMS** (ESI) for $C_{14}H_{20}O_3NBNa$ $[M+Na]^+$ requires 284.1434 found 284.1430.

***N*-(4-Fluorobenzyl)formamide (3.35):**

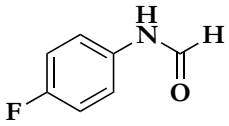


To a 100 mL round bottom flask charged with ethyl formate (25 mL) was added (4-fluorophenyl)methanamine (2.17 mL, 19 mmol). The reaction was left to stir for 24 hours at 45 °C. After this time the mixture was concentrated *in vacuo,* then purified *via* silica gel flash column chromatography using ethyl acetate/cyclohexane (2/3-1/0) yielding **3.35** as pale yellow solid (2.5 g, 16.34 mmol, 86%).

Major isomer given: **^{1}H-NMR** (400 MHz, $CDCl_3$): δ 8.22 (s, 1H, C*H*O), 7.27-7.23 (m, 2H, Ar*H*), 7.04-6.99 (m, 2H, Ar*H*), 6.35 (br.s, 1H, N*H*), 4.43 (d, *J* = 6.0 Hz, 2H, CH_2NH). **^{13}C-NMR** (101 MHz, $CDCl_3$): δ 164.5, 162.2 (d, *J* = 246.4 Hz), 133.3 (d, *J* = 3.2 Hz), 129.4 (d, *J* = 8.3 Hz), 115.5 (d, *J* = 22.3 Hz), 41.3. **^{19}F-NMR** (377 MHz, $CDCl_3$): δ -114.8.

Data consistent with literature values.[17]

***N*-(4-fluorophenyl)formamide (3.41):**



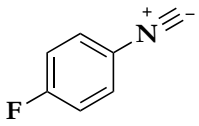
A round bottom flask containing 4-fluoroaniline (1.00 mL, 10.6 mmol,) in ethyl formate (5 mL) was fitted with a reflux condenser and heated to 70 °C for 16 hours. After this

time the mixture was left to cool to room temperature and subsequently concentrated *in vacuo*. Purification was achieved *via* silica gel flash column chromatography using petroleum ether/ethyl acetate (3/2-0/1) yielding **3.41** as a white solid (1.03 g, 7.42 mmol, 70 % yield).

Major isomer given: **^{1}H NMR** (400 MHz, DMSO-d_6): δ 10.23 (br.s, 1H, N*H*), 8.23 (d, *J* = 2.0, 1H, C*H*O), 7.61-7.58 (m, 2H, Ar*H*), 7.25-7.11 (m, 2H, Ar*H*). **^{13}C NMR** (101 MHz, DMSO-d_6): δ 160.5, 159.1 (d, *J* = 245.4 Hz), 135.3 (d, *J* = 3.2 Hz), 121.4 (d, *J* = 8.1 Hz), 115.7 (d, *J* = 22.4 Hz). **^{19}F NMR** (377 MHz, DMSO-d_6): δ -118.7.

Data consistent with literature values.[18]

1-Fluoro-4-isocyanobenzene (3.42):

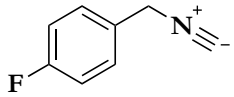


To **3.41** (400 mg, 2.88 mmol) in DCM (10 mL) at 0 °C was added dropwise triethylamine (1.20 mL, 8.64 mmol), and phosphorous (V) oxychloride (268 µL, 2.88 mmol). The reaction was stirred for 3 hours at 0 °C and was kept at this temperature for the addition of aqueous sodium carbonate (305 mg in 10 mL H_2O, 2.88 mmol). After stirring for a further hour at 0 °C, the reaction was extracted with DCM (3 x 10 mL), the combined organic fractions dried over $MgSO_4$ and the solvent removed *in vacuo*. Purification by silica gel flash column chromatography using petroleum ether/ethyl acetate (9/1) afforded **3.42** as a green oil (198 mg, 1.64 mmol, 57 %).

^{1}H NMR (400 MHz, $CDCl_3$): δ 7.39 (dd, *J* = 8.8 Hz, *J* = 4.5 Hz, 2H, Ar*H*), 7.12-7.05 (m, 2H, Ar*H*). **^{13}C NMR** (101 MHz, $CDCl_3$): δ 164.5 (t, *J* = 5.6 Hz), 163.4 (d, *J* = 252.5 Hz), 128.4 (d, *J* = 9.6 Hz), 122.8 (td, *J* = 14.4 Hz, *J* = 3.2 Hz), 116.6 (d, *J* = 24.0 Hz). **^{19}F NMR** (377 MHz, $CDCl_3$): δ -108.6

Data consistent with literature values.[19]

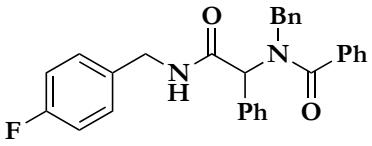
1-Fluoro-4-(isocyanomethyl)benzene (3.32):



To **3.35** (153 mg, 1 mmol) in DCM (5 mL) at 0 °C was added dropwise triethylamine (416 µL, 3 mmol), and phosphorous (V) oxychloride (93 µL, 1 mmol). The reaction was stirred for 3 hours at 0 °C and was kept at this temperature for the addition of aqueous sodium carbonate (106 mg in 5 mL H_2O, 1 mmol). After stirring for a further hour at 0 °C, the reaction was extracted with DCM (3 x 10 mL), the combined organic fractions dried over $MgSO_4$ and the solvent removed *in vacuo*. Purification by silica gel flash column chromatography using petroleum ether/ethyl acetate (9/1) afforded **3.32** as a green oil (81 mg, 0.60 mmol, 60 %).

^{1}H-NMR (400 MHz, $CDCl_3$): δ 7.30-7.27 (m, 2H, Ar*H*), 7.06-7.01 (m, 2H, Ar*H*), 4.37 (s, 2H, CH_2NC). **^{13}C NMR** (101 MHz, $CDCl_3$): δ 165.4 (t, *J* = 5.1 Hz), 163.7 (d, *J* = 245.5 Hz), 133.2 (d, *J* = 3.2 Hz), 129.5 (d, *J* = 8.3 Hz), 115.6 (d, *J* = 22.1 Hz) 47.4 (t, *J* = 11.3 Hz). **^{19}F NMR** (377 MHz, $CDCl_3$): δ -110.3. **IR** (*v*, cm^{-1}): 2152, 1511, 1501, 1312, 1252, 1002, 813, 735. **LRMS:** Not found by ESI.

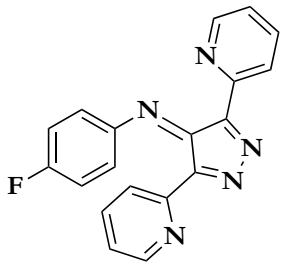
***N*-Benzyl-*N*-(2-((4-fluorobenzyl)amino)-2-oxo-1-phenylethyl)benzamide (3.36):**



To benzaldehyde (41 µL, 0.40 mmol) in EtOH (400 µL) in a pressure tube was added benzyl amine (44 µL, 0.40 mmol), benzoic acid (54 mg, 0.44 mmol) and **3.32** (54 mg, 0.40 mmol). The reaction was stirred for 30 minutes at 80 °C before concentration *in vacuo*. Purification of the crude residue by silica gel flash column chromatography using petroleum ether/ethyl acetate (9/1-7/3) as eluent, afforded **3.36** as a white solid (71 mg, 0.15 mmol, 39 %).

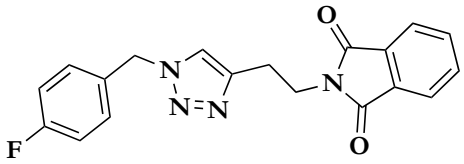
Mp: 68-70 °C. **^{1}H NMR** (400 MHz, $CDCl_3$): 8.29 (br.s, 1H, N*H*), 7.56-7.30 (m, 12H, Ar*H*), 7.24-7.16 (m, 3H, Ar*H*), 7.12- 7.05 (m, 2H, Ar*H*), 6.99-6.89 (m, 2H, Ar*H*), 5.76 (s, 1H, C*H*), 4.81 (d, *J* = 16.5 Hz, 1H, CH_2), 4.57 (d, *J* = 15.4 Hz, 1H, CH_2), 4.46 (d, *J* = 5.9 Hz, 2H, CH_2NH). **^{13}C NMR** (101 MHz, $CDCl_3$): 170.6, 167.7, 161.2 (d, *J* = 245.4 Hz), 136.9, 135.6, 134.3, 133.4, 130.2, 129.4, 129.0, 128.9, 128.5, 128.3, 127.3, 127.0, 126.9, 122.0, 115.4, 65.4, 53.2, 41.5. **^{19}F-NMR** (377 MHz, $CDCl_3$): δ -114.1. **IR** (*v,* cm^{-1}): 3287, 1695, 1618, 1455, 1100, 828, 730. **HRMS** (ESI) for $C_{29}H_{25}FN_2NaO_2$ $[M+Na]^+$ calc. 475.1798, found 475.1790.

***N*-(4-Fluorophenyl)-3,5-di(pyridin-2-yl)-4*H*-pyrazol-4-imine (3.43):**



To a solution of 3,6-di(pyridine-2-yl)-1,2,4,5-tetrazine (55 mg, 0.23 mmol) in DCM (2mL) was added **3.42** (28 mg, 0.23 mmol). The reaction was left to stir at room temperature for 1 hour, concentrated in *vacuo* and subjected to silica gel flash column chromatography methanol/DCM (1/10-1/0) which yielded **3.43** as a deep red solid (42 mg, 0.13 mmol, 55%). **Mp:** 175-177 °C. **^{1}H-NMR** (400 MHz, DMSO-d_6): δ 8.68 (s, 1H, Pyr*H*), 8.52 (d, *J* = 4.1 Hz, 1H, Pyr*H*), 8.43 (d, *J* = 6.5 Hz, 1H, Pyr*H*), 8.19-8.10 (m, 2H, Pyr*H*), 7.94 (d, *J* = 8.0 Hz, 1H, Pyr*H*), 7.75 (t, *J* = 7.7 Hz, 1H, Pyr*H*), 7.40 (t, *J* = 6.0 Hz, 1H, Pyr*H*), 7.30 (t, *J* = 8.3 Hz, 1H, Ar*H*), 7.23 (d, *J* = 9.7 Hz, 1H, Ar*H*), 7.08 (dd, *J* = 21.9, 7.0 Hz, 2H, Ar*H*). **^{13}C-NMR** (101 MHz, DMSO-d_6): δ 158.0 (d, *J* = 238.4 Hz), 155.6, 155.1, 148.3, 146.8, 143.3, 142.8, 140.2, 137.9, 136.6, 133.9, 133.4 (d, *J* = 9.0 Hz), 122.9, 122.1 (d, *J* = 8.2 Hz), 120.7, 119.5, 118.1 (d, *J* = 22.2 Hz), 117.5 (d, *J* = 24.0 Hz) 117.3. **^{19}F-NMR** (377 MHz, DMSO-d_6): δ -120.9. **IR** (*v,* cm^{-1}): 3242, 3063, 2162, 1625, 1524, 1416, 1150, 1021, 961, 863. **HRMS** (ESI) for $C_{19}H_{13}N_5F_1$ $[M+H]^+$ requires 330.1150 found 330.1152.

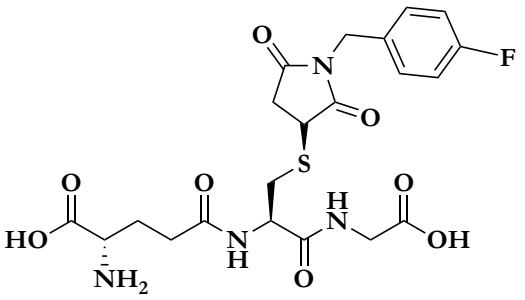
2-(2-(1-(4-Fluorobenzyl)-1*H*-1,2,3-triazol-4-yl)ethyl)isoindoline-1,3-dione (3.25):



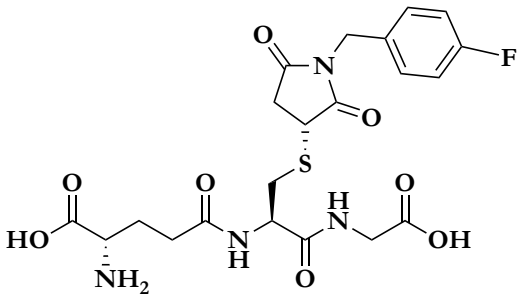
A 25 ml round bottomed flask was charged with **3.9** (151 mg, 1 mmol), *N*-(3-butynyl)phtalimide (200 mg, 1 mmol), $Cu(OTf)_2(py)_4$ (670 mg, 1 mmol), sodium ascorbate (300 mg, 1.5 mmol), DMF (4 ml) and H_2O (1 ml). The reaction was left to stir for 30 minutes at 60 °C before being concentrated *in vacuo*. The crude reaction mixture was subjected to silica gel flash column chromatography using ethyl acetate/cyclohexane as eluent (3/7) affording **3.20** as an off white solid (291 mg, 0.83 mmol, 83% yield).

Mp: 83-85 °C. ^{1}**H-NMR** (400 MHz, $CDCl_3$): δ 7.76-7.65 (m, 4H, Ar*H*), 7.30 (s, 1H, C=C*H*), 7.16 (dd, *J* = 8.8, 5.2 Hz, 2H, Ar*H*), 6.99 (t, *J* = 8.8 Hz, 2H, Ar*H*), 5.41 (s, 2H, CH_2), 3.95 (t, *J* = 7.2 Hz, 2H, CHCH_2), 3.09 (t, *J* = 7.2 Hz, 2H, CHCH_2). ^{13}**C-NMR** (101 MHz, $CDCl_3$): δ 168.0, 162.6 (d, *J* = 248.0 Hz), 144.7, 133.8, 131.8, 130.6 (d, *J* = 3.2 Hz), 129.6 (d, *J* = 7.9 Hz), 123.1, 121.2, 115.9 (d, *J* = 21.8 Hz), 53.1, 37.32, 24.75. ^{19}**F-NMR** (377 MHz, $CDCl_3$): δ -113.01. **IR** (*ν*, cm^{-1}): 2980, 2360, 2341, 1770, 1704, 1510, 1395, 1222, 772. **HRMS** (ESI) for $C_{19}H_{16}FN_4O_2$ $[M + H]^+$ requires 351.1257 found 351.1245.

N^5-((2*R*)-1-((Carboxymethyl)amino)-3-((1-(4-fluorobenzyl)-2,5-dioxopyrrolidin-3-yl)thio)-1-oxopropan-2-yl)-*L*-glutamine (3.27):



A

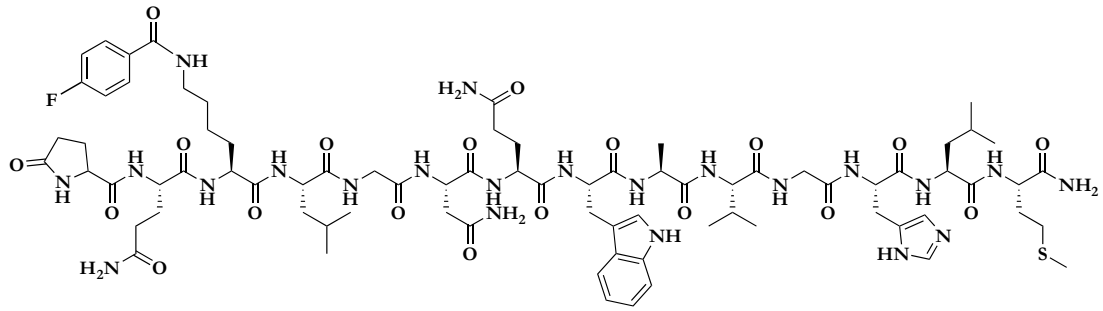


B

To a 1.5 mL vial was added glutathione reduced (25 mg, 81 µmol) in 300 µL of phosphate buffer (pH 7.4) and **3.15** (18 mg, 89 µmol) in 200 µL of acetonitrile. The reaction was left to stir at room temperature for 1 hour before being concentrated *in vacuo*. The crude material was re-dissolved in DCM (1 ml) and H_2O (1 ml) and the aqueous layer was subsequently washed with DCM (3 x 1 ml) and left aside. Furthermore, the organic layer was extracted with H_2O (3 x 1 ml) and the combined fractions were lyophilised to yield **3.27** as a white powder (34 mg, 66 µmol, 82%).

Mp: 182-184 °C. **^{1}H NMR** (400 MHz, Deuterium Oxide): δ = 7.28 (m 4H, [A]Ar*H* + [B]Ar*H*), 7.06 – 6.99 (m, 4H, [A]Ar*H* + [B]Ar*H*), 4.60 (m, 4H, [A]CH_2 + [B]CH_2), 4.57 – 4.52 (m, 2H, [A]C*H* + [B]C*H*), 4.05 – 3.95 (m, 4H, [A]CH_2 + [B]CH_2), 3.94 (s, 2H, [A]CH_2), 3.92 (s, 2H, [B]CH_2), 3.27 (m, 2H, [A]CH_2 + [B]CH_2), 3.17 (dd, *J*=14.1, 5.3, 1H, [A]CH_2), 3.10 (dd, *J*=14.0, 5.5, 1H, [B]CH_2), 3.02 (dd, *J*=14.0, 8.0, 1H, [A]CH_2), 2.89 (dd, *J*=14.0, 8.7, 1H, [B]CH_2), 2.68 (dd, *J*=8.1, 3.9, 1H, [A]CH_2), 2.63 (dd, *J*=8.1, 3.9, 1H, [B]CH_2), 2.50 (m, 4H, [A]CH_2 + [B]CH_2), 2.21 – 2.08 (m, 4H, [A]CH_2 + [B]CH_2). **^{13}C NMR** (126 MHz, Deuterium Oxide): δ 179.0, 178.9, 177.7, 177.7, 174.2, 174.2, 172.8, 172.7, 172.1, 172.1, 171.8, 162.3 (d, J = 243.8 Hz), 130.9 (d, J = 3.1 Hz), 129.8 (d, J = 8.5 Hz), 115.4 (d, J = 21.8 Hz) 53.0, 52.5, 52.4, 41.7, 41.0, 40.4, 39.8, 35.9, 35.7, 32.4, 32.2, 30.8, 30.8, 25.4, 25.4. **^{19}F-NMR** (377 MHz, Deuterium Oxide): δ -114.81. **IR** (*ν*, cm^{-1}): 2980, 1699, 1392, 1251, 1153, 965, 829, 803. **HRMS** (ESI) for $C_{21}H_{24}N_4O_8FS$ $[M - H]^-$ requires 511.1293 found 511.1304.

4-Fluorobenzoyl-[Lys³]-bombesin (3.28):



A 2 mL vial containing [Lys³]-bombesin (1 mg, 0.624 μmol) in 250 μL of sodium borate buffer (50 mmol/L, pH 8.3) was charged with 100 μL of MeCN containing **3.1** (148 μg, 0.624 μmol). The reaction contents were gently stirred for 60 minutes at 40 °C prior to addition of 1 ml H_2O. Purification of **3.28** was achieved by loading the reaction contents directly onto a 2 mL HPLC loop and injecting onto a semi-prep HPLC column (phenomenex C-18 luna) eluting with gradiant A (shown below). The combined fractions were lyophilised to yield **3.28** as a white powder (0.5 mg, 0.262 μmol, 42%). **HRMS** (ESI) for $C_{78}H_{115}FN_{22}O_{19}S$ $[M + 2H]^{2+}$ requires 857.4201 found 857.4188.

HPLC gradient A: water/acetonitrile containing 0.1 mg/mL TFA, 1 mL/min, Phenomenex C18 luna Column, 5 μm, 4.6 x 250 mm)

0-3 min (5% MeCN containing 0.1 mg/mL TFA) isocratic

3-33 min (5% MeCN containing 0.1 mg/mL TFA to 65% MeCN containing 0.1 mg/mL TFA) linear increase

33-43 min (65% MeCN containing 0.1 mg/mL TFA to 5% MeCN containing 0.1 mg/mL TFA) linear decrease.

5.3.2 Radiochemistry

[^{18}F]Fluoride Preparation:

[^{18}F]Fluoride was produced by Alliance Medical (UK) *via* the $^{18}O(p,n)^{18}F$ reaction and delivered as [^{18}F]fluoride in ^{18}O-enriched-water. Radiosynthesis and azeotropic drying was performed on a NanoTek microfluidic device (Advion).

Buffer Preparation:

1 litre of 100 mM PBS, 50 mM Bicarbonate

Start with 800 ml of distilled water.

Add 8 g of NaCl.

Add 0.2 g of KCl.

Add 1.44 g of Na_2HPO_4.

Add 0.24 g of KH_2PO_4.

Add in 0.42 g of $NaHCO_3$

Add distilled water to a total volume of 1 litre.

Adjust pH accordingly to 7.4 if needed.

Borate Buffer 50 mM

Dissolve 3.84 g sodium tetraborate in 200 mL of distilled water.

1.24 g boric acid, dissolve in 800 mL distilled water.

Combine the two, adjust the pH by adding HCl to pH 8.3

Analysis:

For all reactions, an aliquot was removed for analysis by radioTLC and radioHPLC.

RadioTLC was carried out on Merck Kiesegel 60 F254 plates in EtOAc/Hexane (1/1) or MeOH/DCM (1/10) and analysed using a plastic scintillator/PMT detector.

HPLC analysis was performed using a Dionex Ultimate 3000 dual channel HPLC system with a shared autosampler, parallel UV-detectors and LabLogic NaI/PMT-radiodetectors with Flowram analogue output.

HPLC Gradient B: Water/MeCN, 1 mL/min, Waters Nova-Pak C18 Column, 4 µm, 3.9 x 150 mm:

0 – 1 min (5 % MeCN) isocratic

1 – 10 min (5 % MeCN to 95 % MeCN) linear increase

10 – 14 min (95 % MeCN) isocratic

14 – 15 min (95 % MeCN to 5 % MeCN) linear decrease

15 – 17 min (5 % MeCN) isocratic.

HPLC gradient C: water/acetonitrile containing 0.1 % TFA, 1 mL/min, Waters Nova-Pak C18 Column, 4 µm, 3.9 x 150 mm

0-3 min (5% MeCN containing 0.1 % TFA) isocratic
1-10 min (5% MeCN containing 0.1 % TFA to 95% MeCN containing 0.1 mg/mL TFA) linear increase
10-14 min (95% MeCN containing 0.1 % TFA) isocratic
14-15 min (95% MeCN containing 0.1 % TFA to 5% MeCN containing 0.1 % TFA) linear decrease
15-17 min (5% MeCN containing 0.1 % TFA) isocratic

Reported radiochemical conversions (RCCs) are decay corrected and calculated by radioTLC taking into account the radiochemical purity as determined by radioHPLC

General Procedure for Azeotropic Drying

Radiosynthesis and azeotropic drying was performed on a NanoTek® microfluidic device (Advion). [^{18}F]Fluoride (3.0 - 4.0 GBq) was separated from ^{18}O-enriched-water using a Chromafix cartridge and subsequently released with 900 µL (in 6 x 150 µL portions) of a solution of $K_{2.2.2}/K_2CO_3$ (Kryptofix 222 (15mg) and K_2CO_3 (3mg) in 1 mL of MeCN/H2O, 4:1) into a 5 mL v-vial containing a magnetic stir bar. The solution was dried with five cycles of azeotropic drying with MeCN (200 µL) under a flow of N_2 at 105°C. The dried [^{18}F]KF/$K_{2.2.2}$ residue was re-dissolved in anhydrous MeCN (500 - 1000 µL) and aliquots used for ^{18}F-fluorination reactions.

General ^{18}F-Fluorination Procedure for Prosthetic Group Radiosynthesis:

A small aliquot (25-30 MBq, 10–50 µL) of a solution of ^{18}F-KF/K_{222} in anhydrous MeCN was dispensed into a V-vial containing $Cu(OTf)_2(py)_4$ (0.03 or 0.02 mmol), aryl pinacol boronate (0.02 mmol) and a magnetic stirrer bar. Air was flushed through the reaction vial using a syringe, and then 300 µL of DMA was added *via* syringe. The sealed vial was then heated at 110 °C for 20 minutes. The reaction was quenched by addition of water (200 µL). An aliquot was removed for analysis by radioTLC and HPLC for radiochemical conversion and product identity. Analysis was performed using the Gradiant B given above with a Waters Nova-Pak C18 column (4 µm, 3.9 x 150 mm) at a flow rate 1 mL/min.

Radiosynthesis of [^{18}F]3.25

A small aliquot (25-30 MBq, 10–50 μL) of a solution of ^{18}F-KF/K_{222} in anhydrous MeCN was dispensed into a V-vial containing $Cu(OTf)_2(py)_4$ (0.02 mmol), **3.19** (5.2 mg, 0.02 mmol) and a magnetic stirrer bar. Air was flushed through the reaction vial using a syringe, and then 300 μL of DMA was added *via* syringe. The sealed vial was then heated at 110 °C for 20 minutes. Thereafter, sodium ascorbate (4.4 mg, 0.022 mmol) in 200 μL of H_2O and **3.25** (4 mg, 0.02 mmol) in 100 μL of DMA was added to the reaction vial *via* syringe. The reaction was heated at 80 °C for 20 minutes and prior to addition of 100 μL of H_2O. An aliquot was removed for analysis by radioTLC and HPLC for radiochemical conversion and product identity. Analysis was performed using the Gradiant B given above with a Waters Nova-Pak C18 column (4 μm, 3.9 x 150 mm) at a flow rate 1 mL/min.

Radiosynthesis of [^{18}F]3.15:

[^{18}F]Fluoride (3.0-4.0 GBq) was separated from ^{18}O-enriched-water using a Waters Sep-Pak Accell Plus QMA Carbonate Plus Light Cartridge, (46 mg, Sorbent per Cartridge, 40 μm Particle Size, 50/pk (Part #186004540 from Waters) and subsequently released with 900 μL (in 6 x 150 μL portions) of a solution of $K_{222}/K_2C_2O_4/K_2CO_3$ (kryptofix 222 (6.3 mg), $K_2C_2O_4$ (1 mg) and K_2CO_3 (0.1 mg) in 1 mL of MeCN/H_2O, 4:1) into a 5 mL V-vial containing a magnetic stir bar in the concentrator. The solution was dried with five cycles of azeotropic drying with MeCN (200 μl) under a flow of N_2 at 105 °C. The 5 mL vial containing the dried [^{18}F]KF/$K_{2.2.2}$ complex was purged with 30 mL of air using a syringe and then a solution of arylboronate precursor **3.19** (6.2 mg, 0.02 mmol) and $Cu(OTf)_2(py)_4$ (14 mg, 0.02 mmol) in anhydrous DMA (400 μL) was added. The mixture was heated at 120 °C for 20 minutes in a sealed vial with stirring, after which, 10ml of H_2O was added to the V-vial. The contents were then loaded onto a C-18 SepPak Plus

cartridge. Flushing the cartridge with 2 mL of H_2O, drying with air and subsequent elution with 2 mL of acetonitrile afforded **[^{18}F]3.15**. An aliquot was removed for analysis by radioTLC and HPLC for product identity. The RCY was calculated by comparing the initial activity (MBq) used, to the percentage of activity (MBq) in the MeCN elute with respect to product purity, determined *via* radioHPLC. Analysis was performed using the Gradiant B with a Waters Nova-Pak C18 column (4 μm, 3.9 x 150 mm) at a flow rate 1 mL/min.

Radiosynthesis of [^{18}F]3.27:

An aliquot (150-400 μl) of the 2 ml MeCN solution containing **[^{18}F]3.15** was subsequently added to a 5 mL V-vial before solvent removal using a stream of N_2 at 100 °C for 2 minutes. A solution of **3.26** (2 mg, 6.5 μmol) in 500 μL of PBS buffer (pH 7.4) was then added to the V-vial and the reaction contents were left to stir for 30 minutes at room temperature. An aliquot was removed for analysis by radioTLC and HPLC for radiochemical conversion and product identity. Analysis was performed using the Gradiant C with a Waters Nova-Pak C18 column (4 μm, 3.9 x 150 mm) at a flow rate 1 mL/min.

Radiosynthesis of [^{18}F]3.1:

[^{18}F]Fluoride (3.0-4.0 GBq) was separated from ^{18}O-enriched-water using a Waters Sep-Pak Accell Plus QMA Carbonate Plus Light Cartridge, (46 mg, Sorbent per Cartridge, 40 μm Particle Size, 50/pk (Part #186004540 from Waters) and subsequently released with 900 μL (in 6 x 150 μL portions) of a solution of $K_{222}/K_2C_2O_4/K_2CO_3$ (kryptofix 222 (6.3 mg), $K_2C_2O_4$ (1 mg) and K_2CO_3 (0.1 mg) in 1 mL of MeCN/H_2O, 4:1) into a 5 mL V-vial containing a magnetic stir bar in the concentrator. The solution was dried with five cycles of azeotropic drying with MeCN (200 μl) under a flow of N_2 at 105 °C. The 5 mL

vial containing the dried [^{18}F]KF/$K_{2.2.2}$ complex was purged with 30 mL of air using a syringe and then a solution of arylboronate precursor **3.16** (7 mg, 0.02 mmol) and $Cu(OTf)_2(py)_4$ (22 mg, 0.03 mmol) in anhydrous DMA (400 μL) was added. The mixture was heated at 120 °C for 20 minutes in a sealed vial with stirring, after which, 10ml of H_2O was added to the V-vial. The contents were then loaded onto a C-18 SepPak Plus cartridge or Oasis WAX cartridge (WAX = Weak Anion Exchange). Flushing the cartridge with 2 mL of H_2O, drying with air and subsequent elution with 2 mL of acetonitrile afforded [^{18}**F**]**3.1**. An aliquot was removed for analysis by radioTLC and HPLC for product identity. The RCY was calculated by comparing the initial activity (MBq) used, to the percentage of activity (MBq) in the MeCN elute with respect to product purity, determined *via* radioHPLC. Analysis was performed using the Gradiant B with a Waters Nova-Pak C18 column (4 μm, 3.9 x 150 mm) at a flow rate 1 mL/min.

Radiosynthesis of [^{18}F]3.28:

The contents of the vial were concentrated to approx. 1 mL under a flow of N_2 (0.4 mL/min) at 70 °C. An aliquot (50-150 μl) of an MeCN solution of [^{18}**F**]**3.1** was subsequently added to a 5 mL V-vial before addition of a solution of **3.26** (0.5 mg, 0.3 μmol) in 250 μL of Borate buffer (pH 8.3) and the reaction contents were left to stir for 30 minutes at 40 °C. An aliquot was removed for analysis by radioTLC and HPLC for radiochemical conversion and product identitfication. Analysis was performed using the Gradiant C with a Waters Nova-Pak C18 column (4 μm, 3.9 x 150 mm) at a flow rate 1 mL/min.

Procedure for radiosynthesis of [^{18}F]3.31 and [^{18}F]3.41:

A small aliquot (25-30 MBq, 10–50 μL) of a solution of ^{18}F-KF/K_{222} in anhydrous MeCN was dispensed into a V-vial containing $Cu(OTf)_2(py)_4$ (0.02 mmol), **3.30**/**3.44** (0.02 mmol) and a magnetic stirrer bar. Air was flushed through the reaction vial using a syringe, and then 300 μL of DMF was added *via* syringe. The sealed vial was then heated at 110 °C for 20 minutes. The reaction was quenched by addition of water (200 μL). An aliquot was removed for analysis by radioTLC and HPLC for radiochemical conversion and product identity. Analysis was performed using the Gradiant B given above with a Waters Nova-Pak C18 column (4 μm, 3.9 x 150 mm) at a flow rate 1 mL/min.

Procedure for attempted dehydration of [^{18}F]3.31 and [^{18}F]3.41, table 3.55 chapter 3:

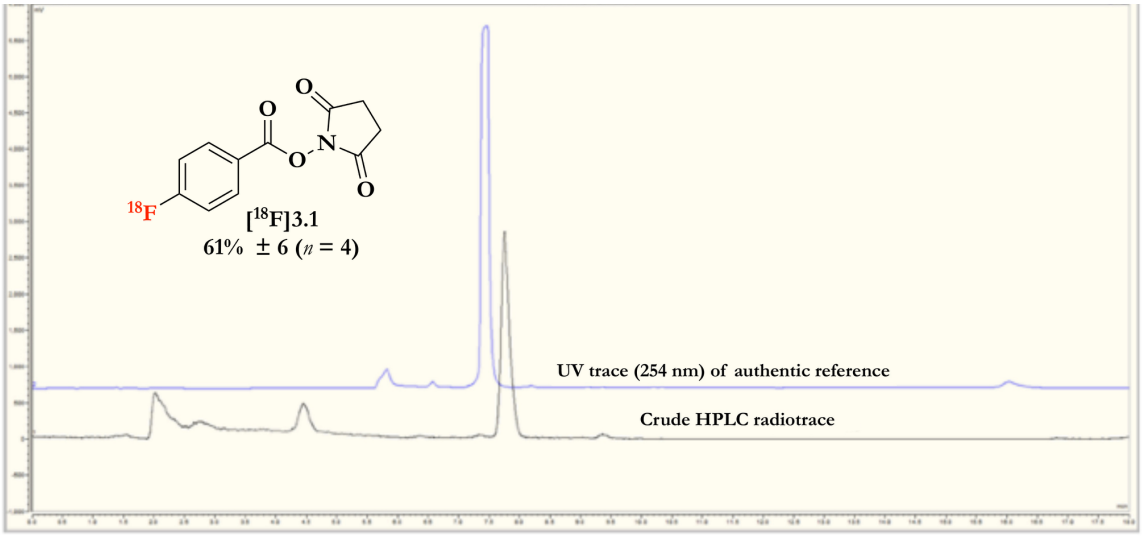
Radiosynthesis and azeotropic drying was performed on a NanoTek® microfluidic device (Advion). [^{18}F]Fluoride (4.0 GBq) was separated from ^{18}O-enriched-water using a Waters Sep-Pak Accell Plus QMA Carbonate Plus Light Cartridge, (46 mg Sorbent per Cartridge, 40 μm Particle Size, 50/pk (Part #186004540 from Waters) and subsequently released with 900 μL (in 6 x 150 μL portions) of a solution of K_{222}/K_2CO_3 (Kryptofix 222 (6.3 mg), $K_2C_2O_4$ (1.0 mg) and K_2CO_3 (0.1 mg) in 1 mL of MeCN/H_2O, 4:1) into a 5 mL V-vial containing a magnetic stir bar in the concentrator. The solution was dried with five cycles of azeotropic drying with MeCN (5 x 200 μl) under a flow of N_2 at 105 °C. The 5 mL vial containing the dried [^{18}F]KF/$K_{2.2.2}$ complex was purged with 30 mL of air using a syringe and then a solution of **3.30**/**3.44** (0.02 mmol) and Cu(OTf)2(py)4 (14 mg, 0.02 mmol) in anhydrous DMF (400 μL) was added. The sealed vial was heated at 120 °C for 20 minutes. The reaction solution was diluted with 8 mL de-ionized water and loaded onto an Oasis HLB Plus LP Extraction Cartridge. The cartridge was then flushed with 2 mL water, followed by 2 mL air. **[^{18}F]3.31** or **[^{18}F3.41** was then eluted into a 5 mL V-vial

with 2 mL of MeCN. An aliquot was removed for analysis by radioTLC and HPLC for product identity. Analysis was performed using Gradiant B with a Waters Nova-Pak C18 column (4 µm, 3.9 x 150 mm) at a flow rate 1 mL/min.

An aliquot (20-40 µl) of the 2 ml MeCN solution containing either **[^{18}F]3.31** or **[^{18}F]3.41** was a added to a 5 ml V-vial. Subsequently a solution of dehydrating reagent (1 equiv. = 0.02 mmol) in 100 µL of DCE/MeCN and a solution of NEt_3 (1 equiv. = 0.02 mmol) in 100 µL of DCE/MeCN was added *via* syringe to the V-vial containing either **[^{18}F]3.31** or **[^{18}F]3.41**. The sealed vial was stirred for 30 minutes before being quenched by addition of ethanol/water, (3:1, 200 µL). An aliquot was removed for analysis by radioTLC and HPLC for radiochemical conversion and product identification. Analysis was performed using the Gradiant B with a Waters Nova-Pak C18 column (4 µm, 3.9 x 150 mm) at a flow rate 1 mL/min. Table 5.3.3 below details the conditions trialled.

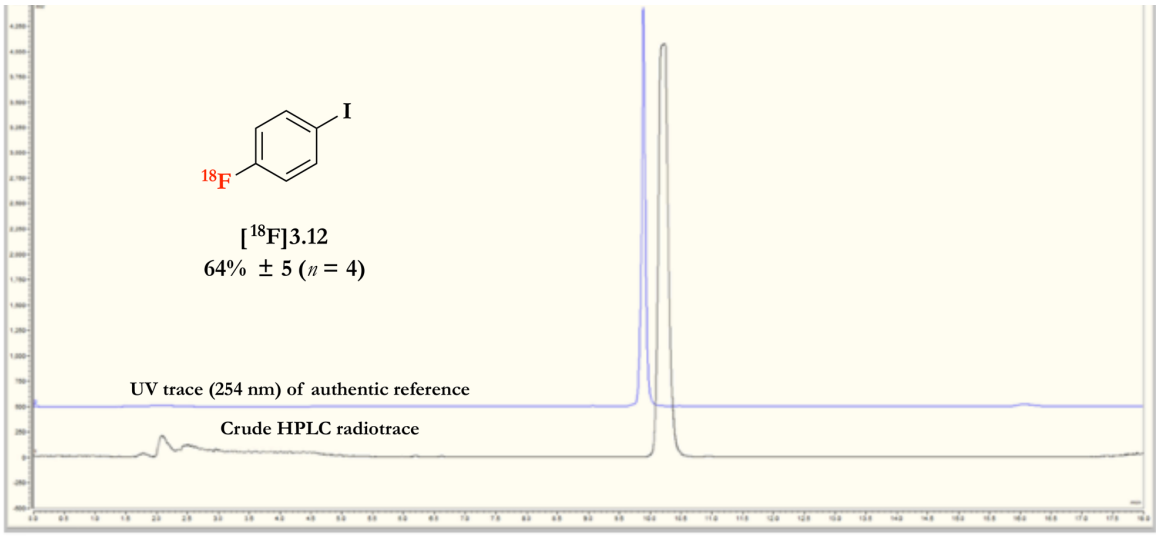
HPLC radiotraces

Radiotrace and RCC of [^{18}F]3.1:



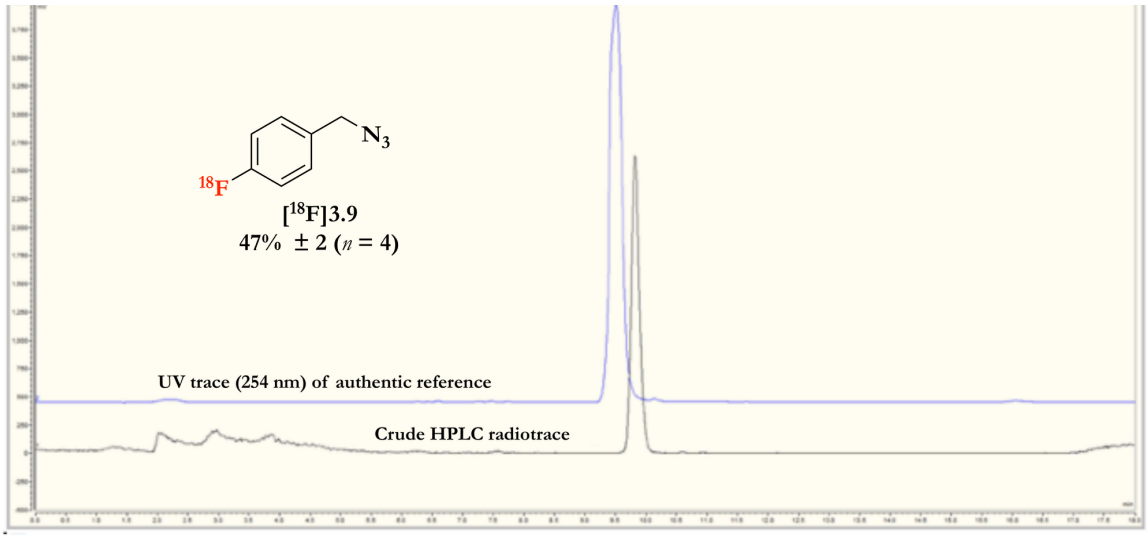
Reaction Number	Radio-TLC (%)	Radiochemical Purity (%)	Radiochemical Conversion (%)
1	91%	80%	73%
2	68%	-	54%
3	81%	88%	71%
4	53%	-	47%
RCC and Standard Error of the Mean			61% ± 6%

Radiotrace and RCC of [^{18}F]3.12:



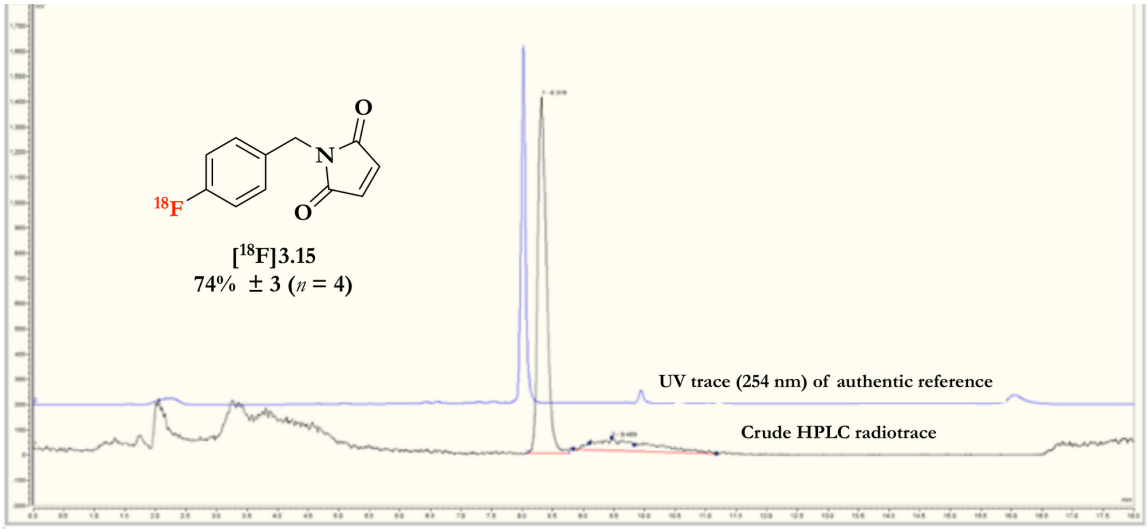
Reaction Number	Radio-TLC (%)	Radiochemical Purity (%)	Radiochemical Conversion (%)
1	80%	>99%	80%
2	59%	-	59%
3	58%	>99%	58%
4	57%	-	57%
RCC and Standard Error of the Mean			64% ± 5%

Radiotrace and RCC of [^{18}F]3.9:



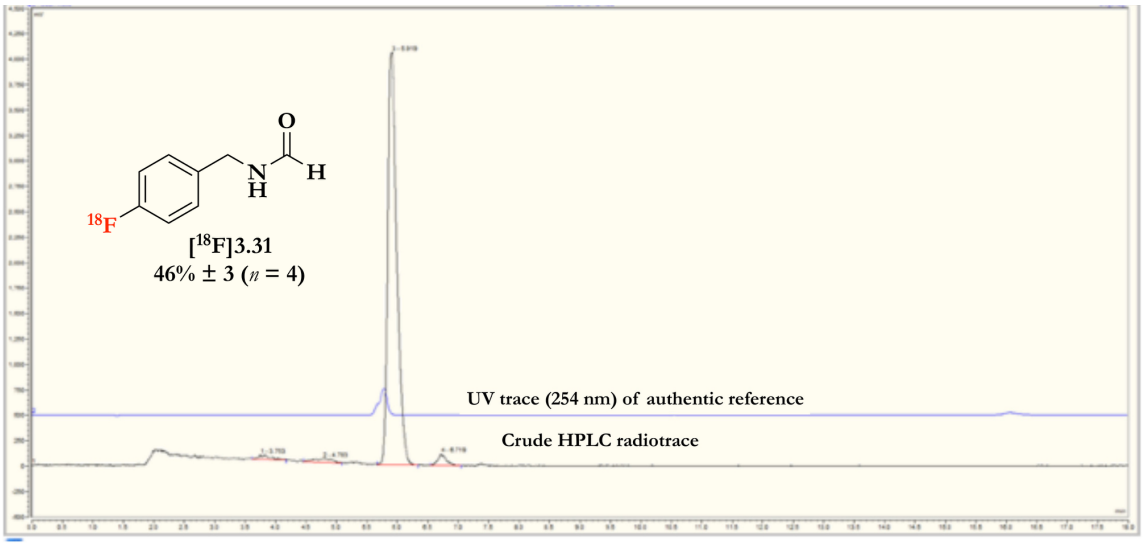
Reaction Number	Radio-TLC (%)	Radiochemical Purity (%)	Radiochemical Conversion (%)
1	54%	98%	53%
2	45%	-	44%
3	51%	95%	48%
4	47%	-	45%
RCC and Standard Error of the Mean			47% ± 2%

Radiotrace and RCC of [^{18}F]3.15:



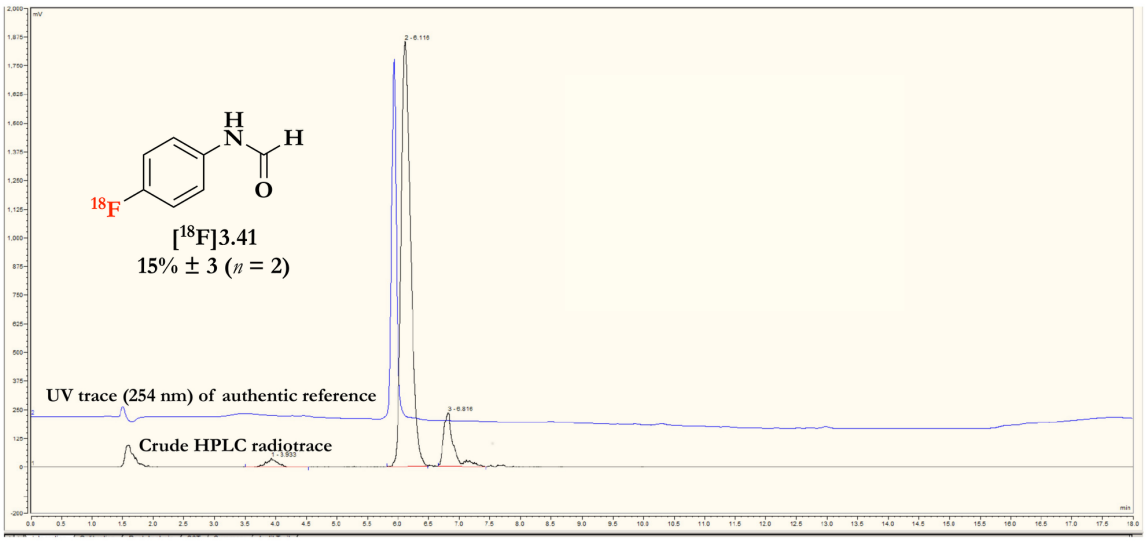
Reaction Number	Radio-TLC (%)	Radiochemical Purity (%)	Radiochemical Conversion (%)
1	80%	95%	76%
2	79%	-	75%
3	67%	95%	64%
4	83%	-	79%
RCC and Standard Error of the Mean			74% ± 3%

Radiotrace and RCC of [^{18}F]3.31:



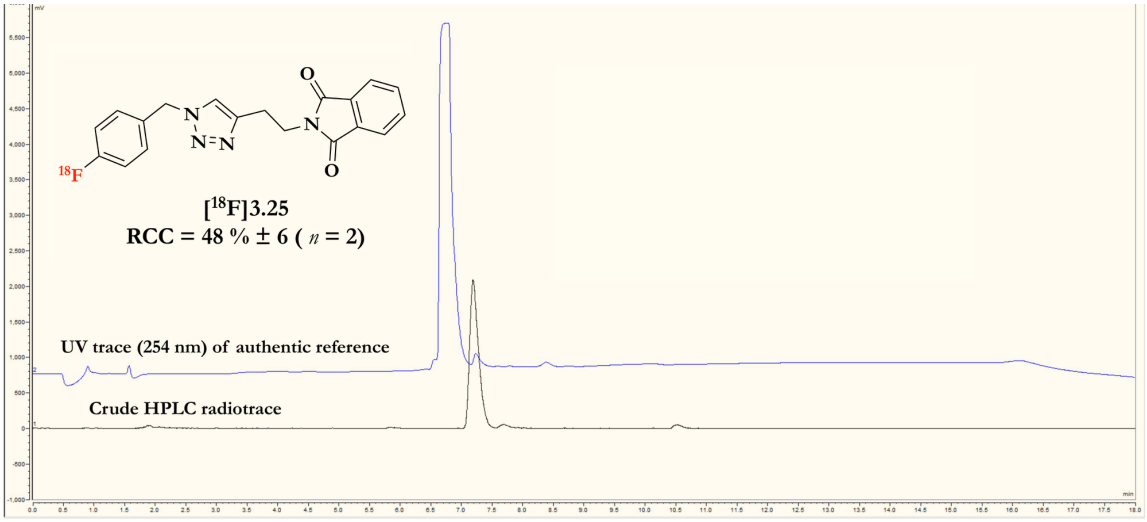
Reaction Number	Radio-TLC (%)	Radiochemical Purity (%)	Radiochemical Conversion (%)
1	51%	92%	47%
2	47%	-	43%
3	41%	95%	39%
4	56%	-	53%
RCC and Standard Error of the Mean			46% ± 3%

Radiotrace and RCC of [^{18}F]3.41:



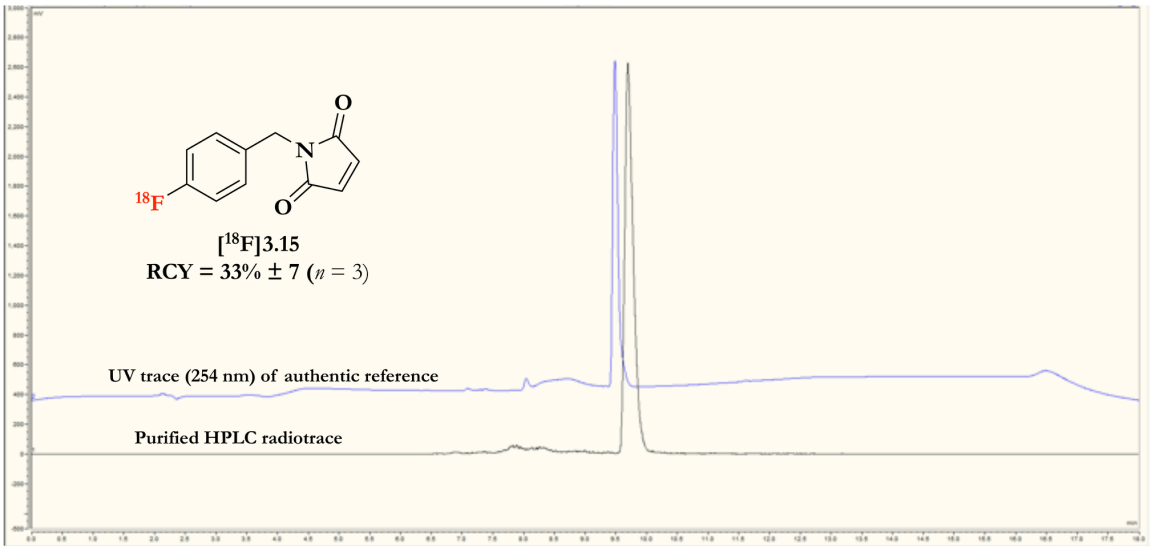
Reaction Number	Radio-TLC (%)	Radiochemical Purity (%)	Radiochemical Conversion (%)
1	21%	86%	18%
2	14%	-	12%
RCC and Standard Error of the Mean			15% ± 3%

Radiotrace and RCC of [^{18}F]3.25:

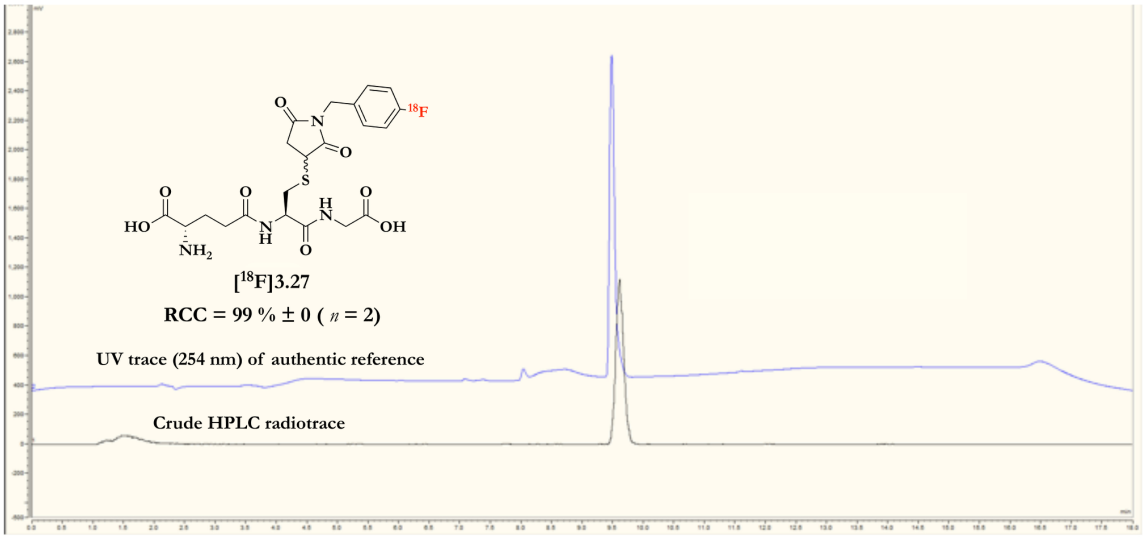


Reaction Number	Radio-TLC (%)	Radiochemical Purity (%)	Radiochemical Conversion (%)
1	63%	86%	54%
2	44%	95%	42%
RCC and Standard Error of the Mean			48% ± 6%

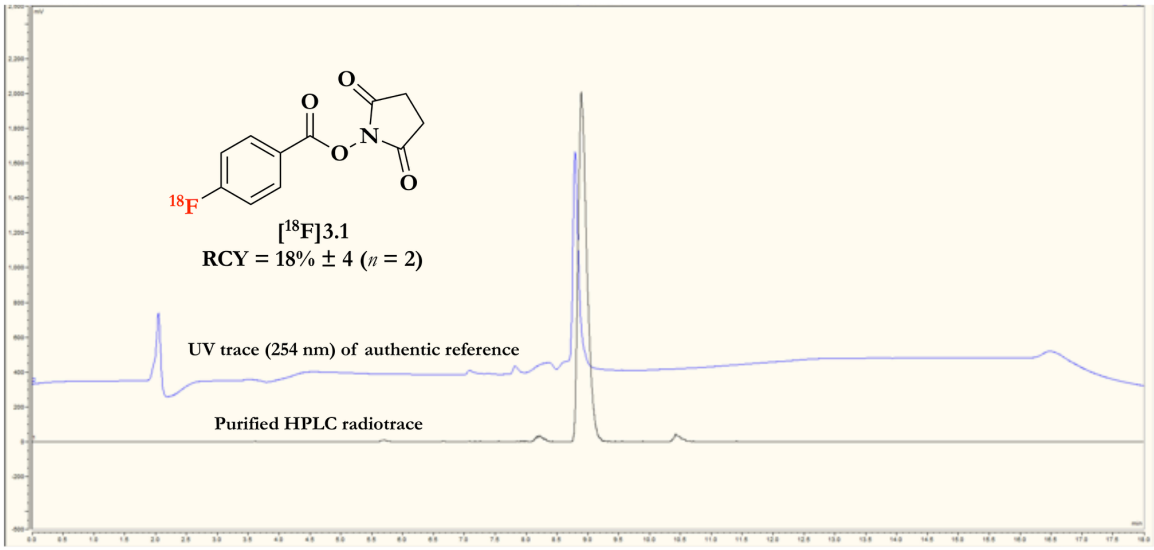
Purified Radiotrace and RCY of [^{18}F]3.15:



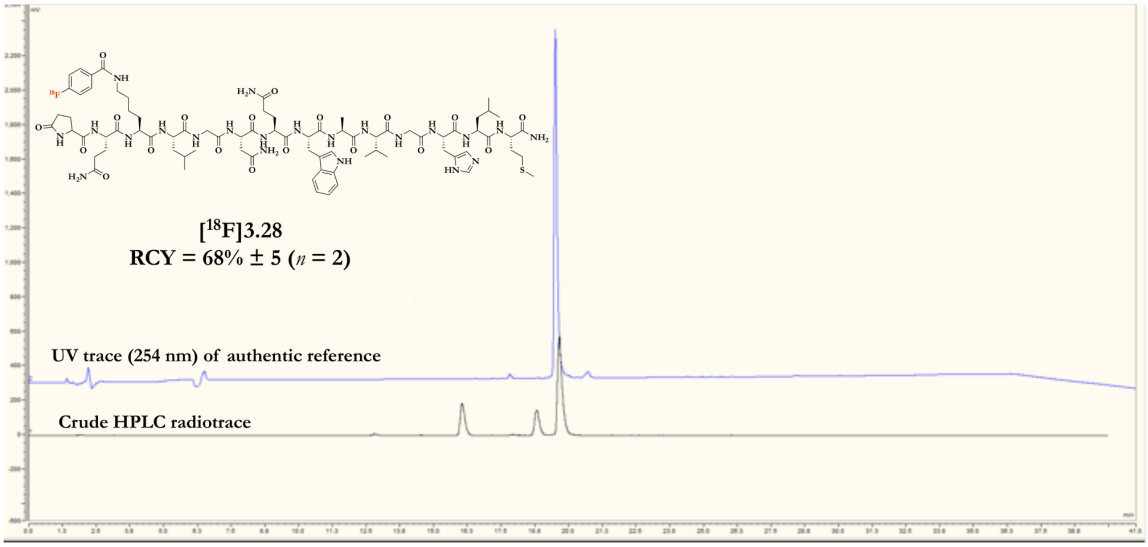
Radiotrace and RCC of [^{18}F]3.27:



Purified Radiotrace and RCY of [^{18}F]3.1:



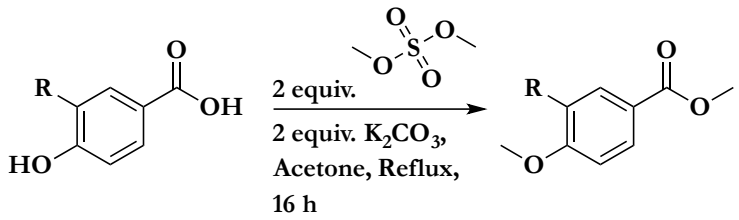
Radiotrace and RCC of [^{18}F]3.28:



5.4 Chapter 4: ^{18}F-DPA 713 a novel second generation radioligand for PET imaging of neuroinflammation

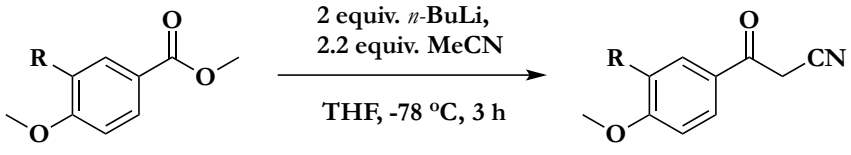
5.4.1 General Procedures

General Procedure 5A:[20]



To a solution of a precursor benzoic acid (6.0 mmol, 1 equiv.) and K_2CO_3 (15 mmol, 2.5 equiv.) in acetone (30 mL) was added dimethyl sulfate (12 mmol, 2.0 equiv.). The reaction mixture was vigorously stirred at reflux overnight, then cooled to room temperature and filtered. The filtered solid was rinsed with acetone. The solution was concentrated until approx. 2 mL of acetone remained. The residue was diluted with saturated $NaHCO_3$ solution and stirred for 5 minutes. The aqueous layer was extracted with EtOAc (3 x 40 mL). The combined organic layers were washed with 1 M aq. HCl, saturated $NaHCO_3$ solution, brine, dried over Na_2SO_4, and concentrated *in vacuo*, yielding the desired compound without the need for further purification.

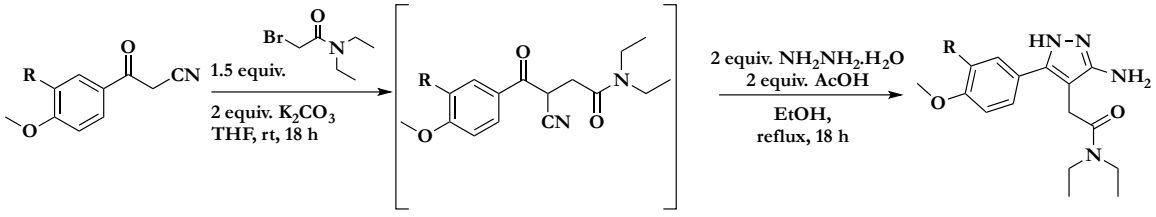
General Procedure 5B:



Under argon at – 78 °C, a solution of MeCN (13.2 mmol, 2.2 equiv.) in THF (10 mL) was added drop-wise over a period of 20 minutes to a solution of *n*-butyllithium (12 mmol, 2 equiv. 2.5 M in *n*-hexane) in 5 mL of THF. The mixture was left to stir at -78 °C for one hour before the chosen benzoate (6 mmol, 1 equiv. in 10 mL THF) was added over a

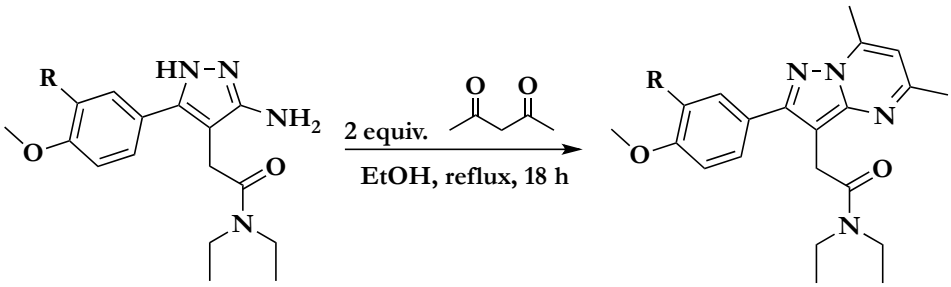
period of 15 minutes. After one hour the reaction was warmed to – 45 °C and the stirring continued until complete consumption of starting material was observed *via* TLC. The reaction was quenched using 2 M aq. HCl (50 mL), diluted with EtOAc (50 mL) and the layers were separated. The organic layer was washed with brine (4 x 40 mL), dried with $MgSO_4$ and concentrated to afford the expected 3-(4-methoxyphenyl)-3-oxopropanenitrile derivative.

General Procedure 5C:



K_2CO_3 (8 mmol, 2 equiv.) was added to a reaction vessel containing the chosen 3-(4-methoxyphenyl)-3-oxopropanenitrile derivative (4 mmol, 1 equiv.) in THF (30 mL). Subsequently, 2-bromodiethylacetamide (6 mmol, 1.5 equiv.) was added drop-wise and the reaction was left to stir overnight. The reaction was quenched using 1 M aq. HCl (50 mL), followed by dilution with EtOAc (60 mL) and the layers were separated. The mixture was washed with brine (4 x 50 mL) dried and concentrated *in vacuo*. The crude sample was flushed through a short plug of silica using EtOAc/cyclohexane (2/8 to 4/6) as the eluent to give an oil. This oil was dissolved in EtOH (30 mL), treated with hydrazine monohydrate (8 mmol, 2 equiv.), glacial acetic acid (8 mmol, 2 equiv.) and was heated to reflux for 18 hours. The solvent was evaporated under reduced pressure and diluted with EtOAc before being washed with saturated Na_2CO_3 (3 x 50 mL). The organic layer was dried with $MgSO_4$ and concentrated i*n vacuo* prior to purification *via* silica gel flash column chromatography using MeOH/DCM (3/7) as the eluent to afford the expected pyrazolo[1,5-*a*]pyrimidin-3-yl]acetamide derivative.

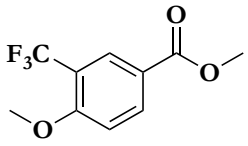
General Procedure 5D:



2,4-Pentanedione (4 mmol, 2 equiv.) was added to a solution of the chosen pyrazolo[1,5-*a*]pyrimidin-3-yl]acetamide derivative (2 mmol, 1 equiv.) in 10 mL of EtOH. The reaction mixture was heated at reflux for 18 hours. Upon cooling to ambient temperature, the solvent was removed in *vacuo*. The crude material was purified *via* silica gel flash column chromatography using MeOH/DCM (1/9) as the eluent to give the expected DPA-713 analogue.

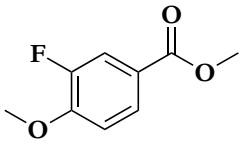
5.4.2 Substrate synthesis

Methyl 4-methoxy-3-(trifluoromethyl)benzoate (4-22):



Synthesized following general procedure 5A, yielding **4-22** (1.4 g, 5.98 mmol, >95%) as a white solid. **MP:** 70-73 °C ^{1}**H-NMR** (400 MHz; $CDCl_3$): δ 8.28 (m, 1H, Ar*H*), 8.21 (ddd, *J* = 8.7, 2.2, 0.4 Hz, 1H, Ar*H*), 7.06 (d, *J* = 8.7 Hz, 1H, Ar*H*), 3.99 (s, 3H, OC*H*$_3$), 3.94 (s, 3H, OC*H*$_3$).^{13}**C-NMR** (101 MHz, $CDCl_3$): δ 165.8, 160.9, 135.1, 129.0 (q, *J* = 5.2 Hz), 123.3 (q, *J* = 262.7 Hz), 121.7, 118.7 (q, *J* = 31.8 Hz), 111.5, 56.2, 52.2. ^{19}**F NMR** ($CDCl_3$, 377 MHz): δ -62.9 (s). **IR** *ν* 2929, 1632, 1508, 1283, 1208, 1069, 807, 774, 630. **HRMS (FI)** calc for $C_{10}H_9F_3O_3$ [M] 234.0504, found 234.0505.

Methyl 3-fluoro-4-methoxybenzoate (4-33):

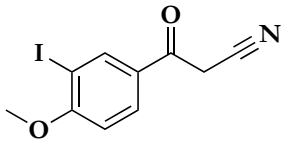


Synthesised following general procedure 5A yielding **4-33** (1.1 g, 5.97 mmol, >95%) as a white powder.

^{1}H-NMR (400 MHz; $CDCl_3$): δ 7.85 (ddd, *J* = 8.5, 2.1, 1.3 Hz, 1H, Ar*H*), 7.77 (dd, *J* = 11.7, 2.1 Hz, 1H, Ar*H*), 7.01 (t, *J* = 8.5 Hz, 1H, Ar*H*), 3.98 (s, 3H, OCH_3), 3.92 (s, 3H, OCH_3). **^{13}C-NMR** (101 MHz, $CDCl_3$): δ 166.0, 151.7 (d, *J* = 10.6 Hz), 151.6 (d, *J* = 246.3 Hz), 126.6 (d, *J* = 3.1 Hz), 122.9 (d, *J* = 6.3 Hz), 117.2 (d, *J* = 19.0 Hz), 112.3 (d, *J* = 1.5 Hz), 56.2, 52.1. **^{19}F NMR ($CDCl_3$, 377 MHz)** δ -134.7 (t, *J* = 10.0 Hz).

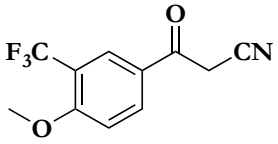
Data was consistent with literature values.[21]

3-(3-Iodo-4-methoxyphenyl)-3-oxopropanenitrile (4-16):



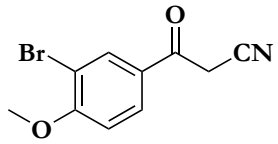
Synthesized following general procedure 5B, yielding **4-16** (1.66 g, 5.52 mmol, 92% yield) as a white powder. **MP** 128-130 °C. **^{1}H NMR** (400 MHz, $CDCl_3$): δ 8.32 (d, *J* = 2.2 Hz, 1H, Ar*H*), 7.92 (dd, *J* = 8.7, 2.2 Hz, 1H, Ar*H*), 6.89 (d, *J* = 8.7 Hz, 1H, Ar*H*), 4.02 (s, 2H, COCH_2), 3.98 (s, 3H, OCH_3). **^{13}C-NMR** (101 MHz, $CDCl_3$): δ 184.5, 163.1, 140.2, 131.0, 128.9, 113.8, 110.5, 86.5, 56.9, 29.2. **IR** *ν*. 2941, 2269, 1707, 1583, 1256, 1203, 935, 818, 662. **HRMS** (ESI) for $C_{10}H_8O_2N^{127}I$ $[M+Na]^+$ requires 323.9492, found 323.9490.

3-(4-Methoxy-3-(trifluoromethyl)phenyl)-3-oxopropanenitrile (4-22):



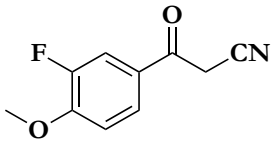
Synthesized following general procedure B, yielding **4-22** (1.45 g, 5.97 mmol, >95%) as a white solid. **M.P**: 95-97 °C **^{1}H-NMR** (400 MHz, $CDCl_3$): δ 8.16-8.13 (m, 2H, Ar*H*), 7.15 (d, *J* = 9.6 Hz, 1H, Ar*H*), 4.10 (s, 2H, COCH_2), 4.04 (s, 3H, OCH_3). **^{13}C-NMR** (101 MHz, $CDCl_3$): δ 184.9, 162.2, 134.4, 128.1 (q, *J* = 5.1 Hz), 126.5, 122.7 (q, *J* = 273.2 Hz), 119.5 (q, *J* = 31.8 Hz), 113.6, 112.2, 56.6, 29.2. **^{19}F-NMR** (377 MHz, $CDCl_3$): δ -63.13. **IR** *ν* 2939, 2254, 1635, 1445, 1285, 1205, 1107, 1005, 848, 721, 639. **HRMS** calc for $C_{11}H_8F_3NO_2$ [M - H] 242.04344, found 242.04344.

3-(3-Bromo-4-methoxyphenyl)-3-oxopropanenitrile (4-29):



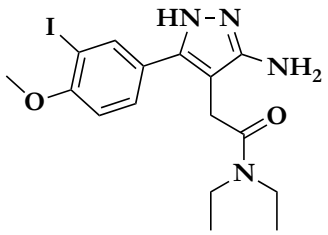
Synthesised following general procedure 5B, yielding **4-29** (1.43 g, 5.63 mmol, 94%) as yellow powder. **MP** 110-112°C. **^{1}H NMR** (400 MHz, $CDCl_3$) δ 8.11 (s, 1H, Ar*H*), 7.88 (d, *J* = 8.7 Hz, 1H, Ar*H*), 6.98 (d, *J* = 8.7 Hz, 1H, Ar*H*), 4.05 (s, 2H, COCH_2), 3.99 (s, 3H, OCH_3). **^{13}C NMR** (400 MHz, $CDCl_3$) δ 184.7, 160.9, 133.9, 129.9, 128.2, 113.8, 112.6, 111.5, 56.8, 29.2. **IR** *ν* 980, 2915, 2255, 1687, 1589, 1285, 1202, 966, 828, 818, 774, 676. **HRMS** (ESI) for $C_{10}H_7O_2N^{79}Br$ $[M-H]^+$ requires 251.9665 found 251.9674.

3-(3-Fluoro-4-methoxyphenyl)-3-oxopropanenitrile (4-33):



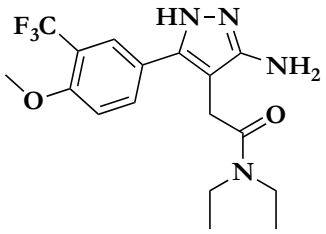
Synthesized following general procedure 5B, yielding **4-33** as a white solid (1.14 g, 5.90 mmol, 98%, 95% purity, processed to the next step without further purifications). **MP** 113-115°C. **^{1}H NMR** (400 MHz, $CDCl_3$) δ 7.69 (ddd, *J* = 8.4, 2.2, 1.0 Hz, 1H, Ar*H*), 7.66 (dd, *J* = 11.4, 2.2 Hz, 1H, Ar*H*), 7.04 (t, *J* = 8.3 Hz, 1H, Ar*H*), 4.03 (s, 2H, COCH_2), 3.98 (s, 3H, OCH_3). **^{13}C NMR** (400 MHz, $CDCl_3$) δ 185.0, 153.5 (d, *J* = 16 Hz), 152.2 (d, *J* = 247 Hz), 127.5 (d, *J* = 5 Hz), 126.3 (d, *J* = 3 Hz), 116.2 (d, *J* = 20 Hz), 113.9, 112.8, 56.6, 29.3. **^{19}F NMR** (376 MHz, $CDCl_3$, {H}) δ -132.6. **IR** *ν* 2946, 2259, 1689, 1465, 1286, 1123, 1007, 866, 842, 762, 723. **HRMS** (ESI) for $C_{10}H_7FNO_2$ $[M-H]^+$ requires 192.0466 found 192.0465.

2-(3-Amino-5-(3-iodo-4-methoxyphenyl)-1*H*-pyrazol-4-yl)-*N*,*N*-diethylacetamide (4-18):



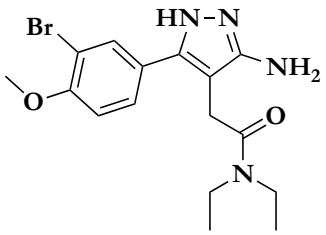
Synthesised following general procedure 5C, yielding **4-18** (941 mg, 2.20 mmol, 55%) as a yellow powder. **MP** 87-89°C. **^{1}H NMR** (400 MHz, $CDCl_3$) δ 7.77 (d, *J* = 2.1 Hz, 1H, Ar*H*), 7.33 (dd, *J* = 8.4, 2.1 Hz, 1H, Ar*H*), 6.80 (d, *J* = 8.5 Hz, 1H, Ar*H*), 5.97 (br. s, 2H, NH_2), 3.89 (s, 3H, OCH_3), 3.46 (s, 2H, CH_2CO), 3.33 (q, *J* = 7.1 Hz, 2H, NCH_2CH$_3$), 3.12 (q, *J* = 7.1 Hz, 2H, NCH_2CH$_3$), 1.09 (t, *J* = 7.1 Hz, 3H, CH$_2$CH_3), 0.98 (t, *J* = 7.1 Hz, 3H, CH$_2$CH_3). (Signal due to pyrazole NH is not observed). **^{13}C-NMR** (101 MHz, $CDCl_3$): δ 170.4, 158.3, 153.9, 141.8, 138.7, 129.3, 125.3, 111.0, 97.8, 86.3, 56.6, 42.6, 40.8, 28.4, 14.4, 13.2. **IR** *ν* 3210, 2968, 1610, 1506, 1432, 1251, 1046, 814. **HRMS** (ESI) for $C_{16}H_{22}O_2N_4{}^{127}I$ $[M+H]^+$ requires 429.0782, found 429.0779.

2-(3-Amino-5-(4-methoxy-3-(trifluoromethyl)phenyl)-1*H*-pyrazol-4-yl)-*N*,*N*-diethylacetamide (4-25):



Synthesised following general procedure 5C yielding **4-25** (880 mg, 2.40 mmol, 60%) as a yellow solid. **M.P:** 79-81 °C. **^{1}H-NMR** (400 MHz, $CDCl_3$): δ 7.57 (d, *J* = 2.2 Hz, 1H, Ar*H*), 7.52 (dd, *J* = 8.5, 2.1 Hz, 1H, Ar*H*), 7.02 (d, *J* = 8.6 Hz, 1H, Ar*H*), 3.92 (s, 3H, OCH_3), 3.46 (s, 2H, CH_2CO), 3.34 (q, *J* = 7.1 Hz, 2H, NCH_2CH$_3$), 3.12 (q, *J* = 7.2 Hz, 2H, NCH_2CH$_3$), 1.09 (t, *J* = 7.1 Hz, 3H, CH$_2$CH_3), 0.98 (t, *J* = 7.2 Hz, 3H, CH$_2$CH_3). (Signal due to pyrazole NH and NH_2 are not observed). **^{13}C-NMR** (126 MHz, $CDCl_3$): δ 170.3, 157.3, 153.2, 142.7, 132.8, 128.4, 126.4 (q, *J* = 5.2 Hz), 123.4 (q, *J* = 272.6 Hz), 118.8 (q, *J* = 31.0 Hz), 112.4, 97.3, 56.0, 42.4, 40.7, 28.3, 14.0, 13.0. **^{19}F-NMR** (377 MHz, $CDCl_3$): δ -62.57. **IR** *ν* 3210, 2978, 2920, 1621, 1501, 1429, 1382, 1245, 1046, 849, 722. **HRMS (ESI)** calc. for $C_{17}H_{21}F_3N_4O_2$ [M - H] 369.15438, found 369.15396.

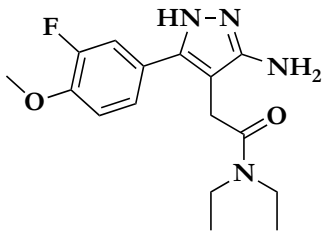
2-(3-Amino-5-(3-bromo-4-methoxyphenyl)-1*H*-pyrazol-4-yl)-*N*,*N*-diethylacetamide (4-31):



Synthesised following general procedure 5C, yielding **4-31** (810 mg, 2.13 mmol, 53%) as a yellow powder. **MP**: 84 – 86 °C. **^{1}H NMR** (400 MHz, $CDCl_3$) δ 7.52 (d, *J* = 2.1 Hz, 1H, Ar*H*), 7.26 (dd, *J* = 8.5, 2.1 Hz, 1H, Ar*H*), 6.82 (d, *J* = 8.5 Hz, 1H, Ar*H*), 3.88 (s, 3H, OCH_3), 3.44 (s,

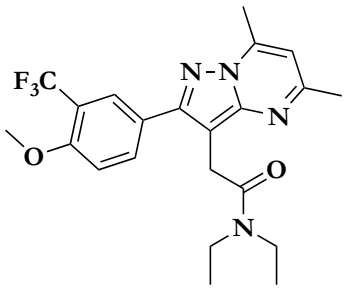
2H, C*H*$_2$CO), 3.31 (q, *J* = 7.1 Hz, 2H, NC*H*$_2$CH$_3$), 3.09 (q, *J* = 7.1 Hz, 2H, NC*H*$_2$CH$_3$), 1.07 (t, *J* = 7.1 Hz, 3H, CH$_2$C*H*$_3$), 0.95 (t, *J* = 7.1 Hz, 3H, CH$_2$C*H*$_3$) (Signal due to pyrazole NH and NH$_2$ are not observed). **^{13}C NMR** (400 MHz, $CDCl_3$) δ 170.3, 155.7, 153.4, 142.3, 132.4, 128.2, 125.1, 111.9, 111.7, 97.2, 56.3, 42.4, 40.6, 28.4, 14.2, 13.2. **IR** *ν* 3542, 2915, 1615, 1595, 1469, 1428, 1229, 1107, 971, 832, 747. **HRMS** (ESI) for $C_{16}H_{21}{}^{79}BrN_4O_2$ $[M-H]^+$ requires 379.0775, found 379.0770.

2-(3-Amino-5-(3-fluoro-4-methoxyphenyl)-1*H*-pyrazol-4-yl)-*N*,*N*-diethylacetamide (4-36):



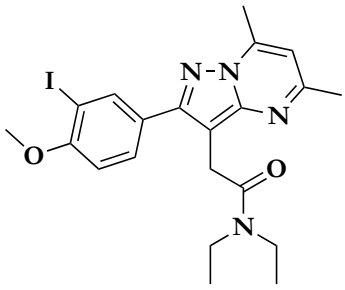
Synthesized following general procedure 5C, yielding 2-[5-amino-3-(3-fluoro-4-methoxyphenyl)-*1H*-pyrazol-4-yl]-*N*,*N*-diethylacetamide (752 mg, 2.35 mmol, 58%) as yellow powder. **MP** 89-90°C. **^{1}H NMR** (400 MHz, CD_3CN) δ 7.24-7.15 (m, 2H, Ar*H*), 7.13-7.08 (m, 1H, Ar*H*), 4.18 (br. s, 2H, N*H*$_2$), 3.87 (s, 3H, OC*H*$_3$), 3.43 (s, 2H, C*H*$_2$CO), 3.29 (q, *J* = 7.1 Hz, 2H, NC*H*$_2$CH$_3$), 3.18 (q, *J* = 7.1 Hz, 2H, NC*H*$_2$CH$_3$), 1.02 (t, *J* = 7.1 Hz, 3H, CH$_2$C*H*$_3$), 0.98 (t, *J* = 7.1 Hz, 3H, CH$_2$C*H*$_3$) (Signal due to pyrazole NH is not observed). **^{13}C-NMR** (126 MHz, CD_3CN): δ 170.2, 153.9, 152.2 (d, *J* = 247.1 Hz), 147.7 (d, *J* = 10.5 Hz), 142.0, 123.8 (d, *J* = 3.2 Hz), 115.5 (d, *J* = 19.2 Hz), 113.7, 97.6, 56.2, 42.3, 40.5, 28.4, 14.1, 13.03. **^{19}F NMR** (376 MHz, CD_3CN, {H}) δ -136.4. **IR** *ν* 3211, 2980, 2934, 1621, 1523, 1380, 1256, 1096, 948, 789. **HRMS** (ESI) for $C_{16}H_{21}FN_4O_2$ $[M-H]^+$ requires 319.1576 found 319.1561.

***N*,*N*-Diethyl-2-(2-(4-methoxy-3-(trifluoromethyl)phenyl)-5,7-dimethylpyrazolo[1,5-*a*]pyrimidin-3-yl)acetamide (4-9):**



Synthesised following general procedure 5D yielding **4-9** (790 mg, 1.82 mmol, 91 %) as a pale yellow solid. **M.P:** 172-175 °C **^{1}H-NMR** (400 MHz, $CDCl_3$): δ 8.09 (dd, *J* = 8.6, 2.1 Hz, 1H, Ar*H*), 8.00 (d, *J* = 2.1 Hz, 1H, Ar*H*), 7.09 (d, *J* = 8.6 Hz, 1H, Ar*H*), 6.53 (s, 1H, Ar*H*), 3.92 (s, 2H, CH_2CO), 3.91 (s, 3H, OCH_3), 3.52 (q, *J* = 7.1 Hz, 2H, NCH_2CH$_3$), 3.40 (q, *J* = 7.1 Hz, 2H, NCH_2CH$_3$), 2.74 (s, 3H, NCCH_3), 2.55 (s, 3H, NCCH_3), 1.22 (t, *J* = 7.1 Hz, 3H, CH$_2$CH_3), 1.10 (t, *J* = 7.1 Hz, 3H, CH$_2$CH_3). **^{13}C-NMR** (126 MHz, $CDCl_3$): δ 169.7, 157.7, 157.5, 153.6, 147.7, 144.7, 133.6, 127.2 (q, *J* = 5.3 Hz), 126.1, 123.6 (q, *J* = 272.4 Hz), 118.7 (q, *J* = 30.9 Hz), 112.1, 108.5, 101.0, 56.0, 42.3, 40.6, 28.0, 24.6, 16.9, 14.3, 13.0. **^{19}F-NMR** (377 MHz, $CDCl_3$): δ -62.33 (s, 3F). **IR** *ν* 2970, 1620, 1588, 1430, 1211, 1186, 1061, 969, 944, 838, 764. **HRMS (ESI)** for $C_{22}H_{25}F_3N_4O_2$ [M - H] requires 433.18568 found 433.18533.

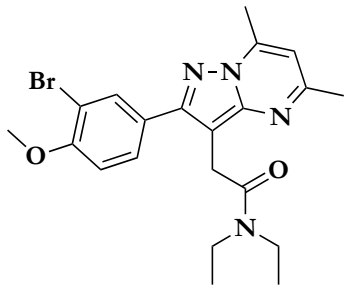
***N*,*N*-Diethyl-2-(2-(3-iodo-4-methoxyphenyl)-5,7-dimethylpyrazolo[1,5-*a*]pyrimidin-3-yl)acetamide (4-7):**



Synthesized following general procedure 5D, yielding **4-7** (827 mg, 1.68 mmol, 84%) as a yellow powder. **MP** 151-152°C. **^{1}H NMR** (400 MHz, $CDCl_3$) δ 8.19 (d, *J* = 2.1 Hz, 1H, Ar*H*),

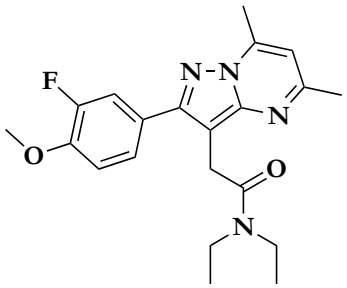
7.87 (dd, *J* = 8.5, 2.1 Hz, 1H, Ar*H*), 6.90 (d, *J* = 8.5 Hz, 1H, Ar*H*), 6.52 (d, *J* = 0.6 Hz, 1H, Ar*H*), 3.93 (s, 2H, CH_2CO), 3.92 (s, 3H, OCH_3), 3.52 (q, *J* = 7.1 Hz, 2H, NCH_2CH$_3$), 3.42 (q, *J* = 7.1 Hz, 2H, NCH_2CH$_3$), 2.74 (d, *J* = 0.6 Hz, 3H, NCCH_3), 2.55 (s, 3H, NCCH_3), 1.24 (t, *J* = 7.1 Hz, 3H, CH$_2$CH_3), 1.13 (t, *J* = 7.1 Hz, 3H, CH$_2$CH_3). **^{13}C NMR** (101 MHz, $CDCl_3$): δ = 169.8, 158.2, 157.7, 153.5, 139.3, 130.1, 128.3, 110.7, 108.4, 101.0, 100.0, 86.1, 56.5, 42.4, 40.7, 28.1, 24.6, 17.0, 14.5, 13.2. **IR** *ν* 3610, 2981, 2886, 1640, 1209, 1182, 1052, 1036, 847, 786, 762. **HRMS** (ESI) for $C_{21}H_{25}O_2N_4{}^{127}I$ [M-H]$^+$ requires 491.0949 found 491.0948.

2-(2-(3-Bromo-4-methoxyphenyl)-5,7-dimethylpyrazolo[1,5-*a*]pyrimidin-3-yl)-*N*,*N*-diethylacetamide (4-27):



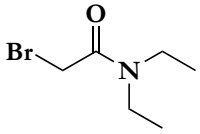
Synthesised following general procedure 5D, yielding **4-27** (792 mg, 1.78 mmol, 89%) as a yellow powder. **MP** 145-146 °C. **^{1}H NMR** (400 MHz, $CDCl_3$) δ 7.99 (d, *J* = 2.1 Hz, 1H, Ar*H*), 7.84 (dd, *J* = 8.5, 2.1 Hz, 1H, Ar*H*), 6.97 (d, *J* = 8.5Hz, 1H, Ar*H*), 6.51 (d, *J* = 0.9 Hz, 1H, Ar*H*), 3.93 (s, 3H, OCH_3), 3.91 (s, 2H, CH_2CO), 3.52 (q, *J* = 7.1 Hz, 2H, NCH_2CH$_3$), 3.41 (q, *J* = 7.1 Hz, 2H, NCH_2CH$_3$), 2.73 (d, *J* = 0.8 Hz, 3H, NCCH_3), 2.53 (s, 3H, NCCH_3), 1.23 (t, *J* = 7.1 Hz, 3H, CH$_2$CH_3), 1.12 (t, *J* = 7.1 Hz, 3H, CH$_2$CH_3). **^{13}C NMR** (400 MHz, $CDCl_3$) δ 169.9, 157.8, 156.0, 153.6, 147.9, 144.9, 133.3, 129.1, 127.9, 111.9, 111.8, 108.5, 101.1, 56.4, 42.5, 40.8, 28.1, 24.8, 17.0, 14.5, 13.2. **IR** *ν* 2980, 1638, 1554, 1225, 1052, 945, 907, 845, 787, 763. **HRMS** (ESI) for $C_{21}H_{24}BrN_4O_2$ [M-H]$^-$ requires 443.1088 found 443.1081.

***N*,*N*-Diethyl-2-(2-(3-fluoro-4-methoxyphenyl)-5,7-dimethylpyrazolo[1,5-*a*]pyrimidin-3-yl)acetamide (4-10):**



Synthesized following general procedure 5D, yielding **4-10** (714 mg, 1.86 mmol, 93%) as a yellow powder. **MP** 100-101°C. **^{1}H NMR** (400 MHz, $CDCl_3$) δ 7.65-7.60 (m, 2H, Ar*H*), 7.03 (t, *J* = 8.4 Hz, 1H, Ar*H*), 6.51 (d, *J* = 0.8 Hz, 1H, Ar*H*), 3.92 (s, 3H, OCH_3), 3.92 (s, 2H, CH_2CO), 3.53 (q, *J* = 7.1 Hz, 2H, NCH_2CH$_3$), 3.41 (q, *J* = 7.1 Hz, 2H, NCH_2CH$_3$), 2.73 (s, 3H, NCCH_3), 2.53 (s, 3H, NCCH_3), 1.23 (t, *J* = 7.1 Hz, 3H, CH$_2$CH_3), 1.11 (t, *J* = 7.1 Hz, 3H, CH$_2$CH_3). **^{13}C-NMR** (101 MHz, $CDCl_3$): δ 169.9, 157.6, 153.7, 152.4 (d, *J* = 245.1 Hz), 147.76 (d, *J* = 14.2 Hz), 147.7, 144.7, 127.0 (d, *J* = 6.6 Hz), 124.6 (d, *J* = 4.3 Hz), 116.3 (d, *J* = 20.1 Hz), 113.2, 108.4, 100.9, 56.3, 42.3, 40.6, 28.0, 24.6, 16.8, 14.3, 13.0. **^{19}F NMR** (376 MHz, $CDCl_3$, {H}) δ -135.4. **IR** *ν* 2971, 1641, 1442, 1271, 1181, 1026, 852, 786, 762, 649. **HRMS** (ESI) for $C_{21}H_{24}FN_4O_2$ $[M-H]^-$ requires 383.1888 found 383.1863.

2-Bromo-*N*,*N*-diethylacetamide:

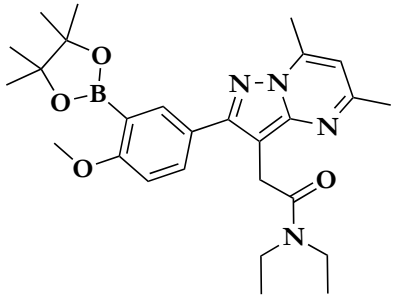


Freshly distilled diethylamine (2 mL, 19.8 mmol) was slowly added to a solution of bromoacetyl bromide (860 µl, 9.90 mmol) in 50 mL DCM at -78 °C. The mixture was allowed to warm to room temperature and left to stir for one hour. 25 mL of H_2O was added and the reaction mixture was extracted with DCM (3 x 40 mL). The combined organic layers were dried with $MgSO_4$ and concentrated, yielding the title compound as a white solid (1.9 g, 9.8 mmol, 98%).

^{1}H NMR (400 MHz; $CDCl_3$): δ = 3.86 (s, 2H, BrC*H*), 3.41 (qd, *J* = 7.2, 2.6 Hz, 4H, *CH*$_2$NC*H*$_2$), 1.27 (t, *J* = 7.2 Hz, 3H, CH_2CH_3), 1.16 (t, *J* = 7.2 Hz, 3H, CH_2CH_3); **^{13}C NMR** ($CDCl_3$, 101 MHz): δ = 165.9, 42.9, 40.5, 26.4, 14.4, 12.5.

Data consistent with literature values.[4]

_N_,_N_-Diethyl-2-(2-(4-methoxy-3-(4,4,5,5-tetramethyl-1,3,2-dioxaborolan-2-yl)phenyl)-5,7-dimethylpyrazolo[1,5-*a*]pyrimidin-3-yl)acetamide (4-8):

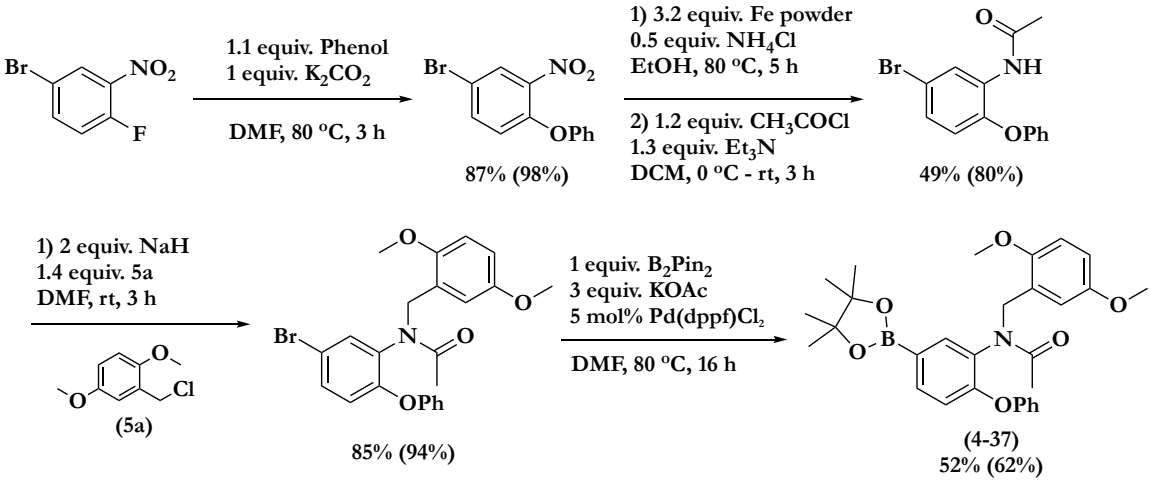


To a 10 mL round bottom flask under argon, charged with 2 mL of toluene was added *N*,*N*-diethyl-2-[2-(3-bromo-4-methoxyphenyl)-5,7-dimethylpyrazolo[1,5-*a*]pyrimidin-3-yl]acetamide **(4-8)** (177 mg, 0.4 mmol), $Pd(dppf)Cl_2.CH_2Cl_2$ (32 mg, 0.04 mmol), potassium acetate (157 mg, 1.6 mmol) and bis(pinacolato)diboron (305 mg, 1.2 mmol). The reaction was left to stir at 85 °C for 18 hours. The reaction was allowed to cool and the solvent removed in *vacuo* before addition of EtOAc (5 mL). The mixture was filtered through a short plug of celite, evaporated and subjected to silica gel flash column chromatography using using acetone/DCM (1/9 to 2/8) as the eluent. Crystallization followed by filtration from petroleum ether and diethylether afforded **2.20** as a white solid (123 mg, 0.25 mmol, 63%).

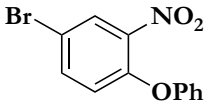
Mp: 120 - 122 °C; **^{1}H NMR** (400 MHz, $CDCl_3$): δ = 8.03 (d, *J* = 2.3 Hz, 1H, Ar*H*), 7.89 (dd, *J* = 8.6, 2.3 Hz, 1H, Ar*H*), 6.94 (d, *J* = 8.6 Hz, 1H, Ar*H*), 6.49 (d, *J* = 0.7 Hz, 1H, Ar*H*), 3.90 (s, 2H, C*H*$_2$CO), 3.87 (s, 3H, OC*H*$_3$), 3.46 (q, *J* = 7.2 Hz, 2H, NC*H*$_2$CH$_3$), 3.39 (q, *J* = 7.1 Hz, 2H, NC*H*$_2$CH$_3$), 2.75 (d, *J* = 0.7 Hz, 3H, NCC*H*$_3$), 2.52 (s, 3H, NCC*H*$_3$), 1.36 (s, 12H,

B(OCCH_3CH_3)$_2$), 1.18 (t, J = 7.2 Hz, 3H, CH_2CH_3), 1.10 (t, J = 7.1 Hz, 3H, CH_2CH_3); **^{13}C NMR** (101 MHz, $CDCl_3$): δ = 170.0, 164.4, 157.3, 155.1, 147.7, 144.7, 136.9, 133.2, 125.8, 110.5, 108.1, 100.9, 83.4, 56.0, 42.3, 40.7, 28.1, 24.9, 24.7, 17.0, 14.4, 13.1 (Signal due to carbon bearing the boron is not observed); **IR** (ν, cm^{-1}): 2974, 1649, 1585, 1398, 1249, 1140, 1067, 1024, 859, 759. **HRMS** (ESI) for $C_{27}H_{38}{}^{11}BN_4O_4$ $[M+H]^+$ requires m/z 493.2978, found 493.2978.

Synthesis of *N*-(2,5-dimethoxybenzyl)-*N*-(2-phenoxy-5-(4,4,5,5-tetramethyl-1,3,2-dioxaborolan-2- yl)phenyl)acetamide (4-37):



5-Bromo-2-phenoxynitrobenzene:



Prepared according to literature procedure.[22]

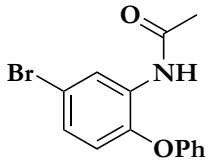
A round bottom flash charged with 5-bromo-2-fluoronitrobenzene (4.40 g, 20.0 mmol), phenol (2.07 g, 22.0 mmol) and potassium carbonate (2.76 g, 20.0 mmol) in anhydrous DMF (40 mL) was stirred at 80°C for 3 hours. The mixture was concentrated *in vacuo* and the residue was partitioned between EtOAc and H_2O. The phases were separated and the organic phase was washed with 1 M aqueous HCl (3 x 50 mL) and brine (3 x 50 mL). The organic phase was dried with $MgSO_4$, filtered and concentrated *in vacuo* to

afford 5-bromo-2-phenoxynitrobenzene (5.12 g, 17.4 mmol, 87%) as a yellow oil, which was used without further purification.

^{1}H NMR (400 MHz, $CDCl_3$): δ = 8.08 (d, *J* = 2.2 Hz, 1H, Ar*H*), 7.61 (dd, *J* = 8.8, 2.2 Hz, 1H, Ar*H*), 7.38-7.45 (m, 2H, Ar*H*), 7.21-7.26 (m, 1H, Ar*H*), 7.04-7.08 (m, 2H, Ar*H*), 6.89 (d, *J* = 8.8 Hz, 1H, Ar*H*); **^{13}C NMR** (101 MHz, $CDCl_3$): δ = 155.1, 150.0, 141.2, 136.8, 130.3, 128.3, 125.0, 121.9, 119.4, 114.8.

Data consistent with literature values.[8,22]

***N*-(5-Bromo-2-phenoxyphenyl)acetamide:**



Prepared according to modified literature procedure.[22]

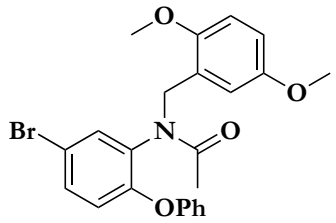
A round bottom flask charged with 5-bromo-2-phenoxynitrobenzene (5.29 g, 18.0 mmol), Fe powder (3.25 g, 58.0 mmol) and NH_4Cl (481 mg, 9.0 mmol) in 20 mL of EtOH/H_2O (3/1) and stirred at 80°C for 5 hours. Upon reaction completion the mixture was filtered. EtOAc and H_2O were added to the filtrate and the phases separated. The organic layer was washed with water (3 x 50 mL), dried with $MgSO_4$ and concentration *in vacuo.* Affording a yellow oil, which was diluted with 30 mL of anhydrous DCM. Acetyl chloride (1.5 mL, 21.6 mmol) was added to the reaction flask drop-wise at 0 °C, succeeding the addition of triethylamine (3.26 mL, 23.4 mmol). The reaction was left to warm to room temperature and left to stir for 3 hours. The mixture was concentrated *in vacuo* and the residue partitioned between EtOAc and H_2O. The phases were separated and the organic phase washed with brine (3 x 50 mL), dried with $MgSO_4$ and concentrated *in vacuo*. Silica gel flash column chromatography using

EtOAc/cyclohexane (1/9 to 2/8) as the eluent afforded *N*-(5-bromo-2-phenoxyphenyl)acetamide (2.69 g, 8.82 mmol, 49%) as a white solid.

^{1}H NMR (400 MHz, $CDCl_3$): δ = 8.61 (d, *J* = 2.2 Hz, 1H, Ar*H*), 7.70 (br. s, 1H, N*H*), 7.29-7.36 (m, 2H, Ar*H*), 7.08-7.14 (m, 1H, Ar*H*), 7.06 (dd, *J* = 8.8, 2.2 Hz, 1H, Ar*H*), 6.99 (d, *J* = 8.0 Hz, 2H, Ar*H*), 6.65 (d, *J* = 8.8 Hz, 1H, Ar*H*), 2.13 (s, 3H, COC*H*$_3$); **^{13}C NMR** (101 MHz, $CDCl_3$): δ = 168.3, 155.8, 144.6, 130.9, 129.7, 126.8, 124.1, 123.5, 119.2, 118.6, 116.4, 25.1

Data consistent with literature values.[8,22]

_N_-(5-Bromo-2-phenoxyphenyl)-_N_-(2,5-dimethoxybenzyl)acetamide



Prepared according to literature procedure.[8,22]

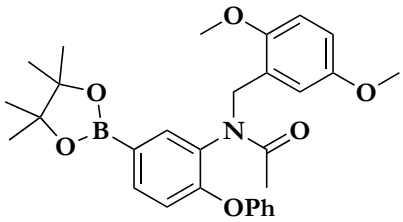
To a solution of *N*-(5-bromo-2-phenoxyphenyl)acetamide (2.45 g, 8.00 mmol) in anhydrous DMF (20 mL) was added NaH (60% in mineral oil, 640 mg, 16 mmol). The mixture was stirred at room temperature for 1 hour before addition of 2,5-dimethoxybenzyl chloride (1.80 g, 11.2 mmol) and the mixture was stirred at room temperature for a further 2 hours. The mixture was poured into water and extracted with EtOAc (3 x 50 mL). The combined organic phases were washed with 1 M aqueous HCl (3 x 40 mL) brine (3 x 50 mL), dried with MgSO4, filtered and concentrated *in vacuo*. Silica gel flash column chromatography using EtOAc/cyclohexane (1/9 to 3/7) afforded *N*-(5-bromo-2-phenoxyphenyl)-*N*-(2,5- dimethoxybenzyl)acetamide (3.10 g, 6.81 mmol, 85%) as a white solid.

^{1}H NMR (400 MHz, $CDCl_3$): δ = 7.34-7.24 (m, 3H, Ar*H*), 7.21 (d, *J* = 2.1 Hz, 1H, Ar*H*), 7.15-7.10 (m, 1H, Ar*H*), 6.95 (d, *J* = 3.0 Hz, 1H, Ar*H*), 6.86-6.82 (m, 2H, Ar*H*), 6.75 – 6.65 (m, 3H,

Ar*H*), 5.04 (d, *J* = 14.5 Hz, 1H, NC*H*H), 4.71 (d, *J* = 14.5 Hz, 1H, NC*H*H), 3.65 (s, 3H, OCH_3), 3.56 (s, 3H OCH_3), 1.97 (s, 3H, COCH_3); **^{13}C NMR** (101 MHz, $CDCl_3$): δ = 170.5, 155.4, 153.5, 153.0, 151.6, 134.4, 133.1, 131.6, 129.9, 126.2, 124.4, 119.3, 119.2, 116.5, 114.3, 113.5, 111.3, 55.7, 55.5, 46.1, 22.2

Data consistent with literature values.[8,22]

_N_-(2,5-Dimethoxybenzyl)-_N_-(2-phenoxy-5-(4,4,5,5-tetramethyl-1,3,2-dioxaborolan-2-yl)phenyl)acetamide (4-37):



Prepared according to modified literature procedure.[23]

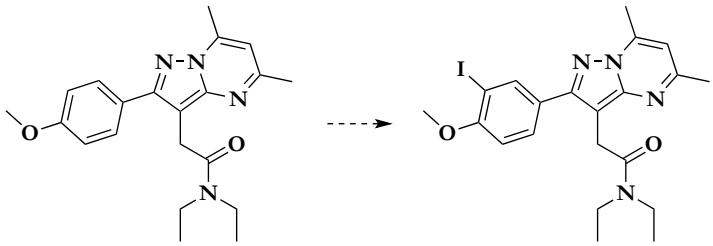
To a 50 mL Schlenk tube under argon was added *N*-(5-bromo-2-phenoxyphenyl)-*N*-(2,5- dimethoxybenzyl)acetamide (456 mg, 1.0 mmol), bis(pinacolato)diboron (254 mg, 1.0 mmol), potassium acetate (295 mg, 3 mmol) and Pd(dppf)Cl_2 (37 mg, 0.05 mmol). Degassed DMF was added *via* syringe and the reaction vessel was sealed and heated at 80 °C for 16 hours. DMF was removed under reduced pressure and the residue was dissolved in EtOAc, passed through a short plug of celite and the filtrate was concentrated *in vacuo*. The elute was further concentrated and subjected to silica gel flash column chromatography using EtOAc/cyclohexane (1/9 to 3/7) yielding **4-37** as a white solid (262 mg, 0.52 mmol, 52 %).

^{1}H NMR (400 MHz, $CDCl_3$): δ 7.60-7.55 (m, 2H, Ar*H*), 7.33 (t, *J* = 8.0 Hz, 2H, Ar*H*), 7.16 (t, *J* = 7.5 Hz, 1H, Ar*H*), 6.98 (d, *J* = 3 Hz, 1H, Ar*H*), 6.86 (d, *J* = 8.0 Hz, 2H, Ar*H*), 6.73 (d, *J* = 8.4 Hz, 1H, Ar*H*), 6.69-6.63 (m, 2H, Ar*H*), 4.97 (d, *J* = 14.6 Hz, 1H, NC*H*H), 4.75 (d, *J* = 14.6 Hz, 1H, NC*H*H), 3.62 (s, 3H, OCH_3), 3.51 (s, 3H, OCH_3), 1.93 (s, 3H, COCH_3), 1.29 (s, 12H, B(OCCH_3CH_3)$_2$); **^{13}C NMR** (101 MHz, $CDCl_3$) δ 171.2, 156.5, 155.5, 153.4, 152.0, 137.1, 135.6,

132.4, 130.0, 126.6, 124.7, 119.7, 116.9, 116.4, 113.5, 111.2, 83.7, 55.7, 55.5, 46.4, 25.3, 25.1, 22.6 (Signal due to carbon bearing the boron is not observed).

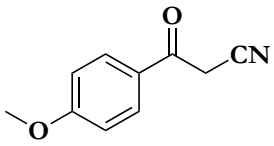
Data consistent with literature values.[8]

5.4.3 Attempted Iodination of DPA-713:



Substrates:

3-(4'-Methoxyphenyl)-3-oxopropanenitrile:

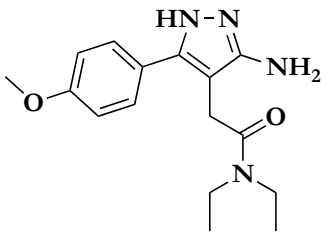


Synthesized following general procedure 5B, yielding **3-(4'-Methoxyphenyl)-3-oxopropanenitrile** as a white powder (1.02 g, 5.81 mmol, >95%).

^{1}H-NMR (400 MHz; $CDCl_3$): δ 7.92 (d, *J* = 9.0 Hz, 2H, Ar*H*), 7.00 (d, *J* = 9.0 Hz, 2H, Ar*H*), 4.05 (s, 2H, COCH_2), 3.92 (s, 3H, OCH_3); **^{13}C NMR ($CDCl_3$, 101 MHz): δ** 185.4, 164.7, 130.9, 127.3, 121.6, 114.3, 114.1, 55.7 29.1

Data consistent with literature values.[24]

2-(3-amino-5-(4-methoxyphenyl)-1H-pyrazol-4-yl)-N,N-diethylacetamide:

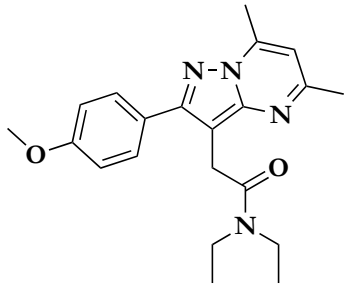


Synthesised following general procedure 5C, yielding **2-(3-amino-5-(4-methoxyphenyl)-1H-pyrazol-4-yl)-N,N-diethylacetamide** as a white powder (728 mg, 2.41 mmol, 60%).

^{1}H-NMR (400 MHz; $CDCl_3$): δ 7.35 (d, *J* = 8.8 Hz, 2H, Ar*H*), 6.97 (d, *J* = 8.8 Hz, 2H, Ar*H*), 3.86 (s, 3H, OCH_3), 3.51 (s, 2H, CH_2CO), 3.33 (q, *J* = 7.1 Hz, 2H, NCH_2CH$_3$), 3.06 (q, *J* = 7.1 Hz, 2H, NCH_2CH$_3$), 1.09 (t, *J* = 7.1 Hz, 3H, CH$_2$CH_3), 0.93 (t, *J* = 7.1 Hz, 3H, CH$_2$CH_3); (Signal due to pyrazole NH and NH_2 are not observed). **^{13}C NMR ($CDCl_3$, 101 MHz):** δ 170.3, 159.9, 154.2, 142.6, 129.2, 122.8, 114.4, 97.3, 55.4, 42.4, 40.5, 28.5, 14.1, 13.0.

Data consistent with literature values.[25]

***N*,*N*-diethyl-2-(2-(4-methoxyphenyl)-5,7-dimethylpyrazolo[1,5-*a*]pyrimidin-3-yl)acetamide (DPA-713):**

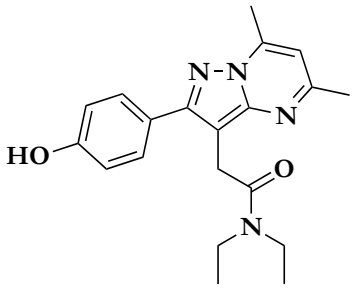


Synthesized following general procedure 5D, yielding **DPA-713** as a white powder (660 mg, 1.8 mmol, 90%).

^{1}H-NMR (400 MHz; $CDCl_3$): δ 7.79 (d, *J* = 8.9 Hz, 2H, Ar*H*), 7.00 (d, *J* = 8.9 Hz, 2H, Ar*H*), 6.52 (s, 1H, Ar*H*), 3.95 (s, 2H, CH_2CO), 3.86 (s, 3H, OCH_3), 3.51 (q, *J* = 7.1 Hz, 2H, NCH_2CH$_3$), 3.43 (q, *J* = 7.1 Hz, 2H, NCH_2CH$_3$), 2.75 (s, 3H, NCCH_3), 2.56 (s, 3H, NCCH_3), 1.24-1.20 (t, *J* = 7.1 Hz, 3H, CH$_2$CH_3), 1.13 (t, *J* = 7.1 Hz, 3H, CH$_2$CH_3). **^{13}C NMR ($CDCl_3$, 101 MHz):** δ 170.1, 159.8, 157.4, 155.1, 147.4, 144.9, 130.0, 126.3, 113.9, 108.1, 100.8, 55.3, 42.3, 40.6, 28.2, 24.5, 16.9, 14.3, 13.1.

Data consistent with literature values.[25]

***N*,*N*-Diethyl-2-(2-(4-hydroxyphenyl)-5,7-dimethylpyrazolo[1,5-*a*]pyrimidin-3-yl)acetamide:**



Prepared according to literature procedure.[26]

A cooled (0 °C) solution of **DPA-713** (395 mg, 1.0 mmol) in DCM (4 mL) was treated portionwise with aluminum chloride (446 mg, 3.3 mmol, 3.3 equiv.). The solution was allowed to warm to room temperature and after several minutes, a heterogeneous mixture formed and was stirred vigorously for 16 hours. The reaction mixture was cooled to 0 °C and treated with saturated aqueous NH_4Cl (40 mL) and subsequently stirred for 2.5 hours at room temperature. The mixture was filtered and the precipitate washed with H_2O (40 mL) and extracted with DCM (3 x 40 mL). The organic layer was further washed with H_2O (3 x 30 mL), brine (4 x 40 mL), dried with $MgSO_4$ and the solvent concentrated *in vacuo*. The crude material was subjected to silica gel flash column chromatography using MeOH/DCM (1/9) yielding *N*,*N*-diethyl-2-(2-(4-hydroxyphenyl)-5,7-dimethylpyrazolo[1,5-*a*]pyrimidin-3-yl)acetamide as a yellow solid (260 mg, 0.74 mmol, 74 %).

^{1}H-NMR (400 MHz; $CDCl_3$): δ 7.66 (d, *J* = 8.5 Hz, 2H, Ar*H*), 7.15 (br. s, 1H, O*H*), 6.89 (d, *J* = 8.5 Hz, 2H, Ar*H*), 6.51 (s, 1H, Ar*H*), 3.95 (s, 2H, CH_2CO), 3.51 (q, *J* = 7.1 Hz, 2H, NCH_2CH$_3$), 3.42 (q, *J* = 7.1 Hz, 2H, NCH_2CH$_3$), 2.74 (s, 3H, NCCH_3), 2.55 (s, 3H, NCCH_3), 1.21 (t, *J* = 7.1 Hz, 3H, CH$_2$CH_3), 1.13 (t, *J* = 7.1 Hz, 3H, CH$_2$CH_3). **^{13}C NMR ($CDCl_3$, 101 MHz):** δ 170.1, 158.8, 157.4, 155.1, 147.7, 145.0, 130.1, 125.8, 114.4, 108.4, 100.8, 42.1, 40.6, 28.4, 24.6, 17.0, 14.3, 13.1.

Data consistent with literature values.[26]

Reactions Attempted:

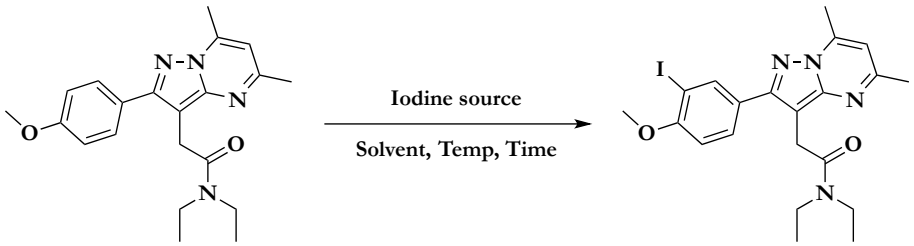


Table 5.4.1 : Attempted iodination of DPA-713

Entry	Iodine Source	Additive	Solvent	Temp [°C]	Time [hr][e]	Yield [%][f]
1	I_2[a]	-	AcOH	rt	16	0
2	I_2[a]	-	AcOH	60	16	0
3	I_2[a]	PIFA[a]	DCM	rt	16	10
4	I_2[b]	PIFA[b]	DCM	rt	16	14
5	I_2[b]	PIFA[b]	MeCN	rt	16	21
6	I_2[b]	PIFA[b]	MeCN	reflux	16	28
7	I_2[b]	PIFA[b]	THF	reflux	16	25
8	NIS[c]	TFA[d]	MeCN	rt	16	15
9	NIS[c]	TFA[c]	MeCN	reflux	16	20
10	NIS[c]	TFA[c]	THF	reflux	16	17
11	NaI[a]	Oxone[a]	MeOH	60	16	28
12	NaI[b]	Oxone[b]	MeOH	60	16	34
13	NaI[a]	Oxone[b]	MeOH	60	16	30

[a]1 equiv. [b]2 equiv. [c]1.5 equiv. [d]0.3 equiv.[e]Reactions monitored *via* TLC and LC/MS every 3 hours.
[f]Determined by ^{1}H NMR, integration relative to an internal standard.

Table 5.4.1 discloses our efforts toward the direct iodination of DPA-713. Unfortunately low product conversion was observed *via* crude ^{1}H NMR and LC/MS under all conditions trialled. Owing to this, an aluminium chloride deprotection of DPA-713 ensued and direct iodination was attempted on the resulting phenolic product. It was hypothesised that the enhanced nucleophilicity of the phenol ring may enable a more facile iodination.[27]

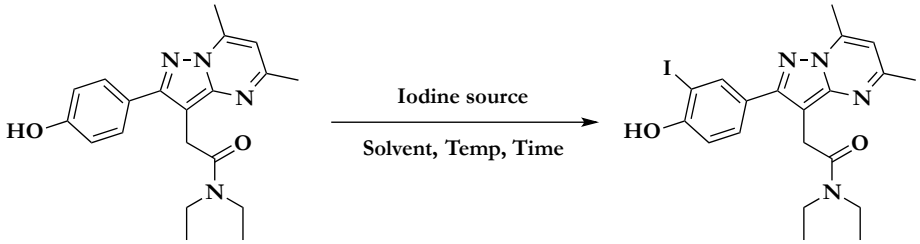


Table 5.4.2: Attempted iodination of *N*,*N*-diethyl-2-(2-(4-hydroxyphenyl)-5,7-dimethylpyrazolo[1,5-*a*]pyrimidin-3-yl)acetamide

Entry	Iodine Source	Additive	Solvent	Temp [°C]	Time [hr][e]	Yield [%][f]
1	I_2[a]	PIFA[a]	MeCN	rt	16	23
2	I_2[a]	PIFA[a]	MeCN	reflux	16	36
3	I_2[a]	PIFA[a]	THF	reflux	16	30
4	NIS[b]	TFA[c]	MeCN	rt	16	28
5	NIS[b]	TFA[b]	MeCN	reflux	16	34
6	NIS[b]	TFA[b]	THF	reflux	16	30
7	NaI[d]	Oxone[d]	MeOH	60	16	38
8	NaI[a]	Oxone[a]	MeOH	60	16	45
9	NaI[d]	Chloramine-T[b]	MeCN	reflux	16	34

[a]2 equiv. [b]1.5 equiv. [c]0.3 equiv. [d]1 equiv.[e]Reactions monitored *via* TLC and LC/MS every 3 hours. [f]Determined by ^{1}H NMR, integration relative to an internal standard.

Unfortunatly low conversions were also observed *via* crude ^{1}H NMR and LC/MS, therefore this direct iodination strategy was abandoned owing to the impracticality of separating the starting material from iodinated product *via* silica gel flash column chromatography i.e. retention factors were identical. HPLC purification may have been utilised, however it was deemed to be too time consuming to facilitate the successful purification of the desired quantities of product required for radiosynthesis.

5.4.4 Radiochemistry

General Information and Procedures

[^{18}F]Fluoride Preparation:

[^{18}F]Fluoride was produced by Alliance Medical (UK) *via* the ^{18}O(*p*,*n*)^{18}F reaction and delivered as [^{18}F]fluoride in ^{18}O-enriched-water. Radiosynthesis and azeotropic drying was performed on a NanoTek microfluidic device (Advion).

Analysis:

For all reactions, an aliquot was removed for analysis by radioTLC and radioHPLC.

RadioTLC was carried out on Merck Kiesegel 60 F254 plates in EtOAc/Hexane (1/1) and analysed using a plastic scintillator/PMT detector.

HPLC analysis was performed using a Dionex Ultimate 3000 dual channel HPLC system with a shared autosampler, parallel UV-detectors and LabLogic NaI/PMT-radiodetectors with Flowram analogue output.

HPLC Gradient A: Water/MeCN, 1 mL/min, Waters Nova-Pak C18 Column, 4 μm, 3.9 x 150 mm:

0 – 1 min (5 % MeCN) isocratic

1 – 10 min (5 % MeCN to 95 % MeCN) linear increase

10 – 14 min (95 % MeCN) isocratic

14 – 15 min (95 % MeCN to 5 % MeCN) linear decrease

15 – 17 min (5 % MeCN) isocratic.

Reported radiochemical conversions are decay corrected and calculated by radioTLC taking into account the radiochemical purity as determined by radioHPLC

General Procedure for Azeotropic Drying

Radiosynthesis and azeotropic drying was performed on a NanoTek® microfluidic device (Advion). [^{18}F]Fluoride (3.0 - 4.0 GBq) was separated from ^{18}O-enriched-water using a Chromafix cartridge and subsequently released with 900 µL (in 6 x 150 µL portions) of a solution of $K_{2.2.2}/K_2CO_3$ (Kryptofix 222 (15mg) and K_2CO_3 (3mg) in 1 mL of MeCN/H2O, 4:1) into a 5 mL v-vial containing a magnetic stir bar. The solution was dried with five cycles of azeotropic drying with MeCN (200 µL) under a flow of N_2 at 105°C. The dried [^{18}F]KF/$K_{2.2.2}$ residue was re-dissolved in anhydrous MeCN (500 - 1000 µL) and aliquots used for ^{18}F-fluorination reactions.

Procedure for radiosynthesis of [^{18}F]4-9:

The dried [^{18}F]KF/K_{222} residue was re-dissolved in anhydrous MeCN (500–1000 µL). Small aliquots of this solution of [^{18}F]KF/K_{222} in MeCN (20-30 MBq, 10-40 µL) were dispensed into a V-vial containing CuI (11 mg, 0.06 mmol) and a magnetic stirrer bar. The solvent was evaporated under a flow of N_2 at 100 °C (2 minutes). The vial was removed from heating and a solution of methyl chlorofluoroacetate (6 µL, 0.06 mmol), TMEDA (9 µL, 0.06 mmol), and aryl iodide (0.037 mmol) in DMF (300 µL) was added *via* syringe. The sealed vial was heated at 150 °C for 20 minutes. The reaction was quenched by addition of water (100 µL). An aliquot was removed for analysis by radioTLC and HPLC for radiochemical conversion and product identity. Analysis was performed using Gradient A given above with a Waters Nova-Pak C18 column (4 µm, 3.9 x 150 mm) at a flow rate 1 mL/min.

Procedure for radiosynthesis of [^{18}F]4-10:

The dried [^{18}F]KF/K_{222} residue was re-dissolved in anhydrous MeCN (500–1000 μL). Small aliquots of this solution of [^{18}F]KF/K_{222} in MeCN (20-30 MBq, 10-40 μL) were dispensed into a V-vial containing $Cu(OTf)_2(py)_4$ (27 mg, 0.04 mmol) aryl pinacol boronate **(4-8)** (15 mg, 0.03 mmol) and a magnetic stirrer bar. Air was flushed through the reaction vial using a syringe and then DMF (300 μL) was added *via* syringe. The sealed vial was heated at 110 °C for 20 minutes. The reaction was quenched by addition of water (200 μL). An aliquot was removed for analysis by radioTLC and HPLC for radiochemical conversion and product identity. Analysis was performed using the Gradiant A given above with a Waters Nova-Pak C18 column (4 μm, 3.9 x 150 mm) at a flow rate 1 mL/min.

Procedure for radiosynthesis of [^{18}F]4-4:

The dried [^{18}F]KF/K_{222} residue was re-dissolved in anhydrous MeCN (500–1000 μL). Small aliquots of this solution of [^{18}F]KF/K_{222} in MeCN (20-30 MBq, 10-40 μL) were dispensed into a V-vial containing $Cu(OTf)_2(py)_4$ (14 mg, 0.02 mmol) aryl pinacol boronate **(4-37)** (10 mg, 0.02 mmol) and a magnetic stirrer bar. Air was flushed through the reaction vial using a syringe and then DMF (300 μL) was added *via* syringe. The sealed vial was heated at 110 °C for 20 minutes. The reaction was quenched by addition of water (200 μL). An aliquot was removed for analysis by radioTLC and HPLC for radiochemical conversion and product identity. Analysis was performed using the Gradiant A given above with a Waters Nova-Pak C18 column (4 μm, 3.9 x 150 mm) at a flow rate 1 mL/min.

Isolation Procedures

Procedure for isolation of [^{18}F]4-9:

[^{18}F]Fluoride (3.0 - 4.0 GBq) was separated from ^{18}O-enriched-water using a Chromafix PS-HCO_3 ^{18}F separation cartridge (45 mg) and subsequently released with 900 µL (in 6 x 150 µL portions) of a solution of of a solution of K_{222}/K_2CO_3 (Kryptofix 222 (15 mg) and K_2CO_3 (3 mg) in 1 mL of MeCN/H_2O, 4:1) into a 5 mL V-vial containing a magnetic stir bar in the concentrator. The solution was dried with five cycles of azeotropic drying with MeCN (5 x 200 µL) under a flow of N2 at 105 °C. A solution of CuI (11 mg, 0.06 mmol), methyl chlorofluoroacetate (6 µL, 0.06 mmol), TMEDA (9 µL, 0.06 mmol), and aryl iodide (0.037 mmol) in DMF (300 µL) was added *via* syringe to the 5 mL vial containing the dried [^{18}F]KF/$K_{2.2.2}$ complex. The sealed vial was heated at 150 °C for 20 minutes, after which, the reaction mixture was diluted with 1 mL of 50% MeCN/ 50% 25 mM NH_4HCOO (aq.) and loaded directly onto a 2 mL HPLC loop and injected on a semi-Prep HPLC column (Synergi 4µm Hydro-RP 250x10mm) and eluted with 50% MeCN/50% 25 mM NH_4HCOO (isocratic 4 mL/min) monitoring with UV (254 nm) and radioactive traces.

Product identity of **[^{18}F]4-9** in the collected fraction was assessed using an analytical Synergi 4µm Hydro-RP 80A, 150 x 4.6 mm with 50% MeCN/50% 25 mM NH_4HCOO (aq.) (isocratic 1 mL/min) monitoring with UV (254 nm) and radioactive traces.

Procedure for isolation of [^{18}F]4-10:

[^{18}F]Fluoride (3.0 - 4.0 GBq) was separated from ^{18}O-enriched-water using a Waters Sep-Pak Accell Plus QMA Carbonate Plus Light Cartridge, (46 mg, Sorbent per Cartridge, 40 µm Particle Size, 50/pk (Part #186004540 from Waters) and subsequently released with 900 µL (in 6 x 150 µL portions) of a solution of $K_{222}/K_2C_2O_4/K_2CO_3$ (kryptofix 222 (6.3 mg), $K_2C_2O_4$ (1 mg) and K_2CO_3 (0.1 mg) in 1 mL of MeCN/H_2O, 4:1) into

a 5 mL V-vial containing a magnetic stir bar in the concentrator. The solution was dried with five cycles of azeotropic drying with MeCN (200 µl) under a flow of N_2 at 105 °C. The 5 mL vial containing the dried [^{18}F]KF/$K_{2.2.2}$ complex was purged with 30 mL of air using a syringe and then a solution of arylboronate precursor **4-8** (15 mg, 0.03 mmol) and $Cu(OTf)_2(py)_4$ (14 mg, 0.02 mmol) in anhydrous DMA (400 µL) was added. The mixture was heated at 120 °C for 20 minutes in a sealed vial with stirring, after which, the reaction mixture was diluted with 1 mL of 50% MeCN/ 50% 25 mM NH_4HCOO (aq.) and loaded directly onto a 2 mL HPLC loop and injected on a semi-Prep HPLC column (Synergi 4µm Hydro-RP 250x10mm) and eluted with 50% MeCN/50% 25 mM NH_4HCOO (isocratic 4 mL/min) monitoring with UV (254 nm) and radioactive traces.
SA of [^{18}**F]4-10** in the collected fraction was assessed using an analytical Synergi 4µm Hydro-RP 80A, 150 x 4.6 mm with 50% MeCN/50% 25 mM NH_4HCOO (isocratic 1 mL/min) monitoring with UV (254 nm) and radioactive traces.

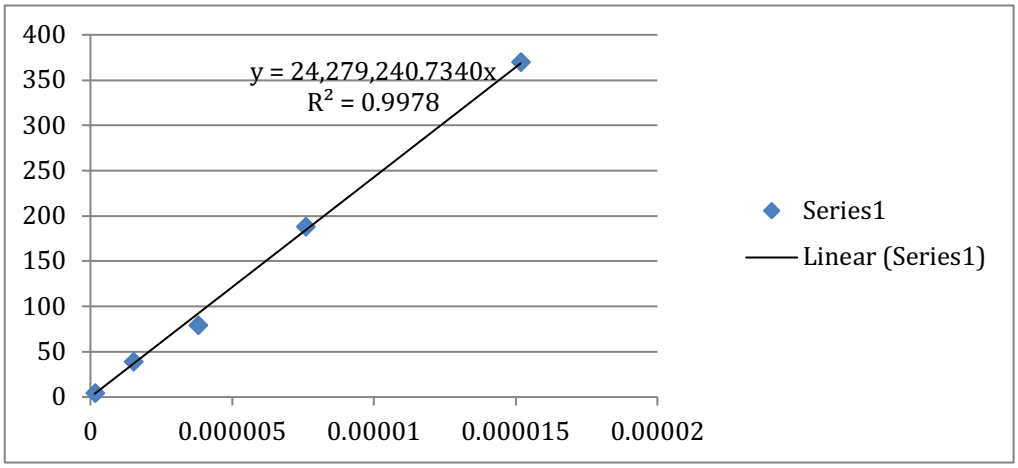
Procedure for isolation of [^{18}F]4-4:
Radiosynthesis and azeotropic drying was performed on a NanoTek® microfluidic device (Advion). [^{18}F]Fluoride (3.0 - 4.0 GBq) was separated from ^{18}O-enriched-water using a Chromafix cartridge and subsequently released with 900 µL (in 6 x 150 µL portions) of a solution of $K_{2.2.2}/K_2CO_3$ (Kryptofix 222 (15mg) and K_2CO_3 (3mg) in 1 mL of MeCN/H_2O, 4:1) into a 5 mL v-vial containing a magnetic stir bar. The solution was dried with five cycles of azeotropic drying with MeCN (200 µL) under a flow of N_2 at 105°C. The dried [^{18}F]KF/$K_{2.2.2}$ residue was re-dissolved in anhydrous MeCN (500 - 1000 µL) and aliquots used for ^{18}F-fluorination reactions. The dried [^{18}F]KF/K_{222} residue was re-dissolved in anhydrous MeCN (500–1000 µL). Small aliquots of this solution of [^{18}F]KF/K_{222} in MeCN (20-30 MBq, 10-40 µL) were dispensed into a V-vial containing $Cu(OTf)_2(py)_4$ (14 mg, 0.02 mmol) aryl pinacol boronate **(4-37)** (10 mg, 0.02 mmol) and a magnetic stirrer bar. Air was flushed through the reaction vial using a syringe and then

DMF (300 µL) was added *via* syringe. The sealed vial was heated at 110 °C for 20 minutes. Subsequently the reaction mixture was diluted with 200 µL of 40% MeCN/ 60% 25 mM NH_4HCOO (aq.) and an aliquot (40 µL) was loaded onto a Dionex Ultimate 3000 dual channel HPLC system *via* autosampler, eluting with 60% MeCN/ 40% 25 mM NH_4HCOO (aq.) (isocratic 4 mL/min) monitoring with UV (254 nm) and radioactive traces.

Product identity of **[^{18}F]4-4** in the collected fraction was assessed using a Dionex Ultimate 3000 dual channel HPLC system with a shared autosampler, parallel UV-detectors and LabLogic NaI/PMT- radiodetectors with Flowram analogue output.

Determination of Specific Activity for [^{18}F]4-10:

Calibration curve



Calculation of Specific Activity for [^{18}F]4-10:

SA of ^{18}F-DPA 713 in collected fraction was assessed using an analytical Synergi 4µm Hydro-RP 80A, 150 x 4.6 mm with 50% MeCN/50% 25 mM NH_4HCOO (isocratic 1 mL/min) monitoring with UV (254 nm) and radioactive traces.

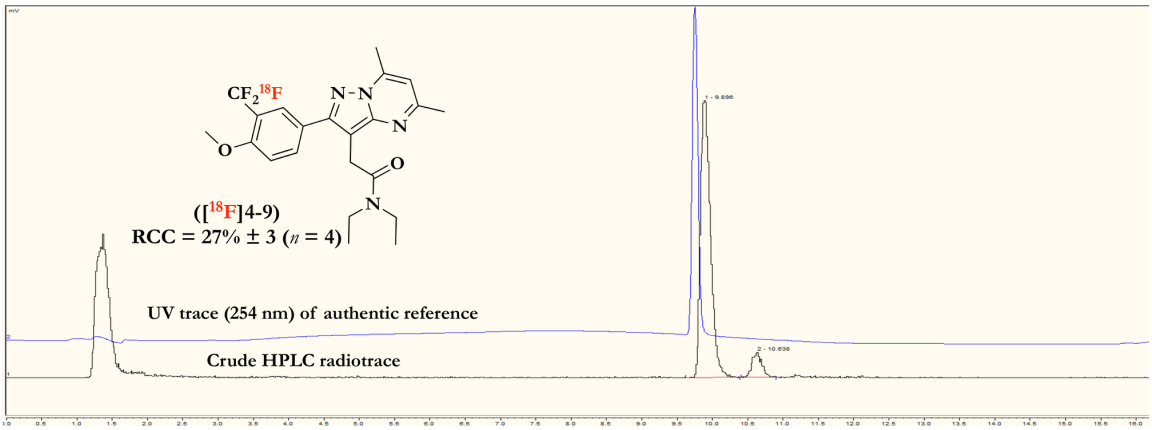
SA (GBq/umol)	*Activity (MBq)*	*mmol*	*Area (mAU*min)*
8.42	3.9	4.63338E-07	11.2495
11.01	1.86	1.68967E-07	4.1024
7.10	1.2	1.68967E-07	4.1024
12.36	4.5	3.64052E-07	8.8389
62.78	0.8	1.27434E-08	0.3094

SA = 20.3 ± 10.6 GBq/µmol.

HPLC Traces

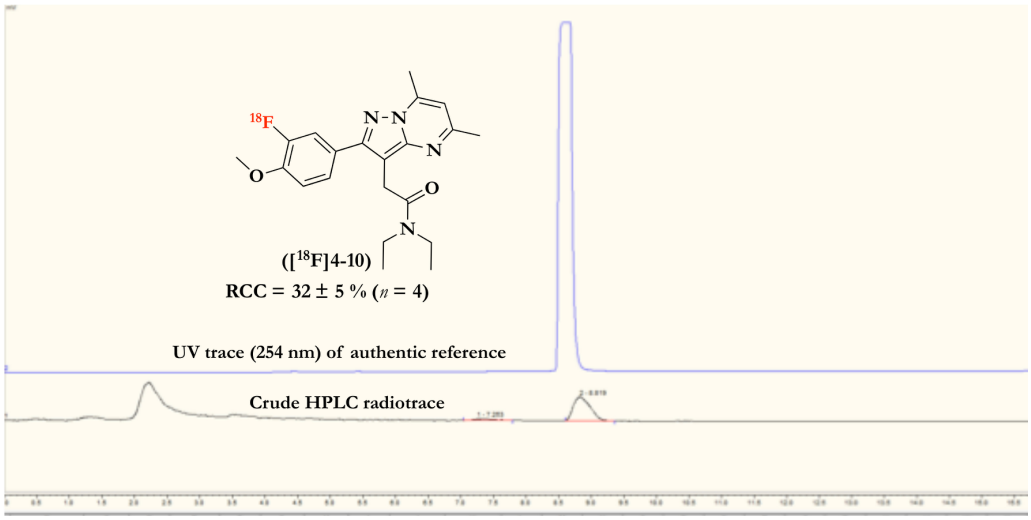
The solid blue line indicates the UV trace for the fluorine-19 reference material and the solid black line is the radio-HPLC trace.

Radiotrace for small scale radiosynthesis of [^{18}F]4-9



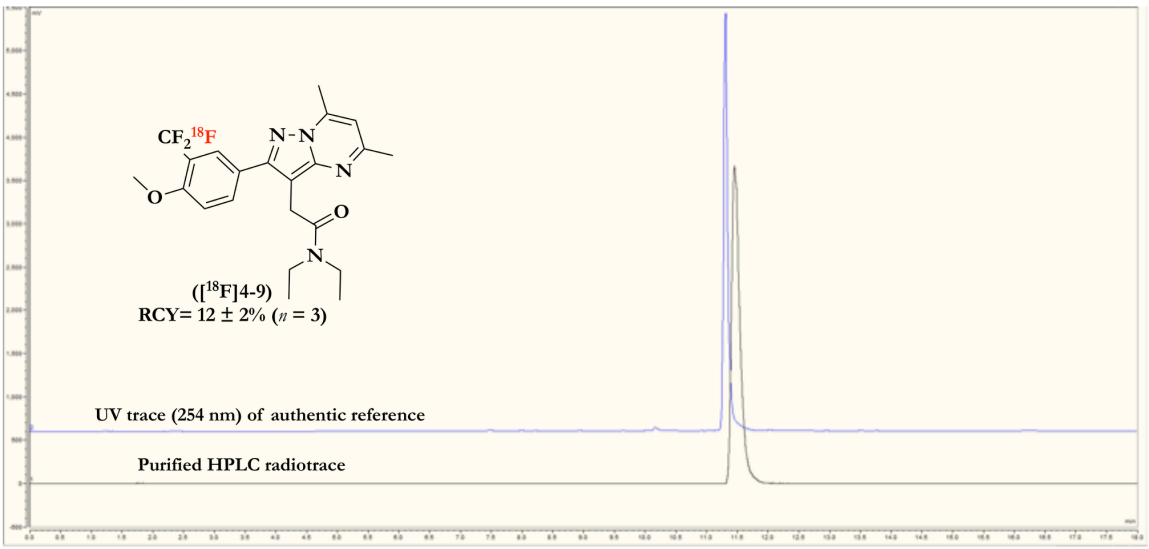
Reaction Number	Radio-TLC (%)	Radiochemical Purity (%)	Radiochemical Conversion (%)
1	34%	87%	30%
2	39%	-	34%
3	27%	85%	23%
4	24%	-	20%
RCC and Standard Error of the Mean			27% ± 3%

Radiotrace for small scale radiosynthesis of [^{18}F]4-10

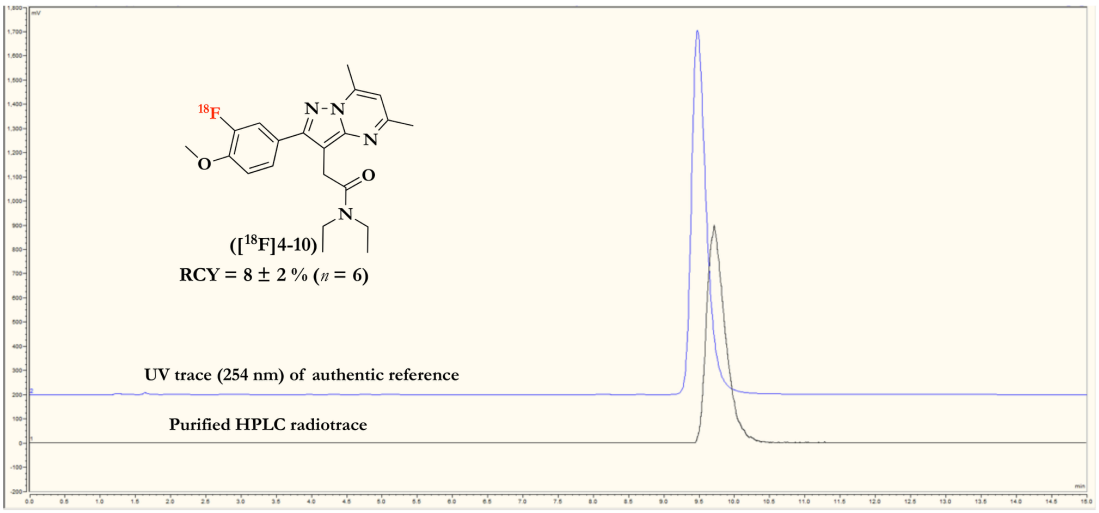


Reaction Number	Radio-TLC (%)	Radiochemical Purity (%)	Radiochemical Conversion (%)
1	37%	>99%	37%
2	21%	-	21%
3	28%	>99%	28%
4	41%	-	41%
RCC and Standard Error of the Mean			32% ± 5%

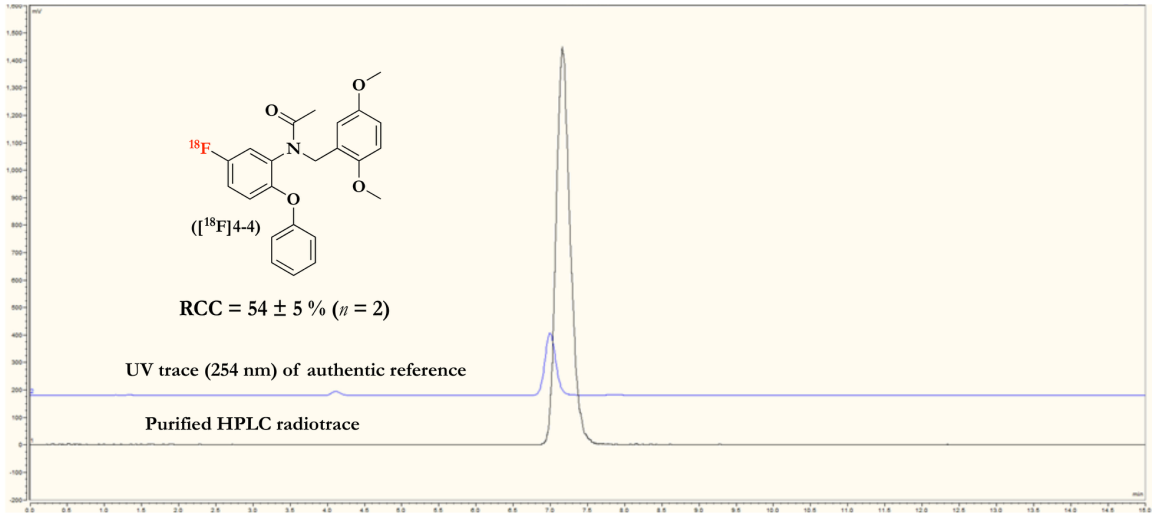
Radiotrace of isolated [^{18}F]4-9:



Radiotrace of isolated [^{18}F]4-10:



Radiotrace of isolated [^{18}F]4-4:



A RCY value was not determined for **[^{18}F]4-4** when isolated for *in vitro* studies.

5.4.5 Biological Methods:

Prof. Daniel Anthony and Dr. Alex Dickens conducted the procedures described in this section. The inclusion of these protocols is primarily as a means of reference for the biological methods described in section 4.8.

Intrastriatal Injection of LPS

LPS (1 µL in saline, *E.Coli* 026:B6, Sigma-Aldrich) was injected into the striatum of male adult C57Bl6 mice (2-3 months) at the following stereotaxic coordinates: bregma +0.5, ML +1.2, DV -1.5. Prior to the injection a small burr-hole was drilled in the skull over the striatum. The animal was anesthetised using isoflurane (2% in O_2).

Induction of Focal EAE

A focal EAE (fEAE) model was established in CD1 mice. On day -14, CD1 mice were immunized by an intradermal injection in the hind legs (25 µl in each side) with a 1:1 MOG35-55peptide (MEVGWYRSPFSRVVHLYRNGK; Innovagen SP-5360-5) (0.5 mg/mL in physiological saline) and CFA (Sigma F5881) emulsion. Fourteen days later, on day 0, when the antibody titer for MOG antibodies was highest, the animals received a 1µl stereotaxic intracranial injection in the left striatum (bregma +0.5, ML +1.2, DV -1.5) with heat-killed Tuberculosis (TB) (DB Difco Mycobacterium Tuberculosis H37Ra) resuspended in physiological saline (0.9%), while anaesthetized with 2 – 3% isoflurane in 70% nitrous oxide/ 30% oxygen mixture. The injection of the TB in non-MOG immunized animals induces a transient acute inflammatory response that resolves within 7 days. In MOG-immunized animals a persistent immune-mediated pathology develops that is characterized by complement deposition on white matter and the generation of a focal demyelinating lesion, with blood-brain barrier (BBB) breakdown, microglial & astrocyte activation, recruitment monocytes and of T and B cells, and loss of axons. These are all the hallmarks of an MS lesions.

Approximately 28 days after the intracerebral injection the BBB breakdown resolves, but the lesion continues to evolve and demyelinate.

Ex Vivo Autoradiography:

Mice with either a focal EAE lesion (n = 3) or vehicle control (n = 3) were anesthetised (3% Isoflourane in oxygen) and a tail vein cannula inserted. ^{18}F-DPA 713 was injected (EAE: 14.1 MBq ± 0.3, Ctl: 15.0 MBq ± 0.3) *via* the tail vein cannula. In order to assess the specificity of the radioligand *in-vivo* autoradiography blocking experiments were also performed. The cold compound PK11195 was injected *via* the tail cannula 20 minutes prior to the injection of ^{18}F-DPA 713 (16.5 MBq ± 0.4) at a concentration of approximately 1000 times greater than the radioactive tracer. The animals were killed by decapitation after 40 minutes to allow binding of the tracer.[28] The brain was removed and snap frozen in an isopentane bath in dry ice. Cryosections from the striatum (20 μM) were collected on positively charged slide. The sections were then dried using a hairdryer and placed in an imaging cassette (GE Healthcare) equipped with a tritium storage phosphor screen plate (19 x 24 cm). The sections were left overnight and the plate read in a typhoon (Amersham) scanner. The images were acquired at a resolution of 100 μm^2.

In-vitro autoradiography

Fresh or PFA fixed tissue were removed from the -20 °C freezer and allowed to defrost and dry at 37 °C for 20 mins. The slides were then rehydrated in TRIS-HCl buffer containing 120 mM $NaCl_2$, 5 mM KCl, 2 mM $CaCl_2$ and 1 mM $MgCl_2$ (ref DOI: 10.1007/s11307-005-7001-6).

For the studies comparing ^{18}F-DPA 713 to a known TSPO radio tracer slides (n = 3) adjacent to sections used in the ^{18}F-DPA 713 *in vitro* experiment were incubated with 19.2 kBq/mL of ^{18}F-DAA1106.

Following the incubation with the radioactivity all the slides were washed twice (5 mins) with TRIS-HCl buffer and then the sections were dried and placed in an imaging cassette and the images collected in the same manner as before.

Histology

Immunohistochemistry (IHC) was performed using the avidin-biotin-peroxidase method. After being post-fixed in ice cold 4% PFA, tissue slides were dried, washed in phosphate buffered saline (PBS) and incubated in methanol with 1% H_2O_2 (30%) to block endogenous peroxidases. Fc receptors in the tissue were blocked with 10% serum. Tissue was stained for Astrocytes (GFAP 1:500, Z0334 DAKO), myelin (MBP 1:1000, ab40390 AbCam), oligodendrocyte progenitor cells (NG2 1:500, AB5320 Millipore), premature oligodendrocytes (APC/ CC1 1:200, OP80 Millipore), presence of the treating antibody (huIgG Fc 1:100, SA5-10134 (Thermo Scienctific). Primary antibodies were incubated overnight at 4°C. For immunohistochemistry (IHC) Vector ABC (Vector Laboratories, CA, USA) was used to amplify the signal, which was revealed using 3,3-diaminobenzidine (DAB) (Sigma D5637). For immunofluorescence (IF), fluorescently labelled secondary antibodies were used. Tissue was counter-stained using cresyl violet after IHC and with DAPI after IF.

Statistical Analysis

The digital images were analysed in image J (NIH) using a set size region of interest which was placed in the ipsi and contralateral striatum. The average intensity in the ROI was then converted to a binding per mm^2 and the background radiation was subtracted. A binding potential was then generated using the following formula:

$$B_{pnd} = ((PSL/cm^2)_{(Lesion)} - (PSL/cm^2)_{(Contralateral)})/(PSL/cm^2)_{(Contralateral)})$$

The top three binding potential values were used from each brain and averaged. This data was then used for subsequent analysis in Prism (v5 Graph Pad).

5.5 References

(1) Pangborn, A. B.; Giardello, M. A.; Grubbs, R. H.; Rosen, R. K.; Timmers, F. J. *Organometallics* **1996**, 1518–1520.

(2) Kabalka, G. W.; Sastry, K. A. R.; Muralidhar, K. *J. Labelled Compd. Radiopharm.* **1982**, *19* (6), 795–799.

(3) Partridge, B. M.; Hartwig, J. F. *Org. Lett.* **2013**, *15* (1), 140–143.

(4) Riches, S. L.; Saha, C.; Filgueira, N. F.; Grange, E.; McGarrigle, E. M.; Aggarwal, V. K. *J. Am. Chem. Soc.* **2010**, *132* (22), 7626–7630.

(5) Wang, H.; Pullambhatla, M.; Guilarte, T. R.; Mease, R. C.; Pomper, M. G. *Biochem. Biophy. Res. Comm.* **2009**, *389* (1), 80–83.

(6) Diwu, Z.; Beachdel, C.; Klaubert, D. H. *Tetrahedron Lett.* **1998**, *39*, 4987–4990.

(7) Zhuang, Z.-P.; Kung, M.-P.; Wilson, A.; Lee, C.-W.; Plössl, K.; Hou, C.; Holtzman, D. M.; Kung, H. F. *J. Med. Chem.* **2003**, *46* (2), 237–243.

(8) Preshlock, S.; Calderwood, S.; Verhoog, S.; Tredwell, M.; Huiban, M.; Hienzsch, A.; Gruber, S.; Wilson, T. C.; Taylor, N. J.; Cailly, T.; Schedler, M.; Collier, T. L.; Passchier, J.; Smits, R. X.; Mollitor, J.; Hoepping, A.; Mueller, M.; Génicot, C.; Mercier, J. X. L.; Gouverneur, V. X. R. *Chem. Commun.* **2016**, *52*, 8361–8364.

(9) de Almeida, A. M.; Andersen, T. L.; Lindhardt, A. T.; de Almeida, M. V.; Skrydstrup, T. *J. Org. Chem.* **2015**, *80* (3), 1920–1928.

(10) Poty, S.; Désorgère, P.; Goze, C.; Boschetti, F.; Dhuys, T.; Schols, D.; Cawthorne, C.; Archibald, S. J.; Maecke, H. R.; Denat, F. *Dalton Trans.* **2015**, *44*, 5004–5016.

(11) Qiu, D.; Jin, L.; Zheng, Z.; Meng, H.; Mo, F.; Wang, X.; Zhang, Y.; Wang, J. *J. Org. Chem.* **2013**, *78* (5), 1923–1933.

(12) Campbell-Verduyn, L. S.; Mirfeizi, L.; Schoonen, A. K.; Dierckx, R. A.; Elsinga, P. H.; Feringa, B. L. *Angew. Chem. Int. Ed.* **2011**, *50* (47), 11117–11120.

(13) White, J. R.; Price, G. J.; Schiffers, S.; Raithby, P. R.; Plucinski, P. K.; Frost, C. G. *Tetrahedron Lett.* **2010**, *51* (30), 3913–3917.

(14) Zhao, X. Z.; Maddali, K.; Metifiot, M.; Smith, S. J.; Vu, B. C.; Marchand, C.; Hughes, S. H.; Pommier, Y.; Burke, T. R., Jr. *Bioorg. Med. Chem. Lett.* **2011**, *21* (10), 2986–2990.

(15) Puerto Galvis, C. E.; Kouznetsov, V. V. *Org. Biomol. Chem.* **2013**, *11* (3), 407–411.

(16) Gerack, C. J.; McElwee-White, L. *Chem. Commun.* **2012**, *48* (92), 11310–11313.

(17) Neochoritis, C. G.; Stotani, S.; Mishra, B.; Dömling, A. *Org. Lett.* **2015**, *17* (8), 2002–2005.

(18) Muchowska, K. B.; Adam, C.; Mati, I. K.; Cockroft, S. L. *J. Am. Chem. Soc.* **2013**, *135* (27), 9976–9979.

(19) Boeyens, J. C. A.; Cook, L. M.; Ding, Y.; Fernandes, M. A.; Reid, D. H. *Org. Biomol. Chem.* **2003**, *1* (12), 2168–2172.

(20) Ogura, T.; Usuki, T. *Tetrahedron* **2013**, *69* (13), 2807–2815.

(21) Chambers, R. D.; Hutchinson, J.; Sparrowhawk, M.; Sanford, G.; Moilliet, J.; Thomson, J. *J. Fluorine Chem.* **2000**, *102*, 169–173.

(22) Zhang, M.-R.; Kumata, K.; Maeda, J.; Haradahira, T.; Noguchi, J.; Suhara, T.; Halldin, C.; Suzuki, K. *J. Med. Chem.* **2007**, *50* (4), 848–855.

(23) Tredwell, M.; Preshlock, S. M.; Taylor, N. J.; Gruber, S.; Huiban, M.; Passchier, J.; Mercier, J.; Génicot, C.; Gouverneur, V. *Angew. Chem. Int. Ed.* **2014**, *53* (30), 7751–7755.

(24) Shen, J.; Yang, D.; Liu, Y.; Qin, S.; Zhang, J.; Sun, J.; Liu, C.; Liu, C.; Zhao, X.; Chu, C.; Liu, R. *Org. Lett.* **2014**, *16* (2), 350–353.

(25) Tang, D.; McKinley, E. T.; Hight, M. R.; Uddin, M. I.; Harp, J. M.; Fu, A.;

Nickels, M. L.; Buck, J. R.; Manning, H. C. *J. Med. Chem.* **2013**, *56* (8), 3429–3433.
(26) Banister, S. D.; Beinat, C.; Wilkinson, S. M.; Bin Shen; Bartoli, C.; Selleri, S.; Da Pozzo, E.; Martini, C.; Chin, F. T.; Kassiou, M. *Eur. J. Med. Chem.* **2015**, *93* (C), 392–400.
(27) O'Brien, E. R.; Kersemans, V.; Tredwell, M.; Checa, B.; Serres, S.; Soto, M. S.; Gouverneur, V.; Leppert, D.; Anthony, D. C.; Sibson, N. R. *J. Nucl. Med.* **2014**, *55* (2), 275–280.
(28) Dickens, A. M.; Vainio, S.; Marjamaki, P.; Johansson, J.; Lehtiniemi, P.; Rokka, J.; Rinne, J.; Solin, O.; Haaparanta-Solin, M.; Jones, P. A.; Trigg, W.; Anthony, D. C.; Airas, L. *J. Nucl. Med.* **2014**, *55* (3), 466–472.